From the Department of Cell and Molecular Biology
Karolinska Institutet, Stockholm, Sweden

CELLULAR RESPONSES TO THE DNA DAMAGING CYTOLETHAL DISTENDING TOXIN

Lina Guerra

Karolinska Institutet

Stockholm 2009

Cover illustration: Human HeLa cells intoxicated with the cytolethal distending toxin from *Haemophilus ducreyi* (green). Nucleus (blue), endoplasmic reticulum (red).

All previously published papers were reproduced with permission from the publishers.
Published by Karolinska Institutet, Stockholm, Sweden

ISBN 978-91-7409-568-5
Printed by Reproprint AB

“What we do in life echoes in eternity”

(Gladiator, 2000)

ABSTRACT

Cytolethal distending toxin (CDT) is a genotoxin, which belongs to a group of bacterial protein toxins called cyclomodulins. These are characterized by their interference with the eukaryotic cell cycle. CDT causes DNA damage, which induces cell cycle arrest and apoptosis. The active holotoxin consists of three subunits CdtA, CdtB and CdtC, where CdtB is the active subunit and has structural and functional similarities with DNase I.

We demonstrated that CDT uses the same internalization pathway as several other bacterial toxins do, such as cholera toxin and Shiga toxin. The binding on the plasma membrane is dependent on cholesterol. The toxin is internalized via the Golgi complex, and retrogradely transported to the endoplasmic reticulum (ER) and found in the nucleoplasmic reticulum. The translocation from the ER to the nucleus does not require either the ER-associated (ERAD) pathway or the Derlin-1 protein. Additionally, we showed that CDT is not farnesylated, a modification known to occur in the cytosol. In contrast, to other AB toxins, CdtB was demonstrated to have heat-stable properties and is not degraded by the 20S proteasome. All these evidence suggest that the toxin is translocated directly from the ER to the nucleus.

In adherent cells the cellular response to the CDT-induced DNA damage involved activation of the RhoA GTPase. We showed that the RhoA-specific Guanine nucleotide exchange factor (GEF) Net1 is dephosphorylated and translocated from the nucleus to the cytosol upon DNA damage. Knock down of Net1 by RNAi prevents RhoA activation, inhibits the formation of stress fibers, and enhances cell death. This indicates that Net1 activation is required for RhoA-mediated response to genotoxic stress. The Net1 and the RhoA dependent signals converge the activation of mitogen-activated protein kinase p38 (p38 MAPK) and its downstream target MAPK-activated protein kinase 2 (MK2). To further investigate this novel cell survival pathway in response to CDT we screened a yeast deletion library for CdtB-sensitive strains. Approximately 4500 yeast deletion strains were transformed with a plasmid containing CdtB. The screen shows that 78 mutated strains were hypersensitive to CdtB. Twenty of the human ortholog genes were found to interact with the actin cytoskeleton regulation network. Our analysis focused on TSG101, FEN1 and Vinculin (VCL). We demonstrated that they are all required to induce actin stress fiber formation in response to DNA damage. FEN1 and VCL also regulate the RhoA GTPase and p38 MAPK activation, and delay cell death in response to CDT intoxication.

In response to DNA damage, Ataxia-telangiectasia mutated (ATM) and ATM and Rad-3-related kinases (ATR) are activated and orchestrate DNA damage response. The transcription factor Myc has multi-functions such as inducing apoptosis in response to DNA damage. The Myc-regulated effectors acting upstream of the mitochorial apoptotic pathway are still unknown. We demonstrated that Myc is required for activation of the ATM-dependent DNA damage checkpoint response in cells exposed to ionizing radiation or CDT. Activation of ATM effectors, such as histone H2AX and the nuclear foci formation of the Nijmegen Berakage Syndrome (Nbs)1 protein, were abolished in the absence of Myc. The cellular response to UV irradiation, known to activate an ATR-dependent checkpoint, was not delayed in the absent of the Myc expression. This data demonstrate that Myc is required for activation of the ATM-dependent pathway.

Our studies highlight the importance of understanding the CDT biology and its mode of action. This knowledge could provide new tools to elucidate the putative involvement of bacteria in carcinogenesis.

SAMMANFATTNING PÅ SVENSKA

Bakterietoxinet cytolethal distending toxin (CDT) är ett genotoxin, det vill säga ett toxin som skadar arvsmassan. CDT tillhör en grupp bakterietoxiner som kallas cyclomoduliner. Dessa karaktäriseras av att de påverkar livscykeln hos celler. När CDT orsakar skador på arvsmassan i cellerna, leder det till stopp i cellens livscykel och så småningom till cellens död. CDT består av tre delar; CdtA, CdtB och CdtC, där CdtB är den verksamma delen.

Vi har visat att CDT tar sig in i värdcellen på samma sätt som många andra bakterietoxiner, exempelvis koleratoxin. Toxinets bindning till cellytan är kolesterolberoende. Väl inne i cellen transporteras toxinet till Golgiapparaten och vidare till det endoplasmatiska nätverket. Transporten från nätverket till cellkärnan är inte beroende av ERAD signalvägen eller av proteinet Derlin-1, vilket är viktigt för andra toxiner. Vi har även visat att CDT inte farnesyleras, vilket endast sker i cytoplasman. CDT kan istället lokaliseras i det nukleärplastiska nätverket nära cellkärnan. Till skillnad från andra toxiner, visade sig CdtB vara värmestabilt och bryts inte ner av destruktionsmekanismen 20S proteasomen. CDT tar sig direkt från nätverket till cellkärnan utan att först passera cytoplasman.

CDT-framkallade skador på arvsmassan leder till aktivering av RhoA GTPase. Vi påvisade att GEF (RhoA-specifika Guanine nucleotide exchange factor), Net1, defosforyleras och transporteras från cellkärnan till cytoplasman när arvsmassan skadas. Nedreglering av Net1 stoppar bildningen av stressfibrer och ökar celldödligheten. Detta visar att aktivering av Net1 är nödvändig för hur cellen skall reagera när arvsmassan skadas. Net1 och RhoA behövs för vidare signalering till molekylerna p38 MAPK och MK2. För att ytterligare undersöka denna nya signalväg som är viktig för cellens överlevnad, tog vi hjälp av ett genetiskt jästbibliotek. En plasmid med CdtB placerades in i cirka 4500 jäststammar. Resultatet visar att 78 av dessa jäststammar är känsliga för CdtB. Hos dessa är 20 stycken mutanter inblandade i kontrollen av cytoskelettet i mänskliga celler. Ytterligare experiment visar att molekylerna TSG101, FEN, och Vinculin (VCL) är viktiga för bildning av stressfibrer när arvsmassan skadats. FEN1 och VCL reglerar även aktiveringen av RhoA GTPase och p38 MAPK och är viktiga för cellens överlevnad när arvsmassan skadats.

ATM (Ataxia-Telangiectasia Mutated) och ATR (ATM and Rad-3-related kinases) är molekyler som aktiveras vid skador på arvsmassan. Myc är ett protein med flera funktioner bland annat vid celldöd. Vi undersökte Mycs roll efter att arvsmassan skadats i cellen. ATM visade sig inte aktiveras lika snabbt i celler utan Myc jämfört med celler med Myc. Celler utan Myc överlevde längre med skador i arvsmassan och vissa molekyler som är inblandade i reparationen av arvmassan aktiverades inte. Detta betyder att Myc är nödvändig för ATMs aktivering efter att arvsmassan skadats med antingen strålning eller CDT. ATR-signalvägen som aktiveras av UV strålning är inte beroende av Myc.

Dessa resultat understrycke vikten av att förstå biologin om CDT och dess mekanismer. Dessa kunskaper om CDT kan bli viktiga för att kunna förstå sambandet mellan bakterieinfektioner och uppkomsten av cancer.

PUBLICATIONS

This thesis is based on the following articles and manuscripts. They will be referred to in the text by their roman numerals.

I Cellular internalization of cytolethal distending toxin: a new end to a known pathway

Lina Guerra, Ken Teter, Brendan N. Lilley, Bo Stenerlöw, Randall K. Holmes, Hidde L. Ploegh, Kirsten Sandvig, Monica Thelestam and Teresa Frisan
Cell Microbiol. 2005 Jul;7(7):921-34

II A Novel Mode of Translocation for Cytolethal Distending Toxin

Lina Guerra, Kathleen N. Nemec, Shane Massey, Suren A. Tatulian, Monica Thelestam, Teresa Frisan, Ken Teter.
Biochim Biophys Acta. 2009 Mar;1793(3):489-95. Epub 2008 Dec 11.

III A bacterial cytotoxin identifies the RhoA exchange factor Net1 as a key effector in the response to DNA damage

Lina Guerra*, Heather S. Carr*, Agneta Richter-Dahlfors, Maria G. Masucci, Monica Thelestam, Jeffrey A. Frost, Teresa Frisan
PLoS ONE 2008 May 28;3(5):e2254

IV Characterization of novel survival signals induced by bacterial genotoxin

Lina Guerra, Riccardo Guidi, Ilse Slot, Ramakrishna Sompallae, Carol L. Pickett, Stefan Åström, Frederik Eisele, Dieter Wolf, Camilla Sjögren, Maria G. Masucci, Teresa Frisan
Manuscript

V Myc is required for activation of the ATM-dependent checkpoints in response to DNA damage

Lina Guerra*, Ami Albihn*, Riccardo Guidi, Susanna Trommersjö, Bo Stenerlöw, Christine Josenhans, James G. Fox, David B. Schauer, Monica Thelestam, Lars-Gunnar Larsson, Marie Henriksson, Teresa Frisan
Manuscript

* These authors contributed equally to the work.

ABBREVIATIONS

A. actinomycetemcomitans	*Aggregatibacter actinomycetemcomitans* (formerly *Actinobacillus*)
ATM	Ataxia-Telangiectasia Mutated
ATR	Ataxia-Telangiectasia and Rad-3-related kinases
BFA	BreFeldin A
C. jejuni	*Campylobacter jejuni*
CagA	Cytotoxin-associated antigen A
Cdk	Cyclin-dependent kinase
CDT	Cytolethal Distending Toxin
Chk	Checkpoint kinase
CHO	Chinese Hamster Ovary cells
Cif	Cycle inhibiting factor
CKI	Cyclin-dependent Kinase Inhibitors
CNF	Cytotoxic Necrotizing Factor
CT	Cholera Toxin
DNA	DeoxyriboNucleic Acid
DNase I	DeoxyriboNuclease I
DNT	DermoNecrotic Toxin
DSB	Double Strand Breaks
ECM	ExtraCellular Matrix
E. coli	*Escherichia coli*
ER	Endoplasmic Reticulum
ERAD	ER-Associated Degradation
ESCRT	Endosomal Sorting Complex Required for Transport
ETA	*Pseudomonas aeruginosa* ExoToxin A
FEN1	Flap EndoNuclease 1
FIP	Fusobacterial Immunosuppressive Protein
GDPases	Guanosine DiphosPhatases
GEFs	Guanine nucleotide Exchange Factors
GPI	GlycosylPhophatidylInositol
GTPases	Guanosine TriphosPhatases
H. ducreyi	*Haemophilus ducreyi*
H. hepaticus	*Helicobacter hepaticus*
H. pylori	*Helicobacter pylori*
HdCDT	*H. ducreyi* CDT
IARC	International Agency for Research on Cancer
IL	InterLeukin
IR	Ionizing Radiation

mβCD	methyl-β-CycloDextrin
M. ulcerans	*Mycobacterium ulcerans*
MK2	MAPK-activated protein Kinase 2
mTOR	mammalian Target Of Rapamycin
Net1	Neuroepithelioma transforming gene 1
NLS	Nuclear Localization Signal
OMVs	Outer Membrane Vesicles
p38 MAPK	Mitogen-Activated Protein Kinase p38
pI	Isoelectric point
PI-3,4,5-P	PhosphatidylInositol (PI)-3,4,5-triphosphate Phosphatase
PI3K	PhosphoInositide 3-Kinases
PMT	*Pasteurella multocida* Toxin
RNAi	RiboNucleic Acid interference
ROCK	RhO-associated, Coiled-coil containing protein Kinase
S. cerevisiae	*Saccharomyces cerevisiae*
S. typhi	*Salmonella typhi*
SSB	Single Strand Breaks
TNF	Tumor Necrosis Factor
TSG101	Tumor Susceptibility Gene 101
UV	UltraViolet
VacA	Vacuolating cytotoxin
VCL	VinCuLin

TABLE OF CONTENTS

1. OBJECTIVES

The objective of this study: to understand the internalization and the cellular response in mammalian cells upon DNA damage induced by the bacterial genotoxin CDT.

The specific aims were to:

- Characterize the internalization pathway of CDT from binding on the cell membrane to its entry into the nucleus where it causes DNA damage.

- Identify key effectors of the RhoA-dependent survival signals in response to DNA damage.

- Investigate the role of the transcription factor Myc in response to radiation- and CDT induced DNA damage.

2. INTRODUCTION

2.1 Background

Cytolethal distending toxin (CDT) is a bacterial toxin affecting many cellular processes, such as cell cycle, actin stress fiber formation and inflammation. To entirely understand the complex biology of CDT and its mode of action, it is necessary to review several of these cellular key pathways.

2.1.1 Cell cycle

The eukaryotic cell cycle consists of four coordinated activities, cell growth, deoxyribonucleic acid (DNA) replication, distribution of the duplicated chromosomes to daughter cells, and cell division. There are four phases: Gap 1 phase (G1), synthesis (S), Gap 2 phase (G2), and mitosis (M) (Figure 1) [143, 173]. During the G1 phase, there is cellular growth and preparation of the chromosomes for replication. Chromosome duplication takes place during the S phase. During the G2 phase, the cell continues to grow, synthesizes protein, and prepares for mitosis. During the M phase, the chromosomes condense, the nuclear envelope breaks down, the cytoskeleton rearranges to form the mitotic spindle, and the chromosomes separate and move to opposite poles. The cell is pinched into two parts, each with a complete set of chromosomes. The chromosomes are enveloped by a nuclear membrane to form a nucleus and cell division takes place. The new daughter cells eventually enter the G1 phase to continue the cycle [98]. If the conditions that signal the transition to the next phase are not present, the cell exits the cell cycle and enters a quiescent stage called G0 [172, 173].

2.1.1.1 Checkpoints

There are several systems, called checkpoints. These systems ensure the proper execution of the cell division, by checking that the essential events of a cell cycle step are completed before progression to the next step. In case of detection of DNA damage, the checkpoints prolong the length of a stage to allow repair [40]. The cell cycle checkpoints, activated by DNA damage, occur at the G1/S transition (G1 checkpoint), S phase progression (S checkpoint), G2/M boundary (G2 checkpoint), and M phase (M checkpoint) (Figure 1) [40, 133].

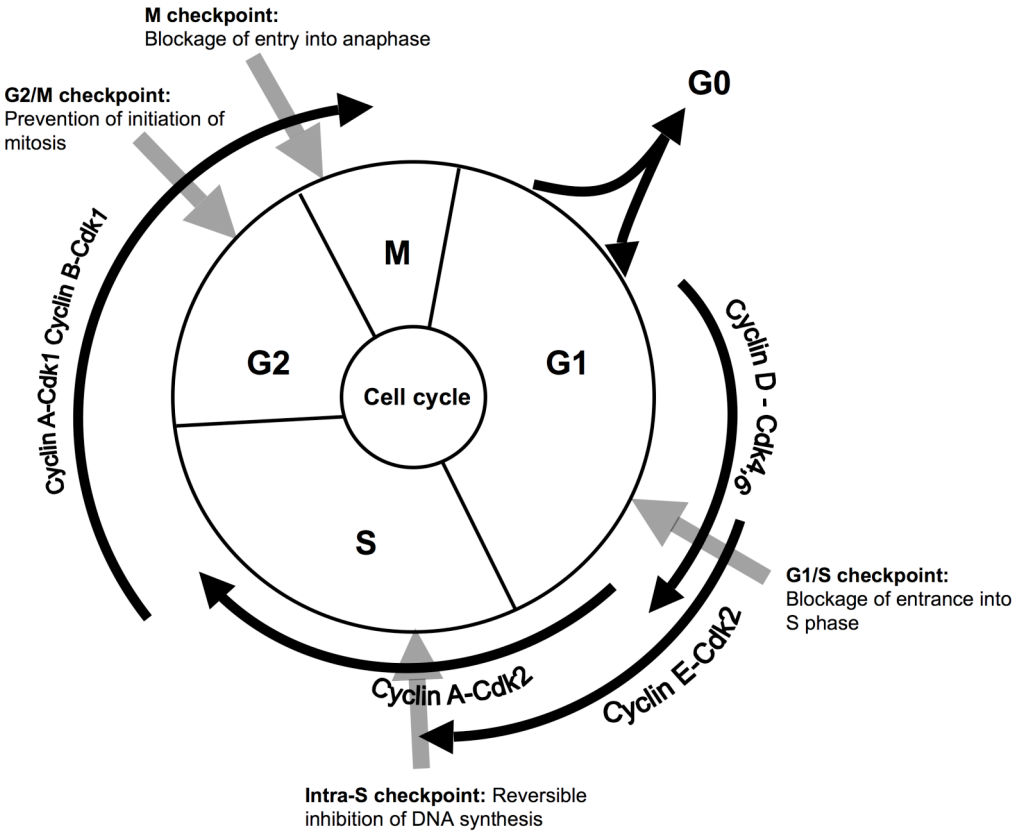

Figure 1. The cell cycle. The cycle is divided into four phases with a checkpoint in each, which is preventing the cell from proceeding in the cycle if any errors occur. Different cyclins and Cdks are regulating the transition from one phase to another.

2.1.1.2 Cyclins and Cdks

The cell cycle of eukaryotes is controlled by a conserved set of protein kinases, which promotes the transition to the next stage of the cycle. Regulatory protein subunits, referred to as cyclins, are associated with these kinases. Distinct pairs of cyclins and cyclin-dependent kinases (Cdks) are the primary regulators of the cell cycle. The levels of cyclins rise and fall through the stages of the cell cycle through periodic synthesis and degradation, but the Cdk levels remain relatively stable. Association with specific cyclins regulates the kinase activity of the Cdks by phosphorylation and dephosphorylation, by the binding of Cdk inhibitors, and by degradation of the attached cyclin. The role of Cdks is to phosphorylate a number of protein substrates that control cell cycle procession [40, 141, 173]. Upstream regulators, such as tumor suppressor genes, like Ataxia-telangiectasia mutated protein kinase (ATM), Rb and p53 control the Cdks.

2.1.2 DNA Damage and checkpoint responses

The genomic integrity of organisms is maintained, generation after generation through a number of mechanisms, like replication, cell cycle checkpoints, and DNA repair. Genomes are subjected to a number of exogenous DNA damaging agents (e.g. ionizing radiation (IR), radiomimetic chemicals and bacterial toxins), or endogenous DNA damaging agents (e.g. reactive radicals, stalled replication forks, meiotic recombination, and immune system maturation) that cause DNA double-strand breaks (DSBs) or single- strand breaks (SSBs) (Figure 2). The DSBs can cause chromosomal rearrangements, senescence, carcinogenesis or cell death [72, 171].

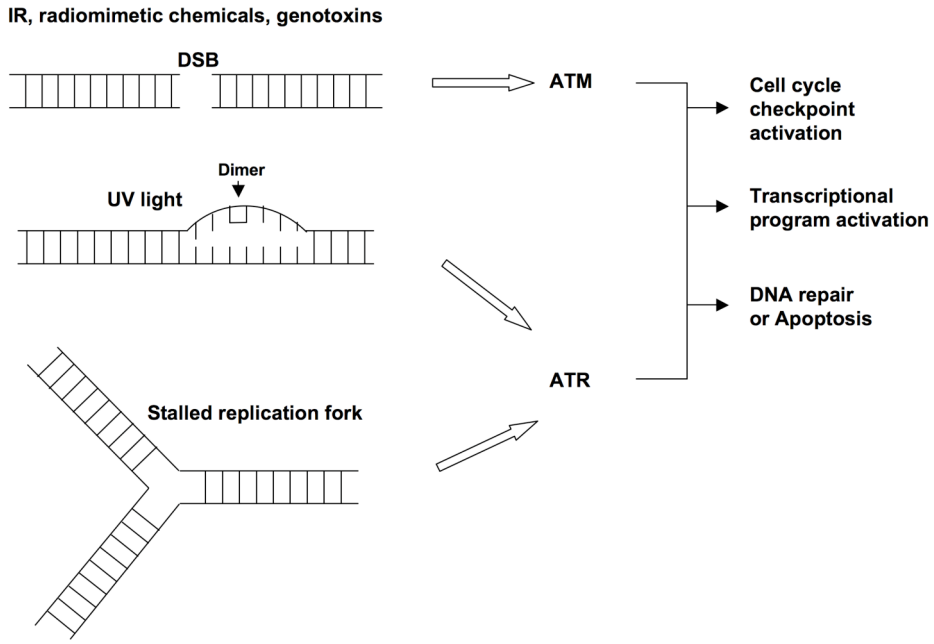

Figure 2. DNA damaging agents and cellular response to DNA damage. Many agents can cause DNA damage and this may have different outcomes. ATM and ATR are the main sensor kinases, activated by different kinds of DNA damage. IR or genotoxins activate preferentially ATM, while ATR is activated by ultraviolet (UV) exposure or stalled replication fork. ATM and ATR activate cascades of signaling pathways, leading to either cell death or attempt to rescue the cell.

The DNA repair is dependent on the family of phosphatidylinositol 3-OH-kinase like kinases (PIKKs), such as ATM and the ataxia-telangiectasia and Rad-3-related kinases (ATR), and DNA protein kinase catalytic subunit (DNA PKcs). The kinases phosphosphorylate a diversity of proteins that transduce DNA damage signals. The signal leads to cell cycle arrest, alternate transcription, start DNA repair or, if the DNA damage cannot be repaired, apoptosis [2, 152].
A recent proteomic analysis of the components in the DNA repair machinery reveals an extensive network of more than 700 proteins [100]. The substrate proteins of ATM and ATR

kinases are involved in nucleic acid and protein metabolism, cell cycle regulation, signal transduction, cell structure and proliferation, oncogenesis, and immunity. In mammalian cells, the activation of ATM is induced by DSBs. The ATM phosphorylation is followed by dissociation of the inactive complex to form the active ATM [6]. Upon treatment of cells with IR, proteins such as the Mre11-Rad50-Nbs1 complex involved in repairing DNA DSBs are moved to the site of the damaged DNA and are required for proper ATM activation [88]. ATM phosphorylates histone H2AX that localizes to the break site along with the Mre11-Rad50-Nbs1 complex [99, 104, 110, 122]. Detection of phosphorylated H2AX is a well-established way to detect and quantify DNA damage in cells [93]. Another known ATM substrate is checkpoint kinase 2 (Chk2), which inactivates CDC25C phosphatase leading to accumulation of hyperphosphorylated (inactive) Cdk1 [133]. ATM also activates p53, which increases the production of the cyclin-dependent kinase inhibiting p21 (Figure 6) [151]. p21 inhibits dephosphorylation of cyclin E/Cdk2, thereby blocking transition from G1 into S of the cell cycle.

2.1.3 Cell death and apoptosis

Apoptosis or programmed cell death is an important mechanism to balance cell proliferation and remove unwanted cells during the development and homeostasis of multicellular organisms [43]. Apoptosis is characterized by shrinkage of the cell, membrane blebbing, chromatin condensation, followed by DNA fragmentation and the appearance of apoptotic bodies, which are then engulfed by the surrounding cells [176]. The apoptotic process can be divided into three main phases: the initiation phase, the effector phase and the execution phase. The two major pathways for apoptosis induction are the death receptor-dependent pathway and the mitochondria-dependent pathway. Activation of either of these pathways ultimately target a family of cystein-dependent aspartate directed proteases, called caspases [174], the main executioners of cell death. The receptor-dependent pathway includes ligation of a death ligand to its transmembrane receptor belonging to the tumor necrosis factor (TNF) receptors super family. The receptor forms a death complex, followed by recruitment and activation of caspases in the death-inducing signalling complex. The mitochondria-dependent pathway is mainly activated by intracellular signals such as DNA damage. Activation of the mitochondria, results in release of caspase-activating proteins into the cytosol, thereby forming the apoptosome where caspases will bind and become activated [172, 174].

2.1.4 The Rho GTPases family

The Rho guanosine triphosphatases (GTPases) are molecular switches that regulate many essential cellular processes, including actin dynamics, gene transcription, cell cycle progression and cell adhesion. Rho GTPases are inactive when bound to GDP, and kept in this form by binding to guanine nucleotide dissociation inhibitors (GDI). They are activated by GDP/GTP exchange, induced by guanine nucleotide exchange factors (GEFs) and are inactivated by hydrolysis of the bound GTP, a process that is mainly facilitated by GTPases-activating proteins (GAPs (Figure 3). The active Rho GTPases interact with a large spectrum of effector proteins to mediate downstream signalling [12, 67, 129].

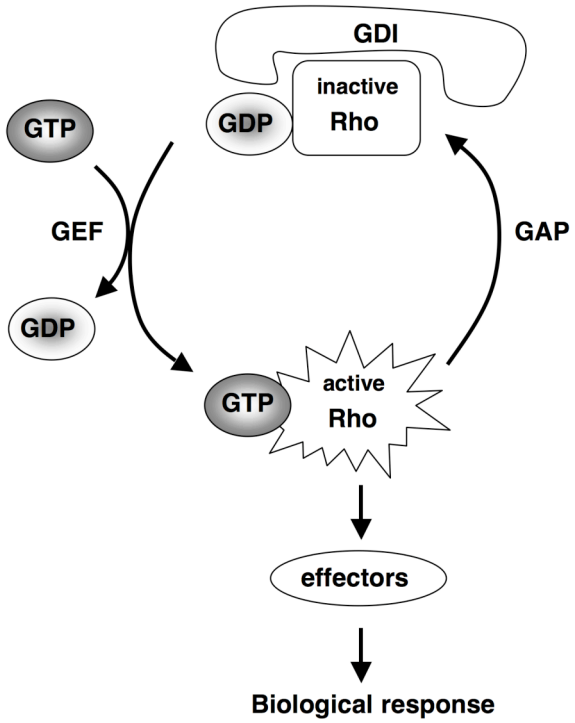

Figure 3. The Rho-GTPase molecular switch. The small GTPases cycle between an inactive GDP-bound state and an active GTP-bound state. GEFs activate the Rho-GTPases by accelerating their GDP/GTP exchange rate and GAPs inactivate the Rho-GTPases.

Members of the Rho family of small GTPases (RhoA, Rac, Cdc42) have shown to be key regulators of the actin cytoskeleton, and furthermore, through their interaction with multiple target proteins, they ensure a coordinated control of other cellular activities like gene transcription and adhesion. The cytoskeleton is a dynamic structure that maintains cell shape, protects the cell, enables cellular motion, and plays an important role in both intracellular transport and cellular division. Eukaryotic cells contain three main types of cytoskeletal filaments; microfilaments, intermediate filaments, and microtubules [145].

Each of the three GTPases regulate distinct processes; RhoA is involved in the formation of stress fibers and focal adhesions, by activating the Rho-associated, coiled-coil containing protein kinase 1 (ROCK1) which stimulates LIM kinase, then stimulates Cofilin that re-organises the actin cytoskeleton. Rac stimulates the polymerisation of actin underneath the plasma membrane leading to membrane ruffles. Cdc42 induces polymerization of actin to produce filopodia [16, 71].

2.2 Bacterial toxins

Bacterial toxins are the most powerful human poisons known and retain high activity at very low concentrations. For example the lethal dose of botulinum toxin in mouse is in the range of 1–5ng/kg [106]. In contrast, the lethal dose of strychnine, a very toxic pesticide, is 2mg/kg [135].

There are two main types of bacterial toxins, lipopolysaccharides (LPS), which are associated with the cell wall of Gram-negative bacteria (endotoxins), and proteins, which are released from the bacterial cells and can act at tissue sites removed from the site of bacterial growth (exotoxins) [91]. Since the attention of my work is to characterize the cellular responses to cytolethal distending toxin (CDT) which regulate the cell cycle, the primarily discussion will be on bacterial toxins that interfere with this process; the bacterial cyclomodulins.

2.2.1 Cyclomodulins

Pathogenic bacteria have developed a complicated arsenal of virulence factors that take over eukaryotic host functions to their own benefits. One of the pathways targeted by several bacterial toxins is the eukaryotic cell cycle. These toxins, termed cyclomodulins, can promote cell proliferation, or in opposition inhibit cell growth and modulate differentation by blocking cell cycle progression (Table 1) [115, 117].

Table 1. Bacterial cyclomodulins. Adapted from [115].

Bacteria	Effectors
Inhibit proliferation	
Escherichia coli *Shigella dysenteriae* *Haemophilus ducreyi* *Campylobacter sp.* *Helicobacter sp.* *Salmonella typhi*	CDT
Escherichia coli	Colibactin
Escherichia coli	Cif
Helicobacter pylori	VacA
Fusobacterium nucleatum	FIP
Mycobacterium ulcerans	Mycolactone
Promote proliferation	
Escherichia coli *Yersinia pseudotuberculosis*	CNF
Helicobacter pylori	CagA
Pasteurella multocida	PMT
Bordetella sp.	DNT

2.2.1.1 Inhibiting cyclomodulins

CDT and Colibactin induce DNA damage in the host cells, resulting in activation of the DNA damage checkpoints [114, 167, 181].

Cif produced by enteropathogenic and enterohemorrhagic *Escherichia coli* (EPEC and EHEC) is injected into the host cell by the bacterial type II secretion system, and inhibits the G2/M transition via constant inhibition of Cdk1, [20, 97]. Cif also induces reorganization of the actin cytoskeleton, although the effect is cell type-dependent, and cell cycle arrest is not a result of the cytoskeleton alterations [114, 162]. Cif is composed of a C-terminal effector domain and an exchangeable N-terminal translocation signal [20]. In contrast to CDT and Colibactin, Cif-induced Cdk1 phosphorylation is not a consequence of DNA damage response and does not

cause phosphorylation of histone H2AX [162]. Cif-induced block of the cell proliferation correlates with induction of cyclin-dependent kinase inhibitor (CKI) p21 and p27 ubiqutination. Fusobacterial immunosuppressive protein (FIP) is produced by *Fusobacterium nucleatum*, a Gram-negative anaerobe involved in various diseases, including periodontitis. FIP suppresses human B- and T-cell responses to antigen and mitogens *in vitro* by arresting the cell cycle in the G1 phase. The G1 arrest is associated with the failure in these cells to express the proliferating cell nuclear antigen (PCNA), an important factor in DNA replication and repair [149].

Mycobacterium ulcerans is a causative agent of Buruli ulcer, a debilitating skin disease found in Australia and West Africa. The disease is characterised by persistent severe necrotic lesions of the skin and underlying fat, and lack of an acute inflammatory response. *M. ulcerans* secretes a polyketide-derived macrolide, named mycolactone, which induces cell rounding, inhibits protein synthesis and causes cell cycle arrest in G0/G1 and eventually cell death [55].

2.2.1.2 Promoting cyclomodulins

Several bacterial products are known to stimulate the proliferation of eukaryotic cells. Cytotoxic necrotizing factor (CNF) from *E. coli* and *Yersinia pseudotuberculosis* and the dermonecrotic toxin (DNT) from *Bordetella* species are transglutaminases. These toxins catalyze deamination or polyamination at Gln63 of RhoA and the corresponding Gln residues of the other members of the GTPase family, Rac and Cdc42. This blocks the essential GAP-stimulated GTP hydrolysis, thereby constitutively activating the GTPases [65]. CNF and DNT trigger the G1/S transition and induce DNA replication in different mammalian cells, such as fibroblasts and osteoblasts [66, 118]. Another toxin acting in these cell types is the *Pasteurella multocida* toxin (PMT), which is a highly potent mitogen for various cell types [109, 134].

2.2.1.3 Helicobacter pylori

Helicobacter pylori is the only bacterium so far classified as a human carcinogen by the International Agency for Research on Cancer (IARC), since it is associated with an increased risk of gastric adenocarcinoma and mucosa-associated lymphoid tissue (MALT) [87]. *H. pylori* produces cyclomodulins that have both inhibitory and promoting properties. They can both induce cell proliferation ans cause cell cycle arrest. Cytotoxin-associated antigen A (CagA), which is encoded by *cagA* in the *cag*-pathogenicity island of *H. pylori* is an important virulence

factor [19]. It has been shown that CagA promotes a rapid progression from G1 into G2/M and p53-independent apoptosis within 72 hours in a gastric cell line [123]. Once CagA is localized in the plasma membrane it is phosphorylated and activates the oncogene tyrosine phosphatase SHP2. CagA activation of SHP2 leads to cellular morphological changes that are reminiscent of unrestrained stimulation by growth factors, and CagA appears to induce cell proliferation by activation of the MAPK pathway via both Ras-dependent and -independent signalling [62, 63].

The virulence factor vacuolating cytotoxin (VacA) is expressed as a precursor protein. VacA action on cells is associated with rapid formation of acidic vacuoles enriched for late endosomal and lysosomal markers [34]. In gastric epithelial cells, VacA has been shown to inhibit cell proliferation through p53-dependent cell cycle arrest in the G1 phase and induce cell death via activation of the mitochondrial-dependent apoptosis pathway [21, 30].

2.2.2 Cellular internalization of bacterial protein toxins

Many protein toxins consist of two parts, one compartment (subunit A) is responsible for the enzymatic activity of the toxin; the other compartment (subunit B) binds to a specific receptor on the target cell membrane and transferres the enzyme across the membrane. The enzymatic component is not active until it is released from the native AB toxin. Isolated A subunits may bind to target cells but lack the ability to enter. On the other hand, isolated B subunits may bind to target cells and enter cells, but are not toxic. The best known mechanism of toxin uptake into target cells is receptor-mediated endocytosis where the native AB toxin is within the endosomal compartments [59, 116]. The specific receptors for the B subunit of toxins on target cells or tissues are usually glycoproteins [82, 90].

Several bacterial protein toxins are internalized rapidly and efficiently by binding to transmembrane proteins entering by clathrin-dependent endocytosis. Diphtheria toxin, cholera toxin (CT) and *Pseudomonas aeruginosa* exotoxin A (ETA) are toxins, which take advantage of the clathrin-dependent pathway [75, 112, 153, 169]. Transmembrane receptors that become concentrated in clathrin-coated pits have an internalization signal in their cytoplasmic domain, which interacts with the adaptor protein 2 (AP2). AP2 binds to clathrin and many other adaptor proteins and the internalization of the coated vesicle takes place [73, 163]. Another molecule important for toxin internalization is the GTP-binding dynamin, which controls the formation of coated pits and is involved in a late step of clathrin-dependent endocytosis [146]. Also cholesterol is important for clathrin-dependent endocytosis [130, 158]. Several protein toxins

can be internalized by an endocytic mechanism that functions independently of clathrin and caveolae. For example the plant toxin ricin as well as CNF is internalized by clathrin- and caveolae- independent endocytosis [24, 138].

A number of bacterial toxins, such as diphtheria toxin and anthrax toxin are translocated directly from the endosome to the cytosol. The trigger for the translocation is the endosomal pH, which induces a conformational change in the B subunit of the toxin, allowing translocation of the A compoment [23, 24, 44]. A number of toxins such as ricin, Shiga toxin and CT are transported to the Golgi apparatus after being endocytosed [70, 136, 138]. Such a toxin can be present in an organelle in concentrations too low to be visualized by microscopy. Biochemical approaches have been developed to quantify the transport and presence of a toxin in the Golgi complex or the ER. Addition of a sulfation sites to the toxin allows it to be sulfated in the Golgi complex. Similarly, addition of glycosylation sites allows one to use glycosylation in the ER to monitor retrograde transport [136]. Cholesterol is important not only in regulating endocytosis, it is also crucial for endosome to Golgi transport of toxins. When reducing the cholesterol levels with methyl-β-cyclodextrin (mβCD) the transport to the Golgi complex is decreased [140].

Toxins that are retrogradely transported to the ER and act on cytosolic targets, such as the ETA, ricin, and CT, are known to enter the cytosol from the ER. The proposed mechanism for their transmembrane translocation involves the ER associated protein degradation (ERAD) pathway [154, 165], known to translocate misfolded secretory and ER membrane proteins into the cytosol for proteolytic degradation [57].

3. CYTOLETHAL DISTENDING TOXINS

3.1 Introduction

CDT is a bacterial genotoxin with the unique ability to induce DNA damage and cell cycle arrest, thereby inhibiting cell proliferation. These cellular responses are identical to those induced by IR, a well-characterized DNA damaging agent. CDT causes cell cycle arrest and progressive cellular distension leading to enlargement of both the cell and nucleus followed by chromatin fragmentation and cell death [27, 50]. It is possible that CDT acts as a cytotoxic agent in the pathogenesis of infection. Because of its genotoxic activity CDT may be a potentially carcinogenic agent.

CDT was first reported by Johnson and Lior in 1987. It was described as a novel type of toxic activity produced by pathogenic strains of *E. coli*. The cytotoxic effect was observed as an extraordinary cell distension, obvious 3-5 days after addition of bacterial culture supernatants to cells growing *in vitro*, and resulting after a few more days in cell death [69]. They named the toxin "cytolethal distending toxin" (CDT) based on the morphological effect on mammalian cells. It has been showed that CDT has an effect on a variety of cells, even yeast cells [58, 168].

CDTs are produced by several Gram-negative bacterial pathogens, including *E. coli, Salmonella typhi, Shigella dysenteriae, Aggregatibacter actinomycetemcomitans, Haemophilus ducreyi, Helicobacter sp* and *Campylobacter spp* (Table 2) [168]. The toxin consists of three subunits CdtA, CdtB and CdtC. Only a *cdtB* gene has been demonstrated in *S. typhi* and is not present in other *S. enterica* reservoirs. There are no homologues of the *cdtA* or *cdtC* genes. The *cdtB* from *S. typhi* forms a complex with *S. typhi* PltA (persussis-like toxin A) and PltB (persussis-like toxin B) [56, 156].

The subunits of CDT appear to be constitutively synthesized, assembled into CDT complex and translocated into the periplasm in bacterial cells. The CDT complex is then secreted into the extracellular medium, probably via CdtA that undergoes post-translational cleavage at its N-terminal signal sequence [61, 170]. A recent study has demonstrated that CDT is released in association with outer membrane vesicles (OMVs) in *E. coli*, suggesting that OMVs could

represent the natural vesicle through which CDT is delivered to the target cells from the bacteria [10].

Table 2. Summary of CDT occurrence in bacteria. Adapted from [168].

Bacteria	Gene(s) detected	Designation
Escherichia coli	*cdt*ABC	EcCDTI
E. coli	*cdt*ABC	EcCDTII
E. coli	*cdt*ABC	EcCDTIII
E. coli	*cdt*ABC	EcCDTIV
Shigella dysenteriae	*cdt*ABC	SdCDT
S. boyii	-	SbCDT
S. sonnei	*cdt*A	SsCdtA
Haemophilus ducreyi	*cdt*ABC	HdCDT
Campylobacter jejuni	*cdt*ABC	CjCdtB
C. coli	*cdt*ABC	CcCdtB
C. fetus	*cdt*B[a]	CfCdtB
C. hyointestinalis	*cdt*B[a]	ChCdtB
C. lari	*cdt*B[a]	ClCdtB
C. upsaliensis	*cdt*B[a]	CuCdtB
Helicobacter hepaticus	*cdt*ABC	HhCdtB
H. pullorum	*cdt*B	HpuCdtB
H. bilis	*cdt*B	HbCdtB
H. canis	*cdt*B	HcaCdtB
H. flexispira	*cdt*B	HfCdtB
H. cinaedi	*cdt*B	HciCdtB
Helicobacter sp (strain 98-6070)	*cdt*B	HspCdtBI
Helicobacter spp (strain 96-1001)	*cdt*B	HspCdtBII
Salmonella typhi	*cdt*B	StCdtB
Aggregatibacter actinomycetemcomitans (formerly *Actinobacillus)*	AaCDT	AaCDT

a. Probably presence of *cdtB* sequences

In our studies we have used CDT derived from *Haemophilus ducreyi,* named HdCDT. *H. ducreyi* is a fastidious Gram-negative rod-shaped bacterium, that is the causative agent of the sexually transmitted disease, chancroid [155]. It has been demonstrated that HdCDT is virtually identical with the CDT produced from *A. actinomycetemcomitans*; the amino acid sequence identities were 91%, 97%, and 94% for CdtA, CdtB, and CdtC, respectively [159]. HdCDT

induces cell distension and cell cycle arrest in HeLa cells [25]. The toxin also has cytotoxic effects on epithelial cells [28], keratinocytes, fibroblasts [157], antigen presenting cells [177] and endothelial cells [161].

HdCDT is not necessary for initiation of the early stages of an infection. It is possible that the cytotoxic effect of CDT on certain cells may be responsible for the slow healing seen in untreated chancroid [161]. The apoptosis induced in B- and T-cells by HdCDT indicates that the consequential immunosuppression would delay or decrease immune function and allow bacterial growth and enhance tissue damage [28, 54, 160].

3.2 The structure of CDT

The CDT holotoxin is composed of the subunits CdtA, CdtB and CdtC with the predicted molecular masses of approximately 26, 30 and 20 kDa [27]. All three components are necessary for cytotoxicity of CDT [51]. The *cdt* gene cluster are generally located on the chromosome of CDT-producing bacteria [53].

3.2.1 Structure and function

HdCDT is a ternary complex with three extensive globular protein-protein interfaces between CdtA-CdtB, CdtA-CdtC and CdtB-CdtC. CdtA and CdtC are both lectin-type structures, homologous to the B-chain repeats of ricin. CdtA and CdtC bind at one end of CdtB, and contact each other by the repeats in the ricin B-chain [107]. HdCdtB is the most conserved of the three holotoxin components and shows sequence similarity to proteins of the deoxyribonuclease I (DNase I) family (approximately 12% identity based on a structural alignment) [64] Mammalian DNase I is a Mg^{2+}-dependent endonuclease which functions as a digestive enzyme [80].

Structure and mutagenesis analysis indicate that two primary features of the combined CdtA and CdtC subunits are responsible for the surface binding ability of CDT, namely a patch of aromatic residues found in CdtA and a deep grove formed by the combined structure of CdtA and CdtC. This deep groove, which likely plays an important role in the cellular receptor, may explain the previous observations that combined CdtA and CdtC bind to cell surfaces much

better than either subunit by itself. This would also explain why the toxicity is higher when both CdtA and CdtC are present together (Figure 4) [111].

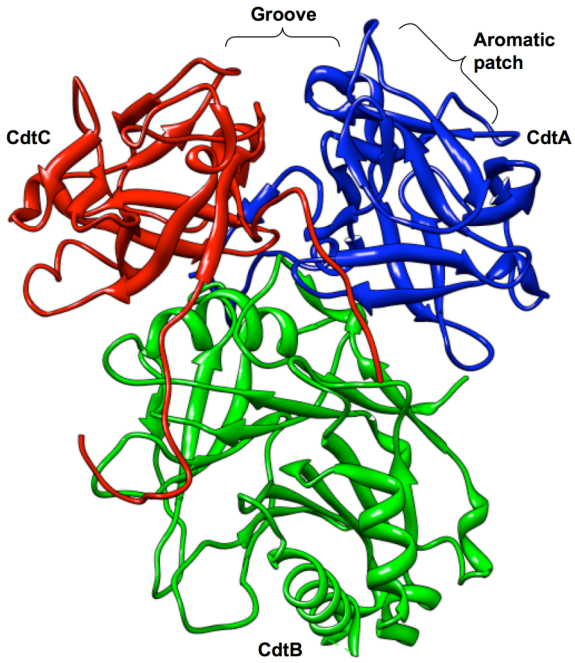

Figure 4. Crystal structure of HdCDT. Adapted from [111].

CDT from other bacteria have also shown DNase I similarities in structure and activity. A significant position-specific amino acid similarity was demonstrated between CdtB-II from *E. coli* and DNase I. Co-incubation of supercoiled plasmid DNA and culture supernatants from CDT-II producing *E. coli* indicated that within 2h, the supercoiled DNA was transformed into linear DNA and by 12h, there was no intact DNA present [42]. Culture supernatants of bacterial strains containing amino acid substitutions in the CdtB protein, corresponding to active sites in DNase I, lacked DNase activity, and did not induce distension or cell cycle arrest in HeLa cells [41, 42]. DNase assays were perfomed with a supercoiled pTRE2 plasmid that was incubated with purified HdCDT in a dose-dependent manner. It demonstrated that indeed a clevage of the supercoiled plasmid into the relaxed and linear form was observed, indicating induction of DNA SSBs and DSBs respectively [92]. Kinetic analysis has shown that also CdtB from *A. actinomycetemcomitans* exhibit DNAse activity *in vitro*.

However, CdtB requires a ten fold higher concentration than DNase I to optimally convert supercoiled to relaxed form of DNA, CdtB is more heat-stable than DNase I and it is not inactivated by actin [38]. These differences are not unexpected since the *cdtB* gene has developed as part of a prokaryotic cytotoxin and would not be expected to be identical to a typical mammalian endonuclease.

3.2.2 The subunits

CdtA is able to bind to target cells, but alone it lacks cytotoxic activity, and the combination of only CdtA and CdtB is without cytotoxicity on HeLa cells [84, 89, 96]. CdtB is the active subunit of the holotoxin and shows DNase I activity *in vitro* and *in vivo.* CdtB is cytotoxic after microinjection or electroporation-facilitated entry into the host cells [41, 83, 96, 178]. In contrast, extracellulary added CdtB is not able to bind to most target cells and therefore is not cytotoxic by itself [53].

It has been demonstrated that the purified recombinant His-tagged *A. actinomycetemcomitans* CdtC alone, delivered to the cytosol, was able to induce cell distension and eventually cell death in Chinese hamster ovary cells (CHO) [96]. However, the effect was not reproduced for CdtC derived from other bacteria. The CdtAC complex is the cell surface binding component and mechanism for the delivery of CdtB of the eukaryotic cells [84, 111]. CdtC has been reported to change the holotoxin environment. The isoelectric point (pI) of the HdCdtC subunit was 1.5 pH units higher in recombinant strains expressing all three subunits than in recombinant strains expressing the CdtC subunit alone [51]. A similar change of pI occurred after mixing the three individual recombinant subunits *in vitro*. Therefore, it was suggested that HdCdtA/CdtB might apply some kind of processing activity on HdCdtC, to make it active [36, 51].

3.3 Cellular internalization of CDT

Different CDTs have the ability to intoxicate cells even after exposure times as short as two to fifteen minutes. It indirectly suggests that CDT binds to cells rapidly and irreversibly, although no specific receptor has been demonstrated [5, 25]. It has been shown that the toxic action of CdtB is dependent on its internalization of the toxin into the target cell [56].

CDT belongs to the AB-type of bacterial protein toxins. The two binding subunits attach to the target regions on the cell membranes; the active subunit enters though the membrane and possesses enzymatic functions [85]. All the subunits are required for its binding to the surface of the target cell and for maximal cytotoxic activity [125, 126, 180]. Studies suggest that the CDT binds to either a fucose-containing glycoprotein [103] or gangliosides [105] on the cell surface.

Cortes-Bratti and colleagues showed that HdCDT enters HeLa cells by endocytosis via clathrin-coated pits. Additionally, the cellular intoxication was completely inhibited under conditions that block the fusion of the endosomal compartment with downstream compartments or after treatment with Brefeldin A (BFA) [26]. Like many AB toxins HdCDT must travel from the plasma membrane to the ER before its active moiety can escape the endomembrane system to reach its target.

Since chromosomal DNA is the target of the CDT action, nuclear translocation of CdtB is necessary to induce DNA damage. Nuclear translocation requires the presence of nuclear localization signal (NLS) sequences. CdtB contains no known conventional NLS. However, it has been demonstrated that CdtB-II from *E. coli* does localize in the nucleus of HeLa cells. Putative bipartite NLS sequences have been located at the C-terminus of the CdtB-II protein. Mutations were introduced into the wild type *cdtB* gene, which affected the NLS sequence without affecting DNase activity. When CdtB-II protein with a NLS mutation was electroporated into HeLa cells, the proteins did not localize in the nucleus and there was no induction of cell cycle arrest [102]. Microinjection experiments in HeLa cells showed that a 76 amino acid stretch in the amino-terminal region in the CdtB from *A. actinomycetemcomitans* forms an unusual NLS. Cells exposed to a holotoxin containing a mutant CdtB did not get intoxicated [113].

3.4 Cellular responses upon CDT intoxication

CDT induces DNA DSBs similar to IR. The DNA damage activates a cascade of pathways including the DNA repair pathway and RhoA activation. The most distinct morphological effect of CDT is the slowly developing cell distension, along with the strongly promoted, actin stress fibers in cells of epithelial origin (Figure 5). The stress fiber promotion has been reported in many different cell types, including CHO cells, HeLa cells and fibroblasts [168]. After several days of toxin exposure, adherent cells begin to round up, show membrane blebbing in some cases, and then diffuse completely. Upon treatment with HdCDT, HEp, HeLa, Don (Chinese hamster lung fibroblasts), and HaCaT (human immortalized keratinocyte) cells undergo irreversible damage resulting in cell enlargement without proliferation and cell cycle arrest followed by cell death [25]. Treating HEp2 cells with CDT caused enlarged cell nuclei

without mitotic spindles, which indicated that cell cycle arrest is at G2 rather than at the M phase [25].

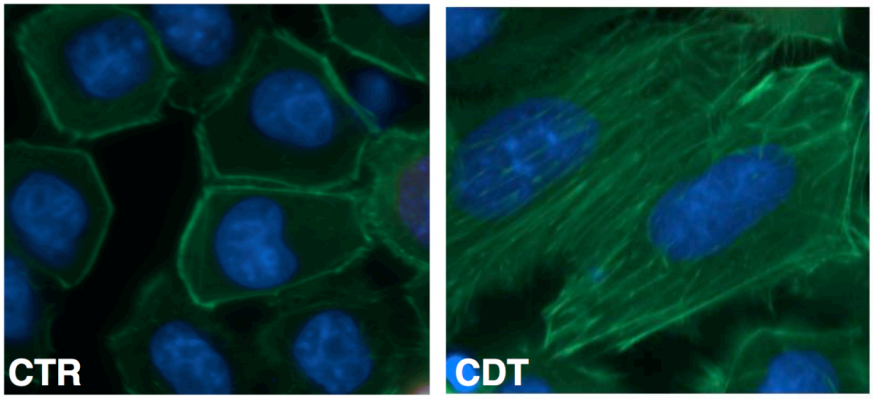

Figure 5. CDT intoxication induces cell distension and promotion of actin stress fibers. Cells intoxicated with CDT for 24h and stained with fluorescein isothiocyanate (FITC)-phalloidin to visualize the actin stress fibers.

3.4.1 CDT causes DNA damage and activates DNA repair pathways

Phosphorylation of two well-known ATM substrates; p53 and Chk2 was demonstrated in intoxicated primary fibroblasts and in HEp2 cells respectively, indicating that the response to CDT is ATM-dependent [28]. The role of ATM in CDT intoxicated cells was further confirmed the delayed p53 phosphorylation and cell cycle arrest in ATM-deficient cells, compared to cells expressing a wild type ATM.

CDT intoxication activates proteins and protein complexes known to coordinate the activation of DNA repair responses such as ATM-dependent phosphorylation of histone H2AX, which localize in nuclear foci, and the relocalization of the Mre11-Rad50-Nbs1 complex at the site of DNA damage (Figure 6) [28, 92]. Therefore, HdCDT similarly to IR induces DNA damage, DNA repair proteins, and cell cycle arrest.

3.4.2 CDT induces cell cycle arrest and cell distension

The effects of HdCDT are cell-specific; B-cells undergo apoptosis, caused by phosphorylation and stabilization of p53 [25]. Normal fibroblasts undergo cell cycle arrest in both G1 and G2 phases of the cell cycle when intoxicated with CDT, thereby hyperphosphorylate Cdk1 and phosphorylate p53, and p21 [11, 25, 28]. p21 inhibits Cdk2 which induces G1 cell cycle arrest. Epithelial cells and normal keratinocytes undergo cell cycle arrest exclusively in the G2 phase.

This was confirmed by the activation of hyperphsophorylation of Cdk1 and prevention of cyclin B translocation into the nucleus (Figure 6) [11, 25, 35]. CDT does not directly inhibit Cdk1 since it can be fully reactivated *in vitro* by CDC25 [35].

The destiny of CDT-intoxicated mammalian cells likely depends on cell types as well on the cell receptor binding specificity of different CdtA/CdtC. In both epithelial cells and fibroblasts the morphological effect of CDT is cell-distending leading within 72h to a 3-to 5-fold increase of the cell size [167]. This is regulated by activation of phosphoinositide 3-kinases (PI3K) and its downstream target mammalian target of rapamycin (mTOR) (Figure 7) [49].

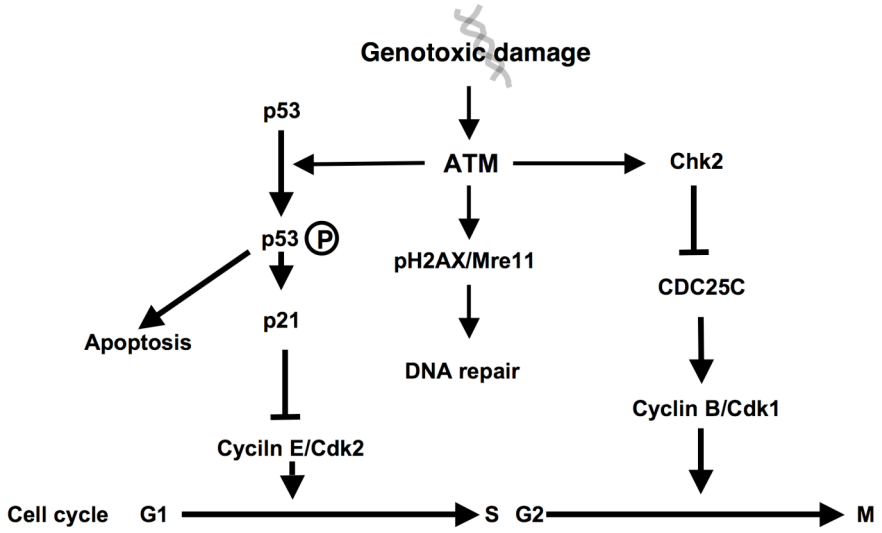

Figure 6. Outline for the mechanisms of cytopathic effects in the nucleus for CDT. DNA damage activates ATM, which activates the DNA repair, and the G1/G2 cell cycle arrest pathway. ATM activation may as well lead to apoptosis.

3.4.3 CDT induces RhoA activation

HdCDT has been found to induce F-actin rearrangement, including pronounced stress fibers development and promotion of membrane ruffling in HEp2 and Don cells [49]. Induction of actin stress fibers is not exclusively a CDT-related effect but was also demonstrated in HEp2 cells and in fibroblasts exposed to IR. This demonstrates that the formation of actin stress fibers is not a strictly toxin induced response, rather a DNA damage response. Promotion of actin stress fibers is dependent on the small GTPase RhoA, since expression of a dominant-negative RhoA prevented the CDT-induced phenotype. Furthermore, biochemical assays demonstrated that RhoA, but not Rac or Cdc42 was activated in a time-dependent manner in intoxicated primary fibroblasts and HeLa cells. RhoA activation in CDT intoxicated cells was dependent on the DNA damage sensor kinase ATM (Figure 7) [49].

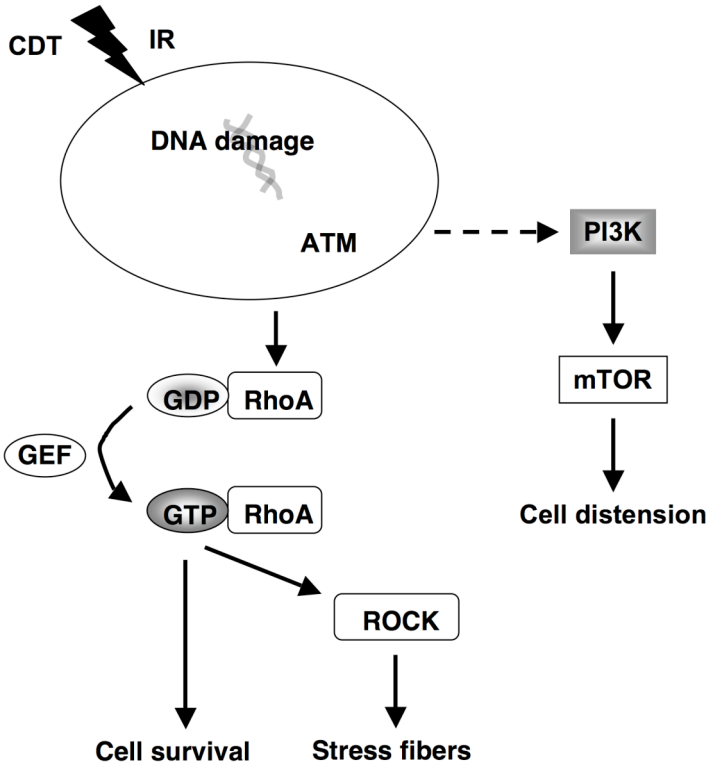

Figure 7. Outline for the mechanisms of cytopathic effects in the cytosol for CDT. CDT intoxication leads to PI3K activation and cell distension. ATM promotes the activation of the RhoA pathway, which induces actin stress fiber formation and enhanced cell survival.

The activation of RhoA was associated with prolonged cell survival. Therefore, it may represent an attempt of intoxicated cells to maintain cell adherence in order to stay alive while some time is given for DNA repair. The ATM-dependent activation of RhoA constitutes a previously unknown type of cell survival response to induction of DNA DSBs.

3.4.4 Cellular responses to CdtB in yeast

In contrast to mammalian cells, yeast cells can not receive CDT from the peripheral medium because of the structure and thickness of the cell wall [74]. Therefore, Hassane and co-workers constructed a plasmid containing each CDT subunit from *Campylobacter jejuni* in *Saccharomyces cerevisiae* under a galactose (GAL) promoter. It was demonstrated that the *C. jejuni* CdtB subunit expressed in *S. cerevisiae* induced irreversible G2/M cell cycle arrest, extensive degradation of chromosomal DNA, and loss of viability. Yeast expressing CdtA or CdtC did not show any damage. The similar effect of the toxin in yeast cells compared to mammalian cells shows that yeast systems can be used to analyze cellular responses to CDT [58].

3.5 CDT in inflammation and cancer

The concept that bacterial infections could lead to cancer was first proposed in the late nineteenth and early twentieth centuries [86]. Several bacteria have been linked to increased risk of cancer, but so far it is only *H. pylori* which has been classified as a human carcinogen by IARC [1]. However, toxins as PMT, CNF and Cif have all been reported to have carcinogenic potential [86]. Since CDT induces DNA DSBs and activates checkpoint responses, it has the potential to function as a biological carcinogen contributing to the initiation, promotion and progression of cancer.

Cancer starts when a cell acquires sufficient mutations to promote cell growth, escape of senescence and inhibition of apoptosis. The cell breakout from its normal status is regulated by extracellular factors and interactions with its surroundings. The carcinogenic processes that arise by accumulation of mutations in crucial genes such as p53, Ras, Rb follow a stepwise sequence. Tumor initiation occurs when mutations free the cells from growth restraints, and the build-up of a small colony of cells takes place. Tumor promotion leads to cells, which are more dysfunctional and have lost more growth controls. As the colony of cells grows it has to obtain its own blood supply by organizing growth of blood vessels into the tumor (angiogenesis). The colony becomes invasive when it acquires the ability to break down local structures. The worst outcome is when cells marsch off from the tumor mass and travel around the body to establish cell colonies (metastases) [86, 101].

Many evidence suggest that chronic inflammation is associated with the initiation of cancer development [45]. Inflammation begins with the production of pro-inflammatory cytokines, such as interleukin-1 (IL-1), IL-8 and TNFα. This attracts infiltration of the tissue mainly by neutrophils, which produce and secrete a number of toxic compounds, which can potentially favour tumor initiation and progression. These include the production of nitric oxide (NO) and reactive oxygen species (ROS), and elevation of levels of cyclooxygenase-2 (COX2). Consecutively, these products result in a complex mixture of effects including direct DNA damage, inhibition of apoptosis, and stimulation of proliferation or inhibition of cell cycle progression, increased angiogenesis and immunosuppression. Each of these outcomes is likely to contribute to the carcinogenic process [29, 86].

3.5.1 CDT and inflammation

Several studies have demonstrated that CDT from different bacteria are involved in inflammation.

The fact that *C. jejuni* enteritis presents with transient watery diarrhoea that progresses to bloody diarrhoea is consistent with the idea that bacterial toxins play a role in this disease. [32]. Sequencing the complete genome of *C. jejuni* has shown that the only toxin genes present in *Campylobacter* are those encoding CDT, no pilus structures are encoded by the chromosome [119]. This made it clear that *C. jejuni*, in contrast to other diarrhoea-causing bacteria, does not express a large number of classical virulence factors. The role of CDT in *C. jejuni* pathogenesis has not been determined yet. However, it might play a role in invasiveness and modulation of the immune response [127]. The CDT-producing bacterium *C. jejuni* has been shown to induce pro-inflammatory activity in NF-κB deficient (3x) mice [47] and promote secretion of IL-8, from human embryo intestinal epithelial (INT407) cells [61, 182]. Therefore, *C. jejuni* CDT might cause intestinal inflammation via its ability to elicit IL-8 secretion from intestinal epithelial cells.

Also the individual CDT subunits from *A. actinomycetemcomitans* have to induce the production of IL-1β, IL-6 and IL-8, but not TNFα, IL-12, or granulocyte-macrophages colony stimulating factor in human peripheral blood mononuclear cells [3]. CDT produced from *A. actinomycetemcomitans* and *H. ducreyi* induce the expression of receptor activator of NF-κB ligand (RANKL) mRNA and RANKL protein [9]. A study performed with IL-$10^{-/-}$ and C57BL/6J (B6) mice, demonstrated that *H. cinaedi* could colonize and cause inflammation of the cecum and colon in the Th1-prediposed IL-$10^{-/-}$ strain, similar to other models using IL-$10^{-/-}$ mice infected with enterohepatic helicobacters [46, 78, 79]. CDT expressed in *H. cinaedi* was not necessary for colonization of the mice, but rather it increases the persistence of the disease, as reported for *C. jejuni* and *H. hepaticus* [147].

3.5.2 CDT and senescence

It has recently been demonstrated that human cells (IMR-90, HeLa) that have been exposed to CDT and survive the acute intoxication phase undergo “premature cellular senescence” [13]. Senescence is a naturally irreversible cell cycle arrest that is known to be induced by DNA damage responses [31]. It is also observed in response to oncogenes and diverse stresses

including genotoxic chemicals [17]. CDT-intoxicated cells demonstrate all the classical senescence criteria, including long-term cell cycle arrest, large flat cellular morphology, positivity for acidic beta-galactosidase, activation of the major suppressor pathways; the p16/RB and p53/p21 cascades, persistent DNA damage signalling, enhanced promyelocytic leukaemia (PML) cellular compartments and induced expression of proinflammatory cytokines, such as IL-6 and IL-8 [13].

3.5.3 CDT as a potentially carcinogenic agent

Genotoxic activity of cyclomodulins, such as that caused by CDT could participate in genetic alterations and act as a promoting factor for the development of cancer. For instance, *H. hepaticus,* which produces CDT, colonizes the liver and causes chronic active hepatitis, which leads to hepatocarcinoma in mice [175]. A recent study of mouse liver carcinogenesis showed that the CDT produced by *H. hepaticus* was not required for induction of chronic hepatitis per se, but it was necessary for the promotion of further development into cancer [52].

It has been shown that survivals of typhoid outbreaks and those who become carriers of *S. typhi*, have 200 fold excess risk of developing hepatobiliary carcinoma compared with people who had acute typhoid and have cleared the infection [18]. Three to five percent of infected individuals who survive become carriers; therefore typhoid carriage could represent a significant cause of this cancer. Since CDT is only found in *S. typhi* and not in other *Salmonella* species, it probably has a specific role in typhoid, and it is appealing to hypothesize that it might be involved in the carcinogenic aspect of *S. typhi* carriage [86].

4. RESULTS AND DISCUSSION

The aim of my PhD thesis was to study several aspects of the CDT biology from the toxin internalization to the characterization of cell survival responses in intoxicated cells.

4.1 CDT internalization through the Golgi apparatus and the endoplasmic reticulum to the nucleus

Little was known about the cellular internalization pathway of CDT. Only one study had been published analyzing the internalization of CDT, and it demonstrated that HdCDT is internalized via clathrin-coated pits and is transported to the Golgi complex [26].

In **paper I** we demonstrate that the binding of the HdCDT on the plasma membrane of sensitive cells is cholesterol dependent, since it was abolished by cholesterol extraction with mβCD. This chemical is a well-known agent, which extracts cholesterol from the plasma membrane and disrupts lipid rafts, which are domains enriched in cholesterol, sphingolipids and glycosylphophatidylinositol (GPI)-anchored proteins [15]. This suggests that CDT may bind to lipid rafts on the cell membrane as many other bacterial toxins do, such as CT and *H. pylori* VacA [139]. Shenker and co-workers found indications that the CdtC subunit contains a cholesterol recognition/interaction amino acid consensus region, called CRAC. Mutation of the CRAC site resulted in decreased binding of the holotoxin to cholesterol containing model membranes as well as to the surface of Jurkat cells. The mutation also inhibited the internalization of CdtB and its toxicity. They suggest that cholesterol can work as a ligand/receptor for CDT [14]. However, there is no convincing evidence of what the receptor for CDT is. Nevertheless, we could for the first time visualize the binding of CDT in CDT-sensitive HeLa cells as compared with CDT-insensitive BalbC3T3 cells by fluorescence microscopy. It indicates that BalbC3T3 cells are resistant to CDT, because they lack the surface receptor.

Is the internalization of CDT necessary to induce cytotoxic effects? Or is it enough to induce DNA damage by transmembrane signalling from the plasma membrane, as suggested by Shenker and colleagues [148]? Indeed, the genotoxic activity of HdCDT was dependent on its

internalization and its DNase activity, since induction of DNA DSBs was prevented in BFA-treated cells and in cells exposed to a catalytically inactive holotoxin.

How is CDT internalized through the cell from the plasma membrane to the nucleus? By constructing a CdtB subunit with a C-terminal-containing sulphation site we could confirm that the toxin is internalized via the Golgi complex. A CdtB-containing sulphation site and three partially overlapping N-linked glycosylation sites, was used to determine that the active subunit is localized in the ER (Figure 8). Data have shown that also CdtC is localized in the Golgi complex (Frisan, unpublished data). This suggests that CdtC may help CdtB to the nuclear compartment. Additional studies have to be perfomed to assess whether CdtC is also retrogradely transported to the ER and if CdtA is following the same pathway.

Further translocation from the ER did not require the ERAD pathway. This is based on that CHO cell clones, which showed an impaired ER to cytosol translocation, were still sensitive to HdCDT. These cell lines have been selected for their resistance to ricin, ETA and CT, which use the ERAD pathway for translocation from the ER to the cytosol. The toxin could also intoxicate a CHO cell line clone that has an enhanced cytosolic degradation. [166]. We could also exclude that HdCDT exits the ER via the Derlin1-ER-cytosol translocation pathway [94, 179], since HeLa cells expressing Derlin-1^{GFP} dominant-negative mutant were still arrested in G2 upon intoxication.

Our results suggest that HdCDT either does not need to transit to the cytosol before entering the nucleus to exert its genotoxic activity, or alternatively its translocation to the cytosol occurs via a different pathway (Figure 8). We hypothesize that the CdtB nuclear translocation requires an uncommon mechanism, which has still not been identified, such as a direct translocation from the ER to the nucleus. In **paper II** we further studied this mechanism. We investigated the biophysical properties of CDT because thermal instability of the toxin active subunit is a common property of toxins that exit the ER by exploiting the mechanism of ERAD. Since HdCDT does not utilize ERAD to exit the ER, we predicted that the biophysical properties of its catalytic subunit would differ from those of ER-translocating toxins.

Fluorescence spectroscopy and far-UV CD were used to examine the thermal stability of HdCdtB. The readings demonstrated that substantial disordering of the HdCdtB tertiary structure did not occur at 37°C. In fact, sample heating to 60°C was required to observe a disordering of the HdCdtB tertiary structure. Analysis of the ellipticity at 220 nm demonstrated

that substantial denaturation of the HdCdtB secondary structure only occurred at temperatures above 50°C. Thus, significant unfolding of HdCdtB did not occur at physiological temperature. To further examine the thermal stability of HdCdtB a protease sensitivity assay was performed. HdCdtB exhibited considerable resistance to proteolysis with thermolysin when incubated at temperatures up to 45°C. Thermolysin is a calcium-dependent metalloprotease that hydrolyzes peptide bonds on the amino side of bulky hydrophobic residues [8].

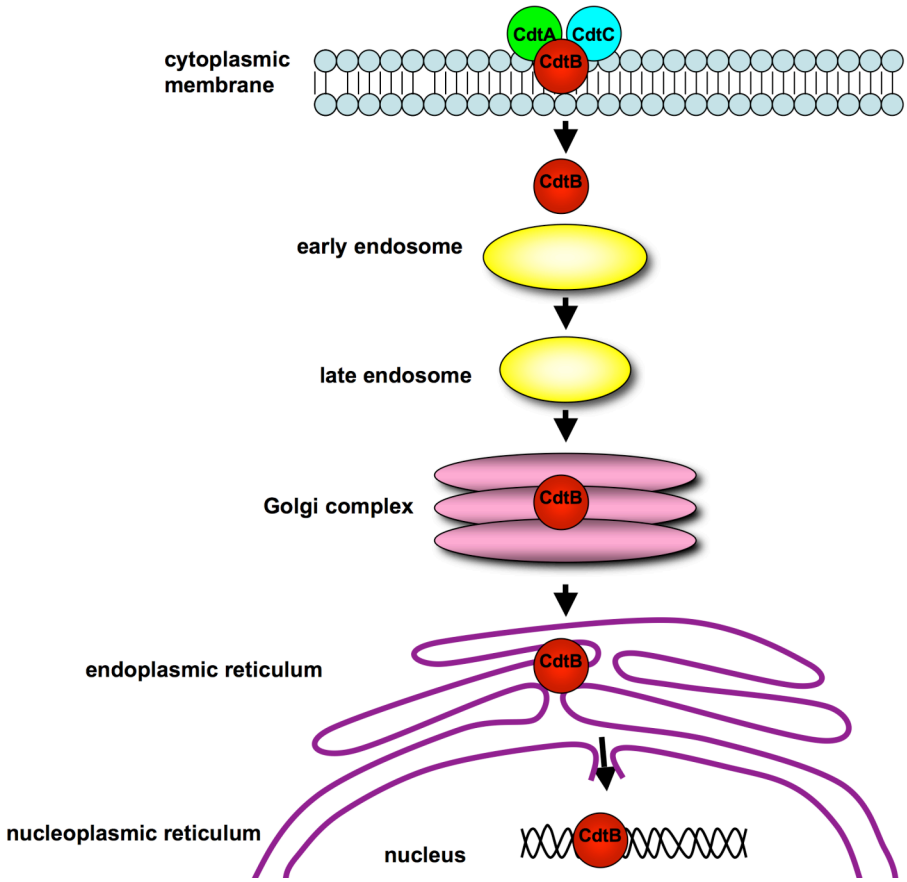

Figure 8. Internalization of HdCDT. CDT binds to the cell as a trimeric holotoxin, CdtB enters the cell through early and late endosomes, is transported to the Golgi, and further retrogradely transported to the ER. From the ER, the toxin is directly transported through the nucleoplasmic reticulum, and enters the nucleus, where it causes DNA damage.

Our data indicate that HdCdtB exhibits remarkable heat stability and thermolysin resistance compared to the active chains of other ER-translocating toxins, such as CT. When testing the sensitivity to degradation by the 20S proteasome, little or no degradation was observed during the 20h time frame of the experiment. Chemical chaperones such as glycerol prevent protein unfolding [131] and block intoxication of ER-translocating toxins, such as ricin and exotoxin A [137]. We showed that the CDT genotoxic activity was not inhibited by glycerol treatment. This result suggests that HdCdtB does not require unfolding before exiting the ER and possibly does not exit the ER at all.

To further examine whether HdCdtB can bypass the cytosol and move directly from the ER to nucleus, we generated a recombinant HdCDT that contains a CVIM-tagged HdCdtB subunit. The C-terminal CVIM farnesylation motif can work as an indicator of protein localization to the cytosol because farnesylation takes place only in the cytosol [22]. The CVIM-tagged HdCdtB could not be found in the cytosolic fraction, suggesting CdtB is not farnesylated in the cytosol. Confocal microscopy detected HdCdtB in a fine, branching intranuclear network that is continuous with the nuclear envelope and the ER, named the nucleoplasmic reticulum [39, 48, 81].

Our results indicate that HdCdtB differs from all other bacterial toxins known to day, and support the hypothesis that CDT might not enter the cytosol before translocation to the nucleus. We could for the first time visualize CdtB in the nucleoplasmic reticulum. This data contribute to a better understanding of the CDT biology and its mode of action, as it demonstrated for the first time how a member of the CDT family is internalized via an intact Golgi, and that it is further retrogradely transported to the ER and probably directly to the nucleus. Furthermore, we showed that DNA damaging activity could only be exerted upon internalization, thereby rejecting previous hypotheses regarding activation of transmembrane signalling pathways.

4.2 Net1 and FEN1 are key proteins in the RhoA-dependent survival pathway

Exposure of adherent cells to DNA damaging agents, such as CDT or IR, activates the small GTPase RhoA, which promotes the formation of actin stress fibers and delays cell death [49] [12, 67]. The signalling intermediates that regulate RhoA activation and promote cell survival were unknown.

GEFs are key activators of small GTPases that regulate the switch between the active GDP-bound and the active GTP-bound form of the GTPase. The majority of the known RhoA-specific GEFs have a cytoplasmic localization. One of the few exceptions is the RhoA-specific GEF encoded by the neuroepithelioma transforming gene 1 (*Net1*) which is normally found in the nucleus of mammalian cells [132]. The regulation of Net1 activity is poorly understood. PAK1 dependent phosphorylation of Net1 inhibits its GEF activity and abolishes Net1-dependent RhoA activation. Activation of RhoA requires translocation of Net1 from the nucleus to the cytoplasm [4, 144]. These data suggested that the activation of Net1 requires both changes in the phosphorylation pattern and shuttling between the nucleus and the cytoplasm. The signals that trigger these events were still unknown. We identified DNA damage as the trigger for Net1 activation.

In **paper III** we demonstrate that DNA damage caused by either CDT or IR induces dephosphorylation of Net1 on its negative regulatory site. Moreover, knock down of endogenous Net1, inhibited the activation of RhoA in response to IR or CDT treatment. We could show that this was not due to a general destruction of the RhoA-dependent response since Net1 knock down did not prevent RhoA activation or the formation of actin stress fibers in cells treated with CNF that constitutively activates RhoA. We further examined whether inhibition of Net1 affected the RhoA-dependent formation of actin stress fibers in cells intoxicated with CDT. Without a doubt, there was a significant decrease in the intensity of fluorescence induced by intoxication in the Net1 ribonucleic acid interference (RNAi) treated cells as compared to controls.

Activation of RhoA also promotes the survival of cells exposed to CDT [49]. In order to investigate whether Net1 is required for this RhoA mediated response, Net1 expression was inhibited by RNAi prior to intoxication, and cell death was observed. Down regulation of Net1

resulted in a 4-5-fold increase in the number of cells presenting chromatin condensation 48h after intoxication. The induction of cell death was also confirmed by cleavage of Poly (ADP-ribose) polymerase (PARP) and activation of the pro-apoptotic protein Bax. These results indicate that Net1 is an essential component in the survival response to DNA damage.

DNA damage has been shown to induce activation of mitogen-activated protein kinase p38 (p38 MAPK) [37]. Therefore, we tested whether exposure to IR or CDT stimulates p38 MAPK activity, and whether this is necessary for protection of cell death. Both CDT and IR induced the activation of p38 MAPK within 3h. Inhibition of p38 MAPK with specific p38 MAPK inhibitors increased by 2-4 folds the number of chromatin condensations 48h after treatment. These results indicate that activation of p38 MAPK protects the cells from death induced by DNA damage. Inhibition of either Net1 or RhoA by RNAi resulted in a potent inhibition of the p38 MAPK activation in treated cells, demonstrating that Net1 and RhoA are upstream signals in the p38 MAPK activation cascade in response to DNA damage. Moreover, the phosphorylation of MAPK activated protein kinase2 (MK2), a direct substrate of p38 MAPK, following irradiation was abolished by knock down of either Net1 or RhoA, indicating that these proteins are required for MK2 activation. Inhibition of ROCKI/ROCKII did not impair the activation of p38 MAPK, demonstrating that ROCKI/ROCKII were not essential for signalling to this MAPK.

These results demonstrate for the first time that genotoxic stress is a trigger for Net1 activation and they contribute to the characterization of a novel survival pathway in response to DNA damage, which involves Net1 and its downstream targets RhoA and p38 MAPK (Figure 10). Our finding that CDT-induced DNA damage is accompanied by activation of survival signals suggests that chronic infection with CDT-producing bacteria may promote genomic instability and favour malignant transformation. The association between bacterial infections and cancer is poorly understood. The only bacterium classified as human carcinogen is *H. pylori*, but a possible involvement in oncogenesis has been suggested for other bacteria, such as for example the Gram-negative, CDT-producing bacterium *S. typhi* [86]. The role of CDT in cancer could be its stimulation of prolonged survival in target cells, instead of inducing apoptosis when DNA is damaged. The prolonged cell survival in potential tumor cells may help the cells to accumulate mutations in crucial genes and progress toward a malignant phenotype.

In **paper IV** we identified more players of the RhoA-dependent survival pathway by screening a yeast deletion library for genes that encode proteins, which promote survival of CdtB-

expressing yeast cells. A total of 4492 yeast strains harboring deletions in nonessential genes were transformed with a CdtB-expression plasmid under a galactose promoter and subsequently screened for delayed growth, which is indicative of defective survival signals. The screen was performed by using *S. cerevisiae* direct transfomation in a 96-well format [142]. All transformed yeast strains where spotted out on selective 2% glucose (CDT off) or on 2% galactose (CDT on) plates for 48h. The strains that showed any signs of CdtB-sensitivity were subjected to dilution series (1:5) on plates containing 2% galactose for CdtB expression or on 2% glucose for control (Figure 9). Mutants that did not grow after the third dilution step out of six were classified as CdtB-hypersensitive strains.

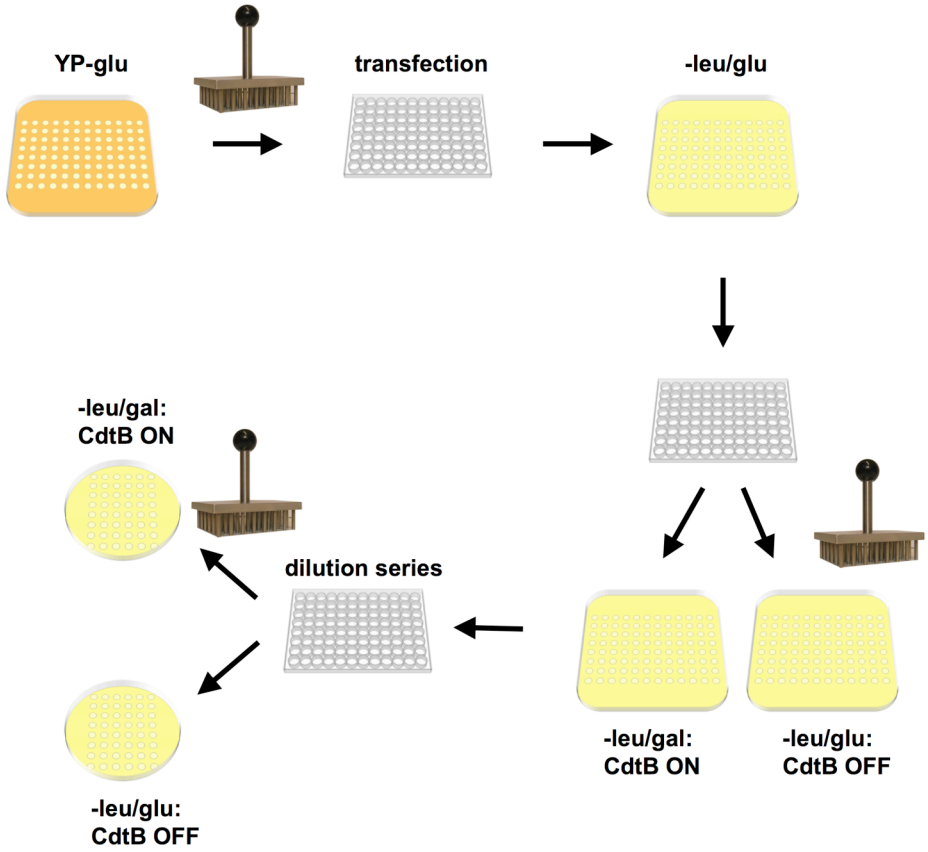

Figure 9. Schematic outline of the yeast screen in a 96-well format using a 48-pin replicator. Wild type deletion strains were transfected in 96-well plates and transferred to selevtive -leucine/glucose (-leu/glu) plates. All transformants were suspended in water and moved to -leucine/galactose (-leu/gal) (CdtB on) or on -leu/glu (CdtB off) plates. All strains that show any indication of CdtB-sensitivity were transferred to 96-well plates for dilution series of 1:5 and replated on -leu/gal (CdtB on) or on -leu/glu (CdtB off) plates.

The screening identified 78 deletion mutants that are CdtB-hypersensitive and further system biology studies demonstrated that 20 of the human orthologs are involved in the actin cytoskeleton regulation. Based on protein-protein interaction networks three genes (the tumor susceptibility gene 101 (TSG101), flap endonuclease 1 (FEN1) and vinculin (VCL)) were selected for further studies in mammalian cells. Knock down assay with specific RNAi

demonstrated that all three genes significatlly reduced actin stress fiber formation in DNA damage cells compared with control cells.

Are these genes involved in the novel RhoA cell survival pathway? Indeed, knock down of FEN1 and VCL completely prevented RhoA activation upon CDT intoxication, whereas TSG101 did not. Cell death was assessed 72h after intoxication by common detection methods, such as monitoring chromatin condensation and detection of the activated Bax. Approximately a 11-fold increase in apoptotic cells was detected in intoxicated cells where FEN1 or VCL have been knocked down, compared with a 3-fold increase of apoptotic cells in control cells. Since both FEN1 and VCL were essential for the RhoA activation, it is conceivable that these genes are also important for p38 MAPK phosphorylation. Downregulation of either FEN1 or VCL showed indeed decrease of p38 MAPK phosphorylation.

In summary; TSG101, FEN1 and VCL are important to induce actin stress fibers. FEN1 and VCL also regulate the activation of RhoA GTPase and its downstream molecule p38 MAPK, resulting in prolonged cell survival (Figure 10).

The finding that FEN1 is one of the key molecules in the RhoA survival pathway is novel and has not previosly been reported. FEN1 has multifunctional endonuclease acitivity. It is involved in RNA primer removal and long-patch base excision repair [7, 93, 95], but also has a 5'-3' exonuclease (EXO), as well as a gap endonulease (GEN) activity [95, 120]. How FEN1 activates the RhoA GTPase remains unknown. It is possible that FEN1 regulates the RhoA specific GEF Net1, which is located in the nucleus, via activation of a specfic phosphatase or inhibition of a kinase. VCL is not present in yeast, but was selected because it has been reported to interact with FEN1 and for its role in focal adhesion complexes and integrin signaling to the actin cytoskeleton proteins [33]. It is not understood whether FEN1 and VCL act consecutively or if they activate different signaling pathways that act on RhoA.

Inhibition of TSG101, did not have any effect on the cell survival nor on the activation of RhoA GTPase or p38 MAPK. TSG101 had a major effect on the formation of stress fibers, demonstrating that TSG101 is important in the regulation of stress fiber formation. TSG101 belongs to one of the four endosomal sorting complex required for transport (ESCRT), the ESCRT I, which controls formation of multivesicular bodies [164]. Several components of the ESCRT complexes or ESCRT-binding proteins were found in the yeast gene screen that promote cell survival in response to CdtB. It has been reported that other members of the

ESCRT proteins induce regulation of the actin cytoskeleton. Our novel data suggest that a number of proteins, which regulate protein and vesicular trafficking may play a role in the regulation of cell adhesion and cell survival in normal or stress conditions, such as DNA damage. The ESCRT protein may function as a scaffold for the compartmentalization of specific signalling complexes. One of these proteins is TSG101,which has already been shown to interact with ROCKI [108, 164]. This suggest that TSG101 activates a part of the RhoA signaling pathway that leads to stress fiber formation, but is not involved the activation of the MAPK pathway or the cell survival pathway.

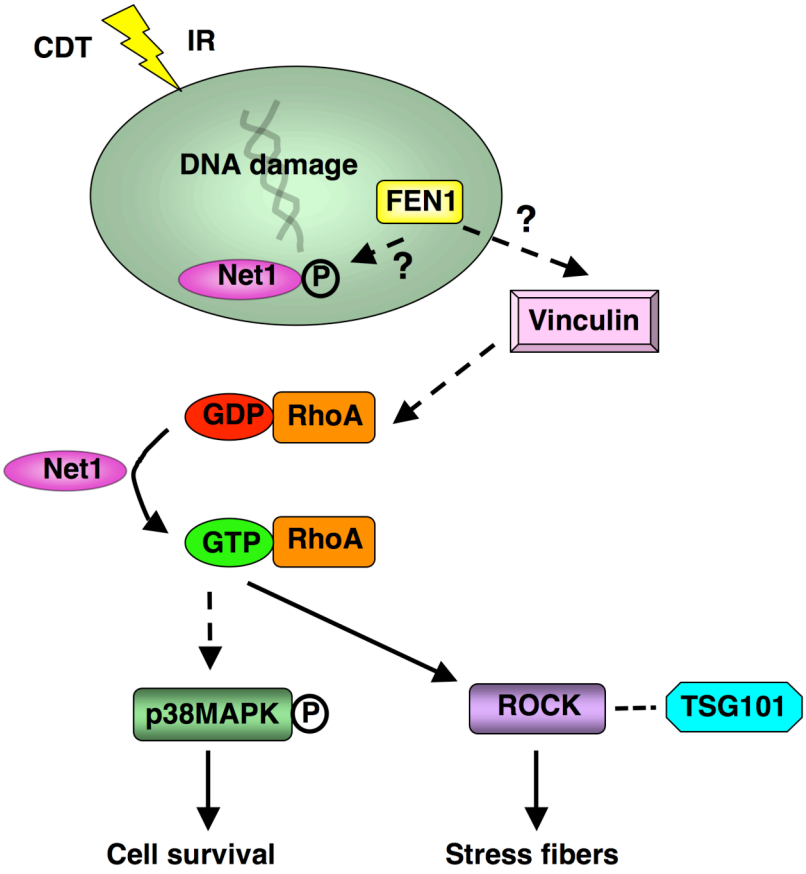

Figure 10. Chart of the Net1/FEN1/VCL regulated cell survival signals upon exposure to DNA damaging agents. Upon DNA damage Net1 is dephosphorylated and transported out from the nucleus to the cytosol. There it activates RhoA, promotes actin stress fibers and increases cell survival. FEN1, located in the nucleus and VCL located in the cytosol are also involved in the regulation of RhoA activation. TSG101 is involved in the induction of actin stress fibers.

This study identified three novel actors FEN1, VCL and TSG101 as important effectors regulating RhoA activation, actin stress fibers, p38 phosphorylation, and ultimately cell survival. This highlights a complex and still poorly characterized cross-talk between DNA damage and the actin cytoskeleton. The cytoskeleton, focal adhesions and integrin activation are important for the cells to maintain the connection with the extracellular matrix (ECM) and

enhanced resistance to IR and cytotoxic drugs [60]. The connection is crucial for the cell survival. If the cell looses the connection to the matrix, it can undergo anoikis, a form of apoptosis induced by detachment from the ECM.

4.3 Myc: an important player in the DNA damage induced ATM activation

In **paper V** we investigate the role of Myc in the DNA damage response. The Myc protein is known to control cellular functions such as differentiation, proliferation, and apoptosis. In response to genotoxic agents, cells expressing Myc undergo apoptosis [124]. However, the Myc-regulated effectors acting upstream of the mitochondrial apoptotic pathway were still unknown. In this study, we demonstrate that expression of Myc is essential to activate the ATM-dependent DNA damage checkpoint responses in cells exposed to IR or CDT and plays an important role in the regulation of the cellular response to genotoxic stress.

Myc positive TGR-1 cells showed G2 cell cycle arrest after 12h compared to 24h to 48h in *myc* null rat cell line HO15.19. Phosphorylation of ATM occurs after 30 minutes in Myc positive cells, whereas it was not detectable in HO15.19 cells. By using an antibody specific for phosphorylated ATM/ATR substrates, we detect two unknown phospho-proteins in the TGR-1 cell but not in the *myc* null rat cells. Phosphorylation of the ATM and its downstream effectors, such as histone H2AX, were delayed in the HO15.19, compared to the Myc positive TGR-1 and HOmyc3 cells. Nuclear foci formation of the Nijmegen breakage syndrome (Nbs)1 protein, essential for efficient ATM activation, was also inhibited in absence of Myc. The data indicate that Myc exerts an additional level of control, apart from gene regulation in the DNA damage-induced activation of up-regulation of Nbs1.

Phosphorylation of the ATR substrate Chk1 was not affected in the HO15.19 cells in response to irradiation. Accordingly, the cellular response to UV irradiation, known to activate an ATR-dependent checkpoint, was similar in all the cell lines, independently of the Myc status (Figure 11). Therefore, our results suggest that Myc regulates the activation of ATM but not the ATR-dependent checkpoint pathway induced by radiation. The DNA damage response and delayed cell death in the *myc* null rat cell line HO15.19 in response to CDT intoxiation may promote or enhance genomic instability and favor carcinogenesis.

Over-expression of Myc can induce DNA damage; thereby contribute to genome instability and chromosomal aberrations. In contrast, expression of physiological levels of Myc is important for the proper activation of DNA damage checkpoint responses. This suggests that Myc may have a tumor-suppressor-like function, by contributing to the DNA repair pathway.

These data demonstrate that Myc is required for the rapid activation and nuclear formation of Nbs1. This activates the ATM and consequent phosphorylation of downstream effectors. If the DNA damage cannot be repaired, the activation of ATM will probably result in mitochondria-dependent apoptosis. Myc may play an important role for maintaining genome stability when expressed at levels observed in non-malignant cells. Myc is a very complex molecule which is involved in many processes in the cell. This study has helped to clarify one more aspect of the complicated regulation in the cell that Myc is controlling.

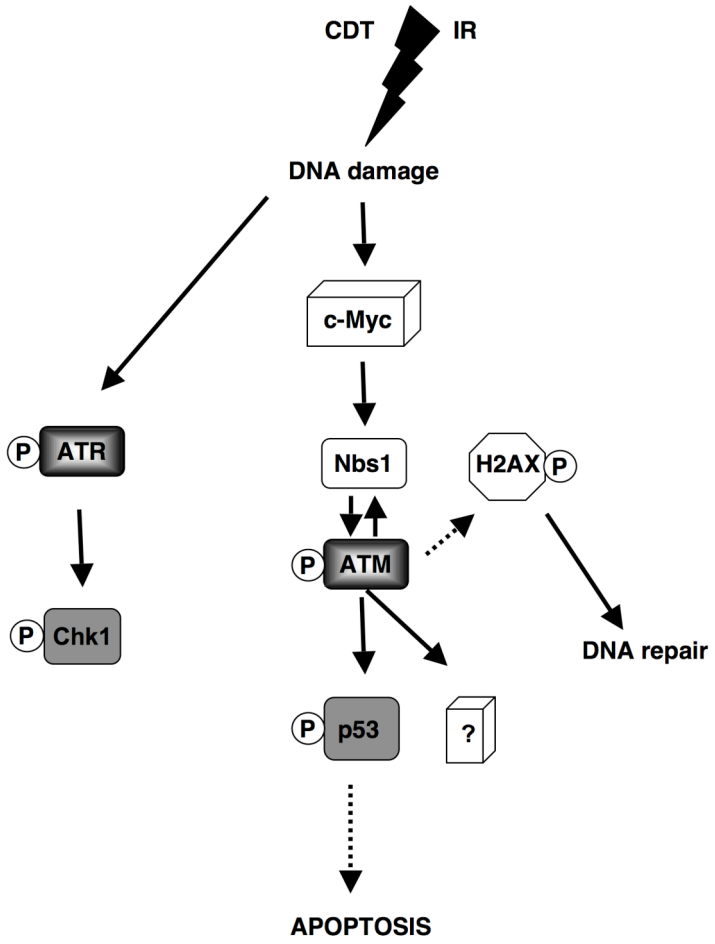

Figure 11. Sketch of the MYC-dependent response to IR or CDT intoxication. Upon DNA damage Myc is activated and regulates the activation of ATM and Nbs1, which leads cell cycle arrest apoptosis. The ATR pathway is not dependent on the activation of Myc.

As discussed in previously in this thesis, chronic infection with CDT-producing bacteria may be associated with increased risk of cancer. How the bacterial infection can contribute to carcinogenesis is still not fully characterized. The loss of Myc and the delayed cell death in chronic infection with CDT-producing bacteria may promote or enhance genomic instability, and favor tumor initiation and/or promotion. This suggests that CDT does not alone cause carcinogenesis but it may require additional factors, such as a mutated or dysfunctional tumor-

suppressor gene. If cells with a non proper functional MYC gene are infected with CDT-producing bacteria, the action of CDT may contribute to carcinogenesis. Cell survival is important for a cell to have the possibility to repair DNA damage, but this may as well lead to accumulation of mutations, which will increased the risk of cancer.

5. CONCLUDING REMARKS

The work described in this thesis has provided new insight on the mechanisms of bacterial genotoxins and their possible role in carcinogenesis. This knowledge has set the platform for further explorations of the biology of CDT and the cellular responses to CDT. Furthermore, it has highlighted many new aspects of CDT and DNA damaging cellular response.

CDT is following the same internalization pathways as many other bacterial toxins for example CT and ETA. In contrast to these other protein toxins, CDT is so far the only toxin that does not exit to the cytosol. It is suggested that the toxin is directly translocated to the nucleus, through a tightly connected ER-nucleus network (**paper I and II**). CDT is heat-stable and not degraded in physiological temperatures by the proteasome (**paper II**). This raises several questions about the complexity of the nuclear translocation of CDTs, emphasizing once more the importance of bacterial toxins as tools for characterization of cellular processes.

The first molecular characterization of a RhoA-dependent survival pathway triggered by DNA damage induced by CDT intoxication or IR was described. The RhoA specific GEF Net1 was identified as the key regulator of RhoA activation upon DNA damage. p38 MAPK was characterized as an important player for cell survival downstream of RhoA **(paper III**). Additional studies of the novel survival pathway were performed with help of a wide genome screen in yeast. The study revealed that both FEN1 and VCL are regulators of RhoA activation and important for cell survival, while TSG101 regulates actin stress fiber formation (**paper IV**). Moreover, we have indications that FEN1 regulates the activation of Net1 since it is demonstrated that downregulation of FEN1 expression by RNAi inhibited dephosphorylation of Net1. Further dissections of this pathway will provide new tools to elucidate the mechanisms of bacterial-induced carcinogenesis, and may also help to design specific inhibitors that can act synergistically with conventional chemotherapy.

A more upstream key player in CDT-induced DNA damage response is Myc, since it regulates the ATM-dependent checkpoint responses to damage (**paper V**). Myc is a complex molecule involved in many different pathways [124]. Further analysis of this phenomenon would be to characterize the two unknown ATM substrates, which are phosphorylated only in the presences of Myc and upon IR treatment (**paper V**, Figure 3).

Studies have shown that CDT beyond any uncertainties acts on the DNA, and has similarities with DNase I [111] Remarkably, DNase I has a significantly more potent DNase activity than CdtB. In contrast, CdtB can enter cells and translocate to the nucleus. How the translocation to the nucleus is carried out is still unclear. It is clear that CDT just like many other bacterial toxins, such a CT uses the endosomal compartments and the retrograde transport to bring itself across the cell to its target destination.

Shenker and colleagues have questioned whether the relevant activity of the CDT family is a DNase-like activity. They suggest that the cytotoxic effect might be triggered upon toxin-induced transmembrane signalling from the cell surface [148, 168]. Shenker and co-workers recently demonstrated that the CdtB subunit has phosphatidylinositol (PI)-3,4,5-triphosphate phosphatase (PI-3,4,5-P) activity in Jurkat cells. Analysis indicated that CdtB hydrolyzes PI-3,4,5-P to PI-3,4-P_2 and therefore functions similar to phsophatidylinositol 5-phosphatases such as the tumor suppressor phosphatase, PTEN and SHIP1. Mutations analysis showed that CDT toxicity correlates with phosphatase activity, and additionally, lymphocytes treated with toxin showed reduced PI-3,4,5-P levels [150]. However, several studies including those presented in this thesis demonstrate beyond any doubt that at least the active CdtB subunit has to be endocytosed and undergo intracellular transport to the nucleus before it can damage the cells and the cell damage is caused by its DNase activity.

The new data presented in this thesis concerning the responses to DNA damage induced by two known DNA damaging agents (CDT and IR) contribute to disclose the complex cellular response to DNA damage. The identification of the novel cell survival pathway, which allows cells to survive in the presence of agents that cause genomic instability, is crucial in the development of more selective therapeutic inhibitors to treat cancer.

Senescence in cells has proven to have a tumor-suppressive fuction and may be the outcome of particularly severe DNA damage. The cells can also undergo apoptosis. It is still unclear what decides the choice between apoptosis and senescence, but the decision may include cell type, intensity, duration and type of damage [31]. The senescence induced by CDT-intoxicated cells may be a dose-dependent response. If cells are intoxicated with higher amount of CDT it causes rapidly DNA damage, resulting in senescence or cell death. If the cells are intoxicated with a lower dose of CDT it may not cause a large extent of DNA damage but instead induce genomic instability. The mutations may force the cell through the cell cycle, and eventually progress into a more malignant phenotype can occur.

The inhibition of cell proliferation and the cell cycle arrest caused by CDTs indicate that CDTs may be virulence factors *in vivo*. While not clearly demonstrated, it is probable that the CDTs produced by *A. actinomycetemcomitans* and *H. ducreyi* are disease determinants since these CDTs induce cell destruction in a number of different cell types and induce apoptosis in immune cells. The antiproliferative and immunosuppressive activities of these CDTs may be responsible for the slow healing and chronic nature of untreated aggressive periodontitis and chancroid diseases.

Is CDT a carcinogenic agent? It has not been established yet that CDT itself can cause cancer, but given that CDT has the abilities to cause DNA damage, mutations and genetic instability resulting in cell cycle arrest, apoptosis and slow healing of ulcers, it could very well be a carcinogen [13]. CDT-producing bacteria have been demonstrated to induce inflammation. It is known that chronic inflammations can initiate tumor progression. Moreover, data have shown that long time low-dose intoxication with HdCDT causes chromosomal aberrations, which are indications for genomic instability, and associated with different types of cancers (Guerra, unpublished data) [13, 128]. As incorrectly repaired DNA can ultimately result in carcinogenesis, insight into how CDT intoxicated cells can survive, may help in designing strategies to prevent tumor development in people that are chronically infected with CDT-producing bacteria.

6. FUTURE PERSPECTIVES

This thesis has contributed to many major findings concerning CDT and its mode of action. However, many questions still need to be answered. Still the receptor is not identified and how CDT translocates from the ER to the nucleus also remains unknown. Even though the cell survival pathways have been to some extent characterized in this thesis, there are still plenty that remain to be clarified.

The toxin is produced by a number of enteric bacteria, however the role of CDT as enteric disease inducer remains unclear. It does not appear that CDT plays a direct role in the induction of diarrhoea; this family of toxins may be responsible for some of the prolonged symptoms seen in diarrhoeal diseases.

Whether the *in vitro* finding of CDTs obtained in cultured cells are possible to be translated *in vivo* still need to be fully assessed. For this purpose a good animal model should to the established, particularly for the human specific CDT-producing bacteria.

Evidence suggests that CDT is a virulence factor that benefits bacterial survival and enhances microbial pathogenicity. CDT is essential for persistent colonization of the host, for example by CDT-producing *H. hepaticus* or *C. jejuni* in mice. It could be of interest to determine whether anti-CDT vaccines generated with catalytic or receptor binding sites-mutated CDT can prevent or clear infection of a human pathogen such as *H. ducreyi*.

Another aspect of the DNA damage and cell killing abilities of CDT is the use of CDT as an immunotoxin. Some bacterial toxins, such as Diphtheria toxin and ETA are in phase I/II in clinical trials for use as immunotoxins. Immunotoxins are bacterial toxins, which are connected with a specific cell binding ligand. The immunotoxin is designed bind to specific cells such as tumor cells, and destroy them [68, 76, 77, 121]. In particular, it has been suggested that CDT could represent a novel immunotoxin for lymphocytes, since these cells are five fold more sensitive to CDT than other cells [150]. Some initial attempts have already been made with CDT, but unfortunately none of these have been particularly successful. It is an assignment for the future.

Further *in vitro* and *in vivo* studies regarding CDT will not only increase the understanding of the virulence properties of CDT but could also provide prophylactic and therapeutic strategies to combat infectious diseases such as diarrhoea, inflammatory bowel disease, fever and chancroid. The characterization of the mode of action of bacterial toxins has led to many developments in the basic and applied medical science. To further investigate the relationship between the DNA damage and the actin cytoskeleton is of great importance since it is a survival pathway, and may be important for bacterial-induced carcinogenesis.

7. ACKNOWLEDGEMENTS

I would like to thank all the people that in any way helped me with this thesis. Some of you I would like especially thank.

First of all I would like to thank my supervisor **Ass**. **Prof**. **Teresa Frisan**, for taking me as her first PhD student and making it an unforgettable adventure. You let me be independent, trying my own ideas and introduced me to so many interesting persons. Thank you for all the interesting and productive discussions and the support during these years. You have made me grow as a person. With your uplifting spirit you make anyone happy on a boring grey Monday morning.

Prof. **em Monica Thelestam**, my co-supervisor, for all the help and support and creative discussion, especially when Teresa was not available.

All co-workers, without you this thesis would not have been made.

I would like to thank all the people at MTC where I did my first years of my PhD studies**. Patricia**, **Juan Carlos**, **Jan**, **Agneta**, **Caroline**, **Henrik**. Everyone in **Prof**. **Agenta Richter-Dahlfors group**: **Margret**, **Keira**, **Jorrit**, **Kalle**, **Lisa**, **Camilla**, **Lisa**, **Peter**, **Sandra**, for all the fun time when we shared lab together. Off course every one else at MTC, especially, **Anna B**, **Meit**, **Jenny A**, **Ami mfl**, for some great lunches at the round table.

To all past and present members of the **Frisan group**:
Ilse, for being a great student and making our work more organized with all the excel files. **Riccardo**, all the fun time in and outside the lab, with video-making, concerts, pub- and disco nights, help with figure 4 and great lab work of course. **Eugenie**, for a great lab and office mate, and teach me the French way of living with late dinners, good wines and great parties. **Javier**, for all extra help, support and good advises. **Ximena and,** for a great lab and office mate, Spanish lessons and teaching me what Central America really is all about. **Nasli**, **Sergey**, **Fabiola** and **Melissa** for making the lab a little bit more special and multicultural.

To all past and present the people in the lab of **Masucci**:
Prof. **Maria G. Masucci**, for the support, good advises, discussions and made me feel like a group member. **Bettina**, for all the great times in and outside the lab. The lunches, fikas, making the movie, our trips and long talks about everything in life etc. **Pino**, for being the happy songbird in the mornings. **Rama**, for being a great travel companion in Portugal and nice chats about life and science. **Bin Zhao**, **Christian**, **Claudia**, **Debora**, **Diego**, **Dimath**, **Gerco**, **Gerry**, **Husam**, **Julia**, **Kristina**, **Mia**, **Micke**, **Nicolay**, **Nina**, **Nouman**, **Omid**, **Sandra**, **Sebastian**, **Siamak**, **Simone**, **Stefan**, **Stefano**, **Susan**. **Thorsten**, **Ulrika**, **Victoria**, for making the lab a great place to go to every day and sharing with me all your different cultures, habits and stories**. Helena**, for keeping the lab in order, all lunches, tea-times, sushi-times and chats talking about everything. **Linda and Yvonne**, for all the fun lunches, and help to organize everything from plane tickets to toothpicks.

Thanks to everyone else in CMB that have help me or made my PhD studies an unforgettable time.

I would like to thank everyone at the University of Würzburg, **Prof. Werner Goebel, Dani and Sabrina**. Everyone at University of Stuttgart, **Prof. Dieter Wolf**, **Frederik**, **Sonja**, **Ann**

and **Oliver**, for taking so good care of me during my time in Germany and sharing German cultures with me, including October and beer festivals.

Great thanks to my friends, for long-lasting friendship and shared laughters and worries throughout the years**. Lindvi**, **Linda**, **Johanna**, **Helena**, **Tara**, **Lisen**, **Bettan**, **Helene**, **Angelica**, **Anna**, **Elisa**, **Melania**

Till sist vill jag tacka min familj som alltid finns där och hjälper mig på alla sätt**. Mamma**, **Pappa**, **Sami**, **Ingela**. **Elias**, **Julia**. Tack till all min släkt runtom i Sverige, Finland och Italien.

Erik, for love and happiness…

The work in this thesis was performed in the Departments of Microbiology, Tumor and Cell biology and Cell and Molecular Biology at Karolinska Institute. The Swedish Cancer Society, Swedish Research Council, the Åke Wiberg fundation, the Robert Lundberg memorial foundation, the European Community Integrated Project on Infection and Cancer (INCA) and Karolinska Institute, founded the work.

8. REFERENCES

[1] Schistosomes, liver flukes and Helicobacter pylori. **IARC Working Group on the Evaluation of Carcinogenic Risks to Humans**. Lyon, 7-14 June 1994, IARC Monogr Eval Carcinog Risks Hum 61 (1994) 1-241.

[2] **Abraham, R.T**., PI 3-kinase related kinases: 'big' players in stress-induced signaling pathways, DNA Repair (Amst) 3 (2004) 883-887.

[3] **Akifusa, S., Poole, S., Lewthwaite, J., Henderson, B., Nair, S.P**., Recombinant Actinobacillus actinomycetemcomitans cytolethal distending toxin proteins are required to interact to inhibit human cell cycle progression and to stimulate human leukocyte cytokine synthesis, Infect Immun 69 (2001) 5925-5930.

[4] **Alberts, A.S., Qin, H., Carr, H.S., Frost, J.A**., PAK1 negatively regulates the activity of the Rho exchange factor NET1, J Biol Chem 280 (2005) 12152-12161.

[5] **Aragon, V., Chao, K., Dreyfus, L.A**., Effect of cytolethal distending toxin on F-actin assembly and cell division in chinese hamster ovary cells, Infection and Immunity 65 (1997) 3774-3780.

[6] **Bakkenist, C.J., Kastan, M.B**., DNA damage activates ATM through intermolecular autophosphorylation and dimer dissociation, Nature 421 (2003) 499-506.

[7] **Bambara, R.A., Murante, R.S., Henricksen, L.A**., Enzymes and reactions at the eukaryotic DNA replication fork, J Biol Chem 272 (1997) 4647-4650.

[8] **Bark, S.J., Muster, N., Yates, J.R., 3rd, Siuzdak, G**., High-temperature protein mass mapping using a thermophilic protease, J Am Chem Soc 123 (2001) 1774-1775.

[9] **Belibasakis, G.N., Johansson, A., Wang, Y., Chen, C., Kalfas, S., Lerner, U.H**., The cytolethal distending toxin induces receptor activator of NF-kappaB ligand expression in human gingival fibroblasts and periodontal ligament cells, Infect Immun 73 (2005) 342-351.

[10] **Berlanda Scorza, F., Doro, F., Rodriguez-Ortega, M.J., Stella, M., Liberatori, S., Taddei, A.R., Serino, L., Gomes Moriel, D., Nesta, B., Fontana, M.R., Spagnuolo, A., Pizza, M., Norais, N., Grandi, G**., Proteomics characterization of outer membrane vesicles from the extraintestinal pathogenic Escherichia coli DeltatolR IHE3034 mutant, Mol Cell Proteomics 7 (2008) 473-485.

[11] **Bielaszewska, M., Fell, M., Greune, L., Prager, R., Fruth, A., Tschape, H., Schmidt, M.A., Karch, H**., Characterization of cytolethal distending toxin genes and expression in shiga toxin-producing Escherichia coli strains of non-O157 serogroups, Infect Immun 72 (2004) 1812-1816.

[12] **Bishop, A.L., Hall, A**., Rho GTPases and their effector proteins, Biochem J 348 Pt 2 (2000) 241-255.

[13] **Blazkova, H., Krejcikova, K., Moudry, P., Frisan, T., Hodny, Z., Bartek, J**., Bacterial Intoxication Evokes Cellular Senescence with Persistent DNA Damage and Cytokine Signaling, J Cell Mol Med (2009).

[14] **Boesze-Battaglia, K., Brown, A., Walker, L., Besack, D., Zekavat, A., Wrenn, S., Krummenacher, C., Shenker, B.J**., Cytolethal distending toxin-induced cell cycle arrest of lymphocytes is dependent upon recognition and binding to cholesterol, J Biol Chem 284 (2009) 10650-10658.

[15] **Brown, D.A., London, E**., Functions of lipid rafts in biological membranes, Annu Rev Cell Dev Biol 14 (1998) 111-136.

[16] **Burridge, K., Wennerberg, K**., Rho and Rac take center stage, Cell 116 (2004) 167-179.

[17] **Campisi, J., d'Adda di Fagagna, F**., Cellular senescence: when bad things happen to good cells, Nat Rev Mol Cell Biol 8 (2007) 729-740.

[18] **Caygill, C.P., Braddick, M., Hill, M.J., Knowles, R.L., Sharp, J.C**., The association between typhoid carriage, typhoid infection and subsequent cancer at a number of sites, Eur J Cancer Prev 4 (1995) 187-193.

[19] **Censini, S., Lange, C., Xiang, Z., Crabtree, J.E., Ghiara, P., Borodovsky, M., Rappuoli, R., Covacci, A**., cag, a pathogenicity island of Helicobacter pylori, encodes type I-specific and disease-associated virulence factors, Proc Natl Acad Sci U S A 93 (1996) 14648-14653.

[20] **Charpentier, X., Oswald, E**., Identification of the secretion and translocation domain of the enteropathogenic and enterohemorrhagic Escherichia coli effector Cif, using TEM-1 beta-lactamase as a new fluorescence-based reporter, J Bacteriol 186 (2004) 5486-5495.

[21] **Cho, S.J., Kang, N.S., Park, S.Y., Kim, B.O., Rhee, D.K., Pyo, S**., Induction of apoptosis and expression of apoptosis related genes in human epithelial carcinoma cells by Helicobacter pylori VacA toxin, Toxicon 42 (2003) 601-611.

[22] **Clarke, S**., Protein isoprenylation and methylation at carboxyl-terminal cysteine residues, Annu Rev Biochem 61 (1992) 355-386.

[23] **Collier, R.J**., Understanding the mode of action of diphtheria toxin: a perspective on progress during the 20th century, Toxicon 39 (2001) 1793-1803.

[24] **Contamin, S., Galmiche, A., Doye, A., Flatau, G., Benmerah, A., Boquet, P**., The p21 Rho-activating toxin cytotoxic necrotizing factor 1 is endocytosed by a clathrin-independent mechanism and enters the cytosol by an acidic-dependent membrane translocation step, Mol Biol Cell 11 (2000) 1775-1787.

[25] **Cortes-Bratti, X., Chaves-Olarte, E., Lagergård, T., Thelestam, M**., The cytolethal distending toxin from the chancroid bacterium *Haemophilus ducreyi* induces cell-cycle arrest in the G2 phase, Journal of Clinical Investigation 103 (1999) 107-115.

[26] **Cortes-Bratti, X., Chaves-Olarte, E., Lagergård, T., Thelestam, M**., Cellular internalization of cytolethal distending toxin from *Haemophilus ducreyi*, Infection and Immunity 68 (2000) 6903-6911.

[27] **Cortes-Bratti, X., Frisan, T., Thelestam, M**., The cytolethal distending toxins induce DNA damage and cell cycle arrest, Toxicon 39 (2001) 1729-1736.

[28] **Cortes-Bratti, X., Karlsson, C., Lagergård, T., Thelestam, M., Frisan, T**., The *Haemophilus ducreyi* cytolethal distending toxin induces cell cycle arrest and apoptosis via the DNA damage checkpoint pathways, Journal of Biological Chemistry 276 (2001) 5296-5302.

[29] **Coussens, L.M., Werb, Z**., Inflammation and cancer, Nature 420 (2002) 860-867.

[30] **Cover, T.L., Krishna, U.S., Israel, D.A., Peek, R.M., Jr**., Induction of gastric epithelial cell apoptosis by Helicobacter pylori vacuolating cytotoxin, Cancer Res 63 (2003) 951-957.

[31] **d'Adda di Fagagna, F**., Living on a break: cellular senescence as a DNA-damage response, Nat Rev Cancer 8 (2008) 512-522.

[32] **Dasti, J.I., Tareen, A.M., Lugert, R., Zautner, A.E., Gross, U**., Campylobacter jejuni: A brief overview on pathogenicity-associated factors and disease-mediating mechanisms, Int J Med Microbiol (2009).

[33] **de Hoog, C.L., Foster, L.J., Mann, M**., RNA and RNA binding proteins participate in early stages of cell spreading through spreading initiation centers, Cell 117 (2004) 649-662.

[34] **De Luca, A., Iaquinto, G**., Helicobacter pylori and gastric diseases: a dangerous association, Cancer Lett 213 (2004) 1-10.

[35] **De Rycke, J., Oswald, E**., Cytolethal distending toxin (CDT): a bacteria weapon to control host cell proliferation?, FEMS Microb. Lett. 203 (2001) 141-148.

[36] **Deng, K., Latimer, J.L., Lewis, D.A., Hansen, E.J**., Investigation of the interaction among the components of the cytolethal distending toxin of Haemophilus ducreyi, Biochem Biophys Res Commun 285 (2001) 609-615.

[37] **Dent, P., Yacoub, A., Fisher, P.B., Hagan, M.P., Grant, S**., MAPK pathways in radiation responses, Oncogene 22 (2003) 5885-5896.

[38] **DiRienzo, J.M., Cao, L., Volgina, A., Bandelac, G., Korostoff, J**., Functional and structural characterization of chimeras of a bacterial genotoxin and human type I DNAse, FEMS Microbiol Lett 291 (2009) 222-231.

[39] **Echevarria, W., Leite, M.F., Guerra, M.T., Zipfel, W.R., Nathanson, M.H**., Regulation of calcium signals in the nucleus by a nucleoplasmic reticulum, Nat Cell Biol 5 (2003) 440-446.

[40] **Elledge, S.J**., Cell cycle check points: preventing an identity crisis, Science 274 (1996) 1664-1672.

[41] **Elwell, C., Chao, K., Patel, K., Dreyfus, L**., *Escherichia coli* CdtB mediates cytolethal distending toxin cell cycle arrest, Infection and Immunity 69 (2001) 3418-3422.

[42] **Elwell, C.A., Dreyfus, L.A**., DNAase I homologous residues in CdtB are critical for cytolethal distending toxin-mediated cell cycle arrest, Mol. Microbiol. 37 (2000) 952-963.

[43] **Evan, G., Littlewood, T**., A matter of life and cell death, Science 281 (1998) 1317-1322.

[44] **Falnes, P.O., Sandvig, K**., Penetration of protein toxins into cells, Curr Opin Cell Biol 12 (2000) 407-413.

[45] **Finch, C.E., Crimmins, E.M**., Inflammatory exposure and historical changes in human life-spans, Science 305 (2004) 1736-1739.

[46] **Fox, J.G., Gorelick, P.L., Kullberg, M.C., Ge, Z., Dewhirst, F.E., Ward, J.M**., A novel urease-negative Helicobacter species associated with colitis and typhlitis in IL-10-deficient mice, Infect Immun 67 (1999) 1757-1762.

[47] **Fox, J.G., Rogers, A.B., Whary, M.T., Ge, Z., Taylor, N.S., Xu, S., Horwitz, B.H., Erdman, S.E**., Gastroenteritis in NF-kappaB-deficient mice is produced with wild-type Camplyobacter jejuni but not with C. jejuni lacking cytolethal distending toxin despite persistent colonization with both strains, Infect Immun 72 (2004) 1116-1125.

[48] **Fricker, M., Hollinshead, M., White, N., Vaux, D**., Interphase nuclei of many mammalian cell types contain deep, dynamic, tubular membrane-bound invaginations of the nuclear envelope, J Cell Biol 136 (1997) 531-544.

[49] **Frisan, T., Cortes-Bratti, X., Chaves-Olarte, E., Stenerlöw, B., Thelestam, M**., The *Haemophilus ducreyi* cytolethal distending toxin induces DNA double strand breaks and promotes ATM-dependent activation of RhoA, Cellular Microbiology 5 (2003) 695-707.

[50] **Frisan, T., Cortes-Bratti, X., Thelestam, M**., Cytolethal distending toxins and activation of DNA damage-dependent checkpoint responses, Int J Med Microbiol 291 (2002) 495-499.

[51] **Frisk, A., Lebens, M., Johansson, C., Ahmed, H., Svensson, L., Ahlman, K., Lagergård, T**., The role of different protein components from the *Haemophilus ducreyi* cytolethal distending toxin in the generation of cell toxicity, Microbial Pathogenesis 30 (2001) 313-324.

[52] **Ge, Z., Rogers, A.B., Feng, Y., Lee, A., Xu, S., Taylor, N.S., Fox, J.G**., Bacterial cytolethal distending toxin promotes the development of dysplasia in a model of microbially induced hepatocarcinogenesis, Cell Microbiol 9 (2007) 2070-2080.

[53] **Ge, Z., Schauer, D.B., Fox, J.G**., In vivo virulence properties of bacterial cytolethal-distending toxin, Cell Microbiol 10 (2008) 1599-1607.

[54] **Gelfanova, V., Hansen, E.J., Spinola, S.M**., Cytolethal distending toxin of *Haemophilus ducreyi* induces apoptotic death of Jurkat T cells, Infect. Immun. 67 (1999) 6394-6402.

[55] **George, K.M., Chatterjee, D., Gunawardana, G., Welty, D., Hayman, J., Lee, R., Small, P.L**., Mycolactone: a polyketide toxin from Mycobacterium ulcerans required for virulence, Science 283 (1999) 854-857.

[56] **Haghjoo, E., Galan, J.E**., Salmonella typhi encodes a functional cytolethal distending toxin that is delivered into host cells by a bacterial-internalization pathway, Proc Natl Acad Sci U S A 101 (2004) 4614-4619.

[57] **Hampton, R.Y**., ER-associated degradation in protein quality control and cellular regulation, Curr Opin Cell Biol 14 (2002) 476-482.

[58] **Hassane, D.C., Lee, R.B., Mendenhall, M.D., Pickett, C.L**., Cytolethal distending toxin demonstrates genotoxic activity in a yeast model, Infect Immun 69 (2001) 5752-5759.

[59] **Hazes, B., Read, R.J**., Accumulating evidence suggests that several AB-toxins subvert the endoplasmic reticulum-associated protein degradation pathway to enter target cells, Biochemistry 36 (1997) 11051-11054.

[60] **Hehlgans, S., Haase, M., Cordes, N**., Signalling via integrins: implications for cell survival and anticancer strategies, Biochim Biophys Acta 1775 (2007) 163-180.

[61] **Hickey, T.E., McVeigh, A.L., Scott, D.A., Michielutti, R.E., Bixby, A., Carroll, S.A., Bourgeois, A.L., Guerry, P**., Campylobacter jejuni cytolethal distending toxin mediates release of interleukin-8 from intestinal epithelial cells, Infect Immun 68 (2000) 6535-6541.

[62] **Higashi, H., Nakaya, A., Tsutsumi, R., Yokoyama, K., Fujii, Y., Ishikawa, S., Higuchi, M., Takahashi, A., Kurashima, Y., Teishikata, Y., Tanaka, S., Azuma, T., Hatakeyama, M**., Helicobacter pylori CagA induces Ras-independent morphogenetic response through SHP-2 recruitment and activation, J Biol Chem 279 (2004) 17205-17216.

[63] **Higashi, H., Tsutsumi, R., Muto, S., Sugiyama, T., Azuma, T., Asaka, M., Hatakeyama, M**., SHP-2 tyrosine phosphatase as an intracellular target of Helicobacter pylori CagA protein, Science 295 (2002) 683-686.

[64] **Holm, L., Sander, C**., Protein structure comparison by alignment of distance matrices, J Mol Biol 233 (1993) 123-138.

[65] **Horiguchi, Y**., Escherichia coli cytotoxic necrotizing factors and Bordetella dermonecrotic toxin: the dermonecrosis-inducing toxins activating Rho small GTPases, Toxicon 39 (2001) 1619-1627.

[66] **Horiguchi, Y., Sugimoto, N., Matsuda, M**., Stimulation of DNA synthesis in osteoblast-like MC3T3-E1 cells by Bordetella bronchiseptica dermonecrotic toxin, Infect Immun 61 (1993) 3611-3615.

[67] **Jaffe, A.B., Hall, A**., Rho GTPases: biochemistry and biology, Annu Rev Cell Dev Biol 21 (2005) 247-269.

[68] **Jain, K.K**., Use of bacteria as anticancer agents, Expert Opin Biol Ther 1 (2001) 291-300.

[69] **Johnson, W.M., Lior, H**., Response of Chinese hamster ovary cells to a cytolethal distending toxin (CDT) of *Escherichia coli* and possible misinterpretation as heat-labile (LT) enterotoxin, FEMS Microbiology Letters 43 (1987) 19-23.

[70] **Joseph, K.C., Stieber, A., Gonatas, N.K**., Endocytosis of cholera toxin in GERL-like structures of murine neuroblastoma cells pretreated with GM1 ganglioside. Cholera toxin internalization into Neuroblastoma GERL, J Cell Biol 81 (1979) 543-554.

[71] **Kaibuchi, K., Kuroda, S., Amano, M**., Regulation of the cytoskeleton and cell adhesion by the Rho family GTPases in mammalian cells, Annu Rev Biochem 68 (1999) 459-486.

[72] **Khanna, K.K., Jackson, S.P**., DNA double-strand breaks: signaling, repair and the cancer connection, Nat Genet 27 (2001) 247-254.

[73] **Kirchhausen, T**., Adaptors for clathrin-mediated traffic, Annu Rev Cell Dev Biol 15 (1999) 705-732.

[74] **Klis, F.M., Boorsma, A., De Groot, P.W**., Cell wall construction in Saccharomyces cerevisiae, Yeast 23 (2006) 185-202.
[75] **Kounnas, M.Z., Morris, R.E., Thompson, M.R., FitzGerald, D.J., Strickland, D.K., Saelinger, C.B**., The alpha 2-macroglobulin receptor/low density lipoprotein receptor-related protein binds and internalizes Pseudomonas exotoxin A, J Biol Chem 267 (1992) 12420-12423.
[76] **Kreitman, R.J**., Immunotoxins in cancer therapy, Current Opinion in Immunology 11 (1999) 570-578.
[77] **Kreitman, R.J., Wilson, W.H., White, J.D., Stetler-Stevenson, M., Jaffe, E.S., Giardina, S., Waldmann, T.A., Pastan, I**., Phase I trial of recombinant immunotoxin anti-Tac(Fv)-PE38 (LMB-2) in patients with hematologic malignancies, J. Clin. Oncol. 18 (2000) 1622-1636.
[78] **Kullberg, M.C., Rothfuchs, A.G., Jankovic, D., Caspar, P., Wynn, T.A., Gorelick, P.L., Cheever, A.W., Sher, A**., Helicobacter hepaticus-induced colitis in interleukin-10-deficient mice: cytokine requirements for the induction and maintenance of intestinal inflammation, Infect Immun 69 (2001) 4232-4241.
[79] **Kullberg, M.C., Ward, J.M., Gorelick, P.L., Caspar, P., Hieny, S., Cheever, A., Jankovic, D., Sher, A**., Helicobacter hepaticus triggers colitis in specific-pathogen-free interleukin-10 (IL-10)-deficient mice through an IL-12- and gamma interferon-dependent mechanism, Infect Immun 66 (1998) 5157-5166.
[80] **Lacks, S.A**., Deoxyribonuclease I in mammalian tissues. Specificity of inhibition by actin, J Biol Chem 256 (1981) 2644-2648.
[81] **Lagace, T.A., Ridgway, N.D**., The rate-limiting enzyme in phosphatidylcholine synthesis regulates proliferation of the nucleoplasmic reticulum, Mol Biol Cell 16 (2005) 1120-1130.
[82] **Lalli, G., Bohnert, S., Deinhardt, K., Verastegui, C., Schiavo, G**., The journey of tetanus and botulinum neurotoxins in neurons, Trends Microbiol 11 (2003) 431-437.
[83] **Lara-Tejero, M., Galan, J.E**., A bacterial toxin that controls cell cycle progression as a deoxyribonuclease I-like protein, Science 290 (2000) 354-357.
[84] **Lara-Tejero, M., Galan, J.E**., CdtA, CdtB and CdtC form a tripartite complex that is required for cytolethal distending toxin activity, Infection and Immunity 69 (2001) 4358-4365.
[85] **Lara-Tejero, M., Galan, J.E**., Cytolethal distending toxin: limited damage as a strategy to modulate cellular functions, Trends Microbiol 10 (2002) 147-152.
[86] **Lax, A.J**., Opinion: Bacterial toxins and cancer--a case to answer?, Nat Rev Microbiol 3 (2005) 343-349.
[87] **Lax, A.J., Thomas, W**., How bacteria could cause cancer: one step at a time, Trends Microbiol 10 (2002) 293-299.
[88] **Lee, J.H., Paull, T.T**., ATM activation by DNA double-strand breaks through the Mre11-Rad50-Nbs1 complex, Science 308 (2005) 551-554.
[89] **Lee, R.B., Hassane, D.C., Cottle, D.L., Pickett, C.L**., Interactions of Campylobacter jejuni cytolethal distending toxin subunits CdtA and CdtC with HeLa cells, Infect Immun 71 (2003) 4883-4890.
[90] **Lencer, W.I., Hirst, T.R., Holmes, R.K**., Membrane traffic and the cellular uptake of cholera toxin, Biochim Biophys Acta 1450 (1999) 177-190.
[91] **Levinson, W**., Review of medical microbiology and immunology, ninth ed., The McGraw-HIll Companies 2006.
[92] **Li, L., Sharipo, A., Chaves-Olarte, E., Masucci, M.G., Levitsky, V., Thelestam, M., Frisan, T**., The *Haemophilus ducreyi* cytolethal distending toxin activates sensors of DNA damage and repair complexes in proliferating and non-proliferating cells, Cellular Microbiology 4 (2002) 87-99.
[93] **Lieber, M.R**., The FEN-1 family of structure-specific nucleases in eukaryotic DNA replication, recombination and repair, Bioessays 19 (1997) 233-240.
[94] **Lilley, B.N., Ploegh, H.L**., A membrane protein required for dislocation of misfolded proteins from the ER, Nature 429 (2004) 834-840.
[95] **Liu, Y., Kao, H.I., Bambara, R.A**., Flap endonuclease 1: a central component of DNA metabolism, Annu Rev Biochem 73 (2004) 589-615.
[96] **Mao, X., DiRienzo, J.M**., Functional studies of the recombinant subunits of a cytolethal distending holotoxin, Cell Microbiol 4 (2002) 245-255.
[97] **Marches, O., Ledger, T.N., Boury, M., Ohara, M., Tu, X., Goffaux, F., Mainil, J., Rosenshine, I., Sugai, M., De Rycke, J., Oswald, E**., Enteropathogenic and enterohaemorrhagic Escherichia coli deliver a novel effector called Cif, which blocks cell cycle G2/M transition, Mol Microbiol 50 (2003) 1553-1567.
[98] **Marshall, C.B., Shankland, S.J**., Cell cycle and glomerular disease: a minireview, Nephron Exp Nephrol 102 (2006) e39-48.
[99] **Maser, R.S., Monsen, K.J., Nelms, B.E., Petrini, J.H.J**., hMre11 and hRad50 nuclear foci are induced during normal cellular response to DNA double-strand breaks, Molecular and Cellular Biology 17 (1997) 6087-6096.

[100] **Matsuoka, S., Ballif, B.A., Smogorzewska, A., McDonald, E.R., 3rd, Hurov, K.E., Luo, J., Bakalarski, C.E., Zhao, Z., Solimini, N., Lerenthal, Y., Shiloh, Y., Gygi, S.P., Elledge, S.J**., ATM and ATR substrate analysis reveals extensive protein networks responsive to DNA damage, Science 316 (2007) 1160-1166.

[101] **Mbeunkui, F., Johann, D.J., Jr**., Cancer and the tumor microenvironment: a review of an essential relationship, Cancer Chemother Pharmacol 63 (2009) 571-582.

[102] **McSweeney, L.A., Dreyfus, L.A**., Nuclear localization of the Escherichia coli cytolethal distending toxin CdtB subunit, Cell Microbiol 6 (2004) 447-458.

[103] **McSweeney, L.A., Dreyfus, L.A**., Carbohydrate-binding specificity of the Escherichia coli cytolethal distending toxin CdtA-II and CdtC-II subunits, Infect Immun 73 (2005) 2051-2060.

[104] **Mirzoeva, O.K., Petrini, J.H.J**., DNA damage-dependent nuclear dymanics of the Mre11 complex, Molecular and Cellular Biology 21 (2001) 281-288.

[105] **Mise, K., Akifusa, S., Watarai, S., Ansai, T., Nishihara, T., Takehara, T**., Involvement of ganglioside GM3 in G(2)/M cell cycle arrest of human monocytic cells induced by Actinobacillus actinomycetemcomitans cytolethal distending toxin, Infect Immun 73 (2005) 4846-4852.

[106] **Montecucco, C., Molgo, J**., Botulinal neurotoxins: revival of an old killer, Curr Opin Pharmacol 5 (2005) 274-279.

[107] **Montfort, W., Villafranca, J.E., Monzingo, A.F., Ernst, S.R., Katzin, B., Rutenber, E., Xuong, N.H., Hamlin, R., Robertus, J.D**., The three-dimensional structure of ricin at 2.8 A, J Biol Chem 262 (1987) 5398-5403.

[108] **Morita, E., Sandrin, V., Chung, H.Y., Morham, S.G., Gygi, S.P., Rodesch, C.K., Sundquist, W.I**., Human ESCRT and ALIX proteins interact with proteins of the midbody and function in cytokinesis, EMBO J 26 (2007) 4215-4227.

[109] **Mullan, P.B., Lax, A.J**., Pasteurella multocida toxin is a mitogen for bone cells in primary culture, Infect Immun 64 (1996) 959-965.

[110] **Nelms, B.E., Maser, R.S., MacKay, J.F., Lagally, M.G., Petrini, J.H.J**., In situ visualization of DNA double-strand break repair in human fibroblasts, Science 280 (1998) 590-592.

[111] **Nesic, D., Hsu, Y., Stebbins, C.E**., Assembly and function of a bacterial genotoxin, Nature 429 (2004) 429-433.

[112] **Nichols, B.J., Kenworthy, A.K., Polishchuk, R.S., Lodge, R., Roberts, T.H., Hirschberg, K., Phair, R.D., Lippincott-Schwartz, J**., Rapid cycling of lipid raft markers between the cell surface and Golgi complex, J Cell Biol 153 (2001) 529-541.

[113] **Nishikubo, S., Ohara, M., Ueno, Y., Ikura, M., Kurihara, H., Komatsuzawa, H., Oswald, E., Sugai, M**., An N-terminal segment of the active component of the bacterial genotoxin cytolethal distending toxin B (CDTB) directs CDTB into the nucleus, J Biol Chem 278 (2003) 50671-50681.

[114] **Nougayrede, J.P., Boury, M., Tasca, C., Marches, O., Milon, A., Oswald, E., De Rycke, J**., Type III secretion-dependent cell cycle block caused in HeLa cells by enteropathogenic Escherichia coli O103, Infect Immun 69 (2001) 6785-6795.

[115] **Nougayrede, J.P., Taieb, F., De Rycke, J., Oswald, E**., Cyclomodulins: bacterial effectors that modulate the eukaryotic cell cycle, Trends Microbiol 13 (2005) 103-110.

[116] **Olsnes, S.a.W., J**., Translation of bacerial proteins toxins into the cytosol, in: M.P. J. Alouf (Ed.), The comprehensive sourcebook of bacterial protein toxins, Elservier, 2006.

[117] **Oswald, E., Nougayrede, J.P., Taieb, F., Sugai, M**., Bacterial toxins that modulate host cell-cycle progression, Curr Opin Microbiol 8 (2005) 83-91.

[118] **Oswald, E., Sugai, M., Labigne, A., Wu, H.C., Fiorentini, C., Boquet, P., O'Brien, A.D**., Cytotoxic necrotizing factor type 2 produced by virulent Escherichia coli modifies the small GTP-binding proteins Rho involved in assembly of actin stress fibers, Proc Natl Acad Sci U S A 91 (1994) 3814-3818.

[119] **Parkhill, J., Wren, B.W., Mungall, K., Ketley, J.M., Churcher, C., Basham, D., Chillingworth, T., Davies, R.M., Feltwell, T., Holroyd, S., Jagels, K., Karlyshev, A.V., Moule, S., Pallen, M.J., Penn, C.W., Quail, M.A., Rajandream, M.A., Rutherford, K.M., van Vliet, A.H., Whitehead, S., Barrell, B.G**., The genome sequence of the food-borne pathogen Campylobacter jejuni reveals hypervariable sequences, Nature 403 (2000) 665-668.

[120] **Parrish, J.Z., Yang, C., Shen, B., Xue, D**., CRN-1, a Caenorhabditis elegans FEN-1 homologue, cooperates with CPS-6/EndoG to promote apoptotic DNA degradation, EMBO J 22 (2003) 3451-3460.

[121] **Pastan, I., Hassan, R., Fitzgerald, D.J., Kreitman, R.J**., Immunotoxin therapy of cancer, Nat Rev Cancer 6 (2006) 559-565.

[122] **Paull, T.T., Rogakou, E.P., Yamazaki, V., Kirchgessner, C.U., Gellert, M., Bonner, W.M**., A critical role for histone H2AX in recruitment of repair factors to nucler foci after DNA danage, Current Biology 10 (2000) 886-895.

[123] **Peek, R.M., Jr., Blaser, M.J., Mays, D.J., Forsyth, M.H., Cover, T.L., Song, S.Y., Krishna, U., Pietenpol, J.A**., Helicobacter pylori strain-specific genotypes and modulation of the gastric epithelial cell cycle, Cancer Res 59 (1999) 6124-6131.
[124] **Pelengaris, S., Khan, M**., The many faces of c-MYC, Arch Biochem Biophys 416 (2003) 129-136.
[125] **Pickett, C.L., Cottle, D.L., Pesci, E.C., Bikah, G**., Cloning, sequencing, and expression of the Escherichia coli cytolethal distending toxin genes, Infect Immun 62 (1994) 1046-1051.
[126] **Pickett, C.L., Pesci, E.C., Cottle, D.L., Russell, G., Erdem, A.N., Zeytin, H**., Prevalence of cytolethal distending toxin production in *Campylobacter jejuni* and relatedness of *Campylobacter* sp. cdtB gene., Infect. Immun. 64 (1996) 2070-2078.
[127] **Purdy, D., Buswell, C.M., Hodgson, A.E., McAlpine, K., Henderson, I., Leach, S.A**., Characterisation of cytolethal distending toxin (CDT) mutants of Campylobacter jejuni, J Med Microbiol 49 (2000) 473-479.
[128] **Raptis, S., Bapat, B**., Genetic instability in human tumors, EXS (2006) 303-320.
[129] **Ridley, A.J**., Rho GTPases and actin dynamics in membrane protrusions and vesicle trafficking, Trends Cell Biol 16 (2006) 522-529.
[130] **Rodal, S.K., Skretting, G., Garred, O., Vilhardt, F., van Deurs, B., Sandvig, K**., Extraction of cholesterol with methyl-beta-cyclodextrin perturbs formation of clathrin-coated endocytic vesicles, Mol Biol Cell 10 (1999) 961-974.
[131] **Romisch, K**., A cure for traffic jams: small molecule chaperones in the endoplasmic reticulum, Traffic 5 (2004) 815-820.
[132] **Rossman, K.L., Der, C.J., Sondek, J**., GEF means go: turning on RHO GTPases with guanine nucleotide-exchange factors, Nat Rev Mol Cell Biol 6 (2005) 167-180.
[133] **Rotman, G., Shiloh, Y**., ATM: a mediator of multiple responses to genotoxic stress, Oncogene 18 (1999) 6135-6144.
[134] **Rozengurt, E., Higgins, T., Chanter, N., Lax, A.J., Staddon, J.M**., Pasteurella multocida toxin: potent mitogen for cultured fibroblasts, Proc Natl Acad Sci U S A 87 (1990) 123-127.
[135] **Safety, I.P.o.C.**, http://www.inchem.org/, vol. 2009.
[136] **Sandvig, K**., Shiga toxins, Toxicon 39 (2001) 1629-1635.
[137] **Sandvig, K., Madshus, I.H., Olsnes, S**., Dimethyl sulphoxide protects cells against polypeptide toxins and poliovirus, Biochem J 219 (1984) 935-940.
[138] **Sandvig, K., Van Deurs, B**., Entry of Ricin and Shiga toxin into cells: molecular mechanisms and medical perspectives, EMBO journal 19 (2000) 5943-5950.
[139] **Sandvig, K., van Deurs, B**., Membrane traffic exploited by protein toxins, Annu Rev Cell Dev Biol 18 (2002) 1-24.
[140] **Sandvig, K., van Deurs, B**., Transport of protein toxins into cells: pathways used by ricin, cholera toxin and Shiga toxin, FEBS Lett 529 (2002) 49-53.
[141] **Satyanarayana, A., Kaldis, P**., Mammalian cell-cycle regulation: several Cdks, numerous cyclins and diverse compensatory mechanisms, Oncogene (2009).
[142] **Schafer, A., Wolf, D.H**., Endoplasmic reticulum-associated protein quality control and degradation: genome-wide screen for ERAD components, Methods Mol Biol 301 (2005) 289-292.
[143] **Schafer, K.A**., The cell cycle: a review, Vet Pathol 35 (1998) 461-478.
[144] **Schmidt, A., Hall, A**., The Rho Exchange Factor Net1 is regulated by nuclear sequestration, Journal of Biological Chemistry 277 (2002) 14581-14588.
[145] **Schmidt, A., Hall, M.N**., Signaling to the actin cytoskeleton, Annu Rev Cell Dev Biol 14 (1998) 305-338.
[146] **Sever, S., Damke, H., Schmid, S.L**., Garrotes, springs, ratchets, and whips: putting dynamin models to the test, Traffic 1 (2000) 385-392.
[147] **Shen, Z., Feng, Y., Rogers, A.B., Rickman, B., Whary, M.T., Xu, S., Clapp, K.M., Boutin, S.R., Fox, J.G**., Cytolethal distending toxin promotes Helicobacter cinaedi-associated typhlocolitis in interleukin-10-deficient mice, Infect Immun 77 (2009) 2508-2516.
[148] **Shenker, B.J., Besack, D., McKay, T., Pankoski, L., Zekavat, A., Demuth, D.R**., Actinobacillus actinomycetemcomitans cytolethal distending toxin (Cdt): evidence that the holotoxin is composed of three subunits: CdtA, CdtB, and CdtC, J Immunol 172 (2004) 410-417.
[149] **Shenker, B.J., Datar, S**., Fusobacterium nucleatum inhibits human T-cell activation by arresting cells in the mid-G1 phase of the cell cycle, Infect Immun 63 (1995) 4830-4836.
[150] **Shenker, B.J., Dlakic, M., Walker, L.P., Besack, D., Jaffe, E., LaBelle, E., Boesze-Battaglia, K**., A novel mode of action for a microbial-derived immunotoxin: the cytolethal distending toxin subunit B exhibits phosphatidylinositol 3,4,5-triphosphate phosphatase activity, J Immunol 178 (2007) 5099-5108.
[151] **Shiloh, Y**., ATM and ATR: networking cellular responses to DNA damage, Current Opinion in Genetics & Development 11 (2001) 71-77.

[152] **Shiloh, Y**., ATM and related protein kinases: safeguarding genome integrity, Nat Rev Cancer 3 (2003) 155-168.

[153] **Shogomori, H., Futerman, A.H**., Cholera toxin is found in detergent-insoluble rafts/domains at the cell surface of hippocampal neurons but is internalized via a raft-independent mechanism, J Biol Chem 276 (2001) 9182-9188.

[154] **Simpson, J.C., Roberts, L.M., Romisch, K., Davey, J., Wolf, D.H., Lord, J.M**., Ricin A chain utilises the endoplasmic reticulum-associated protein degradation pathway to enter the cytosol of yeast, FEBS Lett 459 (1999) 80-84.

[155] **Smith, J.L., Bayles, D.O**., The contribution of cytolethal distending toxin to bacterial pathogenesis, Crit Rev Microbiol 32 (2006) 227-248.

[156] **Spano, S., Ugalde, J.E., Galan, J.E**., Delivery of a Salmonella Typhi exotoxin from a host intracellular compartment, Cell Host Microbe 3 (2008) 30-38.

[157] **Stevens, M.K., Latimer, J.L., Lumbley, S.R., Ward, C.H., Cope, L.D., Lagergård, T., Hansen, E.J**., Characterization of a *Haemophilus ducreyi* mutant deficient in the production of the cytolethal distending toxin, Infection and Immunity 67 (1999) 3900-3908.

[158] **Subtil, A., Gaidarov, I., Kobylarz, K., Lampson, M.A., Keen, J.H., McGraw, T.E**., Acute cholesterol depletion inhibits clathrin-coated pit budding, Proc Natl Acad Sci U S A 96 (1999) 6775-6780.

[159] **Sugai, M., Kawamoto, T., Peres, S.Y., Ueno, Y., Komatsuzawa, H., Fujiwara, T., Kurihara, H., Suginaka, H., Oswald, E**., The cell cycle-specific growth-inhibitory factor produced by *Actinobacillus actinomycetemcomitans* is a cytolethal distending toxin, Infect. Immun. 66 (1998) 5008-5019.

[160] **Svensson, L., Tarkowski, A., Thelestam, M., Lagergård, T**., The impact of *Haemophilus ducreyi* cytolethal distending toxin on cells involved in immune response, Microb. Pathog. 30 (2001) 157-166.

[161] **Svensson, L.A., Henning, P., Lagergard, T**., The cytolethal distending toxin of Haemophilus ducreyi inhibits endothelial cell proliferation, Infect Immun 70 (2002) 2665-2669.

[162] **Taieb, F., Nougayrede, J.P., Watrin, C., Samba-Louaka, A., Oswald, E**., Escherichia coli cyclomodulin Cif induces G2 arrest of the host cell cycle without activation of the DNA-damage checkpoint-signalling pathway, Cell Microbiol 8 (2006) 1910-1921.

[163] **Takei, K., Haucke, V**., Clathrin-mediated endocytosis: membrane factors pull the trigger, Trends Cell Biol 11 (2001) 385-391.

[164] **Tanaka, N., Kyuuma, M., Sugamura, K**., Endosomal sorting complex required for transport proteins in cancer pathogenesis, vesicular transport, and non-endosomal functions, Cancer Sci 99 (2008) 1293-1303.

[165] **Teter, K., Holmes, R.K**., Inhibition of endoplasmic reticulum-associated degradation in CHO cells resistant to cholera toxin, Pseudomonas aeruginosa exotoxin A, and ricin, Infect Immun 70 (2002) 6172-6179.

[166] **Teter, K., Jobling, M.G., Holmes, R.K**., A class of mutant CHO cells resistant to cholera toxin rapidly degrades the catalytic polypeptide of cholera toxin and exhibits increased endoplasmic reticulum-associated degradation, Traffic 4 (2003) 232-242.

[167] **Thelestam, M., Frisan, T**., Cytolethal distending toxins, Rev Physiol Biochem Pharmacol 152 (2004) 111-133.

[168] **Thelestam, M., Frisan, T**., Cytolethal distending toxins, in: J. Alouf, M. Popoff (Eds.), The comprehensive sourcebook of bacterial protein toxins, vol. 448- 467, Elsevier, 2006.

[169] **Torgersen, M.L., Skretting, G., van Deurs, B., Sandvig, K**., Internalization of cholera toxin by different endocytic mechanisms, J Cell Sci 114 (2001) 3737-3747.

[170] **Ueno, Y., Ohara, M., Kawamoto, T., Fujiwara, T., Komatsuzawa, H., Oswald, E., Sugai, M**., Biogenesis of the Actinobacillus actinomycetemcomitans cytolethal distending toxin holotoxin, Infect Immun 74 (2006) 3480-3487.

[171] **van Gent, D.C., Hoeijmakers, J.H., Kanaar, R**., Chromosomal stability and the DNA double-stranded break connection, Nat Rev Genet 2 (2001) 196-206.

[172] **Vermeulen, K., Berneman, Z.N., Van Bockstaele, D.R**., Cell cycle and apoptosis, Cell Prolif 36 (2003) 165-175.

[173] **Vermeulen, K., Van Bockstaele, D.R., Berneman, Z.N**., The cell cycle: a review of regulation, deregulation and therapeutic targets in cancer, Cell Prolif 36 (2003) 131-149.

[174] **Vermeulen, K., Van Bockstaele, D.R., Berneman, Z.N**., Apoptosis: mechanisms and relevance in cancer, Ann Hematol 84 (2005) 627-639.

[175] **Ward, J.M., Fox, J.G., Anver, M.R., Haines, D.C., George, C.V., Collins, M.J., Jr., Gorelick, P.L., Nagashima, K., Gonda, M.A., Gilden, R.V., et al**., Chronic active hepatitis and associated liver tumors in mice caused by a persistent bacterial infection with a novel Helicobacter species, J Natl Cancer Inst 86 (1994) 1222-1227.

[176] **Wyllie, A.H., Kerr, J.F., Currie, A.R**., Cell death: the significance of apoptosis, Int. Rev. Cytol. 68 (1980) 251-305.

[177] **Xu, T., Lundqvist, A., Ahmed, H.J., Eriksson, K., Yang, Y., Lagergard, T**., Interactions of Haemophilus ducreyi and purified cytolethal distending toxin with human monocyte-derived dendritic cells, macrophages and CD4+ T cells, Microbes Infect 6 (2004) 1171-1181.

[178] **Yamamoto, K., Tominaga, K., Sukedai, M., Okinaga, T., Iwanaga, K., Nishihara, T., Fukuda, J**., Delivery of cytolethal distending toxin B induces cell cycle arrest and apoptosis in gingival squamous cell carcinoma in vitro, Eur J Oral Sci 112 (2004) 445-451.

[179] **Ye, Y., Shibata, Y., Yun, C., Ron, D., Rapoport, T.A**., A membrane protein complex mediates retro-translocation from the ER lumen into the cytosol, Nature 429 (2004) 841-847.

[180] **Young, V.B., Chien, C.C., Knox, K.A., Taylor, N.S., Schauer, D.B., Fox, J.G**., Cytolethal distending toxin in avian and human isolates of Helicobacter pullorum, J Infect Dis 182 (2000b) 620-623.

[181] **Zhou, B.B., Elledge, S.J**., The DNA damage response: putting checkpoints in perspective, Nature 408 (2000) 433-439.

[182] **Zilbauer, M., Dorrell, N., Wren, B.W., Bajaj-Elliott, M**., Campylobacter jejuni-mediated disease pathogenesis: an update, Trans R Soc Trop Med Hyg 102 (2008) 123-129.

Cellular Microbiology (2005) **7**(7), 921–934 doi:10.1111/j.1462-5822.2005.00520.x

Cellular internalization of cytolethal distending toxin: a new end to a known pathway

Lina Guerra,[1] Ken Teter,[2] Brendan N. Lilley,[3] Bo Stenerlöw,[4] Randall K. Holmes,[5] Hidde L. Ploegh,[3] Kirsten Sandvig,[6] Monica Thelestam[1] and Teresa Frisan[1]*

[1]*Microbiology and Tumorbiology Center, Karolinska Institutet, Stockholm, Sweden.*
[2]*Biomolecular Science Center, Department of Molecular Biology and Microbiology, University of Central Florida, Orlando, FL, USA.*
[3]*Department of Pathology, Harvard Medical School, Boston, MA, USA.*
[4]*Division of Biomedical Radiation Sciences, Rudbeck Laboratory, Uppsala University, Sweden.*
[5]*Department of Microbiology, University of Colorado Health Sciences Center, Denver, CO, USA.*
[6]*Institute for Cancer Research, The Norvegian Radium Hospital, Oslo, Norway.*

Summary

The cytolethal distending toxins (CDTs) are unique in their ability to induce DNA damage, activate checkpoint responses and cause cell cycle arrest or apoptosis in intoxicated cells. However, little is known about their cellular internalization pathway. We demonstrate that binding of the *Haemophilus ducreyi* CDT (HdCDT) on the plasma membrane of sensitive cells was abolished by cholesterol extraction with methyl-β-cyclodextrin. The toxin was internalized via the Golgi complex, and retrogradely transported to the endoplasmic reticulum (ER), as assessed by N-linked glycosylation. Further translocation from the ER did not require the ER-associated degradation (ERAD) pathway, and was Derlin-1 independent. The genotoxic activity of HdCDT was dependent on its internalization and its DNase activity, as induction of DNA double-stranded breaks was prevented in Brefeldin A-treated cells and in cells exposed to a catalytically inactive toxin. Our data contribute to a better understanding of the CDT mode of action and highlight two important aspects of the biology of this bacterial toxin family: (i) HdCDT translocation from the ER to the nucleus does not involve the classical pathways followed by other retrogradely transported toxins and (ii) toxin internalization is crucial for execution of its genotoxic activity.

Received 8 November, 2004; revised 31 January, 2005; accepted 14 February, 2005. *For correspondence. E-mail Teresa.Frisan@mtc.ki.se; Tel. (+46) 8 52487163; Fax (+46) 8 342651.

Introduction

Cytolethal distending toxins (CDTs) are produced by several Gram-negative bacteria, including *Escherichia coli*, *Campylobacter* spp., *Shigella* spp., *Haemophilus ducreyi* and *Actinobacillus actinomycetemcomitans* (reviewed in Thelestam and Frisan, 2004a). In the producing bacterium, three linked genes, named as *cdtA*, *cdtB* and *cdtC*, encode three polypeptides, with the predicted molecular masses of 26, 30 and 20 kDa respectively (reviewed in Dreyfus, 2003). The CdtA, CdtB and CdtC proteins form a biologically active tripartite complex (Lara-Tejero and Galan, 2001), which is able to bind to the cell surface of the target cells (Lee *et al*., 2003).

The classical effects of CDT intoxication are cell distension and block of cellular proliferation, which occurs at different stages of the cell cycle, in a cell type-dependent manner. Human fibroblasts are arrested in the G1 and G2 phases of the cell cycle, while other cell types, such as HeLa cells, are exclusively arrested in G2 (reviewed in Thelestam and Frisan, 2004a). The molecular pathways leading to the CDT-induced cell cycle arrest are identical to the checkpoint responses induced by ionizing radiation, a well-known DNA-damaging agent, including phosphorylation of histone H2AX and hyperphosphorylation of the cyclin-dependent kinase (cdc) 2 (Cortes-Bratti *et al*., 2001; Li *et al*., 2002; Hassane *et al*., 2003). Activation of the DNA damage checkpoint responses in CDT-treated cells is consistent with the demonstration that the CdtB subunit shares functional and structural homology with the mammalian DNase I (Elwell and Dreyfus, 2000; Lara-Tejero and Galan, 2000). The crystal structure of the *H. ducreyi* CDT (HdCDT) has been recently solved, and it reveals that the toxin consists of an enzyme belonging to the DNase I family (CdtB), bound to two lectin-like domains (CdtA and CdtC) with homologies to the cell binding component of the plant toxin ricin (Nesic *et al*., 2004). Furthermore, the CdtB subunit from *E. coli* causes DNA degradation in an *in vitro* system (Elwell and Dreyfus, 2000), CdtB from *Campylobacter jejuni* (CjCdtB) induces nuclear collapse when microinjected or ectopically transfected in eukaryotic cells (Lara-Tejero and Galan, 2000), and DNA double-stranded breaks (DSBs)

were induced by CjCdtB expressed in yeast (Hassane *et al*., 2001) and by HdCDT intoxication in mammalian cells (Frisan *et al*., 2003). Point mutations in residues important for catalysis, Mg^{2+} or DNA binding completely prevent cellular intoxication by CDTs (Elwell and Dreyfus, 2000; Lara-Tejero and Galan, 2000). However, some controversy still exists regarding the mechanism of action of CDTs, as it has been recently suggested that cellular intoxication could be mediated by CDT-induced signals from the cell membrane (Shenker *et al*., 2004).

Internalization of several cytosolic acting toxins, such as ricin, cholera toxin and *Pseudomonas aeruginosa* exotoxin A (ETA), requires translocation via the endosomal compartment, transit through the Golgi complex and transport to the endoplasmic reticulum (ER) (reviewed in Sandvig and van Deurs, 2002). It is noteworthy that among the bacterial toxins discovered so far, CDT is the only one acting as a DNase, and therefore needs to gain access to the nuclear compartment.

Few studies have addressed the issue of CDT internalization and its requirement for nuclear translocation. It has been shown that HdCDT enters HEp-2/HeLa cells by endocytosis via clathrin-coated pits. Furthermore, the cellular intoxication was completely inhibited under conditions that block the fusion of the endosomal compartment with downstream compartments or after treatment of cells with Brefeldin A (BFA) (Cortes-Bratti *et al*., 2000).

Nishikubo *et al*. (2003) recently identified an atypical nuclear localization signal (NLS) within the N-terminal region of the A. *actinomycetemcomitans* CdtB (AaCdtB), which was essential for nuclear translocation of the recombinant His-tagged CdtB-GFP. Cells exposed to a holotoxin containing a mutant CdtB, with 11-amino-acid deletion, did not present any sign of intoxication. On the other hand, two NLS sequences, designated as NLS1 and NLS2, have been identified in the C-terminal region of the *E. coli* CdtB-II (EcCdtB-II). Deletion of these two regions prevented induction of cell cycle arrest and nuclear localization of the holotoxin, without affecting its DNase activity, as tested in *in vitro* assays (McSweeney and Dreyfus, 2004).

The knowledge concerning the mechanism of action of CDTs has increased exponentially over the past 4 years. However, some relevant questions still need to be answered regarding this unusual family of bacterial toxins, such as the nature of the toxin receptor and the complete characterization of its internalization pathway. In this study, we have addressed some of these questions.

Results

Binding of HdCDT on sensitive cells is cholesterol dependent

To establish a reliable method to detect surface binding of HdCDT, HeLa cells were exposed for 20 min on ice to: (i) CdtA+CdtC+GST-CdtB, (ii) CdtA+CdtC and (iii) GST-CdtB alone. After extensive washing, bound toxin was detected by fluorescence microscopy via a fluorescein-conjugated anti-GST antibody. A distinct membrane staining was observed in HeLa cells exposed to CdtA+CdtC+GST-CdtB, while we could not detect any signal in cells incubated with CdtA+CdtC, or the GST-CdtB subunit alone, which were used as negative control (Fig. 1A). Similar results were obtained using a reconstituted toxin containing a fluorescein-conjugated CdtB subunit (data not shown).

To show that HdCDT binding detected by fluorescence microscopy was a general phenomenon, not limited to a cell cluster, FACS analysis was performed. As shown in Fig. 1B, the majority of HeLa cells exposed to reconstituted toxin showed an increased fluorescence intensity compared with control cells exposed only to GST-CdtB.

It has been previously shown that proliferation of BalbC3T3 mouse fibroblasts is not affected by HdCDT (Cortes-Bratti *et al*., 1999). In line with this observation, HdCDT failed to induce cell cycle arrest 24 h and 48 h after treatment (Fig. 1C), and we did not detect phosphorylation of the histone H2AX 4 h after toxin exposure (Fig. 1D) in these cells. However, arrest in the G1 and G2 phases of the cell cycle and H2AX phosphorylation were observed in BalbC3T3 cells exposed to ionizing radiation (Fig. 1C and D). The lack of toxin sensitivity of these cells correlated with their inability to bind HdCDT, as shown in Fig. 1E.

To test whether HdCDT intoxication and binding were dependent on the presence of cholesterol, cells were exposed to 5 mM and 10 mM methyl-β-cyclodextrin (mβCD) for 30 min, before intoxication or binding was measured. mβCD is a well-characterized agent, which extracts cholesterol from the plasma membrane and disrupts lipid rafts (Orlandi and Fishman, 1998). The drug concentration and the incubation time used did not affect cell viability (data not shown). Ninety-five per cent of HeLa cells exposed to HdCDT in the absence of mβCD were arrested in the G2 phase of the cell cycle, while a dose-dependent reduction of the G2 population to 65% and 51% was observed upon intoxication of 5 mM and 10 mM mβCD-treated cells respectively (Fig. 2A).

To assess whether the effect of mβCD on cellular intoxication resulted from inhibition of toxin binding, cells were left untreated or treated with 5 mM mβCD and exposed for 20 min on ice either to HdCDT containing the GST-tagged CdtB subunit or CdtA+CdtC alone as control, and fluorescence microscopy analysis was performed (Fig. 2B). As expected a distinct membrane staining was observed in untreated cells exposed to the reconstituted HdCDT, while binding was completely prevented upon mβCD treatment.

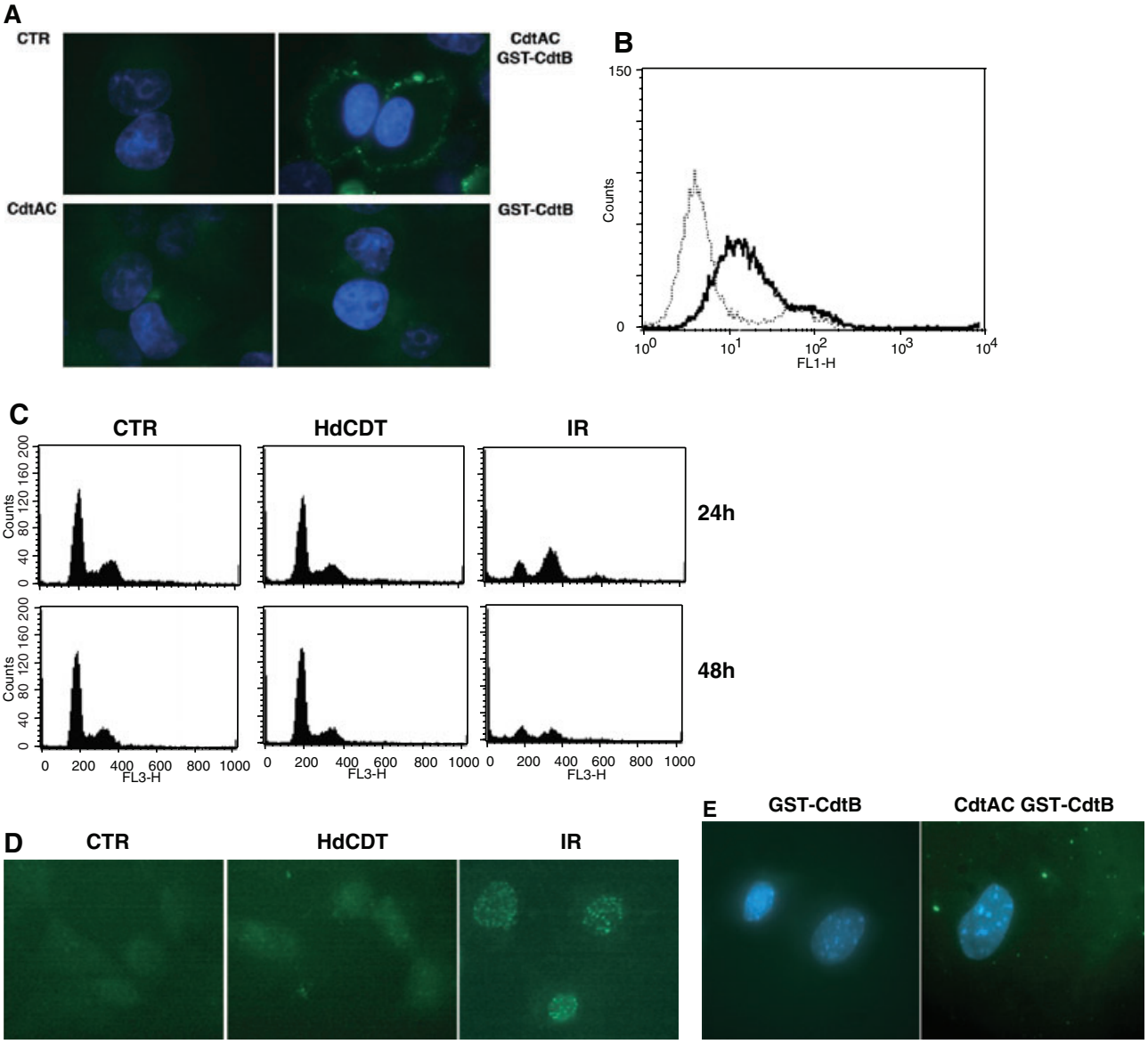

Fig. 1. HdCDT binds to the cell membrane of sensitive cells.
A. HeLa cells were left untreated or exposed to the following subunit combinations: (i) CdtA+CdtC, (ii) GST-CdtB alone and (iii) CdtA+CdtC+GST-CdtB for 20 min on ice. The final concentration of each subunit was 0.2 μg μl^{-1}. Binding and fluorescence staining was performed as described in *Experimental procedures*. Nuclei were counterstained with Hoechst 33258.
B. HeLa cells were exposed to the following subunit combinations: (i) GST-CdtB (dotted line) alone; (ii) CdtA+CdtC+GST-CdtB (thick line) for 20 min on ice. The final concentration of each subunit was 0.2 μg μl^{-1}. Binding was assayed by FACS analysis as described in *Experimental procedures*.
C. BalbC3T3 cells were either left untreated, or intoxicated with reconstituted HdCDT (2 μg ml^{-1}), or irradiated (20 Gy) and further incubated for 24 h and 48 h. Analysis of the cell cycle distribution was assessed by PI staining and flow cytometry as described in *Experimental procedures*.
D. BalbC3T3 cells were either incubated with medium alone or treated with reconstituted HdCDT (2 μg ml^{-1}) or irradiated (20 Gy), fixed 4 h after treatment and stained with anti-phospho-H2AX-specific rabbit serum as described in *Experimental procedures*.
E. BalbC3T3 cells were exposed to GST-CdtB alone or CdtA+CdtC+GST-CdtB as described in (A). Binding and fluorescence staining was performed as described in *Experimental procedures*.
One out of three independent experiments is shown.

HdCDT requires transit via the Golgi complex to exert its genotoxic effect

We have previously shown that disruption of the Golgi integrity by BFA treatment (Fujiwara *et al*., 1988) could prevent HdCDT intoxication of HeLa cells, suggesting that Golgi is an important organelle for its internalization (Cortes-Bratti *et al*., 2000). However, BFA can affect also transit through endosomes (Prydz *et al*., 1992; van Dam *et al*., 2002 and reviewed in Robinson, 2004). To discrim-

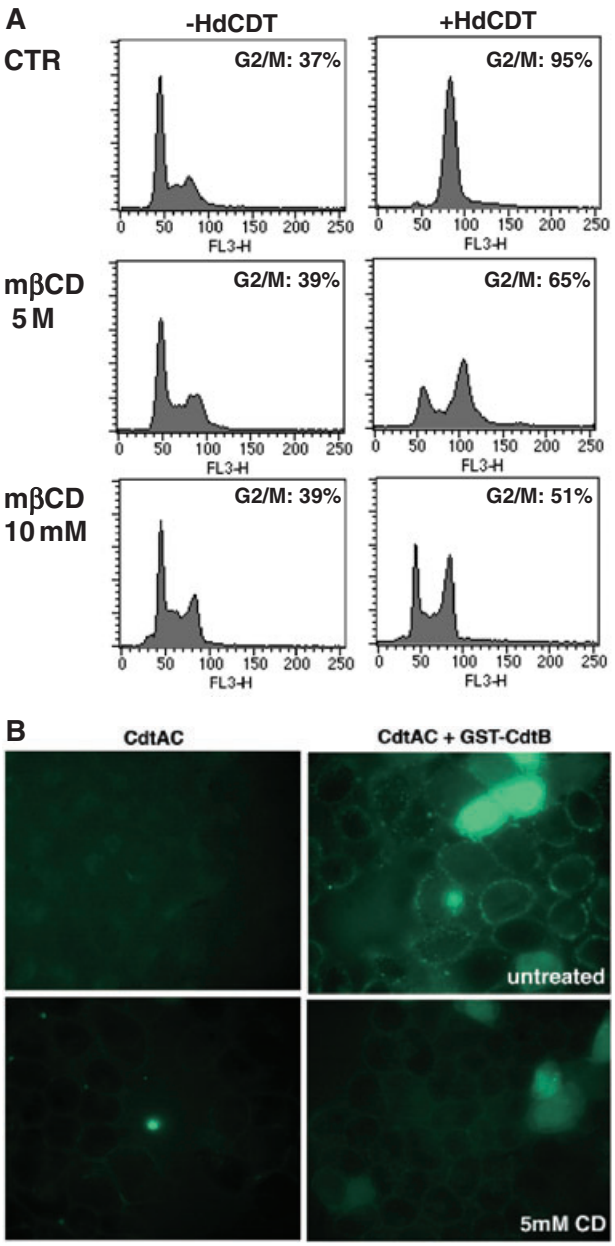

Fig. 2. Methyl-β-cyclodextrin (mβCD) prevents HdCDT intoxication and binding.
A. HeLa cells were pre-incubated for 30 min with the indicated concentrations of mβCD in FCS-free medium, and further exposed to HdCDT (2 μg ml^{-1}) for 15 min on ice. After extensive washing the cells were incubated for 24 h in RPMI complete medium. Cell cycle distribution was assessed by PI staining and flow cytometry analysis as described in *Experimental procedures*.
B. HeLa cells were pre-incubated for 30 min with the indicated concentrations of mβCD in FCS-free medium, and further exposed to: (i) CdtA+CdtC and (ii) CdtA+CdtC+GST-CdtB for 20 min on ice. The final concentration of each subunit was 0.2 μg μl^{-1}. Binding and fluorescence staining was performed as described in *Experimental procedures*.
One out of two independent experiments is shown.

inate whether HdCDT is internalized via the Golgi-dependent or a Golgi-independent pathway, we performed a set of experiments where HdCDT intoxication was assessed in parallel in BFA-treated HeLa and MDCK cell lines. MDCK cells were chosen, as their Golgi complex, but not the endosomal compartment, has been shown to be BFA resistant (Hunziker *et al*., 1991).

Two parameters of HdCDT-induced intoxication were assessed: (i) phosphorylation of the histone H2AX, which was previously shown to occur in intoxicated cells as early as 1 h after HdCDT exposure (Li *et al*., 2002) and (ii) accumulation of the hyperphosphorylated form of the cyclin-dependent kinase cdc2 (Cortes-Bratti *et al*., 1999), which is required for induction of the G2 arrest.

Phosphorylation of H2AX and cdc2 was completely prevented in BFA- and HdCDT-treated HeLa cells, compared with the cells intoxicated in the absence of BFA (Fig. 3A and B). In contrast, BFA treatment did not induce any significant change in intoxication of MDCK cells. These data indicate that transit via the Golgi complex is the main pathway followed by HdCDT.

Haemophilus ducreyi CDT has been shown to cause DNA DSBs in intoxicated cells (Frisan *et al*., 2003). However, some authors still doubt that CDTs act as DNase and that cellular internalization is required for the toxin activity (Shenker *et al*., 2004). To address this issue, we assessed whether a structurally intact Golgi complex is required for the HdCDT genotoxic activity. Disruption of the Golgi structure by BFA, not only prevented the downstream effects caused by CDT intoxication [induction of G2 arrest (Cortes-Bratti *et al*., 2000), H2AX phosphorylation and cdc2 hyperphosphorylation], but completely prevented the induction of DNA DSBs in HeLa cells (Fig. 3C). The amount of DNA DSBs induced in HdCDT-treated cells was comparable to a radiation dose of 27 Gy, and was reduced by sevenfold in cells intoxicated in the presence of BFA.

HdCDT is retrograde transported from the Golgi to the endoplasmic reticulum

The sets of experiments showed in Fig. 3 strongly suggested that HdCDT required an intact Golgi complex for a successful intoxication. To strengthen these observations and to investigate whether HdCDT is further retrogradely transported to the ER, we constructed two CdtB mutants containing either a sulphation site (CdtB-Sulf1), or a sulphation and three partially overlapping N-linked glycosylation sites (CdtB-Sulf2) at the C-terminus of the protein. Protein sulphation is a post-translational modification, which occurs exclusively in the *trans*-Golgi (Baeuerle and Huttner, 1987), while N-linked glycosylation occurs exclusively in the ER (reviewed in Helenius and Aebi, 2004).

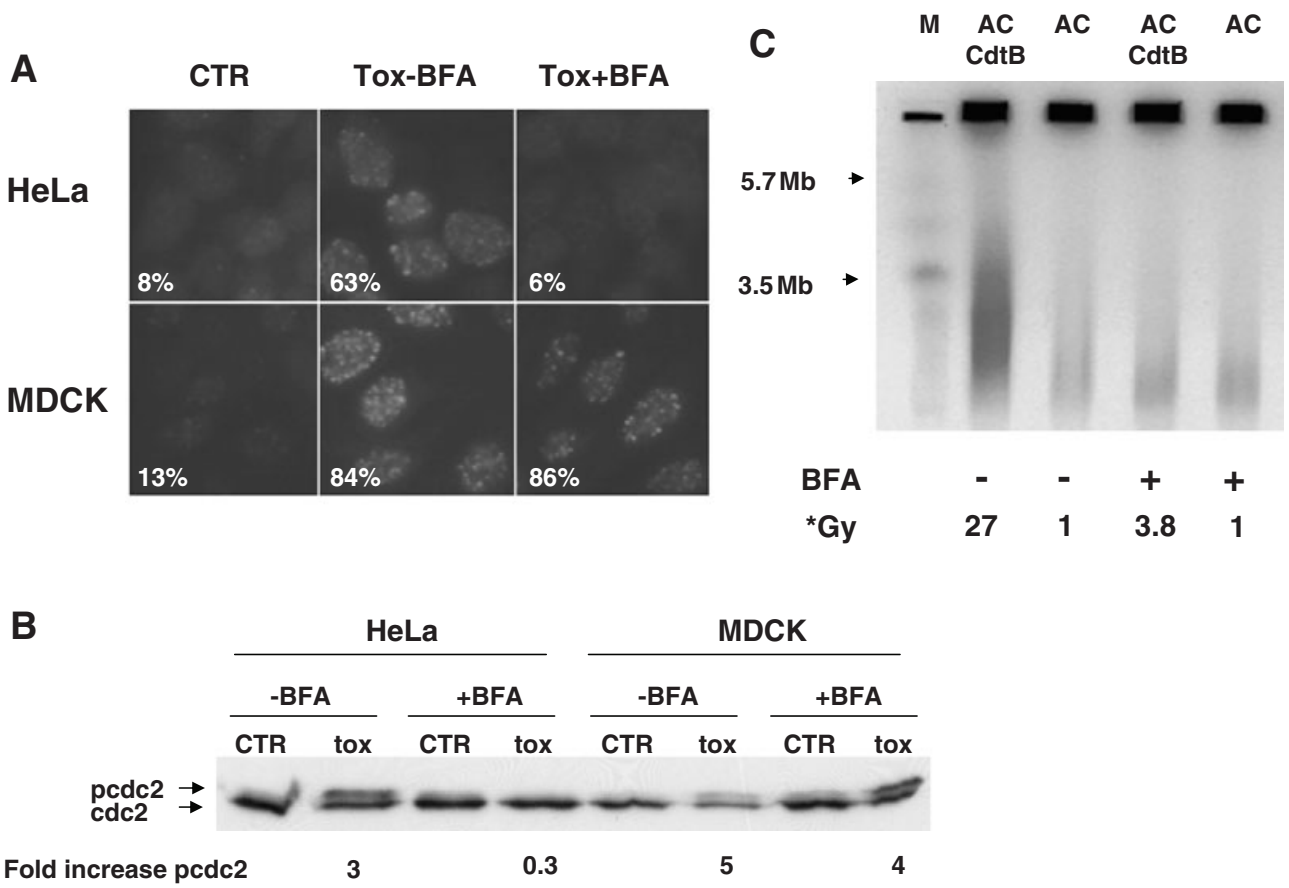

Fig. 3. HdCDT requires an intact Golgi complex to induce DNA double-stranded breaks (DSBs).
A and B. HeLa and MDCK cells were pre-incubated in the presence or absence of BFA (2.5 μg ml^{-1}) for 1 h in RPMI complete medium, and further exposed to HdCDT (2 μg ml^{-1}) for 4 h. Samples were analysed for phosphorylation of H2AX by indirect immunofluorescence (A), where the numbers represent the percentage of cells expressing pH2AX foci, or phosphorylation of cdc2 (pcdc2) by Western blot (B), where fold increase represents the increase of the phosphorylated cdc2 in HdCDT-treated cells compared with the untreated control cells. One out of three independent experiments is shown.
C. Twenty-five thousand HeLa cells per well were grown in 12-well plates in RPMI complete medium containing 4000 Bq ml^{-1} [methyl-^{14}C]-thymidine for 48 h. The cells were then washed three times in PBS and chased for 2 h in complete medium, and further pre-incubated in the presence or absence of BFA (2.5 μg ml^{-1}) for 1 h in RPMI complete medium. Cells were then exposed to: (i) CdtA+CdtC (negative control) and (ii) CdtA+CdtC+CdtB (the final concentration of the CdtB subunit was 20 μg ml^{-1}) for 8 h, and processed for pulsed-field gel electrophoresis analysis. We already showed that HdCdtB alone does not induce DNA DSBs above the control (Frisan *et al.*, 2003).
M, molecular weight marker. *Gy: equivalent radiation dose. One out of two independent experiments is shown.

Reconstituted HdCDTs containing either the CdtB-Sulf1 or the CdtB-Sulf2 subunits were equally efficient as the toxin preparation containing the wild-type CdtB in inducing G2 arrest in HeLa cells (Fig. 4A). Sulphation of HdCDT was assessed in HeLa cells incubated in the presence of $Na_2{}^{35}SO_4$ and further exposed to: (i) CdtA+CdtC, (ii) CdtA+CdtC+GST-CdtB-Sulf1 and (iii) GST-CdtB-Sulf1 alone. A labelled protein corresponding to the molecular weight of GST-CdtB-Sulf1 (approximately 60 kDa) was present only in cells exposed to the reconstituted toxin (Fig. 4B). Transit to the ER was monitored by testing mannosylation of a holotoxin containing the GST-CdtB-Sulf2 subunit in HeLa cells incubated in the presence of [^{3}H]-mannose. A specific band of approximately 60 kDa corresponding to the GST-CdtB-Sulf2 was recovered only in cells exposed to the reconstituted toxin, but not in control cells (i.e. untreated or exposed to CdtA+CdtC, Fig. 4C, or exposed to GST-CdtB-Sulf2 alone, data not shown).

Trafficking of HdCDT does not involve known ER–cytosol translocation pathways

Impairment of the ER-associated degradation (ERAD) pathway interferes with the ER to cytosol translocation of plant and bacterial toxins, such as ricin, ETA and cholera toxin (Simpson *et al.*, 1999; Teter and Holmes, 2002). To assess whether this pathway is also necessary for an efficient translocation and intoxication of target cells by HdCDT, we used a set of Chinese hamster ovary (CHO) clones, which have been selected for resistance to the

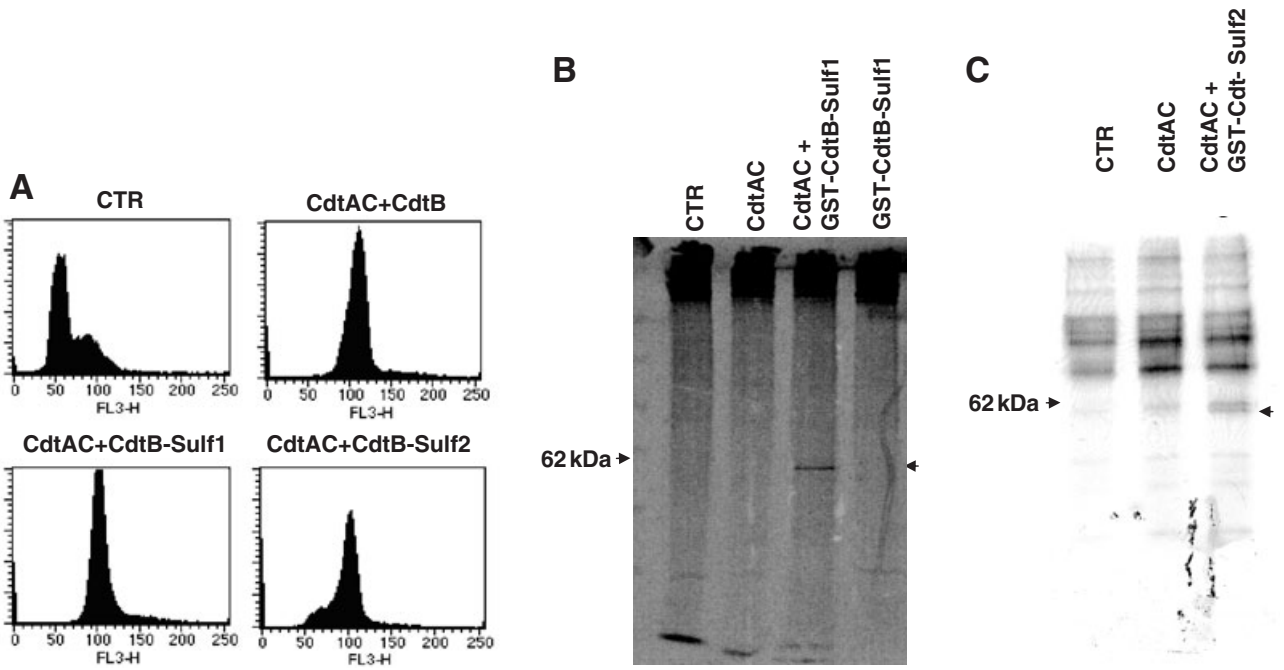

Fig. 4. HdCDT is retrogradely transported from the Golgi complex to the ER.
A. HeLa cells were left untreated or exposed to a reconstituted toxin (2 μg ml^{-1}), containing the wild-type CdtB, or the modified CdtB-Sulf1 (carrying a sulphation site at the C-terminus), or CdtB-Sulf2 (carrying a sulphation site and three overlapping N-glycosylation sites at the C-terminus) for 24 h in RPMI complete medium. Cell cycle distribution was assessed as described in Fig. 1.
B and C. Five hundred thousand HeLa cells were incubated with 600 μCi ml^{-1} $Na_2{}^{35}SO_4$ in DMEM without sulphate (B) or 100 μCi [^{3}H]-mannose in DMEM without glucose (C) for 4 h at 37°C. Cells were then exposed to: (i) CdtA+CdtC, (ii) CdtA+CdtC+GST-CdtB-Sulf1 (B) or GST-CdtB-Sulf2 (C) (20 μg ml^{-1}) and (iii) GST-CdtB-Sulf1 alone (B) for 4 h. GST fusion proteins were recovered as described in *Experimental procedures*, and fractionated in a 10% SDS-polyacrylamide gel. Labelled proteins were detected by PhosphoImager analysis.
One out of two independent experiments is shown.

ricin, ETA and cholera toxins, due to an altered ERAD system (Teter and Holmes, 2002; Teter *et al*., 2003). The CHO mutant cell lines are subgrouped in two different classes: (i) a clone that presents a deficient translocation of proteins from the ER to the cytosol (CHO 16D) and (ii) two clones which present an enhanced cytosolic degradation of the retrotranslocated proteins (CHO 23G and CHO 24D). Parental CHO cells were used as control. In order to avoid artefact due to high toxin concentration, titration experiments were performed to choose the minimal toxin concentration able to induce cell cycle arrest in the CHO parental cells (Fig. 5A). As shown in Fig. 5B, all three CHO mutant cell lines were equally sensitive to HdCDT intoxication (4 μg ml^{-1}) as the parental cells, as judged by the percentage of cells arrested in the G2 phase of the cell cycle, 24 h after intoxication. HdCDT sensitivity of the CHO cell lines was further confirmed with a colony assay. CHO parental cells and the CHO 16D and CHO 23G clones were left untreated or exposed to HdCDT (4 μg ml^{-1}). Two weeks after intoxication a striking difference in colony outgrowth was evident. Untreated cells grew to form distinct colonies, detected by Giemsa staining, while a very limited number of colonies were observed in HdCDT-exposed cells, independently of the status of the ERAD pathway (Fig. 5C).

Resistance of the CHO 16D, CHO 23G and CHO 24D cells to ETA was confirmed in parallel experiments (data not shown).

It has been recently shown that retrotranslocation into the cytoplasm of a subset of proteins involves a human homologue of the yeast Der1 protein, named Derlin-1 (Lilley and Ploegh, 2004; Ye *et al*., 2004). The homologous protein Derlin-2, which shared 36% identity with Derlin-1 and whose function is at present unknown, was not involved in this process (Lilley and Ploegh, 2004). To assess whether HdCDT internalization was Derlin-1 dependent, we investigated the sensitivity to HdCDT of HeLa cells expressing Derlin-1^{GFP}, which acts in a dominant negative manner, blocking the Cytomegalovirus-dependent dislocation of MHC class I proteins from the ER to the cytosol (Lilley and Ploegh, 2004). Cells transduced with empty vector (pMSCV) or Derlin-2^{GFP} were used as controls.

Titration experiments showed that the minimal toxin concentration inducing a complete G2 arrest in HeLa pMSCV was 1 μg ml^{-1} (Fig. 6A), and HeLa cells express-

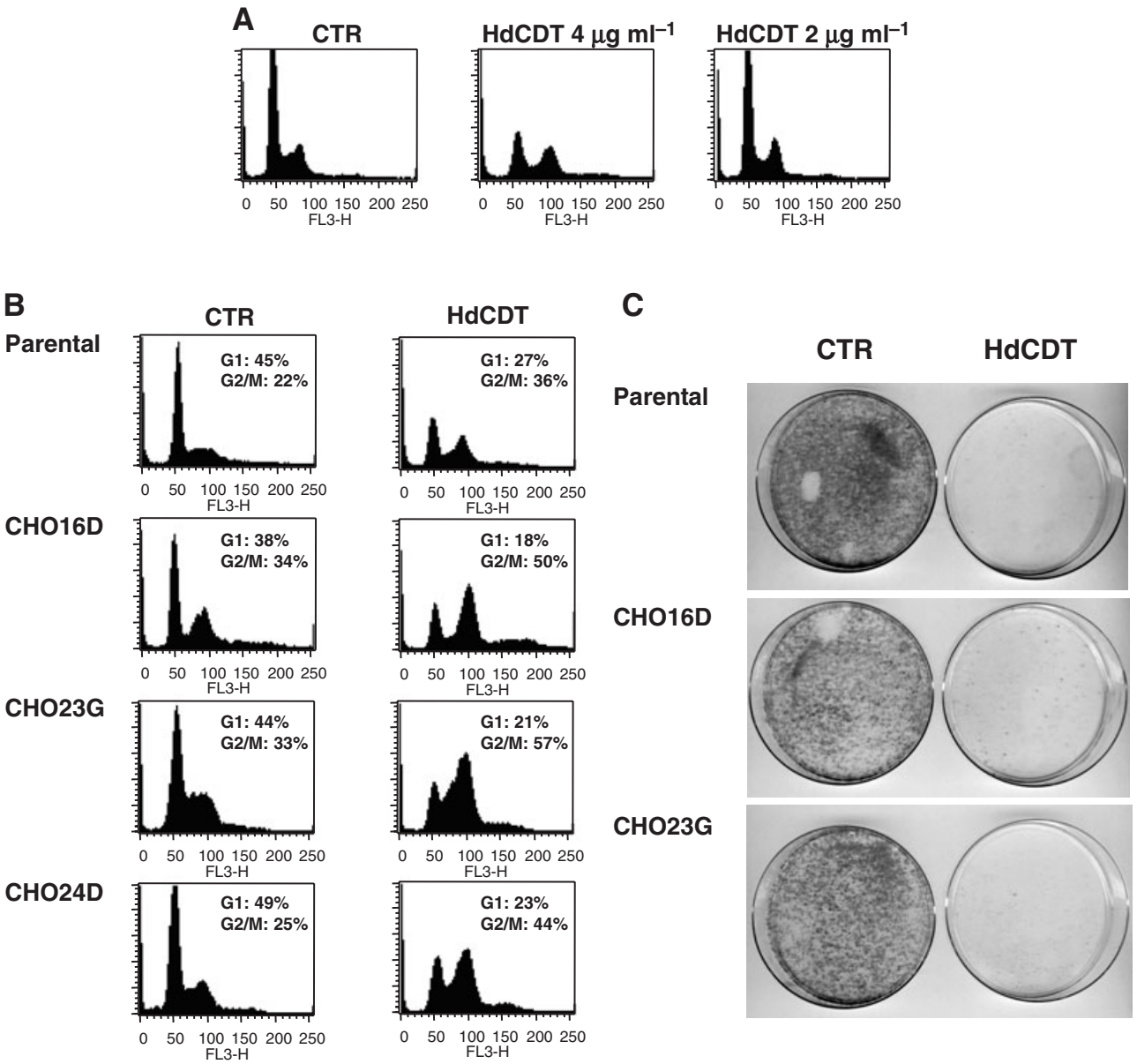

Fig. 5. Intoxication by HdCDT does not require the ERAD pathway.
A. CHO parental cells were exposed to HdCDT at the indicated concentration for 24 h. Cell cycle analysis was performed as described in Fig. 1.
B and C. CHO parental cells or CHO clones selected for resistance to ricin, ETA and cholera (CHO16D, CHO23G, CHO24D) were left untreated or exposed to HdCDT (4 μg ml^{-1}) for 24 h (B, one out of four experiments is shown) or 2 weeks (C, one out of two independent experiments is shown) in Ham's F21 complete medium. Cell cycle analysis (B) and colony assay (C) were performed as described in *Experimental procedures*.

ing the dominant negative Derlin-1^{GFP} were equally sensitive to the toxin as the control cell lines (Fig. 6B).

Mutation of the CdtB Mg^{2+} binding site prevents induction of DNA DSBs

Mutations at the Mg^{2+} binding sites and at residues important for the catalytic activity of the *E. coli* (Elwell and Dreyfus, 2000) and *C. jejuni* (Lara-Tejero and Galan, 2000) CdtB are known to abolish the cytotoxic effects, and expression of the CjCdtB mutated subunit in yeast prevents DNA degradation (Hassane *et al.*, 2001). However, it was not previously investigated whether these mutations affect the ability of CDTs to induce DNA DSBs in naturally intoxicated mammalian cells. We constructed a CdtB subunit where the Asp residue relevant for Mg^{2+} binding in position 273 was substituted by site-directed mutagenesis with an Arg residue. HdCDT containing the mutated CdtB subunit (D273R) failed to block cellular proliferation in the G2 phase of the cell cycle (Fig. 7A), and did not exert any

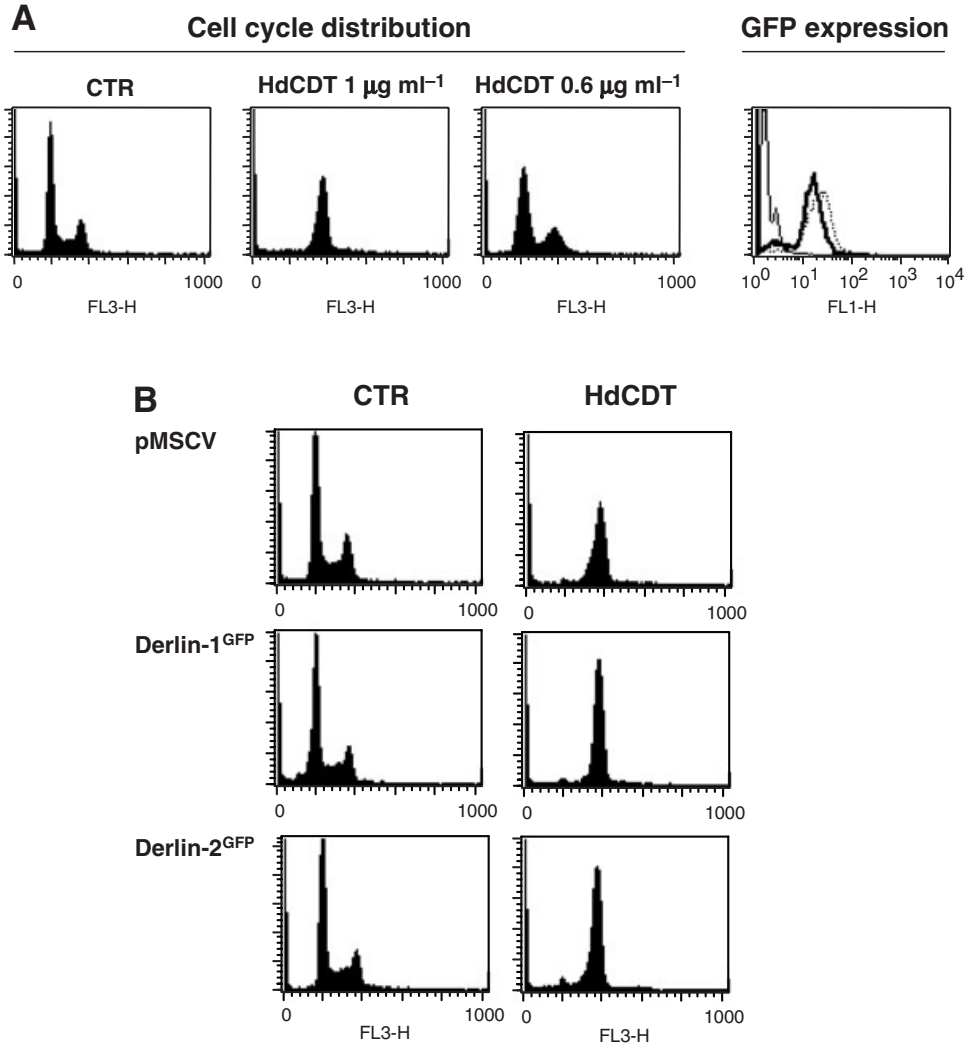

Fig. 6. HdCDT intoxication is Derlin-1 independent.
A. HeLa cells transduced with vector control (pMSCV) were exposed to the HdCDT holotoxin at the indicated concentration for 24 h in RPMI complete medium containing 0.5 μg ml^{-1} puromycin. Cell cycle distribution was assessed as described in Fig. 1. Expression of Derlin-1^{GFP} (thick line) and Derlin-2^{GFP} (dotted line) was assessed by FACs analysis (GFP expression). The vector control cells HeLa pMSCV were used as negative control (thin line).
B. HeLa cells transduced with vector control (pMSCV), Derlin-1^{GFP} or Derlin-2^{GFP} were exposed to HdCDT (1 μg ml^{-1}) for 24 h in RPMI complete medium containing 0.5 μg ml^{-1} puromycin. Cell cycle distribution was assessed as described in Fig. 1.
One out of two independent experiments is shown.

genotoxic activity, as judged by its inability to cause DNA DSBs (Fig. 7B).

Discussion

HdCDT is transported to the ER, but further transit does not require known translocation pathways

Internalization of several cytosolic acting toxins, such as ricin, cholera toxin and *P. aeruginosa* ETA, requires translocation via the endosomal compartment, transit through the Golgi complex and transport to the ER (reviewed in Sandvig and van Deurs, 2002). So far only one study has analysed the internalization of CDTs (Cortes-Bratti *et al*., 2000). Cortes-Bratti *et al*. demonstrated that HdCDT is internalized via clathrin-coated pits, based on: (i) HeLa cells expressing the dominant negative form of dynamin, (ii) removal of clathrin coats by potassium depletion and (iii) use of inhibitors, which prevent assembly of coated pits at the cell surface. Further transit via the Golgi complex was suggested, as BFA treatment could prevent cellular intoxication. However, BFA can also impair translocation through the endosomal compartment (Prydz *et al*., 1992; van Dam *et al*., 2002). Thus, BFA treatment

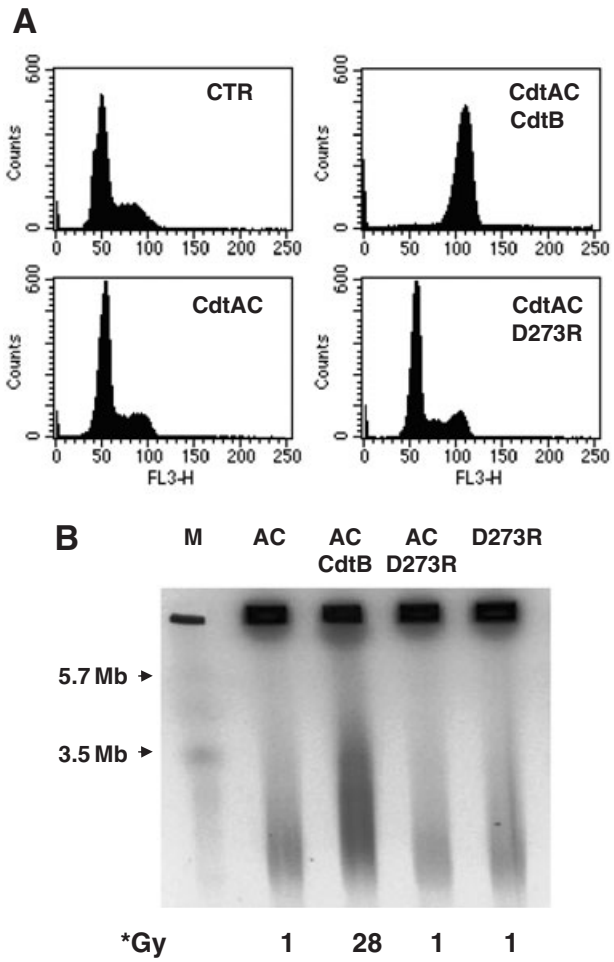

Fig. 7. HdCDT DNase activity is required to induce DNA double-stranded breaks (DSBs).
A. HeLa cells were exposed to the HdCDT toxin (2 μg ml^{-1}) containing either the wild-type CdtB or the mutated CdtBD273R for 24 h. Untreated cells or cells exposed to CdtA+CdtC were used as negative control. Cell cycle distribution was assessed as described in Fig. 1.
B. Twenty-five thousand HeLa cells per well were grown in 12-well plates in complete medium containing 4000 Bq ml^{-1} [methyl-^{14}C]-thymidine for 48 h. The cells were then washed three times in PBS, chased for 2 h in RPMI complete medium, and then exposed for 8 h to: (i) CdtA+CdtC (negative control), (ii) HdCDT containing wild-type CdtB (at the concentration of 20 μg ml^{-1}), (iii) HdCDT containing the mutated CdtBD273R (at the concentration of 20 μg ml^{-1}) and (iv) CdtBD273R alone (20 μg ml^{-1}). Cells were processed for pulsed-field gel electrophoresis analysis.
M, molecular weight marker. *Gy: equivalent radiation dose. One out of two independent experiments is shown.

of HeLa cells alone cannot completely rule out that HdCDT uses alternative internalization pathways. Indeed, an alternative transport of ricin was demonstrated in cells with an impaired Golgi to ER transport, due to a defect in the ε-coatomer protein (Llorente *et al.*, 2003). To better clarify whether the Golgi complex is required for HdCDT intoxication, two different approaches were used: (i) we assessed whether BFA has different effects on intoxication of MDCK cells, carrying a BFA-insensitive Golgi, compared with HeLa cells, carrying a BFA-sensitive Golgi (Fig. 3) and (ii) we constructed a CdtB subunit with a C-terminal sulphation site (Fig. 4). Both these experiments indicated that HdCDT transits via the Golgi apparatus. Detection of early signs of intoxication, such as phosphorylation of H2AX, and sensitivity of BFA- and HdCDT-treated MDCK cells, clearly rules out the possibility that BFA treatment could directly interfere with the cell cycle progression in the present experimental set-up (Mordente *et al.*, 1998).

The data collected so far demonstrated that HdCDT and toxins such as ricin, ETA and cholera follow a similar internalization pathway down to the ER. However, a major difference was observed when the requirement for the ERAD pathway was tested.

The ERAD pathway translocates misfolded secretory and ER membrane proteins into the cytosol for proteolytic degradation (reviewed in Hampton, 2002). Several lines of evidence suggest that the ERAD pathway, using the Sec61p translocon, is essential for mediating cytosolic translocation of intracellularly acting toxins such as ricin and Shiga toxins. Both CHO (Teter and Holmes, 2002) and *Saccharomyces cerevisiae* (Simpson *et al.*, 1999) cells defective in various aspects of the ERAD pathway are resistant to ricin intoxication. Furthermore, sulphated and glycosylated ricin can be co-precipitated with anti-Sec61p-specific antibodies (Wesche *et al.*, 1999). Also cholera toxin is associated with and requires a functional Sec61p complex to be translocated from microsomes derived from porcine pancreas (Schmitz *et al.*, 2000). We used two different classes of CHO mutant cells, which have been selected for their resistance to ricin, ETA and cholera toxin (Teter and Holmes, 2002; Teter *et al.*, 2003).

Our results (Fig. 5) suggest that HdCDT either does not need to transit to the cytosol before entering the nucleus to exert its genotoxic activity, or alternatively its translocation to the cytosol occurs via a different pathway. Data presented in this work favour the former hypothesis, because: (i) the clone CHO16D, which showed an impaired ER to cytosol translocation, was still sensitive to HdCDT and (ii) HdCDT could still intoxicate CHO cells that have an enhanced cytosolic proteolytic degradation (clones CHO23G and 24D). Furthermore, we could exclude that HdCDT exits the ER via the other known ER–cytosol translocation pathway (Lilley and Ploegh, 2004; Ye *et al.*, 2004), as HeLa cells expressing Derlin-1^{GFP} were still arrested in the G2 phase of the cell cycle upon intoxication (Fig. 6).

How the nuclear translocation of the CdtB subunit takes place is still an open question. Two recent reports have identified several NLSs located at the N-terminus of AaCdtB and the C-terminus of EcCdtB-II respectively.

Nishikubo *et al*. (2003) showed that: (i) a 11-amino-acid deletion (aa 114–124) was sufficient to abolish nuclear translocation of the GFP–AaCdtB fusion protein and (ii) a holotoxin containing the Δ11-124 AaCdtB failed to induce cell cycle arrest in sensitive cells. Two different C-terminal NLSs were instead identified in the *E coli* CdtB-II subunit, named ΔNLS1 and ΔNLS2 (McSweeney and Dreyfus, 2004). Interestingly, deletion of each of these sequences produced a differential localization of the active toxin subunit. Cells intoxicated with a holotoxin containing the EcCdtB-II-ΔNLS1 displayed a perinuclear distribution, which is consistent with trapping of the active toxin component in the late endosome and/or ER compartment. A diffuse cytoplasmic staining was observed in cells exposed to the EcCdtB-II-ΔNLS2 containing toxin. It is possible that this second NLS may act as scavenger motif to retrieve CdtB molecules, which have escaped to the cytosol, similar to the suggested ER retention function of the KDEL sequence in cholera toxin (Lencer and Tsai, 2003).

It is difficult to reconcile the results presented for the NLSs in the Aa-CdtB and Ec-CdtB-II. We hypothesize that the CdtB nuclear translocation requires an atypical mechanism, which has still not been identified, such as a direct translocation from the ER to the nucleus. Very recently, a new reticular network has been identified, and designated as nucleoplasmic reticulum (Echevarria *et al*., 2003). This organelle is described as a fine, branching intranuclear network that is continuous with the nuclear envelope and the ER. A high degree of complexity of the ER network is further demonstrated by the fact that specific ER molecules can be found on phagosomes, upon phagocytosis (reviewed in Desjardins, 2003). Interaction between phagosomes and the ER might also explain how the *Salmonella typhi* CdtB (StCdtB), expressed upon bacterial internalization in the absence of CdtA and CdtC, could gain access to the nuclear compartment (Haghjoo and Galan, 2004).

These studies highlight that the ER has a central role in regulation and execution of processes involving intracellular trafficking, some of which are still unknown. In this context, elucidation of the mechanism by which CdtB is translocated into the nucleus becomes an important issue, and our data show that this translocation does not occur via any of the pathways so far described.

HdCDT requires internalization to exert its genotoxic activity

In a recent paper, Shenker and colleagues questioned whether the relevant activity of the CDT family of toxins is a DNase-like activity, and suggested that the cytotoxic effects might be triggered upon toxin-induced transmembrane signalling from the cell membrane (Shenker *et al*., 2004; Thelestam and Frisan, 2004b). Data shown in Fig. 3 demonstrate that inhibition of toxin internalization abolished all the parameters relevant for CDT-mediated intoxication, such as induction of DNA DSBs, phosphorylation of histone H2AX, hyperphosphorylation of the cyclin-dependent kinase cdc2 and cell cycle arrest. Consistent with the data of Elwell and Dreyfus (2000), Lara-Tejero and Galan (2000) and Hassane *et al*. (2003) on EcCDT-II and CjCDT, we also showed that HdCDT carrying a mutation interfering with the DNase activity could not induce cell cycle arrest, and this lack of effect resulted from the inability of the mutant toxin to cause DNA DSBs (Fig. 7A and B). It was previously shown that mutation of the Asp-222 residue critical for the CjCdtB DNase activity inhibits DNA degradation when the mutated CdtB gene was expressed in yeast (Hassane *et al*., 2001). Our data strengthen this observation and represent the first direct demonstration of lack of induction of DNA DSBs in naturally intoxicated mammalian cells by a toxin containing a mutated CdtB subunit.

Taken together these data exclude that induction of DNA DSBs and activation of DNA damage checkpoint responses can be induced by transmembrane signalling.

Binding of HdCDT requires cholesterol

Binding of CDT to the plasma membrane of target cells has recently been well documented by Lee *et al*. (2003) (CjCDT) and McSweeney and Dreyfus (2004) (EcCDT-II). These authors used either an enzyme-linked immunosorbent assay on living cells (CELISA) or FACS analysis. In line with these observations, we could also detect by immunofluorescence analysis binding of HdCDT on the surface of the CDT-sensitive HeLa cells (Fig. 1A and B) but not on the mouse BalbC3T3 cells (Fig. 1E), which are completely resistant to the toxin treatment (Fig. 1C and D). These data indicate that the BalbC3T3 resistance results from a lack of the surface receptor, which is still not identified. It is noteworthy that this is the first time that CDT binding was directly visualized by fluorescence microscopy in CDT-sensitive compared with CDT-insensitive cells.

Cytolethal distending toxins are considered to act as AB toxins, where CdtB is the active subunit ('A' unit), which alone is unable to bind to the cell surface, while CdtA and CdtC are required for toxin binding ('B' unit) (Lee *et al*., 2003; McSweeney and Dreyfus, 2004 and Fig. 1). Interestingly, both these subunits could compete with each other and inhibit binding of the holotoxin, suggesting that CdtA and CdtC bind to the same receptor (Lee *et al*., 2003; McSweeney and Dreyfus, 2004). An increasing number of bacterial toxins, such as cholera toxin, *Aeromonas hydrophila* aerolysin, *Clostridium perfringens* Iota-toxin and *Helicobacter pylori* VacA, have been shown to interact with

microdomains in the plasma membrane, known as lipid rafts (Orlandi and Fishman, 1998; Wolf *et al*., 1998; Abrami and van Der Goot, 1999; Zitzer *et al*., 1999; Waheed *et al*., 2001; Schraw *et al*., 2002). These domains are enriched in cholesterol, sphingolipids and glycosylphosphatidylinositol (GPI)-anchored proteins (reviewed in Brown and London, 1998), and their integrity can be disrupted by drugs which extract cholesterol from the plasma membrane, such as mβCD. It is therefore not surprising that treatment of HeLa cells with mβCD abolished cellular intoxication and HdCDT binding (Fig. 2). We still have to identify the toxin receptor and we are currently pursuing a more detailed analysis of HdCDT binding within lipid rafts.

Our study strongly contributes to the understanding of the CDT biology, as it demonstrates for the first time how a member of the CDT family is internalized via an intact Golgi, and that it is further retrogradely transported to the ER. We show beyond any doubt that the DNA damaging activity of the toxin can be exerted only upon internalization, thereby rejecting previous hypotheses regarding activation of transmembrane signalling pathways. These data also suggest that the toxin may be translocated directly from the ER to the nucleus and raise several questions about the complexity of the nuclear translocation of CDTs, highlighting once more the importance of bacterial toxins as tools for characterization of cellular processes.

Experimental procedures

Cell lines

HeLa and BalbC3T3 (ATCC) cells were cultivated in RPMI 1640 medium supplemented with 10% fetal calf serum (FCS), 5 mM L-glutamine, penicillin (100 units ml^{-1}) and streptomycin (100 μg ml^{-1}) (RPMI complete medium) in a humid atmosphere containing 5% CO_2. HeLa cell lines stably expressing GFP fusion Derlin-1 and Derlin-2 proteins (Derlin-1^{GFP} and Derlin-2^{GFP}) were produced in Dr Hidde Ploegh's laboratory, and will be described in details elsewhere.

Chinese hamster ovary parental cells, and clones CHO16D, CHO23G and CHO24D, selected for resistance to cholera toxin, *P. aeruginosa* ETA and ricin (Teter and Holmes, 2002; Teter *et al*., 2003) were cultivated in Ham's F12 medium supplemented with 10% FCS, 5 mM L-glutamine, penicillin (100 units ml^{-1}) and streptomycin (100 μg ml^{-1}) (Ham's F12 complete medium) in a humid atmosphere containing 5% CO_2.

Reconstitution of the HdCDT holotoxin and intoxication

Reconstitution of the HdCDT toxin was achieved by incubation of the purified CdtA, CdtB or GST-tagged CdtB (when specified) and CdtC subunits for 30 min at 37°C. We have used the following nomenclature throughout this article: non-tagged CdtB subunit is indicated as CdtB, while the GST fusion protein is indicated as GST-CdtB. Similar nomenclature is used for the CdtB-Sulf1 and CdtB-Sulf2 proteins. The term HdCDT indicates the reconstituted toxin containing the non-tagged-CdtB subunit.

The reconstituted toxin containing the GST-CdtB subunit was still able to induce cell cycle arrest in HeLa cells, as assessed by propidium iodide staining, although with a 5- to 10-fold lower efficiency than the holotoxin containing the non-tagged-CdtB subunit (data not shown).

Treatments

Methyl-β-cyclodextrin (mβCD) treatment. Exponentially growing cells were pre-incubated with mβCD (5 mM or 10 mM) for 30 min in FCS-free medium at 37°C. Cells were cooled on ice for 20 min and washed twice with cold phosphate-buffered saline (PBS), before addition of the ice-cold toxin. After toxin exposure on ice for 20 min, cells were washed five times with cold PBS and either incubated for 24 h at 37°C in complete medium for the cell cycle analysis, or processed for the toxin binding analysis as described below.

Brefeldin A (BFA) treatment. Cells were pre-treated with BFA (2.5 μg ml^{-1}) for 1 h at 37°C, and then exposed either to HdCDT or to the negative control, in the presence of BFA, for the indicated period. Cells were then processed for Western blot, phospho-H2AX staining, or pulsed-field gel electrophoresis analysis as described below.

Ionizing radiation. Cells were irradiated (20 Gy), washed once with PBS and incubated for the indicated time periods in RPMI complete medium.

Exotoxin A (ETA) treatment. Sensitivity of the CHO parental cells and the clones CHO16D, CHO23G and CHO24D was tested as previously described (Teter and Holmes, 2002).

Production and purification of the recombinant HdCDT subunits

GST-CdtB. Construction, expression and purification of GST-CdtB was previously described (Frisan *et al*., 2003).

CdtA and CdtC. The pGEX-CdtA and pGEX-CdtC expression vectors were constructed by polymerase chain reaction (PCR) amplification of the *H. ducreyi cdtA* and *cdtC* genes from the pAF-tac1cdtA and pAF-tac1cdtC plasmids, respectively (Frisk *et al*., 2001), using the following primers:

CdtA_1 5′-ATTCGGATCCTGTTCATCAAATCAACGAATGA-3′
CdtA_2 5′-TACCGAATTCTTAATTAACCGCTGTTGCTTCTAAT-3′
CdtC_1 5′-ATTCGGATCCAGTCATGCAGAATCAAATCCTGA-3′
CdtC_2 5′-TACCGAATTCTTAGCTACCCTGATTTCTT-3′.

Each PCR fragment was cloned into the *Bam*HI and *Eco*RI restriction sites of the pGEX4T3 expression vector (Amersham Biosciences, Little Chalfont, Buckinghamshire, UK). Purification and thrombin cleavage of CdtA and CdtC was performed as previously described (Lee *et al*., 2003).

GST-CdtB-Sulf1 and GST-CdtB-Sulf2. A C-terminal extension containing a sulphation site (CdtB-Sulf1) was introduced using as template the *cdtB* nucleotide sequence from the pGEX-CdtB plasmid (Frisan *et al*., 2003). The following primers were used:

CdtB-Sulf1_1 5′-ATTCGGATCCAACTTGAGTGACTTCAAAGTAGC-3′
CdtB-Sulf1_2 5′-TACCGAATTCTCAAGATGGGTATTCGTAGTCTTCTGCGCTGCGATCACGAACAAAACTAAC-3′.

The CdtB-Sulf2 subunit, containing a sulphation and three partly

overlapping N-linked glycosylation sites, was amplified using the CdtB-Sulf1 as template. The following primers were used:

CdtB-Sulf1_1 5′-ATTCGGATCCAACTTGAGTGACTTCAAAGTAGC-3′
CdtB-Sulf2_2 5′-TACCGAATTCTCACTGGGATGTGTTATTTTTGGTGCCGTTAGATGGGTATTCGTAGTCTTCTGCGCT-3′.

The PCR fragment was cloned into the *Bam*HI and *Eco*RI restriction sites of the pGEX4T3 expression vector (Amersham Biosciences). Purification and thrombin cleavage of the fusion protein from the *E. coli* BL21 DE3 strain was performed according to the instructions of the manufacturer (Amersham Biosciences).

CdtBD273R. Mutagenesis of the *cdtB* gene, where the Asp residue in position 273, important for the Mg^{2+} binding was substituted with an Arg residue, was performed using the QuickChange II Site-Directed mutagenesis kit from Stratagene (La Jolla, CA, USA) according to the instructions of the manufacturer. The pGEX-CdtB plasmid (Frisan *et al.*, 2003) was used as template, and the following primers were used:

CdtBD273R_1 5′-CGCTCACAAATTACATCCAGACATTTTCCTGTTAG-3′
CdtBD273R_2 5′-CTAACAGGAAAATGTCTGGATGTAATTTGTGAGCG-3′.

Purification and thrombin cleavage of the CdtBD273R protein, which was found in inclusion bodies in the insoluble fraction, was performed as previously described (Lee *et al.*, 2003).

HdCDT binding assay

Fluorescence microscopy analysis. One hundred thousand cells were grown on 13 mm slides for 24 h. Cells were washed twice with cold PBS and cooled down on ice for 20 min. Cells were left untreated or exposed for 20 min on ice to the following combinations of subunits: (i) CdtA+CdtC, (ii) GST-CdtB alone and (iii) CdtA+CdtC+GST-CdtB, washed five times with cold PBS, and then fixed for 30 min in 1% formaldehyde in PBS on ice. Following fixation, cells were washed twice with PBS, and then further incubated with a goat serum anti-GST fluorescein-conjugated antibody (1:50, Abcam, Cambridge, UK) for 30 min at 25°C. Nuclei were counterstained with Hoechst 33258 (0.5 μg ml^{-1}, Sigma, St Louis, MO, USA), and slides were mounted and viewed via fluorescence microscopy.

FACS analysis. Five hundred thousand cells were grown in 60 mm culture dishes for 24 h. Cells were trypsinized and cooled down on ice for 20 min. Cells were left untreated or exposed for 20 min on ice to the following combinations of subunits: (i) GST-CdtB alone and (ii) CdtA+CdtC+GST-CdtB. After five times washing with cold PBS, cells were fixed for 30 min in 1% formaldehyde in PBS on ice, and then further incubated with a goat serum anti-GST fluorescein-conjugated antibody (1:50, Abcam, Cambridge, UK) for 30 min on ice. Flow cytometry analysis was performed using a FACSort flow cytometer (Becton and Dickinson, Mountain View, CA). Data from 10^4 cells were collected and analysed using the CellQuest software (Becton and Dickinson).

Detection of DNA DSBs by pulsed-field gel electrophoresis

Twenty-five thousand HeLa cells per well were grown in 12-well plates in complete medium containing 4000 Bq [methyl-^{14}C]-thymidine for 48 h. The cells were then washed three times in PBS and chased for 2 h in complete medium. Cells were treated with HdCDT (20 μg ml^{-1}) for the indicated time periods or left untreated for 8 h. Irradiated cells (20 Gy) were used as positive control for detection of DSBs. Cells were washed once in PBS, and trypsinized in a 150 μl volume. The cell suspension was mixed with low gelling-point agarose (InCert, BMA, Rockland, ME, USA) at 37°C to a final agarose concentration of 0.6% and 1×10^6 cells ml^{-1} and pipetted into plastic moulds for 100 μl plugs. Moulds were incubated at 4°C for 20 min to solidify the plugs. The solid plugs were transferred into 1 ml of ice-cold lysis buffer (2% sarkosyl, 1 mg ml^{-1} proteinase K, in 0.5 M Na_3-EDTA, pH 8.0) overnight at 4°C, followed by a second lysis step in high salt solution (1.85 M NaCl, 0.15 M KCl, 5 mM $MgCl_2$, 2 mM EDTA, 4 mM Tris, 0.5% Triton X-100, pH 7.5) overnight at 4°C (Stenerlow *et al.*, 2003). Plugs were washed three times for 1 h in 0.1 M EDTA and double-stranded DNA was separated on an agarose gel (0.8% SeaKem Gold, BMA) in a PFGE unit (Gene Navigator, Amersham Bioscience, Uppsala, Sweden) in TBE ×0.5 as previously described (Stenerlow *et al.*, 2003). Following electrophoresis, the gels were sliced at the position of the 5.7 Mb chromosome from *S. pombe* (BMA), and ^{14}C in the gel segments was measured by liquid scintillation. The fraction of radioactivity corresponding to DNA smaller than 5.7 Mb was used to quantify the number of DSBs (Stenerlöw *et al.*, 1999). The number of DNA DSBs was translated into the equivalent radiation dose (Gy) generating the same amount of DNA DSBs, assuming an induction of 25 DSBs per diploid cell per Gy (Stenerlow *et al.*, 2003).

Sulphation and mannosylation

Sulphation and mannosylation of GST-CdtB-Sulf1 and GST-CdtB-Sulf2 were performed as previously described (Llorente *et al.*, 2003). Briefly, 500 000 HeLa cells were incubated with 600 μCi ml^{-1} $Na_2{}^{35}SO_4$ in DMEM without sulphate or with 100 μCi [^{3}H]-mannose in DMEM without glucose for 4 h at 37°C. HdCDT containing either GST-CdtB-Sulf1 or GST-CdtB-Sulf2 (20 μg ml^{-1}) was added, and the incubation was continued for additional 4 h. Negative controls included: (i) untreated cells, (ii) cells exposed to CdtA+CdtC and (iii) cells exposed to the GST-CdtB-Sulf1 or GST-CdtB-Sulf2 alone. Cells were then washed five times with cold PBS, and lysed in 1 ml lysis buffer (0.1 M NaCl, 10 mM Na_2HPO_4, 1 mM EDTA, 1% Triton X-100, 1 mM PMSF) for 30 min on ice. Nuclei were removed by centrifugation, and the GST fusion proteins were recovered with Gluthatione sepharose as described by the manufacturer (Amersham Biosciences), and analysed by SDS-PAGE as previously described (Rapak *et al.*, 1997). Labelled proteins were detected by PhosphoImager analysis.

Western blot analysis

Proteins were fractionated by 12% SDS-polyacrylamide gels, transferred to PVDF membranes (Millipore, Bedford, MA) and probed with anti-cdc2 (Transduction Laboratories, Lexinton, KY). Blots were developed with enhanced chemoluminescence (ECL; Amersham Biosciences), using the appropriate horseradish peroxidase-labelled secondary antibody, according to the instructions of the manufacturer (Amersham Biosciences).

Fluorescence microscopy

Fifty thousand cells were seeded on 13 mm diameter slides (Merck, Darmstadt, Germany) in 24-well plates in 1 ml of RPMI complete medium and allowed to adhere for 24 h. Cells were treated as specified in the figure legends (Figs 1D and 3A) and fixed with ice cold methanol for 20 min at −20°C. Slides were washed twice in PBS, blocked in 10% FCS in PBS for 30 min at room temperature, and incubated for 1 h at 37°C with the phospho-H2AX-specific rabbit serum (Upstate Biotechnology, Lake Placid, NY, USA), diluted 1:200 in 1% BSA in PBS. Slides were washed three times for 5 min in PBS, and then incubated with the appropriate fluorescein isothiocyanate (FITC)-conjugated secondary antibody (Dako, Glostrup, Denmark, diluted 1:40 in 1% BSA in PBS) for 30 min at 37°C. Nuclei were counter-stained with Hoechst 33258 (Sigma, 0.5 μg ml^{-1} for 1 min at 20°C). Slides were mounted and viewed via fluorescence microscopy. Cells were scored positive for pH2AX foci formation when more than five foci/nucleus were detected.

Cell cycle analysis

Cells were trypsinized, centrifuged and washed once with PBS. The cell pellet was resuspended and fixed on ice for 15 min with 1 ml of cold 70% ethanol. The cells were subsequently centrifuged and resuspended in 1 ml of propidium iodide (PI) solution (0.05 mg ml^{-1} PI; 0.02 mg ml^{-1} RNase; 0.3% NP40; 1 mg ml^{-1} sodium citrate) for 1 h at 4°C. Flow cytometry analysis was performed using a FACSort flow cytometer (Becton and Dickinson, Mountain View, CA). Data from 10^4 cells were collected and analysed using the CellQuest software (Becton and Dickinson).

Colony assay

Ten thousand cells were grown in 100 mm culture dishes in 10 ml of Ham's F12 complete medium for 24 h. Cells were intoxicated or left untreated and further incubated for 2 weeks (medium was changed every fourth day). Cell growth was monitored as formation of foci (colonies). Cell colonies were stained with haematoxylin and eosin as follows: cells were washed twice with PBS, and then stained with 2 ml of haematoxylin and eosin solution (Giemsa solution, Merck Darmstadt, Germany) for 10 min at 22°C, and excess dye was removed by gentle washing with distilled water. Plates were allowed to dry at 22°C.

Acknowledgements

We are grateful to Dr Katja Pokrovskaja for advice on fluorescence microscopy. This work was supported by the Swedish Research Council (#05969 and #15012), the Swedish Cancer Society (#4972-B04-01XAB) and the Karolinska Institutet. T.F. is supported by the Swedish Research Council (#K2005-16P-15440-01A).

References

Abrami, L., and van Der Goot, F.G. (1999) Plasma membrane microdomains act as concentration platforms to facilitate intoxication by aerolysin. *J Cell Biol* **147:** 175–184.

Baeuerle, P.A., and Huttner, W.B. (1987) Tyrosine sulfation is a *trans*-Golgi-specific protein modification. *J Cell Biol* **105:** 2655–2664.

Brown, D.A., and London, E. (1998) Functions of lipid rafts in biological membranes. *Annu Rev Cell Dev Biol* **14:** 111–136.

Cortes-Bratti, X., Chaves-Olarte, E., Lagergård, T., and Thelestam, M. (1999) The cytolethal distending toxin from the chancroid bacterium *Haemophilus ducreyi* induces cell-cycle arrest in the G2 phase. *J Clin Invest* **103:** 107–115.

Cortes-Bratti, X., Chaves-Olarte, E., Lagergård, T., and Thelestam, M. (2000) Cellular internalization of cytolethal distending toxin from *Haemophilus ducreyi*. *Infect Immun* **68:** 6903–6911.

Cortes-Bratti, X., Karlsson, C., Lagergård, T., Thelestam, M., and Frisan, T. (2001) The *Haemophilus ducreyi* cytolethal distending toxin induces cell cycle arrest and apoptosis via the DNA damage checkpoint pathways. *J Biol Chem* **276:** 5296–5302.

van Dam, E.M., Ten Broeke, T., Jansen, K., Spijkers, P., and Stoorvogel, W. (2002) Endocytosed transferrin receptors recycle via distinct dynamin and phosphatidylinositol 3-kinase-dependent pathways. *J Biol Chem* **277:** 48876–48883.

Desjardins, M. (2003) ER-mediated phagocytosis: a new membrane for new functions. *Nat Rev Immunol* **3:** 280–291.

Dreyfus, L.A. (2003) Cytolethal distending toxins. In *Bacterial Protein Toxins*. Burns, D.L., Barbieri, J.T., Iglewski, B.H., and Rappuoli, R. (eds). Washington, DC: American Society for Microbiology Press, pp. 257–270.

Echevarria, W., Leite, M.F., Guerra, M.T., Zipfel, W.R., and Nathanson, M.H. (2003) Regulation of calcium signals in the nucleus by a nucleoplasmic reticulum. *Nat Cell Biol* **5:** 440–446.

Elwell, C.A., and Dreyfus, L.A. (2000) DNase I homologous residues in CdtB are critical for cytolethal distending toxin-mediated cell cycle arrest. *Mol Microbiol* **37:** 952–963.

Frisan, T., Cortes-Bratti, X., Chaves-Olarte, E., Stenerlöw, B., and Thelestam, M. (2003) The *Haemophilus ducreyi* cytolethal distending toxin induces DNA double strand breaks and promotes ATM-dependent activation of RhoA. *Cell Micro* **5:** 695–707.

Frisk, A., Lebens, M., Johansson, C., Ahmed, H., Svensson, L., Ahlman, K., and Lagergård, T. (2001) The role of different protein components from the *Haemophilus ducreyi* cytolethal distending toxin in the generation of cell toxicity. *Microb Pathog* **30:** 313–324.

Fujiwara, T., Oda, K., Yokota, S., Takatsuki, A., and Ikehara, Y. (1988) Brefeldin A causes disassembly of the Golgi complex and accumulation of secretory proteins in the endoplasmic reticulum. *J Biol Chem* **263:** 18545–18552.

Haghjoo, E., and Galan, J.E. (2004) *Salmonella typhi* encodes a functional cytolethal distending toxin that is delivered into host cells by a bacterial-internalization pathway. *Proc Natl Acad Sci USA* **101:** 4614–4619.

Hampton, R.Y. (2002) ER-associated degradation in protein quality control and cellular regulation. *Curr Opin Cell Biol* **14:** 476–482.

Hassane, D.C., Lee, R.B., Mendenhall, M.D., and Pickett, C.L. (2001) Cytolethal distending toxin demonstrates genotoxic activity in a yeast model. *Infect Immun* **69:** 5752–5759.

Hassane, D.C., Lee, R.B., and Pickett, C.L. (2003) *Campylobacter jejuni* cytolethal distending toxin promotes DNA

repair responses in normal human cells. *Infect Immun* **71:** 541–545.
Helenius, A., and Aebi, M. (2004) Roles of N-linked glycans in the endoplasmic reticulum. *Annu Rev Biochem* **73:** 1019–1049.
Hunziker, W., Whitney, J.A., and Mellman, I. (1991) Selective inhibition of transcytosis by brefeldin A in MDCK cells. *Cell* **67:** 617–627.
Lara-Tejero, M., and Galan, J.E. (2000) A bacterial toxin that controls cell cycle progression as a deoxyribonuclease I-like protein. *Science* **290:** 354–357.
Lara-Tejero, M., and Galan, J.E. (2001) CdtA, CdtB and CdtC form a tripartite complex that is required for cytolethal distending toxin activity. *Infect Immun* **69:** 4358–4365.
Lee, R.B., Hassane, D.C., Cottle, D.L., and Pickett, C.L. (2003) Interactions of *Campylobacter jejuni* cytolethal distending toxin subunits CdtA and CdtC with HeLa cells. *Infect Immun* **71:** 4883–4890.
Lencer, W.I., and Tsai, B. (2003) The intracellular voyage of cholera toxin: going retro. *Trends Biochem Sci* **28:** 639–645.
Li, L., Sharipo, A., Chaves-Olarte, E., Masucci, M.G., Levitsky, V., Thelestam, M., and Frisan, T. (2002) The *Haemophilus ducreyi* cytolethal distending toxin activates sensors of DNA damage and repair complexes in proliferating and non-proliferating cells. *Cell Micro* **4:** 87–99.
Lilley, B.N., and Ploegh, H.L. (2004) A membrane protein required for dislocation of misfolded proteins from the ER. *Nature* **429:** 834–840.
Llorente, A., Lauvrak, S.U., van Deurs, B., and Sandvig, K. (2003) Induction of direct endosome to endoplasmic reticulum transport in Chinese hamster ovary (CHO) cells (LdlF) with a temperature-sensitive defect in epsilon-coatomer protein (epsilon-COP). *J Biol Chem* **278:** 35850–35855.
McSweeney, L.A., and Dreyfus, L.A. (2004) Nuclear localization of the *Escherichia coli* cytolethal distending toxin CdtB subunit. *Cell Microbiol* **6:** 447–458.
Mordente, J.A., Konno, S., Chen, Y., Wu, J.M., Tazaki, H., and Mallouh, C. (1998) The effects of brefeldin A (BFA) on cell cycle progression involving the modulation of the retinoblastoma protein (pRB) in PC-3 prostate cancer cells. *J Urol* **159:** 275–279.
Nesic, D., Hsu, Y., and Stebbins, C.E. (2004) Assembly and function of a bacterial genotoxin. *Nature* **429:** 429–433.
Nishikubo, S., Ohara, M., Ueno, Y., Ikura, M., Kurihara, H., Komatsuzawa, H., *et al.* (2003) An N-terminal segment of the active component of the bacterial genotoxin cytolethal distending toxin B (CDTB) directs CDTB into the nucleus. *J Biol Chem* **278:** 50671–50681.
Orlandi, P.A., and Fishman, P.H. (1998) Filipin-dependent inhibition of cholera toxin: evidence for toxin internalization and activation through caveolae domains. *J Cell Biol* **141:** 905–915.
Prydz, K., Hansen, S.H., Sandvig, K., and van Deurs, B. (1992) Effects of brefeldin A on endocytosis, transcytosis and transport to the Golgi complex in polarized MDCK cells. *J Cell Biol* **119:** 259–272.
Rapak, A., Falnes, P.Ø., and Olsnes, S. (1997) Retrograde transport of mutant ricin to the endoplasmic reticulum with subsequent translocation to cytosol. *Proc Natl Acad Sci USA* **94:** 3783–3788.
Robinson, M.S. (2004) Adaptable adaptors for coated vesicles. *Trends Cell Biol* **14:** 167–174.
Sandvig, K., and van Deurs, B. (2002) Membrane traffic exploited by protein toxins. *Annu Rev Cell Dev Biol* **18:** 1–24.
Schmitz, A., Herrgen, H., Winkeler, A., and Herzog, V. (2000) Cholera toxin is exported from microsomes by the Sec61p complex. *J Cell Biol* **148:** 1203–1212.
Schraw, W., Li, Y., McClain, M.S., van der Goot, F.G., and Cover, T.L. (2002) Association of *Helicobacter pylori* vacuolating toxin (VacA) with lipid rafts. *J Biol Chem* **277:** 34642–34650.
Shenker, B.J., Besack, D., McKay, T., Pankoski, L., Zekavat, A., and Demuth, D.R. (2004) *Actinobacillus actinomycetemcomitans* cytolethal distending toxin (Cdt): evidence that the holotoxin is composed of three subunits: CdtA, CdtB, and CdtC. *J Immunol* **172:** 410–417.
Simpson, J.C., Roberts, L.M., Romisch, K., Davey, J., Wolf, D.H., and Lord, J.M. (1999) Ricin A chain utilises the endoplasmic reticulum-associated protein degradation pathway to enter the cytosol of yeast. *FEBS Lett* **459:** 80–84.
Stenerlöw, B., Höglund, E., and Carlsson, J. (1999) Induction and rejoining of large DNA fragments after ion radiation. *Radiat Res* **151:** 642–648.
Stenerlow, B., Karlsson, K.H., Cooper, B., and Rydberg, B. (2003) Measurement of prompt DNA double-strand breaks in mammalian cells without including heat-labile sites: results for cells deficient in nonhomologous end joining. *Radiat Res* **159:** 502–510.
Teter, K., and Holmes, R.K. (2002) Inhibition of endoplasmic reticulum-associated degradation in CHO cells resistant to cholera toxin, *Pseudomonas aeruginosa* exotoxin A, and ricin. *Infect Immun* **70:** 6172–6179.
Teter, K., Jobling, M.G., and Holmes, R.K. (2003) A class of mutant CHO cells resistant to cholera toxin rapidly degrades the catalytic polypeptide of cholera toxin and exhibits increased endoplasmic reticulum-associated degradation. *Traffic* **4:** 232–242.
Thelestam, M., and Frisan, T. (2004a) Cytolethal distending toxins. *Rev Physiol Biochem Pharmacol* **152:** 111–133.
Thelestam, M., and Frisan, T. (2004b) *A. actinomycetemcomitans* cytolethal distending toxin. *J Immunol* **172:** 5813; author reply 5813–5814.
Waheed, A.A., Shimada, Y., Heijnen, H.F., Nakamura, M., Inomata, M., Hayashi, M., *et al.* (2001) Selective binding of perfringolysin O derivative to cholesterol-rich membrane microdomains (rafts). *Proc Natl Acad Sci USA* **98:** 4926–4931.
Wesche, J., Rapak, A., and Olsnes, S. (1999) Dependence of ricin toxicity on translocation of the toxin A-chain from the endoplasmic reticulum to the cytosol. *J Biol Chem* **274:** 34443–34449.
Wolf, A.A., Jobling, M.G., Wimer-Mackin, S., Ferguson-Maltzman, M., Madara, J.L., Holmes, R.K., and Lencer, W.I. (1998) Ganglioside structure dictates signal transduction by cholera toxin and association with caveolae-like membrane domains in polarized epithelia. *J Cell Biol* **141:** 917–927.
Ye, Y., Shibata, Y., Yun, C., Ron, D., and Rapoport, T.A. (2004) A membrane protein complex mediates retrotranslocation from the ER lumen into the cytosol. *Nature* **429:** 841–847.
Zitzer, A., Zitzer, O., Bhakdi, S., and Palmer, M. (1999) Oligomerization of *Vibrio cholerae* cytolysin yields a pentameric pore and has a dual specificity for cholesterol and sphingolipids in the target membrane. *J Biol Chem* **274:** 1375–1380.

Biochimica et Biophysica Acta 1793 (2009) 489–495

Contents lists available at ScienceDirect

Biochimica et Biophysica Acta

journal homepage: www.elsevier.com/locate/bbamcr

A novel mode of translocation for cytolethal distending toxin

Lina Guerra [a], Kathleen N. Nemec [b], Shane Massey [b], Suren A. Tatulian [c], Monica Thelestam [a], Teresa Frisan [a], Ken Teter [b,*]

[a] Department of Cell and Molecular Biology, Karolinska Institutet, Stockholm, Sweden
[b] Department of Molecular Biology and Microbiology, Burnett School of Biomedical Science, College of Medicine, University of Central Florida, Orlando, Florida, USA
[c] Department of Physics, University of Central Florida, Orlando, Florida, USA

ARTICLE INFO

Article history:
Received 18 July 2008
Received in revised form 10 November 2008
Accepted 20 November 2008
Available online 11 December 2008

Keywords:
Cytolethal distending toxin
Circular dichroism
Endoplasmic reticulum
Fluorescence spectroscopy
20S proteasome
Toxin translocation

ABSTRACT

Thermal instability in the toxin catalytic subunit may be a common property of toxins that exit the endoplasmic reticulum (ER) by exploiting the mechanism of ER-associated degradation (ERAD). The *Haemophilus ducreyi* cytolethal distending toxin (HdCDT) does not utilize ERAD to exit the ER, so we predicted the structural properties of its catalytic subunit (HdCdtB) would differ from other ER-translocating toxins. Here, we document the heat-stable properties of HdCdtB which distinguish it from other ER-translocating toxins. Cell-based assays further suggested that HdCdtB does not unfold before exiting the ER and that it may move directly from the ER lumen to the nucleoplasm. These observations suggest a novel mode of ER exit for HdCdtB.

1. Introduction

The *Haemophilus ducreyi* cytolethal distending toxin (HdCDT) is an AB-type genotoxin that consists of a catalytic A moiety (HdCdtB) and a cell-binding B moiety (HdCdtA+HdCdtC) [1]. Like many AB toxins, HdCDT must travel from the plasma membrane to the endoplasmic reticulum (ER) before its A moiety can escape the endomembrane system to reach its target [2,3]. Translocation of the A chain from the ER to the cytosol is thought to involve the ER-associated degradation (ERAD) quality control system [4,5], but HdCDT intoxication is not inhibited by alterations to ERAD that generate resistance against five other ER-translocating toxins: *Pseudomonas aeruginosa* exotoxin A, *Escherichia coli* heat-labile toxin IIb, cholera toxin (CT), plasmid-encoded toxin, and ricin [3,6–9]. Thus, exit of HdCdtB from the ER occurs by an ERAD-independent mechanism or by an ERAD mechanism that is significantly different from the pathway utilized by many other ER-translocating toxins. HdCDT is also unique in that it must reach the nucleus in order to function whereas other ER-translocating toxins act in the cytosol.

ERAD-mediated toxin translocation may depend upon the heat-labile nature of the isolated toxin A chain. The catalytic CTA1 polypeptide, the A subunit of pertussis toxin (PT S1), and ricin A chain are all in partially or fully unfolded states at near-physiological temperatures [10–12]. However, thermal instability is not apparent when the toxin A chain is present in a holotoxin [13–15]. A/B subunit dissociation, an event that occurs in the ER translocation site, could thus serve as the trigger for toxin unfolding. This structural shift would identify the toxin A chain as a misfolded protein and would thereby promote its ERAD-mediated export into the cytosol. Most ERAD substrates are rapidly degraded in the cytosol by the ubiquitin-26S proteasome system, but the A chains of ER-translocating toxins are thought to avoid this fate because they have a paucity of the lysine residues that serve as ubiquitin attachment sites [4]. The translocated A chains may instead be degraded by a relatively slow, ubiquitin-independent mechanism involving the core 20S proteasome [11,12,16].

The distinctive nature of the HdCDT translocation mechanism suggested that HdCdtB may not exhibit the same physical characteristics observed for the A chains of other ER-translocating toxins. To test this prediction, biophysical and biochemical experiments were performed on the purified HdCdtB protein. We found that, in contrast to the A chains of other ER-translocating toxins, HdCdtB was heat-

Abbreviations: CT, cholera toxin; CD, circular dichroism; CDT, cytolethal distending toxin; ER, endoplasmic reticulum; ERAD, endoplasmic reticulum-associated degradation; GST, glutathione S-transferase; HdCDT, *Haemophilus ducreyi* cytolethal distending toxin; EC_{50}, half-maximal effective concentration; PT, pertussis toxin

* Corresponding author. Biomolecular Research Annex, 12722 Research Parkway, Orlando, Florida 32826, USA. Tel.: +1 407 882 2247; fax: +1 407 384 2062.
E-mail address: kteter@mail.ucf.edu (K. Teter).

0167-4889/$ – see front matter © 2008 Elsevier B.V. All rights reserved.
doi:10.1016/j.bbamcr.2008.11.017

stable and resistant to degradation by the 20S proteasome. Cell-based assays further suggested that HdCdtB does not unfold before exiting the ER and that it may move directly from the ER lumen to the nucleoplasm. These results highlight the distinctive nature of CDT and suggest the cellular processing of HdCdtB differs from host–toxin interactions involving other ER-translocating toxins.

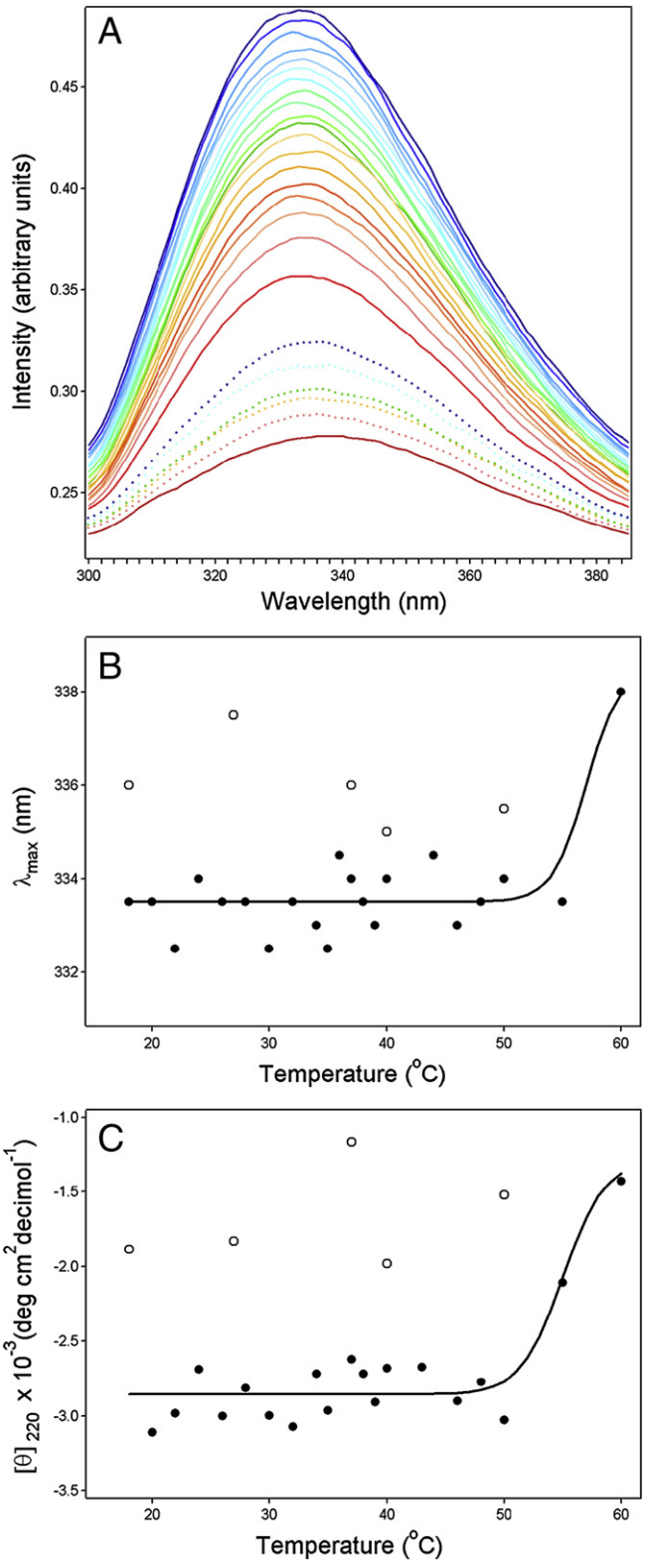

2. Materials and methods

2.1. Biophysical studies

HdCdtB was purified from *E. coli* transformed with a glutathione S-transferase (GST)-CdtB expression vector as previously described [17]. After removal of the GST tag, biophysical measurements were performed on 0.15 mg HdCdtB in 0.2 ml 10 mM Hepes (pH 7.0) with 1 mM $CaCl_2$ as described [11]. For fluorescence measurements, the samples were excited at 280 nm and emission spectra recorded between 300 to 400 nm. For circular dichroism (CD) measurements, ellipticity, θ, was measured between 200 nm and 250 nm using a J-810 spectrofluoropolarimeter (Jasco Corp., Tokyo, Japan). After subtracting the spectra of the buffer, the mean residue molar ellipticity was calculated as $[\theta]=\theta\ /ncl$, where θ is the measured ellipticity in millidegrees, n is the number of residues per molecule, c is the molar concentration, and l is the optical path-length in mm. The temperature dependencies of the maximum fluorescence emission wavelengths or the ellipticities were fitted with theoretical curves as described previously [11].

2.2. Degradation assays

The protease sensitivity assay and the 20S proteasome assay were performed as previously described [11]. The CTA1/CTA2 heterodimer was purchased from Calbiochem (La Jolla, CA); thermolysin was purchased from Sigma-Aldrich (St. Louis, MO); and the 20S proteasome was purchased from Boston Biochem (Cambridge, MA).

2.3. Toxicity assays

The assay for HdCDT induction of H2AX phosphorylation was performed as previously described [18]. HdCDT was reconstituted from individual subunits as described in [3]. The 2 μg/ml concentration of HdCDT used for this assay represents the minimal amount of toxin required to elicit an effect in 100% of the cells after 2 h of intoxication. Toxicity assays with ricin (Vector Laboratories, Burlingame, CA) were based upon the toxin-induced inhibition of protein synthesis as described in [16].

2.4. Construction of CdtB-CVIM

A C-terminal extension containing the -CVIM farnesylation site was introduced into CdtB using the *cdtB* nucleotide sequence from the pGEX-CdtB-sulf1 plasmid [3] as a template. The following primers were used:

5′-ATTCGGATCCAACTTGAGTGACTTCAAAGTAGC-3′ and 5′-TACCGAATTCTCACATGATCACACACCCAGATGGGTATTCGTAGTCTTCTG-CGCTGCGATCACGAACAAAACTAAC-3′

The PCR fragment was cloned into the BamHI and EcoRI restriction sites of the pGEX4T3 expression vector (GE Healthcare, Piscataway, NJ). Purification of the fusion protein produced in *E. coli* strain BL21

Fig. 1. HdCdtB thermal stability. Temperature-induced changes to the structure of HdCdtB were monitored by fluorescence spectroscopy (A, B) and far-UV CD (C). Both measurements were conducted near-simultaneously on the same sample after equilibration at each temperature for 3 min. Three scans per spectra were collected and averaged to improve the signal-to-noise ratio. (A) The change in color from blue to red corresponds to a step-wise increase in temperature from 18 °C to 60 °C. Dotted lines are spectra of samples cooled to 50 °C, 40 °C, 37 °C, 25 °C, and 18 °C after HdCdtB was heated to 60 °C; colors indicate the same temperatures as the solid lines. (B) The maximum emission wavelengths (λ_{max}) from panel A were plotted as a function of temperature. Data points from the cooled HdCdtB spectra are presented as open circles. (C) For far-UV CD analysis, the mean residue molar ellipticities at 220 nm ($[\theta]_{220}$) were plotted as a function of temperature. Data points from the cooled HdCdtB spectra are presented as open circles. The solid lines in panels B and C are best fit curves simulated as described in Ref. [11].

DE3 was performed according to the instructions of the manufacturer (GE Healthcare).

2.5. Farnesylation assays

Detergent phase partitioning of lysates from cells exposed for 4 h to 50 μg/ml of a CDT holotoxin containing the GST-CdtB-CVIM subunit was performed as previously described [19]. GST-CdtB-CVIM was recovered from aqueous and detergent phases of the lysates by affinity purification with glutathione sepharose 4B for 1 h at 4 °C. Western blot was then performed using a horse radish peroxidase-conjugated anti-GST antibody (Novus Biologicals, Littleton, CO). In vitro farnesylation of GST-CdtB-CVIM was demonstrated by mixing 5 μg of the protein with 35 μl rabbit reticulocyte lysate (Sigma-Aldrich), 1 mM $MgCl_2$, and 5 mM farnesyl pyrophosphate (Sigma-Aldrich) for 1 h at 37 °C. Detergent phase partitioning of the reaction product was performed as described in [19].

2.6. Confocal microscopy

HeLa cells grown on coverslips were transfected with 2 μg of the pDSRed2-ER vector (Clontech, Mountain View, CA) using the Lipofectamine 2000 Reagent (Invitrogen, Carlsbad, CA) according to the manufacturer's instructions. The pDSRed2-ER vector encodes a recombinant protein consisting of a *Discosoma* sp. red fluorescent protein appended with an amino-terminal signal sequence for co-translational targeting to the ER lumen and a carboxy-terminal KDEL ER retention motif. At 24 h post-transfection, cells were exposed for 4 h to 10 μg/ml of a CDT holotoxin containing a GST-tagged CdtB subunit [17]. The cells were then fixed with 4% paraformaldehyde and permeabilized with 0.2% Triton X-100 in phosphate buffered saline for 10 min at 22 °C. Non-specific antibody binding was blocked by incubation with 3% bovine serum albumin in phosphate buffered saline for 30 min at 22 °C. GST-CdtB was visualized using a fluorescein-conjugated goat anti-GST antibody (Abcam, Cambridge, MA) at 1:50 dilution for 30 min at 25 °C. Cells were viewed with a Nikon TE 300 confocal microscope, and images were captured using the Perkin Elmer (Waltham, MA) UltraViewERS software.

3. Results

3.1. Thermal stability of HdCdtB

Fluorescence spectroscopy and far-UV CD were used to examine the thermal stability of HdCdtB (Fig. 1), a 29 kDa protein with ~13% α-helix content and ~40% β-sheet content [20,21]. Measurements were conducted with buffer conditions (pH 7.0, 1 mM Ca^{2+}) that approximated the physiological conditions of the ER (pH 7.2, 0.5 mM Ca^{2+}) [22–25]. Fluorescence spectroscopy detected the solvent exposure of previously buried aromatic residues by a red shift in the maximum emission wavelength (Fig. 1A and B). These readings demonstrated that substantial disordering of the HdCdtB tertiary structure did not occur at 37 °C. In fact, sample heating to 60 °C was required to observe the disordering of HdCdtB tertiary structure. Near-simultaneous measurements of fluorescence and CD spectra were performed on the same HdCdtB sample in a 4 mm×4 mm optical path-length rectangular quartz cuvette in order to reduce sample-to-sample variability. This procedure generated some noise in the far-UV CD spectra because of the relatively large optical path-length (not shown). Nevertheless, analysis of the ellipticity at 220 nm (which reflects the α-helical and β-sheet secondary structures) demonstrated that substantial denaturation of the HdCdtB secondary structure only occurred at temperatures above 50 °C (Fig. 1C). Thus, significant unfolding of HdCdtB did not occur at physiological temperature. The conformational changes that occurred at high temperatures were not completely reversible, as the red shift of the fluorescence spectra and the reduced ellipticity did not return to their initial values upon sample cooling to 18 °C (Fig. 1B and C).

3.2. Proteolysis of HdCdtB

The thermal stability of HdCdtB was also examined with a protease sensitivity assay (Fig. 2A). This technique is often used to probe the folding state of a protein, as properly folded proteins are generally more resistant to proteolysis than unfolded variants of the same protein [10,26–28]. To detect temperature-induced changes in the folding state of HdCdtB, toxin samples were incubated at temperatures ranging from 4 °C to 45 °C for 45 min. The samples were then placed on ice and incubated with thermolysin for another 45 min at 4 °C. Finally, EDTA and sample buffer were added to halt the proteolytic digestions. Thermolysin is a calcium-dependent metalloprotease that hydrolyzes peptide bonds on the amino side of bulky hydrophobic residues [27]. The use of this specific protease thus allowed us to detect temperature-induced conformational changes that resulted in the exposure of previously buried hydrophobic residues. For comparative purposes, parallel experiments were run with the reduced CTA1/CTA2 heterodimer. Reduction of the CTA1/CTA2 disulfide bond normally occurs in the ER of an intoxicated cell [29]; this event was reproduced in vitro by including 10 mM β-mercaptoethanol in the assay buffer. Previous work has demonstrated the complete dissociation of CTA1 from CTA2 under this reducing condition [12].

HdCdtB exhibited considerable resistance to proteolysis with thermolysin when incubated at temperatures up to 45 °C. In contrast, reduced CTA1 was completely degraded at temperatures ≥41 °C, and substantial degradation of the CTA1 sample pre-incubated at 37 °C was observed as well. Temperatures ≥33 °C also induce PT S1 to assume a thermolysin-sensitive conformation [11]. Thus, at physiological temperature CTA1 and PT S1 contain surface-exposed hydrophobic residues that could trigger the ERAD translocation mechanism. HdCdtB, in contrast, exhibited remarkable heat stability and thermolysin resistance when compared to the A chains of other ER-translocating toxins.

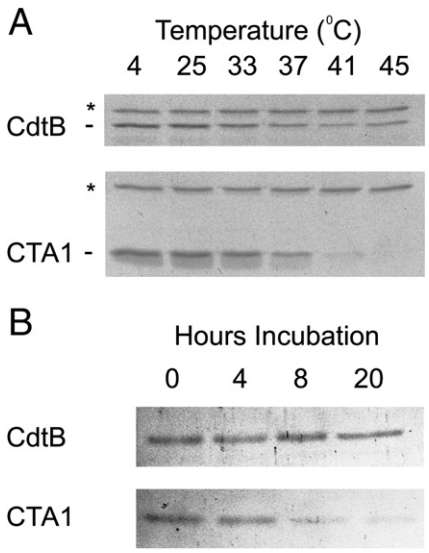

Fig. 2. HdCdtB proteolysis. (A) HdCdtB or the CTA1/CTA2 heterodimer was placed in 20 mM Na-phosphate buffer (pH 7.0) containing 10 mM β-mercaptoethanol. After incubation at the indicated temperatures for 45 min, thermolysin was added for an additional 45 min at 4 °C. Proteolysis was halted by the addition of EDTA and sample buffer. The toxins were then visualized by SDS-PAGE and Coomassie staining. For both gels, the upper thermolysin band is denoted with an asterisk. (B) HdCdtB or the reduced CTA1/CTA2 heterodimer was placed in assay buffer with 100 nM of the 20S proteasome. Proteolysis was halted after 0, 4, 8, or 20 h of incubation at 37 °C. The toxins were then visualized by SDS-PAGE and Coomassie staining.

In vitro, reduced CTA1 and reduced PT S1 are susceptible to ubiquitin-independent degradation by the core 20S proteasome [11,12]. As the 20S proteasome only acts upon unfolded substrates [30], toxin processing by this form of the proteasome is likely linked to thermal instability in the toxin A chain. The relatively heat-stable nature of HdCdtB would therefore render it resistant to degradation by the 20S proteasome. To test this prediction, we incubated HdCdtB or the reduced CTA1/CTA2 heterodimer with the purified 20S proteasome (Fig. 2B). Little to no degradation of HdCdtB occurred during the 20 h time frame of this experiment. In contrast, degradation of the reduced 21 kDa CTA1 polypeptide was evident at 4 h of incubation and was nearly complete by 8 h of incubation. Thus, HdCdtB was not an effective substrate for the 20S proteasome.

3.3. Unique features of HdCdtB translocation

Most proteins require at least partial unfolding in order to move from the ER to the cytosol, yet our data indicated that the isolated HdCdtB subunit is in a folded conformation at 37 °C. To examine the role of A chain unfolding in HdCDT intoxication, we performed toxicity assays with glycerol-treated HeLa cells (Fig. 3). Chemical chaperones such as glycerol prevent protein unfolding [31] and block intoxication with five distinct ER-translocating toxins: ricin [32], exotoxin A [32], plasmid-encoded toxin [33], CT, and Shiga toxin 2 (Teter et. al, unpublished observations). An inhibition of HdCDT activity in glycerol-treated cells would therefore suggest that a chaperone-assisted unfolding step may be necessary for HdCdtB to reach its target.

Toxicity assays were performed on HdCDT-treated HeLa cells incubated in the absence or presence of 10% glycerol (Fig. 3A, B). Cells were exposed to HdCDT and glycerol for a 2 h co-incubation before screening for toxic effects. In parallel experiments, cells were also pre-incubated with glycerol for 1 h before a 2 h co-incubation with HdCDT and glycerol. Prolonged incubation with glycerol was toxic to the cells, so we could not assess HdCDT intoxication by its long-term effect of cell cycle arrest. Phosphorylation of the histone H2AX has been shown to occur early in the CDT intoxication process [18] and was therefore used as an alternative measure of intoxication. Exposure to glycerol did not prevent the phosphorylation of H2AX in HdCDT-treated cells (Fig. 3A, B), but it did block intoxication with ricin (Fig. 3C). The latter result demonstrated that our experimental procedure was sufficient to inhibit the activity of a prototypical ER-translocating toxin. Importantly, glycerol treatment alone did not result in the phosphorylation of H2AX (Fig. 3A, B). These collective observations emphasized the unusual aspects of HdCDT intoxication, a process which may not require A chain unfolding prior to translocation.

We have previously suggested that HdCdtB may bypass the cytosol and move directly from the ER to the nucleus [1,3]. This atypical translocation mechanism would be distinct from the ERAD-mediated pathway that exports heat-labile toxin A chains to the cytosol. To further examine this putative translocation route, we generated a recombinant HdCDT that contains a CVIM-tagged HdCdtB subunit. The C-terminal CVIM farnesylation motif can serve as an indicator of protein localization to the cytosol because farnesylation, which increases the hydrophobicity of the target protein, is a cytosolic modification [34]. The recombinant HdCdtB also contained an N-terminal GST tag to facilitate protein purification and detection.

A farnesylated protein will partition into the detergent phase of Triton X-114, whereas an unmodified variant of the same protein will partition into the aqueous phase. We confirmed that GST-HdCdtB-CVIM behaved in this predicted manner by performing an in vitro farnesylation assay. Purified GST-HdCdtB-CVIM partitioned into the aqueous phase of Triton X-114 (Fig. 4A, left panel). However, GST-HdCdtB-CVIM partitioned into the detergent phase of Triton X-114 when it was exposed to the farnesylation machinery present in a reticulocyte lysate (Fig. 4A, right panel). The farnesylation of GST-HdCdtB-CVIM could therefore be detected by detergent phase partitioning of the modified toxin.

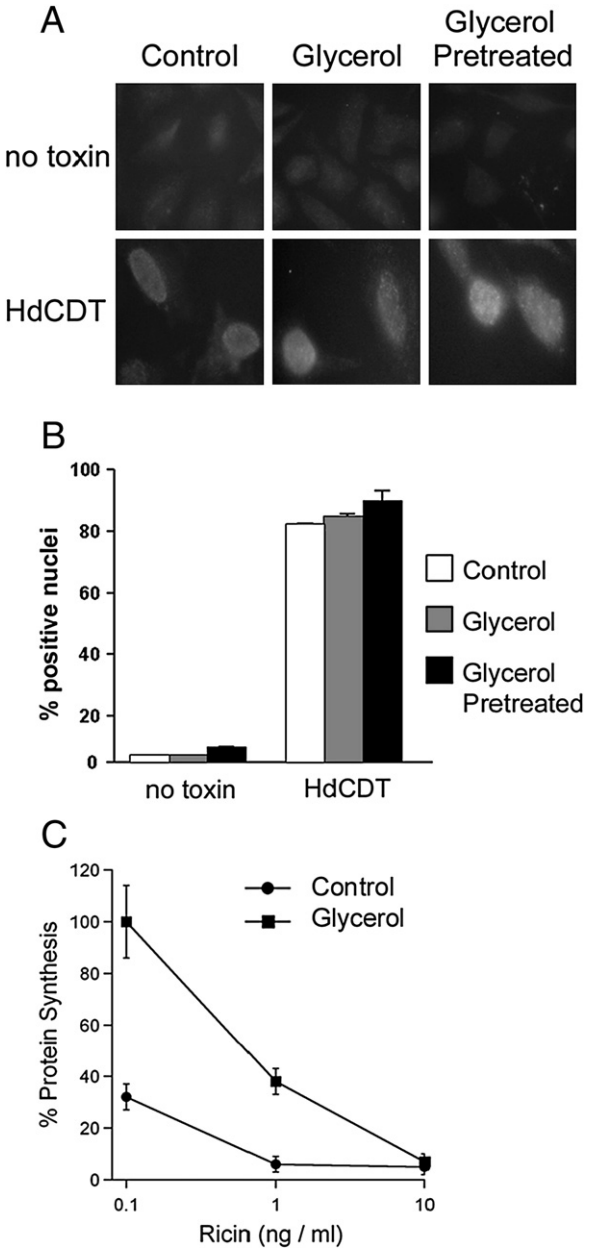

Fig. 3. HdCDT toxicity. (A, B) HeLa cells were incubated with no toxin or with 2 μg/ml of HdCDT for 2 h in medium alone (control) or medium supplemented with 10% glycerol. As indicated, one set of cells were pretreated with 10% glycerol medium for 1 h before a further 2 h incubation with glycerol in the absence (no toxin) or presence of HdCDT. (A) Toxin-induced phosphorylation of histone H2AX was visualized in fixed cells with a rabbit anti-phospho-H2AX antibody and a FITC-conjugated swine anti-rabbit IgG antibody. One of two experiments is shown. (B) The graph charts the average percentage (±range) of nuclei positive for H2AX foci from both experiments. (C) HeLa cells were incubated with various concentrations of ricin for 4 h in the absence or presence of 10% glycerol before protein synthesis levels were quantified. Measurements taken from unintoxicated cells incubated in the absence or presence of glycerol were used to establish the 100% value for the corresponding experimental condition. The average±range of two independent experiments with triplicate samples is shown.

For in vivo experiments, we incorporated GST-HdCdtB-CVIM into a CDT holotoxin. HeLa cells were exposed to 50 μg/ml of the recombinant holotoxin for 4 h before cell extracts were generated with a Triton X-114 lysis buffer. As shown in Fig. 4B, GST-HdCdtB-CVIM could only be found in the aqueous phase of the cell extract. This indicated that no detectable pool of HdCdtB was modified by

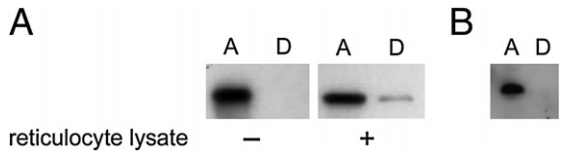

Fig. 4. HdCdtB translocation. (A) Purified GST-HdCdtB-CVIM was incubated in the absence or presence of rabbit reticulocyte lysate before placement in cold 1% Triton X-114. Aqueous (A) and detergent (D) phases of Triton X-114 were isolated by centrifugation of the warmed samples. The distribution of GST-HdCdtB-CVIM was then determined by Western blot analysis of the separate detergent and aqueous phases. (B) For in vivo farnesylation of GST-HdCdtB-CVIM, HeLa cells were exposed for 4 h to 50 μg/ml of a recombinant CDT holotoxin that contained the GST-HdCdtB-CVIM subunit. After lysis in 1% Triton X-114, aqueous (A) and detergent (D) phases were separated. GST-HdCdtB-CVIM was recovered by affinity purification and visualized by Western-blot analysis as described in Materials and methods.

the cytosolic farnesylation machinery. Cells exposed to an HdCdtA/HdCdtC heterodimer or to GST-HdCdtB-CVIM alone did not produce an HdCdtB signal (data not shown). This demonstrated that the protein detected in vivo was GST-HdCdtB-CVIM and that, as expected, an intact holotoxin was required to deliver GST-HdCdtB-CVIM into the target cell. Given the robust HdCdtB signal present in the aqueous phase of the HeLa cell extract, any trace amount of farnesylated GST-HdCdtB-CVIM would represent an exceedingly small pool of the total protein.

Methods such as Western blot analysis that directly monitor the toxin itself are less sensitive than toxicity assays and therefore require higher toxin doses for experimentation. Thus, it was necessary to use 25-fold more HdCDT for the farnesylation assay than for the toxicity assay of Fig. 3. The relatively short-term intoxication periods of 2–4 h for our in vivo experiments also required the use of high toxin concentrations. In our previous work, a 4 h exposure to 20 μg/ml of HdCDT was required to detect sulfation and mannosylation of the recombinant HdCdtB subunit [3]. This toxin concentration did not alter the cellular responses in terms of biochemical signaling. Likewise, the 4 h exposure to 50 μg /ml of toxin that was required for our farnesylation assay did not alter the cell morphology as determined by actin and nuclear staining. Furthermore, the cellular distension that is only seen after long-term intoxications was not observed in cells exposed to 50 μg/ml of HdCDT for 4 h. Collectively, these observations indicated that the high toxin concentration required for our farnesylation assay did not alter the cellular response to HdCDT intoxication.

A direct ER-to-nucleoplasm translocation route would bypass the cytosolic farnesylation machinery and therefore leave HdCdtB in an unmodified state. Confocal microscopy was used to further examine this putative translocation route (Fig. 5). HeLa cells were exposed for 4 h to 10 μg/ml of a recombinant CDT holotoxin that contained a GST-tagged CdtB subunit [17]. The cellular location of GST-CdtB was then compared to the distribution of DsRed2-ER, a fluorescent marker for the ER. GST-CdtB and DsRed2-ER could be found in a branching, tubularized network that was contiguous with the nuclear envelope (arrows). GST-CdtB could also be found in the nucleus but could not be detected in the cytosol. As with the farnesylation data, this suggested that HdCdtB bypasses the cytosol and moves directly from the ER to the nucleus. Finally, GST-CdtB and DsRed2-ER were visualized in invaginations of the nuclear envelope that protruded into the nucleus (arrowheads). These structures have been previously visualized in unintoxicated cells and are morphologically defined as the nucleoplasmic reticulum [35–37]. By visualizing DsRed2-ER in unintoxicated HeLa cells, we confirmed that the tubular protrusions were a normal cellular structure rather than a byproduct of HdCDT intoxication and that the DsRed2-ER signal did not bleed into the fluorescein channel used to visualize GST-CdtB (not shown). Localization to the nucleoplasmic reticulum (i.e., the nuclear protrusions) has not been reported for other toxins that have been visualized in the ER [19,24,38–40]. This again emphasized the unique aspects of HdCDT intoxication. The functional relevance of these nuclear protrusions in regards to CDT intoxication has yet to be determined.

4. Discussion

CDTs are produced by numerous Gram-negative pathogens [1]. They are the only known bacterial AB toxins that function primarily by direct damage to the host cell DNA. CdtB accordingly acts within the nucleus, whereas other toxin A chains act within the cytosol. Our current study demonstrates that, in addition to its unique target and unique site of action, CdtB also exhibits unique structural properties which affect its interaction with the host cell and distinguish it from the A chains of other ER-translocating toxins.

With the exception of the *Salmonella* Typhi CDT [41], the family of CDTs are tripartite toxins composed of a cell-binding CdtA/CdtC subunit and a catalytic CdtB subunit. Both CdtA and CdtC are required for the optimal biological activity of CDT, but the two proteins do not appear to play equivalent roles in cell binding and cellular uptake [1,42–46]. Although the exact roles of CdtA and CdtC in toxin endocytosis and intracellular trafficking remain to be determined, it is well-established that CdtB must exit the endomembrane system and reach the nucleus in order to elicit a cytotoxic effect [2,3,45,47]. HdCdtB escape from the endomembrane system occurs at the level of the ER and involves an ERAD-independent mechanism or an ERAD mechanism that is significantly different from the pathway utilized by other ER-translocating toxins [3].

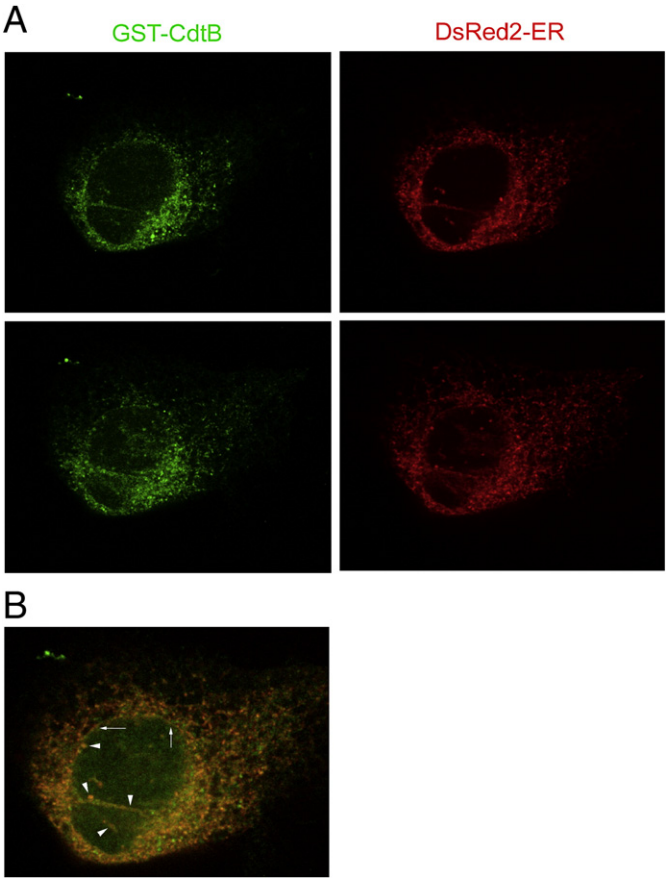

Fig. 5. Intracellular distribution of HdCdtB. Transfected HeLa cells expressing DsRed2-ER, a fluorescent marker for the ER, were exposed for 4 h to 10 μg/ml of a recombinant CDT holotoxin that contained a GST-HdCdtB subunit. The cells were then fixed and stained with a fluorescein-conjugated anti-GST antibody. (A) Labeling patterns for DsRed2-ER and GST-CdtB from two Z-sections of a single cell. (B) The merged image of DsRed2-ER and GST-CdtB distributions. Arrows denote the nuclear envelope; arrowheads denote invaginations of the nucleoplasmic reticulum.

Many ER-translocating toxins exploit ERAD for passage into the cytosol [4,5]. For three of these toxins – CT, PT, and ricin – thermal instability in the isolated catalytic subunit may activate the ERAD mechanism [10–12]. The heat-labile nature of the toxin A chain could also facilitate its ubiquitin-independent degradation by the 20S proteasome. Our results provide previously unknown evidence that HdCdtB maintains its folded conformation at 37 °C in buffer conditions that mimic the physiology of the ER. This offers a structural basis for the previously reported ERAD-independent mechanism of HdCdtB export from the ER [3]: since HdCdtB does not unfold at 37 °C, it is not recognized as an ERAD substrate. The thermal stability of HdCdtB also protects it from degradation by the 20S proteasome, a proteolytic machine that can only act upon unfolded proteins. Finally, CDT is the only known ER-translocating toxin that can function in glycerol-treated cells. The structural and cellular events involved with HdCdtB export from the ER are therefore distinct from those events involving other ER-translocating toxins.

The productive intoxication of glycerol-treated cells suggests that HdCdtB unfolding is not required for its exit from the ER. It is structurally feasible for HdCdtB to exit the ER in a folded state, as passage of folded proteins through the Sec61 translocon pore has been documented [48]. The translocon, which can dilate to 60 Å in diameter [49], could accommodate the 45 Å diameter of an isolated, folded CdtB subunit [50]. Flexibility in the structure of CdtB [50] could also allow the folded toxin to assume a conformation suitable for passage through the Sec61p translocon or other pores in the ER membrane.

Our data further suggest that HdCdtB follows a unique translocation route involving direct passage from the ER to the nucleus. However, we cannot currently discount the possibility that HdCdtB first enters the cytosol and then rapidly moves into the nucleus through the nuclear pore complex. Atypical nuclear localization sequences in other CdtB subunits [51,52] are often used as evidence for a cytosol-to-nucleus transport route, but these sequences could also serve as retrieval motifs to return an escaped pool of toxin to the nucleus. Likewise, the KDEL motif in CT is thought to act as an ER retention motif rather than as a primary ER targeting motif [53]. Given the many unique aspects of HdCdtB translocation, we favor the ER-to-nucleus model of HdCdtB translocation and are currently working to define the molecular details of this process.

Acknowledgements

This work was supported by NIH grants K22 AI054568 and R01 AI073783 to K. Teter. T. Frisan was supported by funds from the Swedish Research Council, the Swedish Cancer Society, The Åke-Wiberg Foundation, and the Karolinska Institutet. We thank Sandra Geden for technical assistance with the in vitro farnesylation assay.

References

[1] M. Thelestam, T. Frisan, Cytolethal distending toxins, in: J.E. Alouf, M.R. Popoff (Eds.), The Comprehensive Sourcebook of Bacterial Protein Toxins, Academic Press, San Diego, 2006, pp. 448–467.
[2] X. Cortes-Bratti, E. Chaves-Olarte, T. Lagergard, M. Thelestam, Cellular internalization of cytolethal distending toxin from *Haemophilus ducreyi*, Infect. Immun. 68 (2000) 6903–6911.
[3] L. Guerra, K. Teter, B.N. Lilley, B. Stenerlow, R.K. Holmes, H.L. Ploegh, K. Sandvig, M. Thelestam, T. Frisan, Cellular internalization of cytolethal distending toxin: a new end to a known pathway, Cell. Microbiol. 7 (2005) 921–934.
[4] B. Hazes, R.J. Read, Accumulating evidence suggests that several AB-toxins subvert the endoplasmic reticulum-associated protein degradation pathway to enter target cells, Biochemistry 36 (1997) 11051–11054.
[5] J.M. Lord, L.M. Roberts, W.I. Lencer, Entry of protein toxins into mammalian cells by crossing the endoplasmic reticulum membrane: co-opting basic mechanisms of endoplasmic reticulum-associated degradation, Curr. Top. Microbiol. Immunol. 300 (2005) 149–168.
[6] S.E. Geden, R.A. Gardner, M.S. Fabbrini, M. Ohashi, O. Phanstiel IV, K. Teter, Lipopolyamine treatment increases the efficacy of intoxication with saporin and an anticancer saporin conjugate, FEBS J. 274 (2007) 4825–4836.
[7] K. Teter, R.K. Holmes, Inhibition of endoplasmic reticulum-associated degradation in CHO cells resistant to cholera toxin, *Pseudomonas aeruginosa* exotoxin A, and ricin, Infect. Immun. 70 (2002) 6172–6179.
[8] K. Teter, M.G. Jobling, R.K. Holmes, A class of mutant CHO cells resistant to cholera toxin rapidly degrades the catalytic polypeptide of cholera toxin and exhibits increased endoplasmic reticulum-associated degradation, Traffic 4 (2003) 232–242.
[9] F. Navarro-Garcia, A. Canizalez-Roman, K.E. Burlingame, K. Teter, J.E. Vidal, Pet, a non-AB toxin, is transported and translocated into epithelial cells by a retrograde trafficking pathway, Infect. Immun. 75 (2007) 2101–2109.
[10] R.H. Argent, A.M. Parrott, P.J. Day, L.M. Roberts, P.G. Stockley, J.M. Lord, S.E. Radford, Ribosome-mediated folding of partially unfolded ricin A-chain, J. Biol. Chem. 275 (2000) 9263–9269.
[11] A.H. Pande, D. Moe, M. Jamnadas, S.A. Tatulian, K. Teter, The pertussis toxin S1 subunit is a thermally unstable protein susceptible to degradation by the 20S proteasome, Biochemistry 45 (2006) 13734–13740.
[12] A.H. Pande, P. Scaglione, M. Taylor, K.N. Nemec, S. Tuthill, D. Moe, R.K. Holmes, S.A. Tatulian, K. Teter, Conformational instability of the cholera toxin A1 polypeptide, J. Mol. Biol. 374 (2007) 1114–1128.
[13] B. Goins, E. Freire, Thermal stability and intersubunit interactions of cholera toxin in solution and in association with its cell-surface receptor ganglioside GM1, Biochemistry 27 (1988) 2046–2052.
[14] T. Krell, F. Greco, M.C. Nicolai, J. Dubayle, G. Renauld-Mongenie, N. Poisson, I. Bernard, The use of microcalorimetry to characterize tetanus neurotoxin, pertussis toxin and filamentous haemagglutinin, Biotechnol. Appl. Biochem. 38 (2003) 241–251.
[15] L.S. Jackson, W.H. Tolleson, S.J. Chirtel, Thermal inactivation of ricin using infant formula as a food matrix, J. Agric. Food Chem. 54 (2006) 7300–7304.
[16] E.D. Deeks, J.P. Cook, P.J. Day, D.C. Smith, L.M. Roberts, J.M. Lord, The low lysine content of ricin A chain reduces the risk of proteolytic degradation after translocation from the endoplasmic reticulum to the cytosol, Biochemistry 41 (2002) 3405–3413.
[17] T. Frisan, X. Cortes-Bratti, E. Chaves-Olarte, B. Stenerlow, M. Thelestam, The *Haemophilus ducreyi* cytolethal distending toxin induces DNA double-strand breaks and promotes ATM-dependent activation of RhoA, Cell. Microbiol. 5 (2003) 695–707.
[18] L. Li, A. Sharipo, E. Chaves-Olarte, M.G. Masucci, V. Levitsky, M. Thelestam, T. Frisan, The *Haemophilus ducreyi* cytolethal distending toxin activates sensors of DNA damage and repair complexes in proliferating and non-proliferating cells, Cell. Microbiol. 4 (2002) 87–99.
[19] K. Teter, R.L. Allyn, M.G. Jobling, R.K. Holmes, Transfer of the cholera toxin A1 polypeptide from the endoplasmic reticulum to the cytosol is a rapid process facilitated by the endoplasmic reticulum-associated degradation pathway, Infect. Immun. 70 (2002) 6166–6171.
[20] L.D. Cope, S. Lumbley, J.L. Latimer, J. Klesney-Tait, M.K. Stevens, L.S. Johnson, M. Purven, R.S. Munson Jr., T. Lagergard, J.D. Radolf, E.J. Hansen, A diffusible cytotoxin of *Haemophilus ducreyi*, Proc. Natl. Acad. Sci. U. S. A. 94 (1997) 4056–4061.
[21] D. Nesic, Y. Hsu, C.E. Stebbins, Assembly and function of a bacterial genotoxin, Nature 429 (2004) 429–433.
[22] M.M. Wu, J. Llopis, S.R. Adams, J.M. McCaffery, K. Teter, M.S. Kulomaa, T.E. Machen, H.P. Moore, R.Y. Tsien, Studying organelle physiology with fusion protein-targeted avidin and fluorescent biotin conjugates, Methods Enzymol. 327 (2000) 546–564.
[23] M.J. Barrero, M. Montero, J. Alvarez, Dynamics of [Ca2+] in the endoplasmic reticulum and cytoplasm of intact HeLa cells. A comparative study, J. Biol. Chem. 272 (1997) 27694–27699.
[24] J.H. Kim, L. Johannes, B. Goud, C. Antony, C.A. Lingwood, R. Daneman, S. Grinstein, Noninvasive measurement of the pH of the endoplasmic reticulum at rest and during calcium release, Proc. Natl. Acad. Sci. U. S. A. 95 (1998) 2997–3002.
[25] A.M. Hofer, I. Schulz, Quantification of intraluminal free [Ca] in the agonist-sensitive internal calcium store using compartmentalized fluorescent indicators: some considerations, Cell Calcium 20 (1996) 235–242.
[26] B. Tsai, C. Rodighiero, W.I. Lencer, T.A. Rapoport, Protein disulfide isomerase acts as a redox-dependent chaperone to unfold cholera toxin, Cell 104 (2001) 937–948.
[27] S.J. Bark, N. Muster, J.R. Yates 3rd, G. Siuzdak, High-temperature protein mass mapping using a thermophilic protease, J. Am. Chem. Soc. 123 (2001) 1774–1775.
[28] J.P. Renn, P.L. Clark, A conserved stable core structure in the passenger domain beta-helix of autotransporter virulence proteins, Biopolymers 89 (2008) 420–427.
[29] P.A. Orlandi, Protein-disulfide isomerase-mediated reduction of the A subunit of cholera toxin in a human intestinal cell line, J. Biol. Chem. 272 (1997) 4591–4599.
[30] O. Coux, K. Tanaka, A.L. Goldberg, Structure and functions of the 20S and 26S proteasomes, Annu. Rev. Biochem. 65 (1996) 801–847.
[31] K. Romisch, A cure for traffic jams: small molecule chaperones in the endoplasmic reticulum, Traffic 5 (2004) 815–820.
[32] K. Sandvig, I.H. Madshus, S. Olsnes, Dimethyl sulphoxide protects cells against polypeptide toxins and poliovirus, Biochem. J. 219 (1984) 935–940.
[33] P. Scaglione, K.N. Nemec, K.E. Burlingame, A. Grabon, J. Huerta, F. Navarro-Garcia, S.A. Tatulian, K. Teter, Structural characteristics of the plasmid-encoded toxin from enteroaggregative *Escherichia coli*, Biochemistry 47 (2008) 9582–9591.
[34] S. Clarke, Protein isoprenylation and methylation at carboxyl-terminal cysteine residues, Annu. Rev. Biochem. 61 (1992) 355–386.
[35] M. Fricker, M. Hollinshead, N. White, D. Vaux, Interphase nuclei of many mammalian cell types contain deep, dynamic, tubular membrane-bound invaginations of the nuclear envelope, J. Cell Biol. 136 (1997) 531–544.
[36] W. Echevarria, M.F. Leite, M.T. Guerra, W.R. Zipfel, M.H. Nathanson, Regulation of calcium signals in the nucleus by a nucleoplasmic reticulum, Nat. Cell Biol. 5 (2003) 440–446.

[37] T.A. Lagace, N.D. Ridgway, The rate-limiting enzyme in phosphatidylcholine synthesis regulates proliferation of the nucleoplasmic reticulum, Mol. Biol. Cell 16 (2005) 1120–1130.
[38] I.V. Majoul, P.I. Bastiaens, H.D. Soling, Transport of an external Lys-Asp-Glu-Leu (KDEL) protein from the plasma membrane to the endoplasmic reticulum: studies with cholera toxin in Vero cells, J. Cell Biol. 133 (1996) 777–789.
[39] L. Johannes, D. Tenza, C. Antony, B. Goud, Retrograde transport of KDEL-bearing B-fragment of Shiga toxin, J. Biol. Chem. 272 (1997) 19554–19561.
[40] M.G. Castro, U. McNamara, N.H. Carbonetti, Expression, activity and cytotoxicity of pertussis toxin S1 subunit in transfected mammalian cells, Cell. Microbiol. 3 (2001) 45–54.
[41] S. Spano, J.E. Ugalde, J.E. Galan, Delivery of a *Salmonella* Typhi exotoxin from a host intracellular compartment, Cell Host Microbe 3 (2008) 30–38.
[42] K. Deng, J.L. Latimer, D.A. Lewis, E.J. Hansen, Investigation of the interaction among the components of the cytolethal distending toxin of *Haemophilus ducreyi*, Biochem. Biophys. Res. Commun. 285 (2001) 609–615.
[43] R.B. Lee, D.C. Hassane, D.L. Cottle, C.L. Pickett, Interactions of *Campylobacter jejuni* cytolethal distending toxin subunits CdtA and CdtC with HeLa cells, Infect. Immun. 71 (2003) 4883–4890.
[44] X. Mao, J.M. DiRienzo, Functional studies of the recombinant subunits of a cytolethal distending holotoxin, Cell. Microbiol. 4 (2002) 245–255.
[45] S. Akifusa, W. Heywood, S.P. Nair, G. Stenbeck, B. Henderson, Mechanism of internalization of the cytolethal distending toxin of *Actinobacillus actinomycetemcomitans*, Microbiology 151 (2005) 1395–1402.
[46] M. Lara-Tejero, J.E. Galan, CdtA, CdtB, and CdtC form a tripartite complex that is required for cytolethal distending toxin activity, Infect. Immun. 69 (2001) 4358–4365.
[47] K. Boesze-Battaglia, D. Besack, T. McKay, A. Zekavat, L. Otis, K. Jordan-Sciutto, B.J. Shenker, Cholesterol-rich membrane microdomains mediate cell cycle arrest induced by *Actinobacillus actinomycetemcomitans* cytolethal-distending toxin, Cell. Microbiol. 8 (2006) 823–836.
[48] E. Fiebiger, C. Story, H.L. Ploegh, D. Tortorella, Visualization of the ER-to-cytosol dislocation reaction of a type I membrane protein, EMBO J. 21 (2002) 1041–1053.
[49] B.D. Hamman, J.C. Chen, E.E. Johnson, A.E. Johnson, The aqueous pore through the translocon has a diameter of 40–60 Å during cotranslational protein translocation at the ER membrane, Cell 89 (1997) 535–544.
[50] J.S. Hontz, M.T. Villar-Lecumberri, B.M. Potter, M.D. Yoder, L.A. Dreyfus, J.H. Laity, Differences in crystal and solution structures of the cytolethal distending toxin B subunit: relevance to nuclear translocation and functional activation, J. Biol. Chem. 281 (2006) 25365–25372.
[51] L.A. McSweeney, L.A. Dreyfus, Nuclear localization of the *Escherichia coli* cytolethal distending toxin CdtB subunit, Cell. Microbiol. 6 (2004) 447–458.
[52] S. Nishikubo, M. Ohara, Y. Ueno, M. Ikura, H. Kurihara, H. Komatsuzawa, E. Oswald, M. Sugai, An N-terminal segment of the active component of the bacterial genotoxin cytolethal distending toxin B (CDTB) directs CDTB into the nucleus, J. Biol. Chem. 278 (2003) 50671–50681.
[53] W.I. Lencer, B. Tsai, The intracellular voyage of cholera toxin: going retro, Trends Biochem. Sci. 28 (2003) 639–645.

OPEN ACCESS Freely available online

PLoS one

A Bacterial Cytotoxin Identifies the RhoA Exchange Factor Net1 as a Key Effector in the Response to DNA Damage

Lina Guerra[1☯], Heather S. Carr[3☯], Agneta Richter-Dahlfors[2], Maria G. Masucci[1], Monica Thelestam[1], Jeffrey A. Frost[3], Teresa Frisan[1]*

1 Department of Cell and Molecular Biology, Karolinska Institutet, Stockholm, Sweden, **2** Department of Neuroscience, Karolinska Institutet, Stockholm, Sweden, **3** Department of Integrative Biology and Pharmacology, University of Texas Health Science Center at Houston, Houston, Texas, United States of America

Abstract

Background: Exposure of adherent cells to DNA damaging agents, such as the bacterial cytolethal distending toxin (CDT) or ionizing radiations (IR), activates the small GTPase RhoA, which promotes the formation of actin stress fibers and delays cell death. The signalling intermediates that regulate RhoA activation and promote cell survival are unknown.

Principal Findings: We demonstrate that the nuclear RhoA-specific Guanine nucleotide Exchange Factor (GEF) Net1 becomes dephosphorylated at a critical inhibitory site in cells exposed to CDT or IR. Expression of a dominant negative Net1 or Net1 knock down by iRNA prevented RhoA activation, inhibited the formation of stress fibers, and enhanced cell death, indicating that Net1 activation is required for this RhoA-mediated responses to genotoxic stress. The Net1 and RhoA-dependent signals involved activation of the Mitogen-Activated Protein Kinase p38 and its downstream target MAPK-activated protein kinase 2.

Significance: Our data highlight the importance of Net1 in controlling RhoA and p38 MAPK mediated cell survival in cells exposed to DNA damaging agents and illustrate a molecular pathway whereby chronic exposure to a bacterial toxin may promote genomic instability.

Citation: Guerra L, Carr HS, Richter-Dahlfors A, Masucci MG, Thelestam M, et al. (2008) A Bacterial Cytotoxin Identifies the RhoA Exchange Factor Net1 as a Key Effector in the Response to DNA Damage. PLoS ONE 3(5): e2254. doi:10.1371/journal.pone.0002254

Editor: Neil Hotchin, University of Birmingham, United Kingdom

Received February 27, 2008; **Accepted** April 16, 2008; **Published** May 28, 2008

Funding: Swedish Research Council, Swedish Cancer Society, the Ake-Wiberg Foundation, Karolinska Institutet, the European Community Integrated Project on Infection and Cancer (INCA), Susan G. Komen Breast Cancer Foundation. None of the funding agencies contributed to design, conduct or analyze the data in this study.

Competing Interests: The authors have declared that no competing interests exist.

* E-mail: Teresa.Frisan@ki.se

☯ These authors contributed equally to this work.

Introduction

Cytolethal distending toxins (CDTs), produced by several pathogenic Gram-negative bacteria, are protein toxins which cause DNA damage (reviewed in [1]). The active holotoxin is a tripartite complex [2,3], formed by the CdtA, CdtB and CdtC subunits, (reviewed in [1]). Cellular intoxication with CDT induces DNA double strand breaks and activation of checkpoint responses that, depending on the cell type, lead to arrest in the G1 or G2 phases of the cell cycle [4–6]. These effects are similar to those caused by ionizing radiation (IR), which is a well-characterized DNA-damaging agent. Activation of the DNA damage responses by CDT is consistent with the functional and structural homology of the CdtB subunit with mammalian DNase I [7–9].

In adherent cells, CDT intoxication and exposure to IR are associated with the formation of actin stress fibers, via activation of the small GTPase RhoA [6]. While a large amount of data is available regarding the activation of RhoA upon stimulation of plasma membrane-bound receptors [10], the molecular mechanisms regulating RhoA activation in response to these and other DNA-damaging agents are still unknown. It is noteworthy that, since RhoA activation occurs in the cytosol, the signals that regulate its activation in response to DNA damage must be then transduced from the nucleus.

Guanine nucleotide exchange factors (GEFs) are key activators of the small GTPases that regulate the switch between the inactive GDP-bound and the active GTP-bound forms of the GTPase (reviewed in [11]). The vast majority of the known RhoA-specific GEFs exhibit a cytoplasmic localization. One remarkable exception is the RhoA-specific GEF encoded by the neuroepithelioma transforming gene 1 (*Net1*) that is normally found in the nucleus of mammalian cells (reviewed in [11]). Net1 was originally isolated in a tissue culture screen for transforming genes in NIH 3T3 cell focus formation assays [12]. The oncogenic form of Net1 isolated from this screen lacked the first 145 amino acids. A deletion mutant of Net1 lacking the first 121 amino acids was shown to be constitutively active and induced: i) formation of actin stress fibers; ii) activation of the Mitogen-Activated Protein Kinase (MAPK) JNK; and iii) activation of the serum response factor (SRF) [13,14].

The regulation of Net1 activity is poorly understood. PAK1-dependent phosphorylation of Net1 on Ser152 and Ser153 inhibits its GEF activity and abolishes Net1-dependent RhoA activation and stress fiber induction [15]. In addition, translocation of Net1 from the nucleus to the cytoplasm is required for activation of RhoA. The amino-terminus of Net1 contains multiple nuclear localization signals, and deletion of this domain is associated with accumulation of a constitutively active Net1 in the cytoplasm [14]. Taken together these data suggest that the activation of Net1 requires both changes in the phosphorylation pattern of specific inhibitory sites and shuttling between the nucleus and the cytoplasm, but the signals that trigger these events are still unknown.

In the present study, we have identified DNA damage as a trigger for Net1 activation. We show that inhibition of Net1 prevents RhoA activation and stress fiber formation, and promotes cell death upon intoxication or irradiation. We also demonstrate that the Net1/RhoA dependent signals converges on the activation of p38 MAPK and its downstream target MK2, indicating that RhoA plays an important role in controlling the activation of this MAPK pathway in response to genotoxic agents.

Results

DNA damage induces Net1 activation

We have previously shown that exposure to DNA damaging agents induces activation of the small GTPase RhoA, which delays cell death [6]. In order to investigate how the signal delivered by DNA damage is transduced from the nucleus to the cytosol, we have studied the activation of the RhoA specific GEF Net1 in response to CDT or IR. These genotoxic agents were chosen since they both induce DNA double strand breaks and activate identical DNA damage checkpoint responses in mammalian cells [4–6]. Decreased phosphorylation of Net1 on the key negative regulatory site Ser152 was used as the hallmark of Net1 activation [15].

Endogenous Net1 was immunoprecipitated from HeLa cells left untreated or exposed to CDT for 12h, and the levels of Ser152 phosphorylation were assessed by western blot using a phospho-specific antibody. As shown in Figure 1A, the phosphorylation of endogenous Net1 on Ser152 (pS152-Net1) was significantly decreased in intoxicated cells. To assess whether dephosphorylation of Net1 is a reproducible effect of DNA damage, HeLa cells were transfected with a plasmid expressing an HA-epitope-tagged Net1A, the major Net1 isoform expressed in these cells [16]. The transfected cells were then exposed to CDT or IR and the expression of total and phosphorylated Net1 was monitored over time. A 70% decrease in the levels of pS152-Net1A was observed within 30 min after irradiation. The effect was similar to that achieved by CDT intoxication where low levels of p152-Net1A were maintained for at least 12h (Figure 1B and data not shown). Thus, exposure to DNA damage induces dephosphorylation of Net1 on its negative regulatory site.

Net1 is required for activation of RhoA and remodelling of the actin cytoskeleton in response to DNA damage

To assess whether Net1 is required for activation of RhoA, the expression of endogenous Net1 was knocked down by RNAi prior to intoxication or irradiation. Transfection with a short hairpin loop interfering RNA expressing plasmid or siRNA oligonucleotides were used to inhibit Net1 expression. Transfection of cells with Net1 specific shRNA resulted in 90% reduction of the endogenous Net1 96h after transfection (Figure 2A), while transfection with a specific siRNA resulted in 60 to 70 percent reduction 72h after transfection (Figure 2B). Since the effects of Net1 specific shRNA or siRNA were reproducibly similar, the

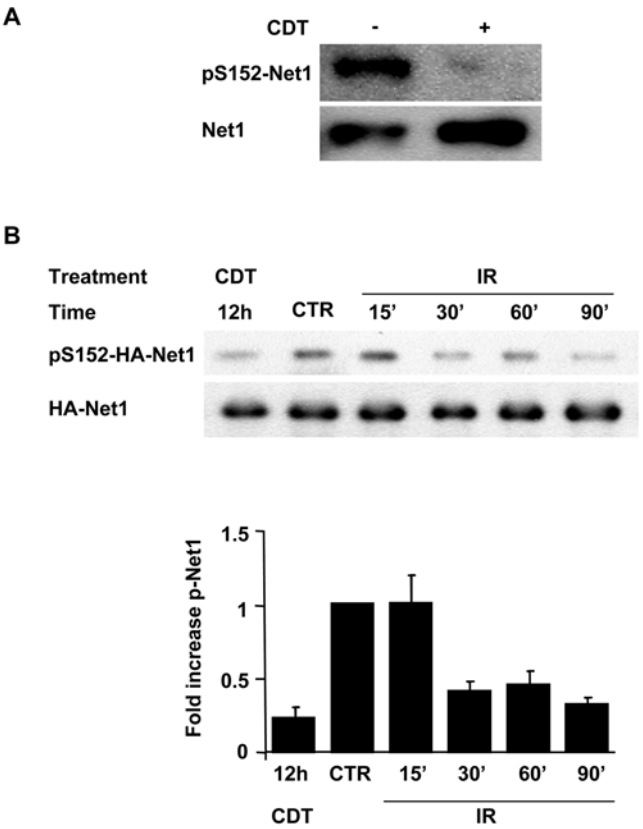

Figure 1. Decreased phosphorylation of Net1 upon induction of DNA damage. A) HeLa cells were left untreated or treated with CDT (2 μg ml^{-1}) for 12h. The endogenous Net1 protein was immunoprecipitated using a goat α-Net1 antibody, and samples were analyzed by western blot using a rabbit serum specific for Net1 phosphorylated on Ser152 (pS152-Net1). **B)** HeLa cells, grown in 12-well plate, were transfected with a HA-epitope tagged Net1A expression plasmid (4 μg/well). Twenty-four hours after transfection, the cells were left untreated (indicated as CTR), or: i) irradiated (20 Gy), and incubated for the indicated time; ii) exposed to CDT (2 μg ml^{-1}) for 12h. The HA-Net1A protein was immunoprecipitated using an α-HA antibody, and the levels of Net1 phosphorylated on Ser152 (pS152-HA-Net1) were assessed as in Figure 1A. The same membrane was re-probed with an α-HA antibody (HA-Net1). The fold increase represents the ratio between the levels of pS152-Net1 in treated cells and the levels of pS152-Net1 in untreated cells (mean±SD of three independent experiments).
doi:10.1371/journal.pone.0002254.g001

results of Net1 knock down experiments have been summarized together and are henceforth indicated as iRNA. Consistent with our previous results [6], a 2- to 4-fold increase in the levels of GTP-bound RhoA was observed in irradiated or intoxicated HeLa cells as compared to the untreated controls. Knock down of endogenous Net1 blocked the activation of RhoA in response to IR or CDT (Figure 2C). Similar results were obtained in cells expressing the dominant negative Net1ΔDH (data not shown). This effect was not due to a general impairment of RhoA-dependent responses since Net1 knock down did not prevent RhoA activation or the formation of actin stress fibers in cells treated with cytotoxic necrotizing factor 1 (CNF1) that constitutively activates RhoA by deamidating Gln-63 and preventing hydrolysis of bound GTP (Figures 2C and 2D).

We next examined whether blockade of Net1 affected the RhoA-dependent formation of actin stress fibers in HeLa cells exposed to CDT. Induction of stress fibers was detected upon intoxication in approximately 80% of control non-transfected cells

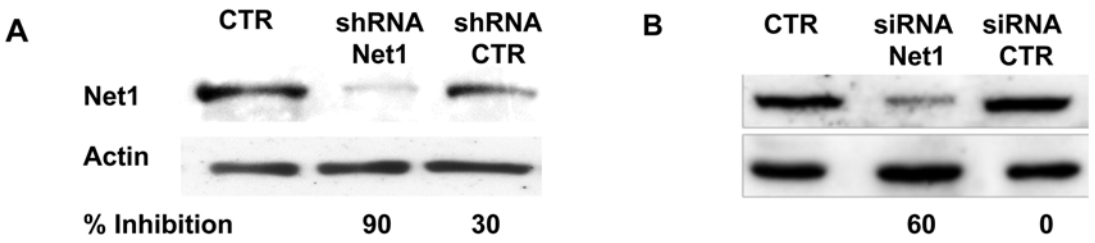

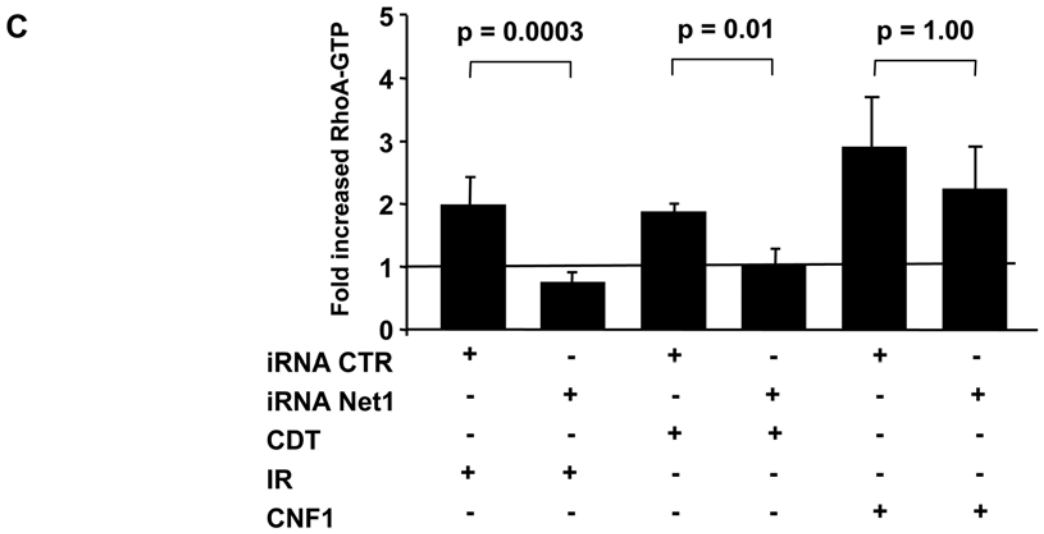

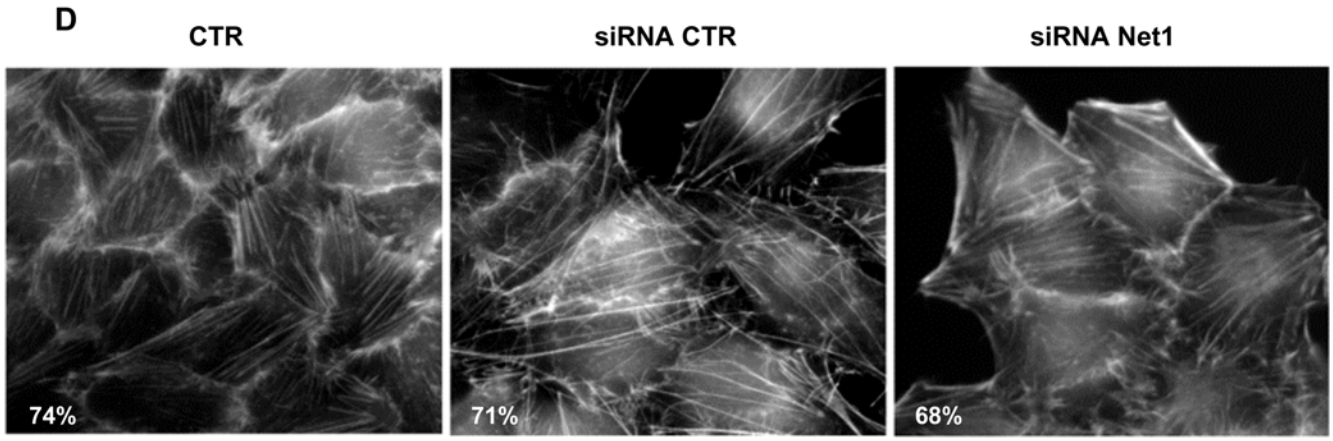

Figure 2. Net1 knock down prevents RhoA activation upon induction of DNA damage. HeLa cells were transfected with plasmids expressing the control or Net1 specific shRNAs (panel **A**), or control or Net1 specific siRNA (panel **B**). Expression of the endogenous Net1 was analysed by western blot 96h (**A**) or 72h (**B**) after transfection. Percentage inhibition was calculated as (1- residual Net1)×100, where residual Net1 is defined as the ratio between the optical density of the Net1 specific band in cells transfected with the Net1 iRNA or control iRNA and the optical density of the Net1 specific band in the non-transfected cells. **C)** HeLa cells, transfected with control or Net1 specific shRNA or shRNA, were left untreated, or exposed to IR (20 Gy), CDT (2 μg ml^{-1}), or CNF-1 (1 μg ml^{-1}), respectively, and further incubated for 4h. Activation of RhoA was assessed by RhoA specific G-LISA™ (mean ±SD of 5 independent experiments for IR and CNF, mean±SD of 3 independent experiments for CDT). Since the effects of transfection with specific Net1 shRNA or siRNA were similar, the data from all these experiments have been summarized together and indicated as iRNA. The fold increase represents the ratio between the levels of GTP-bound RhoA in treated cells and the levels of GTP-bound RhoA in untreated cells. According to the paired *t* test, the reduced RhoA activation in irradiated or intoxicated cells transfected with Net1 iRNA is statistically significant, while the effect of iRNA on the CNF1-induced RhoA activation is not statistically significant. **D)** HeLa cells non-transfected or transfected with control or Net1 specific siRNA were exposed to CNF1 (1 μg ml^{-1}) for 6h. The actin cytoskeleton was visualized by TRITC-phalloidin staining. The values represent the percentage of cells with stress fibers. Cells exhibiting more than 5 stress fibers were scored as positive.
doi:10.1371/journal.pone.0002254.g002

or cells transfected with non-silencing siRNA or shRNA. In contrast, knock down of endogenous Net1 expression prior to intoxication resulted in significant reduction in the number of cells presenting actin stress fibers (Figures 3A and 3B). This effect was quantified by measuring the intensity of the phalloidin staining using the ImageJ software. A significant decrease in the intensity of fluorescence induced by intoxication was demonstrated in the Net1 RNAi treated cells as compared to controls (Figure 3C).

Net1 regulates cell survival in response to DNA damage

Activation of RhoA promotes the survival of cells exposed to CDT [6]. In order to investigate whether Net1 is required for this RhoA mediated response, Net1 expression was inhibited by RNAi prior to intoxication and cell death was assessed by monitoring chromatin condensation. Down-regulation of Net1 resulted in a 4- to 5-fold increase in the number of cells presenting chromatin condensation 48h after intoxication (Figure 4A). Similar results were obtained in cells expressing the dominant negative Net1ΔDH (data not shown). Induction of cell death upon Net1 knock down was confirmed by cleavage of the caspase-3 substrate PARP, as detected by western-blot analysis (Figure 4B), and activation of the pro-apoptotic protein Bax, as detected by immunostaining using the conformation-dependent antibody 6A7 (Figures 4C and 4D). The effect was already observed after 24h and became highly significant within 48h of treatment. The late occurrence of CDT-induced cell death observed upon Net1 knock down was similar to that observed in cells expressing a dominant negative RhoA (RhoAN19) [6]. These results indicate that Net1 is an essential component in the survival response to DNA damage.

Net1/RhoA-dependent activation of p38 MAPK is required for cell survival in intoxicated or irradiated cells

DNA damage was shown to induce activation of p38 MAPK [17]. We therefore tested whether exposure of HeLa cells to CDT or IR stimulates p38 MAPK activity, and whether this is required for protection from cell death. Both CDT intoxication and irradiation induced activation of p38 MAPK within 3h after treatment and this effect was maintained for at least 24h, as assessed by western blot using a p38 MAPK phospho-specific antibody (p-p38) (Figure 5A). The kinetics of p38 MAPK phosphorylation is in line with the previously reported kinetics of RhoA activation, which peaks at 4h after exposure to CDT or IR

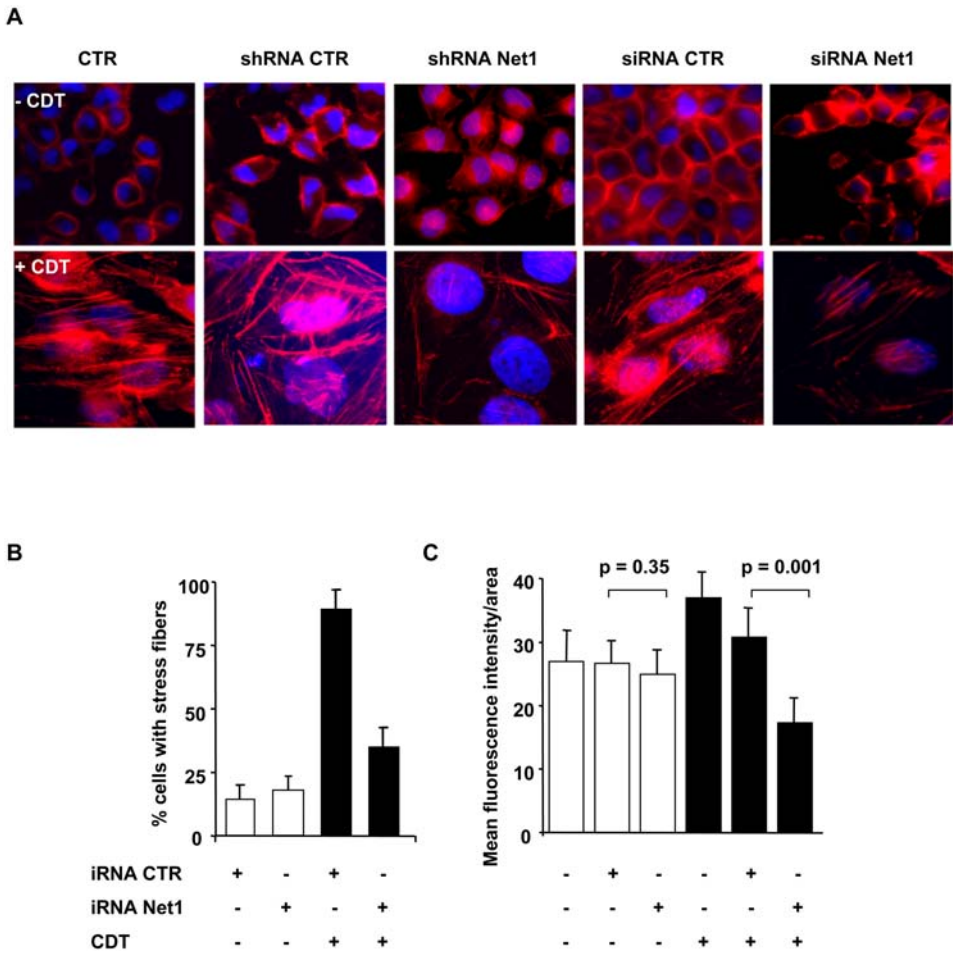

Figure 3. Net1 knock down prevents actin stress fiber formation upon intoxication. A) HeLa cells non-transfected, or transfected with control or Net1 specific shRNA or siRNA, were left untreated or treated with CDT (2 μg ml^{-1}) for 24h. The actin cytoskeleton was visualized by TRITC-phalloidin staining (red). **B)** Quantification of cells with actin stress fibers (mean±SD of 5 independent experiments: three performed with shRNA and two performed with siRNA). One hundred and fifty cells were counted for each experiment. Cells carrying more than 5 stress fibers were scored as positive. **C)** The fluorescence intensity per each cell was quantified using the *ImageJ* software. Data are presented as ratio between the mean fluorescence intensity and the cell area. iRNA is defined as in Figure 2B.
doi:10.1371/journal.pone.0002254.g003

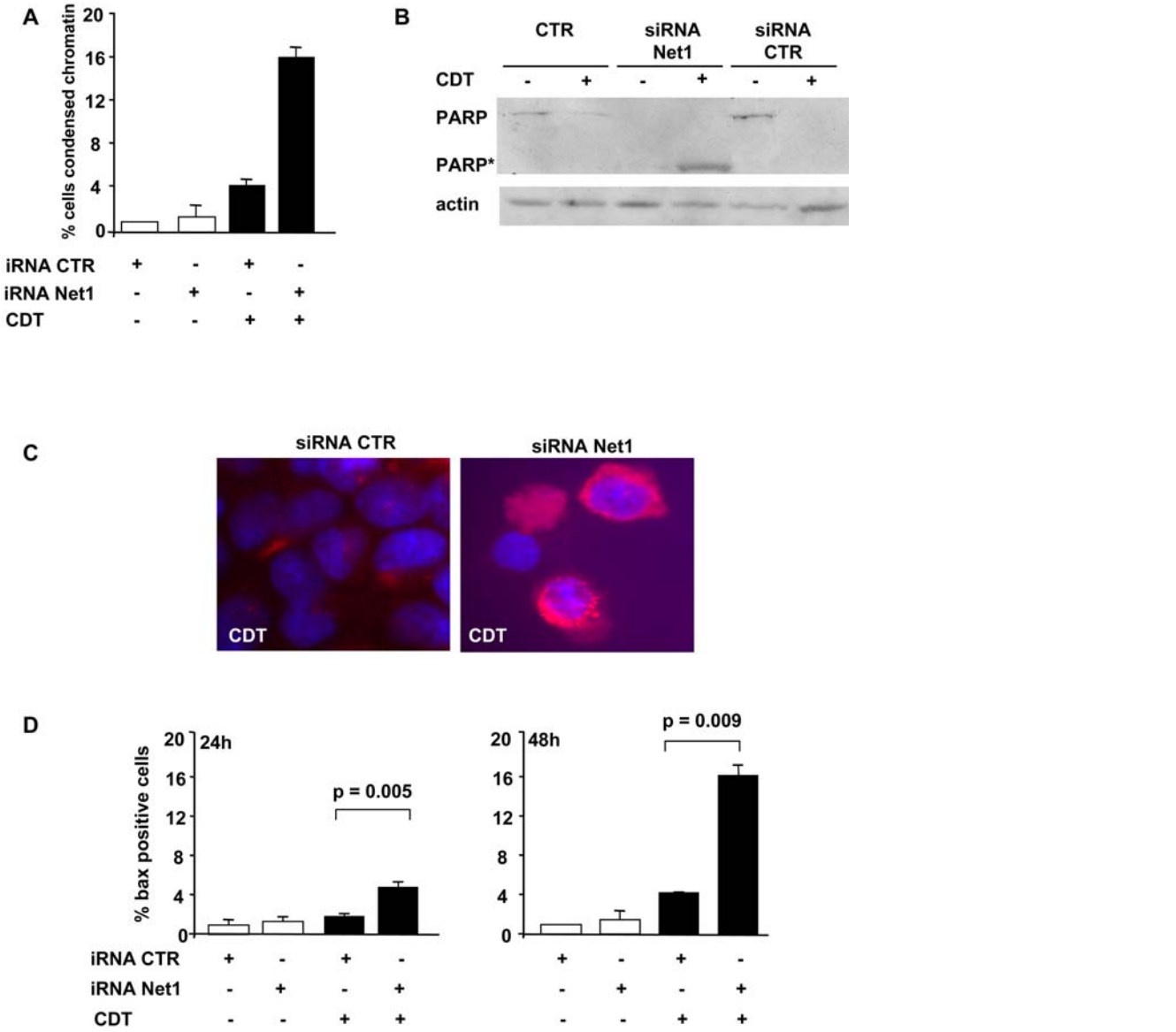

Figure 4. Net1 knock down increases the rate of cell death upon induction of DNA damage. HeLa cells were transfected with control or Net1 specific shRNA or siRNA and exposed to CDT (2 μg ml^{-1}) for 48h. Cell death was assessed by quantifying the percentage of cells presenting chromatin condensation by Hoechst 33258 staining (panel **A**), detection of the cleaved form of PARP (PARP*) by western-blot (panel **B**) and detection of activated Bax, using the anti-Bax 6A7 antibody (red; panel **C**). **D)** Quantification of the Bax positive cells (mean±SD of 5 independent experiments: three performed with siRNA and two performed with shRNA). iRNA is defined as in Figure 2B. According to the *t* test, the increased number of cells expressing the activated form of Bax upon transfection with Net1 specific iRNA is statistically significant both at 24h and 48h after intoxication.
doi:10.1371/journal.pone.0002254.g004

[6]. To determine whether p38 MAPK activation is important for cell survival, the cells were treated with the p38 MAPK specific inhibitors SB203580 or SB202190 (20 μM) prior to irradiation or intoxication. Inhibition of p38 MAPK was associated with a 2- to 4-fold increase in the number of cells exhibiting chromatin condensation 48h after treatment (Figure 5B and data not shown). The increased rate of cell death was confirmed by monitoring activation and increased expression of Bax (Figures 5C and 5D). Activation of p38 MAPK in response to DNA damage was also observed in the colorectal carcinoma cell line HCT116 upon irradiation (Figure 6A). As in HeLa cells, pre-treatment of HCT116 cells with SB203580 prior to irradiation was associated with increased activation of Bax (Figure 6B). Quantification of the Bax positive cells in this set of experiments was hampered by the low number of cells that survived irradiation upon pre-treatment with SB203580 (Figure 6C). These results indicate that activation of p38 MAPK protects the cells from death induced by DNA damage.

To assess whether the activation of p38 MAPK was dependent on RhoA and its regulator Net1, the levels of irradiation-induced phosphorylation were assessed in cells where the expression of the two proteins was independently knocked down by RNAi. Transfection with two independent RhoA specific siRNA oligonucleotides consistently induced a 70 to 80 percent reduction of the endogenous levels of RhoA (Figure 7A), and this effect was associated with a strong inhibition of p38 MAPK activation in response to IR and CDT (Figures 7B and 7C). Similar levels of inhibition were obtained by blocking RhoA activity using the cell

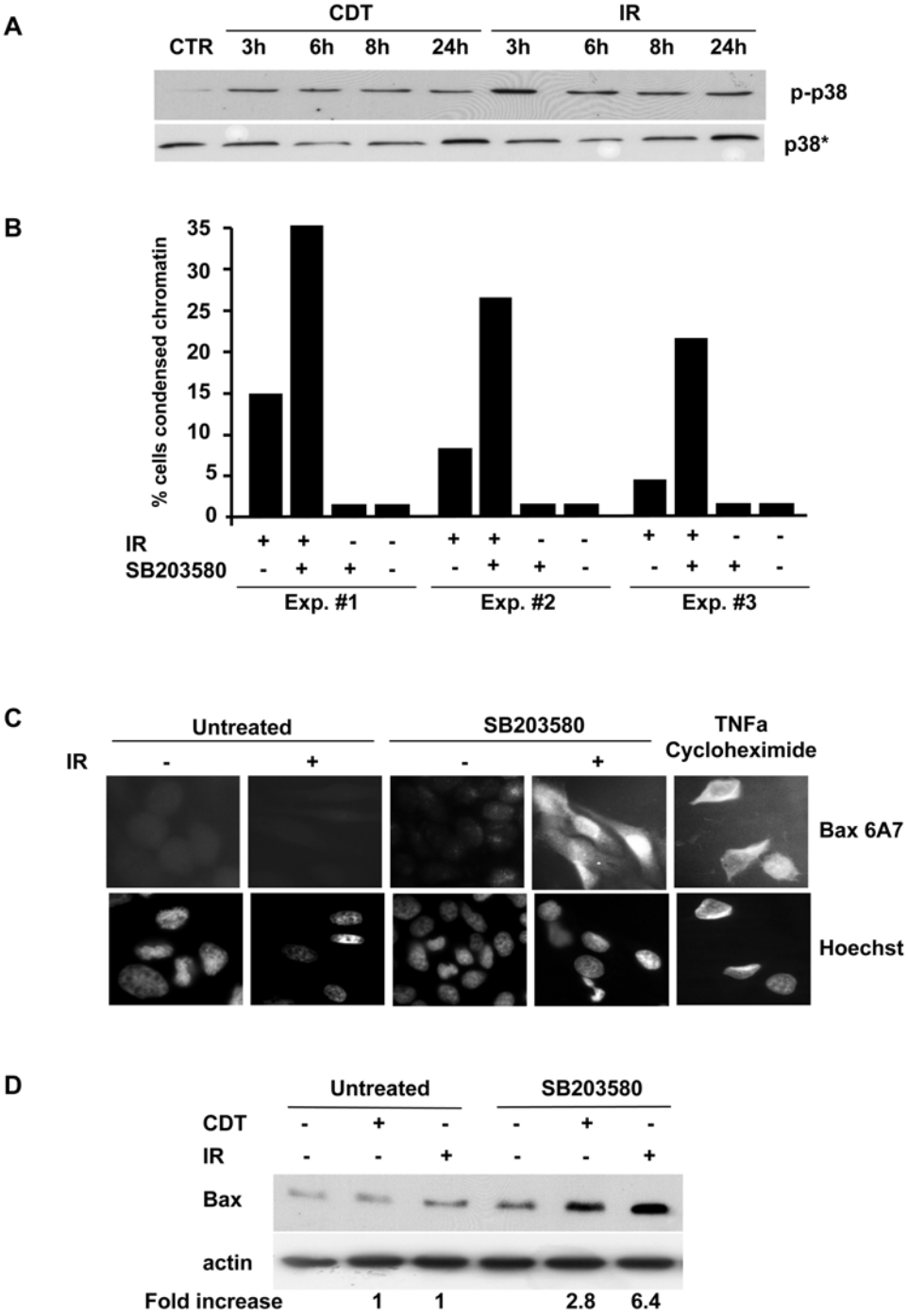

Figure 5. p38 MAPK regulates cell survival in response to DNA damage. A) HeLa cells were: i) left untreated; ii) exposed to CDT (2 μg ml^{-1}) for the indicated time periods; iii) irradiated (20 Gy) and further incubated in complete medium for the indicated time periods. Samples were subjected to western blot analysis using a α-p38 antibody (p38*) or a p38 phospho-specific antibody (p-p38). **B)** HeLa cells, pre-treated with the specific p38 MAPK inhibitor SB203580 (20 μM) in complete medium for 30 min, were left untreated, or irradiated (20 Gy) and further incubated for 48h. Cell death was assessed by quantifying the number of cells presenting chromatin condensation by Hoechst 33258 staining. **C)** HeLa cells were treated as described in Figure 5B, and the activated form of Bax was detected by indirect immunofluorescence using the anti-Bax 6A7 antibody (upper panel). Nuclei were counterstained with Hoechst 33258 (lower panel). As a positive control for Bax staining the cells were treated with 50 ng/ml TNFα and 100 μg/ml cyclohexmide in complete medium for 6h at 37°C. **D)** HeLa cells, pre-treated with the specific p38 MAPK inhibitor SB203580 (20 μM) in complete medium for 30 min, were left untreated, treated with CDT (2 μg ml^{-1}) for 48h, or irradiated (20 Gy) and further incubated for 48h. Expression of Bax was detected by western blot analysis using antibodies specific for Bax or actin. Fold increase represents the ratio between the optical density of the Bax specific band in treated cells and optical density of the Bax specific band in the untreated cells.
doi:10.1371/journal.pone.0002254.g005

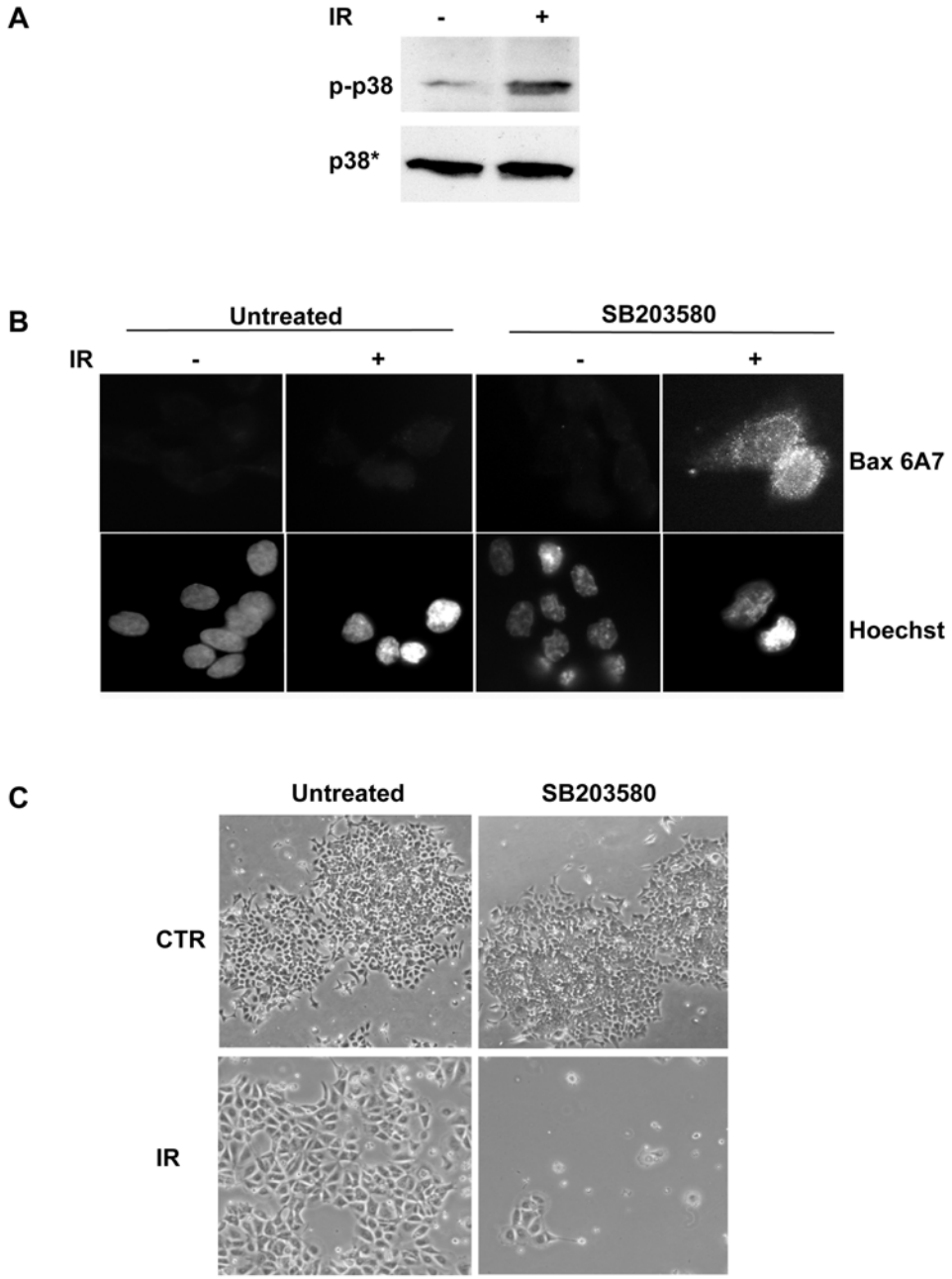

Figure 6. DNA damage activates p38 MAPK in HCT116 cells. A) HCT116 cells were left untreated or irradiated (20 Gy) and further incubated in complete medium for 3h. Samples were subjected to western blot analysis as described in Figure 5A. **B)** HCT116 cells, pre-treated with the specific p38 MAPK inhibitor SB203580 (20 μM) in complete medium for 30 min, were left untreated or irradiated (20 Gy) and further incubated for 48h. Cell death was assessed by detection of activated Bax, using the anti-Bax 6A7 antibody (upper panel). Nuclei were counterstained with Hoechst 33258 (lower panel). **C)** HCT116 cells, pre-treated with the specific p38 MAPK inhibitor SB203580 (20 μM) in complete medium for 30 min, were irradiated (20 Gy) and further incubated for 48h. Cells were visualized by contrast phase microscopy.
doi:10.1371/journal.pone.0002254.g006

permeable inhibitor C3 transferase (data not shown). Knock down of endogenous Net1 expression, by either siRNA or shRNA, resulted in an equally potent inhibition of p38 MAPK activation in irradiated cells (Figures 8A and 8B). These results indicate that Net1 and RhoA are upstream signals in the p38 MAPK activation cascade in response to DNA damage.

To determine whether the RhoA activated kinases ROCKI and ROCK II are required for p38 MAPK activation, HeLa cells were treated with the ROCKI/II inhibitors H-1152 or Y27632 prior to irradiation. As expected, pre-treatment of control HeLa cells with both inhibitors altered the organization of the actin cytoskeleton and prevented the formation of actin stress fibers upon irradiation (Figure 9A), confirming that these effectors were efficiently blocked. However, the treatment did not impair the activation of p38 MAPK (Figure 9B), indicating that ROCKI/II were not required for signalling to this kinase.

The MAPK-activated protein kinase 2 (MK2) is a direct substrate of the p38 MAPK α-and β-isoforms [18]. We asked

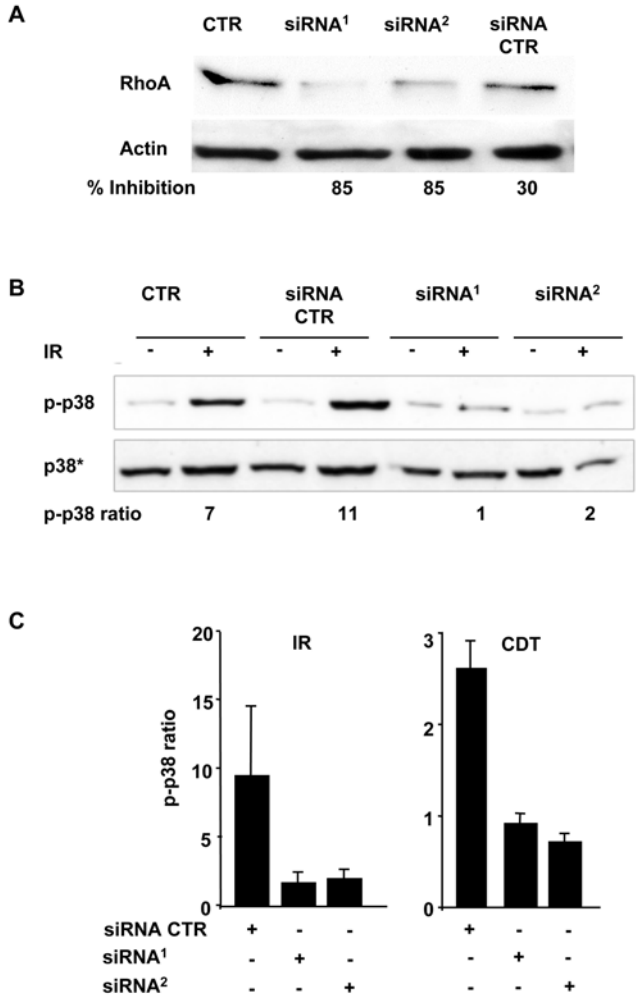

Figure 7. DNA damage-induced p38 phosphorylation is RhoA-dependent. A) HeLa cells were transfected with the control siRNA or two independent RhoA specific siRNA (siRNA[1]: Hs_RHOA_6; siRNA[2]: Hs_RHOA_7). Expression of the endogenous RhoA levels was analysed by western blot. Percentage inhibition was calculated as in Figure 2A. **B)** Untransfected HeLa cells or cells transfected with control siRNA, or two independent RhoA specific siRNA were left untreated or irradiated (20 Gy), and further incubated for 4h in complete medium. p38 phosphorylation was assessed as in Figure 5A. p-p38 ratio represents the ratio between the optical density of the phospho-p38 band in treated cells and optical density of the phospho-p38 band in the untreated cells. **C)** Quantification of the changes in the levels of p38 phosphorylation in HeLa cells transfected with control siRNA, RhoA specific siRNA[1] or siRNA[2]. Mean±SD of 6 independent experiments performed with cells exposed to IR (left panel), and 3 independent experiments performed cells exposed to CDT (right panel) cells. p-p38 ratio is defined as in Figure 7B.
doi:10.1371/journal.pone.0002254.g007

therefore whether this protein is also activated in a Net1- and RhoA-dependent manner upon induction of DNA damage. As illustrated in Figure 10, a 2- to 4-fold increase in the phosphorylation of MK2 on its activating site Thr334 (p-MK2) was observed in HeLa cells 4h after irradiation or intoxication (Figure 10A), and a similar effect was observed in irradiated HCT116 cells (Figure 10B). As expected, this effect was prevented by pre-treatment with the p38 MAPK specific inhibitor SB203580 (Figure 10A). Importantly, the phosphorylation of MK2 following irradiation was abrogated by knock down of either Net1 or RhoA, indicating that these proteins are required for MK2 activation (Figures 10C and 10D).

Discussion

The transforming ability of a truncated form of Net1 described by Chen et al. [12] suggests that this protein may be involved in regulating the delicate balance between cell growth and cell death. This possibility is substantiated by our finding that Net1 regulates the activation of RhoA and p38 MAPK, and promotes cell survival in response to genotoxic agents. Furthermore, our data identify genotoxic stress as a trigger for Net1 activation and contribute to the characterization of a novel DNA damage-induced survival pathway involving Net1 and its downstream targets RhoA and p38 MAPK.

Net1 is activated and regulates RhoA-dependent actin stress fiber formation upon induction of DNA damage

Alberts *et al.* have previously shown that phosphorylation of Net1 on Ser152 prevents RhoA activation and concluded therefore that pSer152 inhibits the GEF activity of Net1 [15]. We now show that exposure to CDT or IR decreases the levels of pSer152 phosphorylation of the endogenous as well as an ectopically expressed Net1 (**Figure 1**), thus identifying genotoxic stress as a signal for Net1 activation in vivo. The mechanisms involved in Net1 de-phosphorylation remain unknown. A constitutively active form of the Rac1-activated protein kinase PAK1 (PAK1*) was identified as the Ser152-specific Net1 kinase *in vitro*, and expression of PAK1* prevented Net1-induced stress fiber formation in Swiss 3T3 cells [15]. We did not observe any significant change in the level of Rac1 or Cdc42 activation in HeLa cells or primary fibroblasts exposed to CDT or IR [6], and PAK1 activity was not changed within 30 min after irradiation, a time when the dephosphorylation of pS152-Net1 was maximal (data not shown). This suggests that the decrease in pSer152-Net1 observed in our experiments does not involve inactivation of PAK1. Conceivably, a different, as yet unknown Net1 specific kinase may be down-regulated. Alternatively, exposure to CDT or IR may enhance the rate of p-S152-Net1 de-phosphorylation by activation of a phosphatase.

Inhibition of endogenous Net1 by RNAi and expression of a dominant negative Net1 demonstrated that this GEF is required for RhoA activation and for the subsequent re-organization of the actin cytoskeleton in response to intoxication or irradiation (**Figures 2 and 3**). It is noteworthy that stress fiber formation is detected in epithelial cells that are arrested in G1 following treatment with TGF-β [19–21], and similar changes occur in cells exposed to bacterial toxins that inhibit, Cycle inhibiting factor (Cif) [22], or promote, *Pasteurella multocida* toxin (PMT) [23], cell cycle progression. Net1 is a major player in the morphological changes that characterize both TGF-β [21] and DNA damage (in this work). It is thereby tempting to speculate that Net1-regulated cytoskeleton rearrangements may be a common feature of the response to stress signals that deregulate the cell cycle.

Net1/RhoA-dependent survival signals

Our RNAi experiments demonstrate that Net1 and RhoA are critical for protecting intoxicated and irradiated cells from cell death induced by DNA damage (**Figure 4**), and identify p38 MAPK as a key mediator in the delivery of the survival signals (**Figures 5 to 9**). The mechanism by which RhoA controls p38 MAPK phosphorylation remains still unclear. Marinissen at al. demonstrated that RhoA stimulates c-jun expression via activation of the p38γ MAPK isoform, resulting in aberrant cell growth and malignant transformation [24]. Interestingly, we have found that

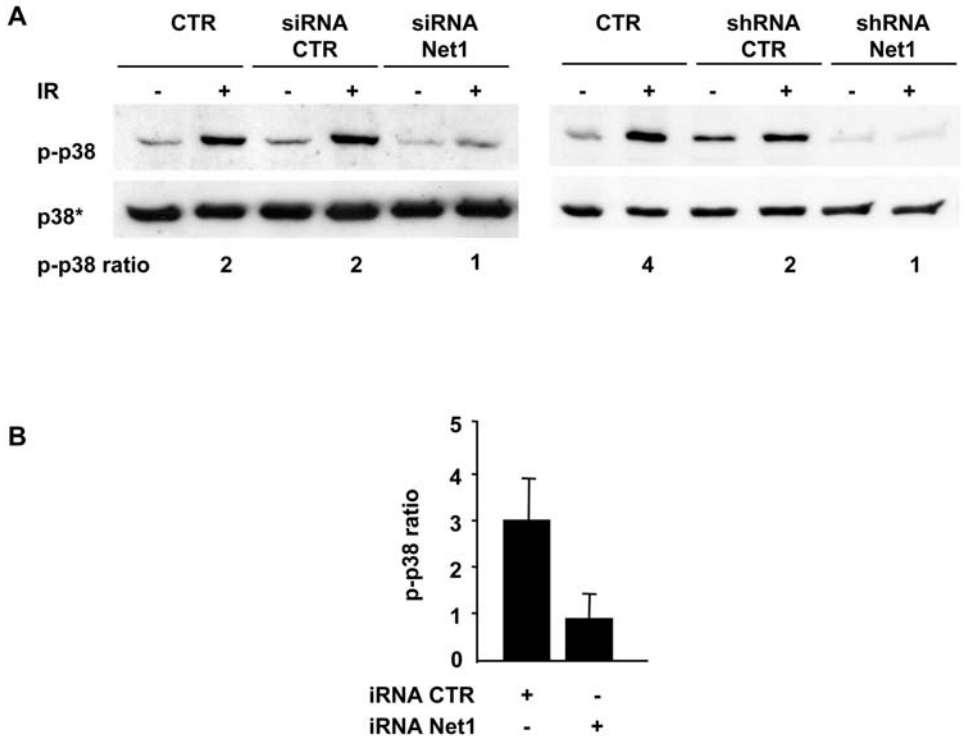

Figure 8. DNA damage-induced p38 phosphorylation is Net1-dependent. A) Untransfected HeLa cells or cells transfected with either the Net1 specific siRNA (left panel) or shRNA (right panel), or the relevant controls were left untreated or irradiated (20 Gy), and further incubated for 4h in complete medium. p38 phosphorylation was assessed as in Figure 5A. **B)** Quantification of the changes in the levels of p38 phosphorylation in irradiated HeLa cells transfected with control or Net1 specific iRNA. iRNA is defined as in Figure 2B. Mean±SD of 6 independent experiments (three performed with siRNA, and three performed with shRNA).
doi:10.1371/journal.pone.0002254.g008

the activation of p38 MAPK in response to DNA damage was abrogated by SB203580 and SB202190 that are specific inhibitors for the α- and β-isoforms of p38 MAPK [25], suggesting that different isoforms may be targeted by RhoA depending on the triggering stimulus. A large number of effector proteins mediate signalling downstream of RhoA [26]. Since the RhoA activated kinases ROCKI and ROCKII regulate many of the cytoskeletal effects of RhoA, we examined whether they transduced the signal from RhoA to p38 MAPK. Interestingly, pre-treatment with pharmacological inhibitors of ROCK did not prevent p38 MAPK activation, but inhibited stress fiber formation (**Figure 9**), suggesting that RhoA may utilize different sets of effector proteins to control these cellular responses. This is likely to require the selective clustering of the downstream effectors on distinct scaffold proteins, as suggested by the finding that the RhoA-dependent activation of JNK involves the association of Net1 and the JNK activators MLK2, MLK3 and MKK7 with the scaffold protein CNK1, while this is not required for induction of stress fibers [27].

The current literature identifies JNK as the main MAPK induced by irradiation [17]. Consistent with our previous results showing that CDT or IR do not activate the JNK regulators Rac and Cdc42 [6], we detected only low levels of JNK phosphorylation and AP1 activation 4h and 12h after intoxication in HeLa cells (data not shown). In contrast, up to 10 fold increase of p38 MAPK phosphorylation was consistently observed both in HeLa and HCT116 cells (**Figures 5 and 6**). This result is not surprising since, depending on the experimental models, p38 MAPK was shown to contribute to either survival or death signals in response to DNA damage [17]. The downstream signals involved in the survival response remain unclear. Reinhardt at al. recently showed that the survival in p53-deficient fibroblasts exposed to cisplatin and doxorubicin is enhanced by ATM-dependent activation of p38 MAPK and its downstream effector MK2 [28]. This pathway has been defined as the third cell cycle-dependent checkpoint, in addition to the well-characterized ATM/Chk2 and ATR/Chk1 responses [28]. Our findings demonstrate that these signals operate also in tumor cells, such as HeLa and HCT116, since blockage of p38 MAPK activation by specific inhibitor abrogates their capacity to survive irradiation or intoxication (**Figures 5 and 6**). Furthermore, we have identified Net1 and RhoA as key molecules controlling the activation of this novel checkpoint pathway (**Figures 7 and 8**). A schematic illustration of the Net1-regulated signal cascade identified in this work is shown in **Figure 11**.

Conclusions

Any event capable of promoting the survival of cell with damaged DNA is detrimental since it would favour tumor initiation and/or progression (reviewed in [29,30]). Our finding that induction of DNA damage by CDT is accompanied by the concomitant activation of survival signals suggests that chronic infection with CDT producing bacteria may promote genomic instability and favour malignant transformation. The association between bacterial infections and cancer is poorly understood. The only bacterium classified as human carcinogen is *Helicobacter pylori*, but a possible involvement in oncogenesis has been suggested for other bacteria, such as for example the Gram-negative bacterium *Salmonella typhi* [31]. Indeed, several Gram-negative bacteria have been shown to produce DNA damaging toxins [32,33]. The work

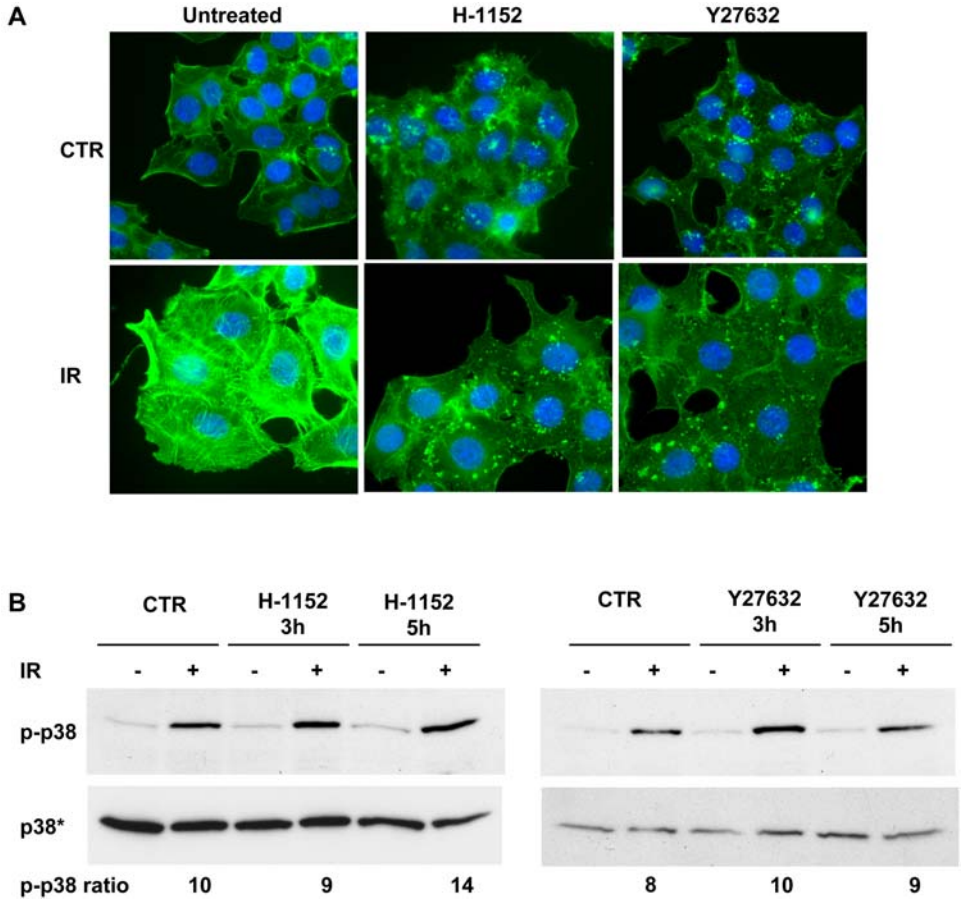

Figure 9. ROCK inhibitors do not prevent DNA damage-induced p38 MAPK phosphorylation. A) HeLa cells, were left untreated or pre-treated with the specific ROCK inhibitors H-1152 or Y27632 (10 μM) in complete medium for 1h prior to irradiation (20 Gy), and further incubated in the presence or absence of the inhibitor for 12h. The actin cytoskeleton was visualized by FITC-phalloidin staining (green). **B**) HeLa cells, pre-treated with the specific ROCK inhibitors H-1152 or Y27632 (10 μM) in complete medium for 1h, were left untreated or exposed to IR (20Gy), and further incubated in the presence or absence of the inhibitors for the indicated periods of time. p38 MAPK phosphorylation was assessed as in Figure 5A.
doi:10.1371/journal.pone.0002254.g009

described in this paper provides the first molecular characterization of a survival pathway triggered by CDT intoxication. Further dissection of this pathway will provide new tools to elucidate the mechanisms of bacterial-induced carcinogenesis, and may also help to design specific inhibitors that can act synergistically with conventional chemotherapy.

Materials and Methods

Cell lines and plasmids

HeLa and HCT116 cell lines were obtained from the ATCC and grown as described [6]. The plasmid expressing the c-Myc epitope-tagged Net1ΔDH was a kind gift from Drs. A. Hall and A. Schmidt (Medical Research Council Laboratory for Molecular Cell Biology, University College London, London, UK). The plasmid expressing the Net1A protein was previously described [16].

CDT and treatments

Production of the *H. ducreyi* CdtA, CdtB and CdtC subunits and reconstitution of the active holotoxin (here named as CDT) was previously described [6,34].

CDT intoxication. Cells were incubated for the indicated time periods with CDT (2 μg ml^{-1}) in complete medium.

Ionizing radiation. Cells were irradiated (20 Gy), washed once with PBS and incubated for the indicated time periods in complete medium.

SB203580/SB202190 treatment. Cells were pre-treated with the p38 MAPK specific inhibitors SB203580 or SB202190 (20 μM) (Calbiochem) in complete medium for 30 min at 37°C, before exposure to CDT or IR.

ROCK inhibitors. Cells were pre-treated with the ROCK inhibitors H-1152 and Y27632 (10 μM) (Calbiochem) in complete medium for 1h at 37°C, before exposure to CDT or IR, and then further incubated in the presence of the inhibitor for the indicated periods of time.

Immunofluorescence

Phalloidin staining. Phalloidin staining of actin filaments was performed as previously described [6].

Bax 6A7 staining. Cells were fixed with 4% paraformaldehyde, and permeabilized with 0.2% Triton X-100 for 2 min at 22°C. Antibody non-specific binding was blocked with 3% BSA in PBS for 30 min at 22°C. Slides were further incubated for 1h at 22°C with the conformation-specific monoclonal antibody (6A7, BD Pharmingen), which recognizes the activated form of Bax. Slides were washed three times with PBS and then incubated with TRITC-conjugated rabbit anti-mouse antibody (DAKO; diluted 1:100 in

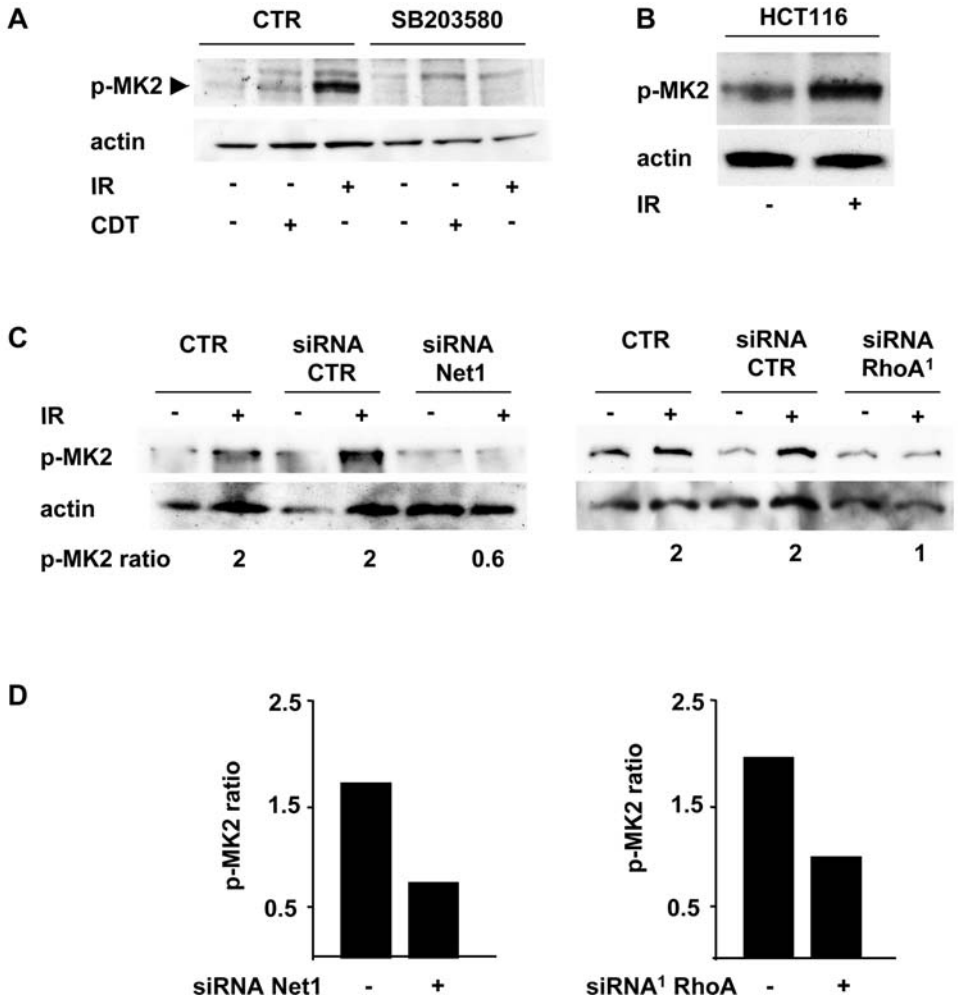

Figure 10. The p38 MAPK effector MK2 is phosphorylated in a Net1- and RhoA-dependent manner in response to genotoxic agents. **A)** Untreated HeLa cells, or cells pre-treated with the specific p38 MAPK inhibitor SB203580 (20 μM) in complete medium for 30 min, were exposed to CDT (2 μg ml^{-1}) for 4h, or irradiated (20 Gy) and further incubated in complete medium for 4h. Samples were subjected to western blot analysis using antibodies specific for phospho-MK2 (p-MK2) or actin. **B)** HCT116 cells were left untreated or irradiated (20 Gy) and further incubated in complete medium for 3h. Samples were subjected to western blot analysis as described in Figure 10A. **C)** HeLa cells transfected with: i) control siRNA; ii) Net1 specific siRNA (left panel); iii) the RhoA specific siRNA[1] (right panel) were left untreated or irradiated (20 Gy), and further incubated for 4h in complete medium. MK2 phosphorylation was assessed as in Figure 10A. p-MK2 ratio represents the ratio between the optical density of the phospho-MK2 band in irradiated cells and optical density of the phospho-MK2 band in the untreated cells. **D)** Quantification of the changes in the levels of MK2 phosphorylation in irradiated HeLa cells: mean of 3 independent experiments performed with the Net1 specific siRNA (left panel) and 2 independent experiment performed with the RhoA specific siRNA (right panel).
doi:10.1371/journal.pone.0002254.g010

PBS) for 30 min at 22°C. Nuclei were counterstained with Hoechst 33258 (Sigma; 0.5 μg ml^{-1}).

iRNA

Net1 shRNA. The following oligonucleotides were used for production of Net1 specific shRNAs:

shRNA-A (target nucleotides: 312–332):

5′-TCTCAATCTCTCCTGTAAGAAATGGACAC-CATTTCTTACAGGAGAGATTCT-3′

5′-CTGCAGAATCTCTCCTGTAAGAAATGGTCTC-CATTTCTTACAGGAGAGATT-3′

shRNA-B (targets nucleotides: 615–635):

5′-TCTCAAAGTTGTCCATCATGTCAGAACATCTGA-CATGATGGACAACTTCT-3′

5′-CTGCAGAAAGTTGTCCATCATGTCAGATGTTCT-GACATGATGGACAACTTT-3′

shRNA-C (targets nucleotides: 819–837):

5′-TCTCCAAAGCTCTTCTTGATCAATTCAAGAGATT-GATCAAGAAGAGCTTTGCT-3′

5′-CTGCAGCAAGCTCTTCTTGATCAATCTCTT-GAATTGATCGSTCAAGAAGAGCTTTG-3′

Non targeting shRNA (scrambled sequence from Dlg1):

5′-TCTCGAGAATGCGAGGTCAAGTTCTTCCTGT-CAAACTTGACCTCGCATTCTCCT-3′

5′-CTGCAGGAGAATGCGAGGTCAAGTTTGACAG-GAACAACTTGACCTCGCATTCTC-3′

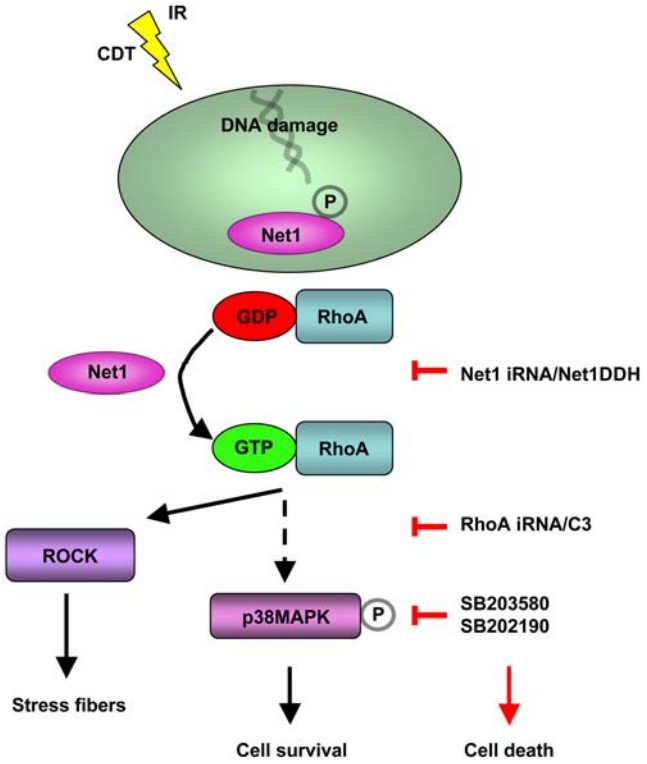

Figure 11. Summary of the Net1-regulated survival signals upon exposure to genotoxic agents. Upon intoxication or irradiation, Net1 is dephosphorylated and induces activation of RhoA, leading to a RhoA dependent phosphorylation of p38 MAPK and its downstream effector protein MK2. This signalling pathway can be blocked at different levels by: i) iRNA knock down of endogenous Net1 levels or expression of the dominant negative Net1ΔDH; ii) C3-mediated RhoA inhibition or iRNA knock down of endogenous RhoA levels; iii) p38 specific inhibitors. In each case, the effect of this interference results in enhanced cell death in response to genotoxic agents.
doi:10.1371/journal.pone.0002254.g011

The oligonucleotides were annealed and ligated into the pGENECLIP-puromycin vector (Promega) according to the manufacturer's instructions.

Efficient down-regulation of the endogenous Net1 levels required co-transfection with the three Net1 specific shRNA expressing plasmids.

siRNA. The Net1 specific siRNA (HP validated 1027400), two RhoA specific siRNAs (Hs_RHOA_6 HP validated SI02654211, and Hs_RHOA_7 HP validated SI02654267), and the Alexa Fluor 488-labelled control siRNA (AATTCTCCGAACGTGTCACGT, 1022076) were purchased from Qiagen.

Transfection

HA-Net1A. Two hundred thousand and one hundred thousand HeLa cells per well were grown in 12-well plates, or 24-well plates, respectively in complete medium. Transfections were performed with the indicated amount of the relevant plasmid using the Lipofectamine 2000 Reagent (Life Technologies), according to the manufacturer's instructions. Twenty-four hours after transfection, cells were either intoxicated or irradiated and incubated for the indicated time periods.

shRNA. One million Hela cells were grown in 6 cm diameter Petri dishes in complete medium, and transfected with the indicated shRNA plasmids (2 μg ml^{-1}) using the Lipofectamine 2000 Reagent. Twenty-four hours after transfection, complete medium supplemented with puromycin (10 μg ml^{-1}) was added and cells were further incubated for 72h.

siRNA. One hundred thousand HeLa cells were grown in 12-well plate in complete medium. Transfection was performed with 75 ng/well of the indicated siRNA with HiPerFect Reagent (Qiagen), according to the manufacturer's instructions, and cells were further incubated for 72h.

RhoA activation

RhoA activation was assessed by the G-LISA™ RhoA Activation Assay Biochem Kit™ (Cytoskeleton) according to the manufacturer's instructions.

Immunoprecipitation

Immunoprecipitations were performed as previously described [15]. The endogenous Net1 protein was immunoprecipitated using a goat α-Net1 specific antibody (Abcam).

Western blot analysis

The following antibodies were used: α-HA, α-Bax (B-9) (Santa Cruz Biotechnology), α-phospho-Net1-Ser152 [15], α-Net1 specific rabbit serum, α-Net1 goat serum (Abcam), α-actin (Sigma), α-phospho-p38, α-p38, α-phospho-MK2 (Thr334), α-RhoA (Cell Signaling), and α-PARP (BD Biosciences). Blots were developed with enhanced chemiluminescence, using the appropriate horseradish peroxidase-labelled secondary antibody, according to the instructions of the manufacturer (GE Healthcare).

Acknowledgments

We thank Drs A. Hall and A. Schmidt for the kind gift of the plasmid expressing the c-Myc epitope-tagged Net1ΔDH.

Author Contributions

Conceived and designed the experiments: TF LG MT. Performed the experiments: TF LG HC. Analyzed the data: MM TF LG MT JF. Contributed reagents/materials/analysis tools: AR HC JF. Wrote the paper: MM TF.

References

1. Thelestam M, Frisan T (2004) Cytolethal distending toxins. Rev Physiol Biochem Pharmacol 152: 111–133.
2. Scott DA, Kaper JB (1994) Cloning and sequencing of the genes encoding *Escherichia coli* cytolethal distending toxins. Infection and Immunity 62: 244–251.
3. Lara-Tejero M, Galan JE (2001) CdtA, CdtB and CdtC form a tripartite complex that is required for cytolethal distending toxin activity. Infection and Immunity 69: 4358–4365.
4. Cortes-Bratti X, Karlsson C, Lagergard T, Thelestam M, Frisan T (2001) The Haemophilus ducreyi cytolethal distending toxin induces cell cycle arrest and apoptosis via the DNA damage checkpoint pathways. J Biol Chem 276: 5296–5302.
5. Li L, Sharipo A, Chaves-Olarte E, Masucci MG, Levitsky V, et al. (2002) The *Haemophilus ducreyi* cytolethal distending toxin activates sensors of DNA damage and repair complexes in proliferating and non-proliferating cells. Cellular Microbiology 4: 87–99.
6. Frisan T, Cortes-Bratti X, Chaves-Olarte E, Stenerlöw B, Thelestam M (2003) The *Haemophilus ducreyi* cytolethal distending toxin induces DNA double strand breaks and promotes ATM-dependent activation of RhoA. Cellular Microbiology 5: 695–707.
7. Elwell CA, Dreyfus LA (2000) DNAase I homologous residues in CdtB are critical for cytolethal distending toxin-mediated cell cycle arrest. Mol Microbiol 37: 952–963.
8. Lara-Tejero M, Galan JE (2000) A bacterial toxin that controls cell cycle progression as a deoxyribonuclease I-like protein. Science 290: 354–357.
9. Nesic D, Hsu Y, Stebbins CE (2004) Assembly and function of a bacterial genotoxin. Nature 429: 429–433.
10. Etienne-Manneville S, Hall A (2002) Rho GTPases in cell biology. Nature 420: 629–635.

11. Rossman KL, Der CJ, Sondek J (2005) GEF means go: turning on RHO GTPases with guanine nucleotide-exchange factors. Nat Rev Mol Cell Biol 6: 167–180.
12. Chan AM, Takai S, Yamada K, Miki T (1996) Isolation of a novel oncogene, NET1, from neuroepithelioma cells by expression cDNA cloning. Oncogene 12: 1259–1266.
13. Alberts AS, Treisman R (1998) Activation of RhoA and SAPK/JNK signalling pathways by the RhoA-specific exchange factor mNET1. Embo J 17: 4075–4085.
14. Schmidt A, Hall A (2002) The Rho Exchange Factor Net1 is regulated by nuclear sequestration. Journal of Biological Chemistry 277: 14581–14588.
15. Alberts AS, Qin H, Carr HS, Frost JA (2005) PAK1 negatively regulates the activity of the Rho exchange factor NET1. J Biol Chem 280: 12152–12161.
16. Qin H, Carr HS, Wu X, Muallem D, Tran NH, et al. (2005) Characterization of the biochemical and transforming properties of the neuroepithelial transforming protein 1. J Biol Chem 280: 7603–7613.
17. Dent P, Yacoub A, Fisher PB, Hagan MP, Grant S (2003) MAPK pathways in radiation responses. Oncogene 22: 5885–5896.
18. Cohen P (1997) The search for physiological substrates of MAP and SAP kinases in mammalian cells. Trends Cell Biol 7: 353–361.
19. Bhowmick NA, Ghiassi M, Aakre M, Brown K, Singh V, et al. (2003) TGF-beta-induced RhoA and p160ROCK activation is involved in the inhibition of Cdc25A with resultant cell-cycle arrest. Proc Natl Acad Sci U S A 100: 15548–15553.
20. Kamaraju AK, Roberts AB (2005) Role of Rho/ROCK and p38 MAP kinase pathways in transforming growth factor-beta-mediated Smad-dependent growth inhibition of human breast carcinoma cells in vivo. J Biol Chem 280: 1024–1036.
21. Shen X, Li J, Hu PP, Waddell D, Zhang J, et al. (2001) The activity of guanine exchange factor NET1 is essential for transforming growth factor-beta-mediated stress fiber formation. J Biol Chem 276: 15362–15368.
22. Marches O, Ledger TN, Boury M, Ohara M, Tu X, et al. (2003) Enteropathogenic and enterohaemorrhagic Escherichia coli deliver a novel effector called Cif, which blocks cell cycle G2/M transition. Mol Microbiol 50: 1553–1567.
23. Zywietz A, Gohla A, Schmelz M, Schultz G, Offermanns S (2001) Pleiotropic effects of Pasteurella multocida toxin are mediated by Gq-dependent and -independent mechanisms. involvement of Gq but not G11. J Biol Chem 276: 3840–3845.
24. Marinissen MJ, Chiariello M, Gutkind JS (2001) Regulation of gene expression by the small GTPase Rho through the ERK6 (p38 gamma) MAP kinase pathway. Genes Dev 15: 535–553.
25. Lee JC, Kassis S, Kumar S, Badger A, Adams JL (1999) p38 mitogen-activated protein kinase inhibitors–mechanisms and therapeutic potentials. Pharmacol Ther 82: 389–397.
26. Bishop AL, Hall A (2000) Rho GTPases and their effector proteins. Biochem J 348 Pt 2: 241–255.
27. Jaffe AB, Hall A, Schmidt A (2005) Association of CNK1 with Rho guanine nucleotide exchange factors controls signaling specificity downstream of Rho. Curr Biol 15: 405–412.
28. Reinhardt HC, Aslanian AS, Lees JA, Yaffe MB (2007) p53-deficient cells rely on ATM- and ATR-mediated checkpoint signaling through the p38MAPK/MK2 pathway for survival after DNA damage. Cancer Cell 11: 175–189.
29. Kastan MB, Bartek J (2004) Cell-cycle checkpoints and cancer. Nature 432: 316–323.
30. Shiloh Y (2003) ATM and related protein kinases: safeguarding genome integrity. Nat Rev Cancer 3: 155–168.
31. Lax AJ (2005) Bacterial toxins and cancer—a case to answer? Nature Reviews Microbiology 3: 343–349.
32. Oswald E, Nougayrede JP, Taieb F, Sugai M (2005) Bacterial toxins that modulate host cell-cycle progression. Curr Opin Microbiol 8: 83–91.
33. Lax AJ (2007) New genotoxin shows diversity of bacterial attack mechanisms. Trends Mol Med 13: 91–93.
34. Guerra L, Teter K, Lilley BN, Stenerlow B, Holmes RK, et al. (2005) Cellular internalization of cytolethal distending toxin: a new end to a known pathway. Cell Microbiol 7: 921–934.

DNA damage induced by a bacterial genotoxin induces FEN1 and vinculin-dependent survival signals

Lina Guerra[1], Riccardo Guidi[1], Ilse Slot[1], Ramakrishna Sompallae[1], Carol L. Pickett[2] Stefan Åström[3], Frederik Eisele[4], Dieter Wolf[4], Camilla Sjögren[1], Maria Masucci[1], Teresa Frisan[1]

[1]Dept. Cell and Molecular Biology, Karolinska Institutet, Stockholm, Sweden, [2]Dept. Microbiology and Immunology, Chandler Medical Center, University of Kentucky, Lexington, Kentucky, USA, [3]Dept. Development Biology, Wenner-Grens Institutet, Stockholm University, Stockholm, Sweden, [4]Institute of Biochemistry, University of Stuttgart, Stuttgart, Germany

Running title: Characterization of novel survival signals induced by the cytolethal distending toxin

Key words: cytolethal distending toxin, DNA damage, vinculin, FEN1, cell survival, TSG101, RhoA, actin cytoskeleton

*Address correspondence to: Teresa Frisan, Dept. Cell and Molecular Biology, Karolinska Institutet, Stockholm, Sweden, Box 285, S-171 77 Stockholm, Sweden.
Tel: +46-8-52486385, Fax: +46-8-337412, e-mail: Teresa.Frisan@ki.se

Abstract

Several human pathogenic Gram-negative bacteria produce a DNA damaging toxin: the cytolethal distending toxin (CDT). Since incorrectly repaired DNA can result in carcinogenesis, insight into how intoxicated cells can survive may help to understand the carcinogenic potential of chronic infections with CDT-producing bacteria.

Activation of the actin regulating protein RhoA and phosphorylation of the downstream Mitogen-Activated Protein Kinase (MAPK) p38 following CDT-induced DNA damage is important to prolong cell survival. The details of this signaling pathway are still unknown. To identify novel CDT-induced survival signals, we screened a *Saccharomyces cerevisiae* deletion library. A total of 4492 mutants, carrying deletions in nonessential genes, were transformed with an inducible CdtB expression vector and screened for delayed growth, which is indicative of defective survival.
The screening identified 78 genes whose deletion confers hypersensitivity to CdtB expression, and 73% of those shared homology with human genes. Systems biology analysis demonstrated that 20 of the proteins encoded by the human orthologs are involved in the regulation of the actin cytoskeleton in higher eukaryotes. We focused our analysis on TSG101 (yeast ortholog VPS23), FEN1 (yeast ortholog RAD27) and vinculin (VCL), and demonstrated that they are all required to induce actin stress fibers formation in response to DNA damage. FEN1 and VCL also regulated the RhoA-dependent p38 MAPK phosphorylation, and delayed cell death in response to CDT intoxication. Our data highlight a complex and still poorly characterized cross-talk between DNA damage and actin cytoskeleton in the regulation of cell survival to genotoxic stresses.

Introduction

The cytolethal distending toxins (CDTs) are produced by a variety of Gram negative bacteria, such as *Escherichia coli*, *Actinobacillus actinomycetemcomitans*, *Haemophilus ducreyi*, *Shigella dysenteriae*, *Campylobacter sp.* and *Helicobacter sp,* and *Salmonella enterica (*reviewed in [1]).

The active holotoxin is a tripartite complex [2,3], formed by the CdtA, CdtB and CdtC subunits. The CdtB component is the active subunit, that shares structural and functional homology with mammalian deoxyribonuclease I (DNase I) [4,5,6]. The CdtA and CdtC subunits are ricin-like lectin domains [6], involved in cellular internalization of the toxin [7,8,9].

CDT induction of DNA double strand breaks (DSBs) was demonstrated in naturally intoxicated mammalian cells by pulsed field gel electrophoresis (PFGE) [10], in agreement with the data reported by Hassane and co-workers who previously observed DSBs in *Saccharomyces cerevisiae* cells transfected with the active CdtB subunit [11]. In both cases, mutations within the DNase conserved motives prevented induction of DNA DSBs.

The cellular effects of CDT intoxication are identical to those induced by exposure to ionizing radiation (IR), a well-characterized DNA-damaging agent. Both CDT and IR stimulate the phosphorylation of histone H2AX and relocalisation of the DNA repair complex Mre11 ([12,13]. In addition, cell cycle checkpoints are activated in a cell type dependent manner. For example, human primary fibroblasts are arrested in the G1 and G2 phases of the cell cycle, while HeLa cells are arrested in G2 upon intoxication [13,14].

In adherent cells, irradiation or CDT intoxication is associated with formation of actin stress fibers [15,16]. This effect is regulated by activation of the small GTPase RhoA, which is dependent on the DNA damage sensor kinase ataxia-telangiectasia mutated protein (ATM). Inhibition of RhoA function in intoxicated cells leads to an increased rate of cell death [10]. Activation of RhoA and actin stress fiber formation in response to CDT is dependent on the RhoA-specific Guanine nucleotide Exchange Factor (GEF) Net1.

The DNA-damage-dependent Net1/RhoA signalling diverges into two different effector cascades: one dependent on the RhoA kinases ROCKI and ROCKII, which controls

formation of actin stress fibers; and one regulated by the Mitogen-Activated Protein Kinase (MAPK) p38 and its downstream target MAPK-activated protein kinase 2, which promotes cell survival [17].

Survival of cells with damaged DNA is detrimental since it may favor tumor initiation and/or progression (reviewed in [18,19]. Characterization of the survival signals activated in response to CDT intoxication are therefore indispensable to elucidate the exact mechanisms by which bacterial infections can contribute to carcinogenesis. To identify novel CDT-induced survival signals, we have screened a yeast deletion library, expressing the CdtB active subunit under the galactose promoter.

The screening identified 78 deletion mutants with reduced growth rate upon induction of CdtB expression. Systems biology analysis demonstrated that 20 human orthologs of these 78 genes are involved in the regulation of the actin cytoskeleton. Further studies on mammalian cells showed that TSG101, FEN1 and Vinculin (VCL) are important to induce RhoA activation and actin stress fibers formation in response to DNA double strand breaks. We further identified FEN1 and VCL as two effectors regulating p38 MAPK phosphorylation, and ultimately cell survival in response to CDT intoxication.

Material and Methods

Cell line

HeLa cell lines were obtained from ATCC and were cultivated in RPMI 1640 medium supplemented with 10% fetal calf serum (FCS), 5mM L-glutamine, penicillin (100 units/ml) and streptomycin (100µg/ml) (complete medium) in a humid atmosphere containing 5% CO_2.

Yeast strains and plasmids

The complete EUROpean *Saccharomyces cerevisiae* ARchive for Functional analysis (EUROSCARF) library, purchased from Open Biosystems, Thermo Scientific, consists of diploid mutants that are homozygous in deletions of non-essential genes [20]. The CdtB and the control plasmids were previously described [11].

The library and the control BY4743 strain (*MATa/MATα, his3Δ1/his3Δ1, leu2Δ/leu2Δmet15Δ0/MET15, LYS2/lys2Δ0, ura3Δ0/ura3Δ0*) were transformed with the pDCH-CdtB [11] or vector control plasmids. Dropout synthetic medium was prepared according to the manufacturer's instructions (Clontech). Transformants were selected and maintained in synthetic dropout medium without leucine (selective medium) supplemented with 2% glucose. For induction of CdtB expression, cells were grown in selective medium supplemented with 2% galactose and 2% raffinose.

Yeast transformation

Systematic yeast transformation experiments were performed using the *S. cerevisiae* direct transformation in 96-well format, previously described in [21] with minor modifications. Yeast deletion strains were grown on yeast extract/peptone/glucose (YPGluc) square plates (12cmx12cm, Greiner Bio-one) for 48h at 30°C. Twenty-five microliters of the transformation solution (27% PEG600, 200mM Litium Acetate, 50mM DTT, Carrier DNA 5µg/µl, and 15µg of the pDCH-CdtB or control plasmids) were added in 96-well plates and the yeast deletions strains were transferred using a 48-pin replicator, mixed well and incubated for 2h at 42°C. After mixing, 10µl aliquots of the mixture were transferred on plates of synthetic dropout selective medium containing 2% glucose using a multi-channel pipette. Plates were let to dry at 22°C and incubated for 4 days at 30°C.

Screening and characterization of CdtB hypersensitive strains

For the first round of selection, transformants were picked, transferred to 100µl of sterile H_2O in 96-well plates and spotted onto square plates containing selective medium supplemented with 2% glucose (CdtB OFF) or 2% raffinose and 2% galactose (CdtB ON) using a 48-pin replicator and incubated for 48h at 30°C. Clones that grew equally in glucose or galactose/raffinose were considered non hypersensitive to CdtB and not further screened.

For the subsequent experiments, the deletion mutants were transferred to 100µl sterile H_2O in 96-well plates, and diluted to a value of optical density at 600nm (OD_{600}) of 1. Three microliters of five-fold dilution series were transferred onto 10cm diameter round plates containing selective medium supplemented with 2% glucose (CdtB OFF) or 2% raffinose/galactose (CdtB ON) using a 48-pin replicator and incubated at 30°C for 48h. Yeast strains that did not grow after the third dilution step in raffinose/galactose were considered as CdtB hypersensitive.

Survival assay

Clones transformed with the pDCH-CdtB or control plasmids were incubated for 24h in medium containing 2% raffinose. Cell were diluted to OD_{600} of 0.3, and transferred to 3ml selective medium containing 2% raffinose and 2% galactose (CdtB ON), and incubated at 30°C. One thousand cells were collected at time 0h and 48h and plated on glucose selective plates (CdtB OFF). Colony forming units (CFUs) were counted after 48h incubation at 30°C.

Flow cytometer analysis

Cells were centrifuged and the cell pellet was resuspended and fixed with 1ml 70% ethanol at 4°C for at least 24h. After an additional centrifugation, cells were resuspended in 0.8ml RNase solution (50mM Tris HCl, pH 7.8, 20μg/ml RNase) and incubated over night at 37°C. Samples were centrifuged and resuspended in 0.5ml PI solution (200mM Tris HCl pH 7.5, 211mM NaCl, 78mM $MgCl_2$, 25μg/ml propidium iodide), and sonicated for 5 seconds at medium voltage. Thirty microliters of cell suspension were mixed in a tube together with 0.6 ml 50mM TrisHCl pH 7.5. Samples were analyzed with a FACS Calibure flow cytometer. Data from 30,000 cells were collected and analyzed using the CellQuest software.

Search for human orthologs

The human orthologs of yeast genes were identified using the Inparanoid database [22], BLAST sequence alignment against all human protein sequences and literature search.

Mapping the actin cytoskeleteon network

The 217 proteins that regulate the actin cytoskeleton re-arrangements were downloaded from the Kyoto Encyclopedia of Genes and Genomes (KEGG) pathway database (KEGG ID: hsa04810) [23]. The protein-protein interaction network (defined henceforth as the actin-network) was then generated using the search tool for the retrieval of interacting genes/proteins (STRING) database [24]. The STRING database contains both experimentally validated and computationally predicted interaction data from different resources. For this analysis, we considered only experimentally reported interactions. Data from the STRING database were further used to add proteins shown experimentally to interact directly with any component of the actin-network. The Cytoscape software [25] was used to generate the extended network depicted in Figure 2A.

CDT and treatments

Production of the *H. ducreyi* CdtB was previously described [10]. The His-tagged CdtA and CdtC were constructed by PCR amplification of the *H. ducreyi cdtA* and *cdtC* genes from the pAF-tac1cdtA and pAF-tac1cdtC plasmids, respectively [26] using the following primers:

CdtA_F 5′- ATTCGGATCCATGTTCATCAAATCAACGAATGA-3

CdtA_R 5'-TACCGAATTCTTAATTAACCGCTGTTGCTTCTAAT-3'

CdtC_F 5′- ATTCGGATCCAAGTCATGCAGAATCAAATCCTGA-3

CdtC_R 5′-5'-TACCGAATTCTTAGCTACCCTGATTTCTT -3'

Each PCR fragment was cloned into the BamHI and EcoRI restriction sites of the pACYC-Duet-1 expression vector (Novagen). Purification of the His-tagged CdtA and CdtC subunits from inclusion bodies was performed as previously described [27].
Reconstitution of the active holotoxin (named as CDT) was previously described [10].

CDT intoxication. Cells were incubated for the indicated time periods with CDT (2μg/ml) in complete medium.

Ionizing radiation. Cells were irradiated (20 Gy), washed once with PBS and incubated for indicated time periods in complete medium.

siRNA and transfections

One hundred thousand HeLa cells were plated in 12-well plate. The siRNA were purchased from Qiagen, and transfection was performed using the fast-forward protocol from Polyplus Transfection, according to the manufacturer's instructions. Gene silencing was assessed by western-blot analysis 72h after transfection. The following siRNA duplex was used: Hs_FEN1_6 #SI02663451; Hs_VCL_10 #SI02664207; Hs_VCL_11 #SI02664214; Hs_TSG101_6 #SI02655184; Hs_TSG101_7 #SI02664522; Allstars Negative Control siRNA #102780.

Immunofluorescence

Immunofluorescence analysis was performed as previously described [10,17], using the conformation-specific monoclonal antibody (6A7, BD Pharmingen), which recognizes the active form of Bax. The actin cytoskeleton was visualized by Phalloidin staining, as previously described [10]. Nuclei were counterstained with DAPI (Vector Laboratories Inc).

RhoA activation

RhoA activation was assessed using the G-LISA^{TM} RhoA Activation Assay Biochem Kit^{TM} (Cytoskeleton), according to the instructions of the manufacturer.

Western blot analysis

Proteins were fractionated by SDS-polyacrylamide gels, transferred to PVDF membranes (Millipore) and probed with the following antibodies: α-phospho-p38, α-p38, α-FEN1 (Cell Signaling), α-TSG101, α-Vinculin and α-Actin (Sigma). Blots were developed with enhanced chemoluminescence, using the appropriate horseradish peroxidase-labelled secondary antibody, according to the instructions of the manufacturer (GE Healthcare).

Results

Screening of the *S. cerevisiae* deletion library

Activation of the small GTPase RhoA and phosphorylation of the downstream p38 MAPK following CDT-induced DNA damage is an important stress response, which leads to delayed cell death. However, the details of this signaling pathway are still unknown [17].

To identify novel CDT-induced survival signals, we screened a *S. cerevisiae* deletion library. In the first set of experiments we expressed the active subunit CdtB derived from the *Campylobacter jejuni* CDT under the galactose promoter into the *S. cerevisiae* control BY4743 strain. Induction of CdtB expression by addition of galactose into the culture medium induced G2 arrest (Figure 1A upper panel) and delayed cell growth (Figure 1A, lower panel) in cells transformed with the pDCH-CdtB plasmid, while no effect was observed in cells grown in the presence of glucose (CdtB OFF) or in cells transformed with the vector control in presence or absence of galactose.

Subsequently, we performed a genome-wide screen using the EUROpean *Saccharomyces cerevisiae* ARchive for Functional analysis (EUROSCARF) library, derived from the BY4743 strain [20]. Deletion strains that showed growth aberrations, for example respiration deficiency (petite strains), were excluded. A total number of 4492 deletion mutants out of the 4793 carrying deletions in nonessential genes were inoculated on YPGluc plates. From the frozen stocks, seven strains could not be recovered. The 4485 recovered strains were successfully transformed with the CdtB-expressing pDCH–CdtB plasmid via the high-throughput yeast transformation method. To select for CdtB-sensitivity, we performed replica plating serial dilutions on plates containing selective medium supplemented with either glucose to inhibit CdtB expression (CdtB OFF), or galactose/raffinose to induce CdtB expression (CdtB ON).

As expected, the wild type cells (wt) presented a inhibited growth in the presence of galactose/raffinose, compared to cells grown in glucose, however, several deletion mutants showed a more pronounced phenotype when CdtB expression was induced (Figure 1B, left panel). Transformants were defined as CdtB hypersensitive when growth was not detected after the third dilution step. This screening was performed three times, and a total of 121 deletion mutants that did not grow after the third dilution step in all the three rounds were considered as CdtB hypersensitive (Figure 1B, right panel). To ensure

that the delayed growth was due only to the expression of CdtB, and not to an intrinsic characteristic of the deletion, each of the 121 deletion mutants were transformed with the vector control plasmid, and a similar serial dilution screening in the presence or absence of galactose/raffinose was performed (data not shown). This analysis restricted the number of CdtB hypersensitive deletion mutants to 78 (Table 1). PCR analysis, performed in 30 out of the 78 mutants, demonstrated that all the cloned tested carried the proper deletion, and validated the quality of the library used in this study (Supplementary Tables 1 and 2).

Hypersensitivity to CdtB, as assessed by the serial dilution assay described above, does not allow to discriminate between delayed growth or cell death induced by the toxin expression. Therefore we performed a survival assay by determining the reduction of colony forming unit (CFU) ability for six deletion mutants hypersensitive to CdtB, two clones that did not show CdtB hypersensitivity, and the wild type cells (Figure 1C).
Each deletion mutant, transformed either with the CdtB expression plasmid or the vector control, was grown in selective medium in the presence of galactose/raffinose (CdtB ON). After 48h, one thousand cells were plated on glucose selective plates (CdtB OFF), and the number of CFU was counted after 48h incubation at 30°C. The data are presented as percentage of the number of CFUs derived from the CdtB expressing cells relative to the number of CFUs derived from cells transformed with the vector control. As shown in Figure 1C, the viability of the hypersensitive CdtB mutants *Δslt2*, *Δrvs161*, and *Δrad27*, was significantly reduced compared to that of the mutants *Δcka2*, *Δsrv2*, and *Δvps23* or the two non-hypersensitive *Δhog1* and *Δsmk1*, indicating that for some of the clones, the reduced cell recovery observed in Figure 1B was associated with enhanced cell death in response to CdtB-induced DNA damage.

The identity of the yeast genes, whose deletion confers hypersensitivity to CdtB, is summarized in Table 1. Based on the annotated function derived from the *Saccharomyces* Genome Database (SGD) [28], we classified these genes into twelve groups, five genes could not be grouped because they encode proteins with unknown function (Figure 1D and Table 1). As expected the majority of them encodes for proteins involved in the regulation of the DNA damage checkpoint responses, genome integrity and DNA repair

(39%, groups 1 to 4). Interestingly, the next larger functional group comprises genes encoding for effectors involved in the control of vesicular transport and endocytosis (13%, group 5). A smaller proportion of the identified genes regulates the actin cytoskeleton (8%, group 7), and this was the target of interest in our screening.

Identification of novel CDT-induced survival signals in higher eukaryotes

The Inparanoid database [22] and BLAST sequence alignment were subsequently used to identify 59 human orthologs of the 78 yeast genes found in the EUROSCARF library screening (Table 1).

To assess whether any of the human orthologs encoded for proteins that regulate cell survival via activation of actin cytoskeleton in response to DNA damage in higher eukaryotes, we constructed a protein-protein interaction network for all the effectors involved in regulation of the actin cytoskeleton and their interacting partners. The network obtained is composed of 185 nodes (proteins) and 448 edges (interactions). The nodes of the pathway are shown in blue circles. Node size and label size indicates that the protein has multiple interacting partners (Figure 2A).

Twenty of the 59 human orthologs were found within the network, and are listed in Table 2, together with their interacting partners. Four clusters were clearly identified. Two encoded for proteins involved either in the regulation of the DNA damage checkpoint (centred on CHK1) and DNA replication and repair (centred on FEN1) (red circles). One comprises proteins of the MAPK pathways (green circle) (Figure 2A). The fourth cluster, marked with the blue circle, included the Ser/Thr protein phosphatase PPM1A, the vacuolar protein sorting TSG101, and the ATPse ATP6V1E1. No homogenous function could be defined for this cluster.

Figure 2B represents part of the network described in Figure 2A, where three key proteins were chosen to perform functional studies in mammalian cells. The selected proteins, marked with green squares, are: TSG101, FEN1 and Vincunlin (VCL). TSG101 (yeast ortholog: VPS23) and FEN1 (yeast ortholog: RAD27) were found in the EURPSCARF library screening, and were selected because TSG101 interacts with the RhoA kinase ROCK, a key factor that promotes actin stress fibers [29], while FEN1 is involved in DNA repair and was found as a central node in one of the clusters defined in Figure 2A. VCL, not present in *S. cerevisiae*, was selected based on its central role in the integrin-dependent regulation of the actin cytoskeleton, and for its reported interaction with FEN1 [30].

FEN1 and VCL prolong cell survival in response to DNA damage

To assess whether TSG101, VCL and FEN1 are important to delayed cell death upon CDT-induced DNA damage, expression of the endogenous proteins were knocked down

by specific siRNAs in HeLa cells 72 h prior intoxication. iRNA interference induced 80% and 60% reduction of TSG101 and VCL expression, respectively, while the levels of expression of endogenous FEN1 were reduced more than 90% (Figure 3A).

Cell death was assessed 72h after intoxication by monitoring chromatin condensation (data not shown) and by detection of the activated form of the pro-apoptotic protein Bax, by immunostaining with the conformation-dependent antibody 6A7 (Figure 3B). Fifteen to twenty percent of apoptotic cells, corresponding to a three-fold increase compared to the untreated cells, were observed in cells transfected with the non-silencing siRNA 72h after intoxication. A similar proportion was observed in cells where expression of TSG101 was knocked down by specific siRNA (Figures 3C and 3D), indicating that this protein does not promote cell survival in response to CDT intoxication. However, approximately a 11-fold increase in apoptotic cells was detected in intoxicated HeLa cells where the endogenous levels of VCL or FEN1 were knocked down by specific siRNA (Figures 3B, 3C and 3D). Down-regulation of FEN1 and TSG101 in mammalian cells recapitulated the phenotype observed in the *S. cerevisiae* mutants, where the orthologs *RAD27* and *VPS23* have been deleted, since the *Δrad27* mutant, but not *Δvps23* showed reduced viability upon induction of CdtB expression. (Figure 1C).

Activation of RhoA and actin stress fibers in response to DNA damage is dependent on TSG101, VCL and FEN1

We have previously shown that exposure to DNA damaging agents, such as IR and CDT, induced actin stress fiber formation, activation of RhoA, and delayed cell death [17], therefore we assessed whether TSG101, VCL and FEN1 were involved in this still poorly characterized signalling pathway. As expected, induction of DNA double strand breaks by CDT intoxication or irradiation induced formation of actin stress fibers in 50% and 40% of control HeLa cells or cells transfected with non-silencing siRNA, respectively (Figures 4A and 4B). This was associated with approximately a three-fold increased of RhoA activation (Figure 4C).

Down-regulation of the endogenous levels of TSG101 or VCL was associated with increased levels of stress fiber formation in untreated cells, but no significant changes were observed upon induction of DNA DSB by irradiation or intoxication (Figures 4A and 4B). FEN1 knock down did not alter the actin cytoskeleton in untreated cells, but significantly reduced stress fiber formation in intoxicated or irradiated cells (Figures 4A

and 4B). These data indicate that all these three proteins regulated induction of actin stress fibers in response to DNA damage. However, only knock down of VCL and FEN1 completely prevented RhoA activation, while, a similar increase of GTP-bound RhoA was observed in irradiated or intoxicated cells transfected with the TSG101 specific siRNA compared to control cells or cells transfected with non-silencing siRNA (Figure 4C). Based on these results, we concluded that FEN1 and VCL regulate activation of RhoA and consequent stress fiber formation, while TSG101 induces the stress fiber formation down-stream of RhoA activation.

Activation of p38 MAPK in response to DNA damage is dependent on VCL and FEN1

Induction of DNA double strand breaks stimulates the activity of the p38 MAPK in a RhoA dependent manner, and this is required to delay cell death in HeLa cells [17]. Since we have demonstrated that VCL and FEN1 are required for RhoA activation, we next assessed whether these two proteins are also important for the activation of p38 MAPK. As previously shown, we observed a four- to five-fold increase in p38 MAPK activation, assessed by western-blot analysis using a p38 MAPK phospho-specific antibody (p-p38) in control HeLa cells or cells transfected with non-silencing siRNA 4h after irradiation (Figures 5A and 5B). In line with the previous results, showing that TSG101 does not affect RhoA activation, similar levels of p38 MAPK phosphorylation were detected in irradiated HeLa cells, where expression of the endogenous levels of TSG101 where knocked down with specific siRNA. Conversely, down-regulation of either VCL or FEN1 resulted in decreased p38 MAPK activation upon induction of DNA damage (Figures 5A and 5B).

These data identified FEN1 and VCL as two important effectors that activate RhoA in response to DNA damage. We further demonstrated that DNA damage triggers two distinct pathways: i) induction of actin stress fibers, which requires both the RhoA kinase ROCKI and II [17], and TSG101 (this work); ii) activation of p38 MAPK, associated with a delayed cell death, which is FEN1 and VCL dependent. Our results are summarized in Figure 6.

Discussion

The exact mechanism by which bacteria contribute to carcinogenesis is still poorly characterized. Several Gram-negative pathogenic bacteria have been shown to produce cytolethal distending toxins (CDTs) that induce DNA damage in their target cells. As incorrect repair of DNA damage may lead to genetic instability and eventually to tumour development, it is conceivable that chronic infection with CDT-producing bacteria can be a risk factor for cancer development. One key factor in the tumorigenic process is activation of survival signals, which can prevent cell death induced by DNA damage and/or oncogene activation. We used *S. cerevisiae* transformed with a CdtB-expressing plasmid as a model for CDT-intoxicated cells and screened a yeast deletion library to identify novel genes required for the CdtB-induced survival response.

A genome-wide screen for the cellular response to CdtB in *S. cerevisiae* has been previously described by Kitagawa *et al.* [31]. However, the focus of their study was the characterization of the DNA damage repair mechanisms in response to CDT intoxication, while we were interested in identifying RhoA-dependent effectors that transduce the stress response of the damaged DNA into survival signals. The identity of the genes that influence the response to CdtB found in our study largely overlap with that reported by Kitagawa and co-workers and with those identified by Bennett *et al.* [32] who performed a genome-wide screen in yeast to identify genes that confer resistance to IR.

Similarly to Kitagawa *et al*, our screen identified: homologous recombination repair genes such as *RAD50*, *RAD51* and *RAD57,* protein products involved in all three known complexes for nonessential replication factor C (RFC) that, in complex with proliferating-cell nuclear antigen (PCNA), forms the replication fork structure [33], the S-phase checkpoint proteins TOF1 and MRC1 [34], the DNA damage mediator Rad9 [34], the SAE2 endonuclease for processing of hairpin DNA [35], the SRS2 helicase required for recovery from stalled replication forks [36], the MUS81-MMS4 endonuclease for replication fork stability [37], and proteins required for efficient sister chromatid cohesion (CHL1 and MCM21) [38].

The overlapping of our data with the two previous reports indicates that the results of our screening are highly reliable.

Systems biology analysis of the actin-cytoskeleton network (Figure 2A) indicates that the link between proteins regulating the actin cytoskeleton and the stress response to DNA damage in the mammalian system is rather complex, and still poorly characterized. To shed some light, we focused our functional analysis on three proteins: two that were identified in the screening (Table 1, Figures 2A and 2B): FEN1 (RAD27) and TSG101 (VPS23), and VCL that is not present in yeast, but was chosen for its reported interaction with FEN1 [30] and for its essential role in transducing the integrin signaling to the actin cytoskeleton regulating proteins.

The FEN1 dependency of RhoA activation, actin stress fiber formation and p38 MAPK phosphorylation in response to DNA DSB induced by CDT is novel and not previously reported. FEN1 (flap endonuclease 1) is a multifunction nuclease that possesses endonuclease activity required for the maturation of the Okazaki fragments during DNA replication and long patch DNA base excision repair [39], but has also a 5'-exonuclease activity (EXO) required for proper homologous DNA recombination, and a gap-dependent endonuclease (GEN), which cleaves the ssDNA region of gapped DNA duplex or DNA forks generating DNA DSBs [40,41]. It has been shown that the EXO and GEN activities can be abrogated by mutation of the Glu to Asp mutation in position 60 (E60D), leading to frequent spontaneous mutations both in yeast and mammalian cells and promotion of cancer progression in a knock-in mouse model [42]. These effects of FEN1 E60D are well on line with its role in maintenance of genomic stability. Interestingly, mouse embryo fibroblasts (MEFs) expressing the E60D FEN1 show also an increased susceptibility to cell death in response to UV irradiation compared to the cells expressing the wild type FEN1, indicating that the EXO and/or GEN activities are required for cell survival in response to certain genotoxic stresses. Our data demonstrate that the role of FEN1 in cells survival is also relevant in response to DNA damage caused by the bacterial genotoxin CDT (Figure 3).

How FEN1 could induce activation of the small GTPase RhoA is still not known. We have previously shown that DNA damage induced by IR or CDT promotes dephosphorylation of the RhoA specific GEF Net1 at the inhibitory site Ser152, essential to trigger its GEF activity [43,44]. It is possible that the FEN1-dependent DNA repair mechanisms, evoked by CDT intoxication, trigger indirectly Net1 dephosphorylation, via

activation of a specific phosphatase or inhibition of a kinase. Preliminary data showed that dephosphorylation of Net1 is inhibited 2h after irradiation in FEN1 knock down HeLa cells (data not shown). Alternatively, FEN1 may exert additional function(s) not related to its nuclease activity in a different subcellular compartment. This has been previously demonstrated for other components of the DNA repair machinery. The DNA-dependent protein kinase (DNA-PK), which forms a complex with the Ku heterodimer (Ku70/Ku80), is an essential component of the non-homologous end-joining recombination (reviewed in [45]). However, a fraction of DNA-PK is localized in the lipid rafts microdomains of the plasma membrane [46], and can phosphorylate Akt at Ser473 [47]. Furthermore, the Ku70/Ku80 heterodimer has been shown to regulate cell adhesion to the extracellular matrix and to protect cells form apoptosis via suppression of the translocation of the pro-apoptotic Bax at the mitochondrial membrane (reviewed in [48]). It is conceivable that also FEN1 may exert additional non-repair function(s), associated with the activation of the actin cytoskeleton.

The down-regulation of the FEN1 and VCL genes exerted similar effects on RhoA activation, stress fiber formation and p38 MAPK phosphorylation (Figures 3 to 5), however, it is nor clear whether these two effector proteins act sequentially or trigger different signaling pathways that converge on RhoA.

Integrin activation and adhesion of cells to ECM confer higher resistance to ionizing radiation and cytotoxic drugs (review in [49]). In a hepatoma cell culture model it was shown that the anti-apoptotic effect of β1-integrin in response to a variety of chemotherapeutic agents, such as cisplatin and doxorubicin, was mediated by the MAPK p42/p44 and p38 [50]. FAK, integrin-linked kinase (ILK), Src-tyrosine kinase, PI3K and several adaptor proteins such as talin and VCL are some of the key players in the integrin-dependent signaling complex, that promote cell survival [51,52]. Therefore, it is possible that VCL may contribute to the formation of an adhesome leading to RhoA activation and consequent p38 MAPK phosphorylation in response to CDT intoxication.

The role of TSG101 in induction of actin stress fibers in response to irradiation or intoxication is very interesting. TSG101, together with VPS28 and VPS37 form one of the four ESCRT complexes, the ESCRT I, that regulate protein sorting into multivesicular bodies (reviewed in [53,54]. We found several components of the ESCRT

complexes or ESCRT-binding proteins in the screen for genes that promote cell growth/survival in response to CdtB, including CHMP3/Vps24, CHMP4B and Vps4 (Table 1).

Several recent reports showed that members of the ESCRT induce regulation of the actin cytoskeleton. Mutation in the Drosophila *Vps28* gene causes early embryonic lethality, associated with perturbation of the actin cytoskeleton [55]. Alix, an ESCRT associated protein, regulates cell morphology and actin stress fiber formation in non-transformed human fibroblasts [56]. Furthermore, knock down of Syntaxin (STX) 6, a v-SNARE protein that mediates vesicle transport [57], leads to decreased expression of the α5-integrin and the FAK kinase, leading to reduced cell adhesion and cell death, via up-regulation of both basal and DNA damage-induced levels of p53 [58]. Interestingly, we also identify a member of the STX family in the yeast genome wide screening: PEP12, which is the yeast orthologue to STX12 (Table 1). Our data suggest that several proteins that regulate protein and vesicular trafficking play a broader role in regulation of cell adhesion and cell survival in basal conditions or in response to stresses, such as DNA damage, possibly by functioning as a scaffold for the compartmentalization of specific signaling complexes.

We demonstrated that TSG101 promoted stress fibers down-stream of RhoA in response to DNA damage, since TSG101 knock down did not affect RhoA activation (Figure 4). The effects of TSG101 down-regulation (Figures 4 and 5) are similar to those observed when the RhoA kinases ROCK I and II are inhibited [17], suggesting that the role of this ESCRT protein is to activate the branch of RhoA signaling that leads to stress fiber formation, but does not alter the activation of the MAPK pathway.

In conclusion, we have identified three novel effector proteins in the signaling pathways that promote actin cytoskeleton re-arrangements and cell survival in response to CDT intoxication: FEN1, VCL and TSG101, as summarized in Figure 6. Our data contribute to disclose the complex net of cellular responses that promote cell survival to genotoxic stresses. Identification of survival signals triggered by chronic infections with CDT-producing bacteria is crucial to understand whether these infections can promote genomic instability and favor malignant transformation. Up to date the mechanisms of bacterial-induced carcinogenesis are still poorly characterized. The only bacterium classified as

human carcinogen is *Helicobacter pylori* [59]. However, a possible involvement in oncogenesis has been suggested for other bacteria, such as for example the Gram-negative bacterium *Salmonella typhi* [60]. Identification of an association between infection with CDT-producing bacteria and cancer promotion/progression can help to develop specific therapeutic protocols aimed at an early and rapid eradication of the bacterial infection, preventing the initial steps of tumor development.

Acknowledgements

This work has been supported by the Swedish Research Council, the Swedish Cancer Society, the Åke-Wiberg Foundation, the Magnus Bergvall Fundation, and the Karolinska Institutet to TF, the European Community Integrated Project on Infection and Cancer, INCA, Project no. LSHC-CT-2005-018704 to MGM. TF is supported by the Swedish Cancer Society.

References

1. Smith JL, Bayles DO (2006) The contribution of cytolethal distending toxin to bacterial pathogenesis. Crit Rev Microbiol 32: 227-248.
2. Scott DA, Kaper JB (1994) Cloning and sequencing of the genes encoding *Escherichia coli* cytolethal distending toxins. Infection and Immunity 62: 244-251.
3. Lara-Tejero M, Galan JE (2001) CdtA, CdtB and CdtC form a tripartite complex that is required for cytolethal distending toxin activity. Infection and Immunity 69: 4358-4365.
4. Lara-Tejero M, Galan JE (2000) A bacterial toxin that controls cell cycle progression as a deoxyribonuclease I-like protein. Science 290: 354-357.
5. Elwell C, Chao K, Patel K, Dreyfus L (2001) *Escherichia coli* CdtB mediates cytolethal distending toxin cell cycle arrest. Infection and Immunity 69: 3418-3422.
6. Nesic D, Hsu Y, Stebbins CE (2004) Assembly and function of a bacterial genotoxin. Nature 429: 429-433.
7. McSweeney LA, Dreyfus LA (2004) Nuclear localization of the Escherichia coli cytolethal distending toxin CdtB subunit. Cell Microbiol 6: 447-458.
8. Lee RB, Hassane DC, Cottle DL, Pickett CL (2003) Interactions of Campylobacter jejuni cytolethal distending toxin subunits CdtA and CdtC with HeLa cells. Infect Immun 71: 4883-4890.
9. McSweeney LA, Dreyfus LA (2005) Carbohydrate-binding specificity of the Escherichia coli cytolethal distending toxin CdtA-II and CdtC-II subunits. Infect Immun 73: 2051-2060.
10. Frisan T, Cortes-Bratti X, Chaves-Olarte E, Stenerlöw B, Thelestam M (2003) The *Haemophilus ducreyi* cytolethal distending toxin induces DNA double strand breaks and promotes ATM-dependent activation of RhoA. Cellular Microbiology 5: 695-707.
11. Hassane DC, Lee RB, Mendenhall MD, Pickett CL (2001) Cytolethal distending toxin demonstrates genotoxic activity in a yeast model. Infect Immun 69: 5752-5759.
12. Li L, Sharipo A, Chaves-Olarte E, Masucci MG, Levitsky V, et al. (2002) The *Haemophilus ducreyi* cytolethal distending toxin activates sensors of DNA damage and repair complexes in proliferating and non-proliferating cells. Cellular Microbiology 4: 87-99.
13. Hassane DC, Lee RB, Pickett CL (2003) Campylobacter jejuni cytolethal distending toxin promotes DNA repair responses in normal human cells. Infect Immun 71: 541-545.
14. Cortes-Bratti X, Karlsson C, Lagergard T, Thelestam M, Frisan T (2001) The Haemophilus ducreyi cytolethal distending toxin induces cell cycle arrest and apoptosis via the DNA damage checkpoint pathways. J Biol Chem 276: 5296-5302.
15. Gelfanova V, Hansen EJ, Spinola SM (1999) Cytolethal distending toxin of *Haemophilus ducreyi* induces apoptotic death of Jurkat T cells. Infect Immun 67: 6394-6402.
16. Cortes-Bratti X, Chaves-Olarte E, Lagergård T, Thelestam M (1999) The cytolethal distending toxin from the chancroid bacterium *Haemophilus ducreyi* induces cell-cycle arrest in the G2 phase. Journal of Clinical Investigation 103: 107-115.
17. Guerra L, Carr HS, Richter-Dahlfors A, Masucci MG, Thelestam M, et al. (2008) A bacterial cytotoxin identifies the RhoA exchange factor Net1 as a key effector in the response to DNA damage. PLoS ONE 3: e2254.
18. Kastan MB, Bartek J (2004) Cell-cycle checkpoints and cancer. Nature 432: 316-323.
19. Shiloh Y (2003) ATM and related protein kinases: safeguarding genome integrity. Nat Rev Cancer 3: 155-168.
20. Cherry JM, Adler C, Ball C, Chervitz SA, Dwight SS, et al. (1998) SGD: Saccharomyces Genome Database. Nucleic Acids Res 26: 73-79.
21. Schafer A, Wolf DH (2005) Endoplasmic reticulum-associated protein quality control and degradation: screen for ERAD mutants after ethylmethane sulfonate mutagenesis. Methods Mol Biol 301: 283-288.
22. O'Brien KP, Remm M, Sonnhammer EL (2005) Inparanoid: a comprehensive database of eukaryotic orthologs. Nucleic Acids Res 33: D476-480.
23. Kanehisa M, Goto S (2000) KEGG: kyoto encyclopedia of genes and genomes. Nucleic Acids Res 28: 27-30.
24. von Mering C, Huynen M, Jaeggi D, Schmidt S, Bork P, et al. (2003) STRING: a database of predicted functional associations between proteins. Nucleic Acids Res 31: 258-261.
25. Shannon P, Markiel A, Ozier O, Baliga NS, Wang JT, et al. (2003) Cytoscape: a software environment for integrated models of biomolecular interaction networks. Genome Res 13: 2498-2504.

26. Frisk A, Lebens M, Johansson C, Ahmed H, Svensson L, et al. (2001) The role of different protein components from the *Haemophilus ducreyi* cytolethal distending toxin in the generation of cell toxicity. Microbial Pathogenesis 30: 313-324.
27. Moberg P, Nilsson S, Stahl A, Eriksson AC, Glaser E, et al. (2004) NMR solution structure of the mitochondrial F1beta presequence from Nicotiana plumbaginifolia. J Mol Biol 336: 1129-1140.
28. Database SpSG http://www.yeastgenome.org/.
29. Morita E, Sandrin V, Chung HY, Morham SG, Gygi SP, et al. (2007) Human ESCRT and ALIX proteins interact with proteins of the midbody and function in cytokinesis. Embo J 26: 4215-4227.
30. de Hoog CL, Foster LJ, Mann M (2004) RNA and RNA binding proteins participate in early stages of cell spreading through spreading initiation centers. Cell 117: 649-662.
31. Kitagawa T, Hoshida H, Akada R (2007) Genome-wide analysis of cellular response to bacterial genotoxin CdtB in yeast. Infect Immun 75: 1393-1402.
32. Bennett CB, Lewis LK, Karthikeyan G, Lobachev KS, Jin YH, et al. (2001) Genes required for ionizing radiation resistance in yeast. Nat Genet 29: 426-434.
33. Majka J, Burgers PM (2004) The PCNA-RFC families of DNA clamps and clamp loaders. Prog Nucleic Acid Res Mol Biol 78: 227-260.
34. Longhese MP, Clerici M, Lucchini G (2003) The S-phase checkpoint and its regulation in Saccharomyces cerevisiae. Mutat Res 532: 41-58.
35. Lengsfeld BM, Rattray AJ, Bhaskara V, Ghirlando R, Paull TT (2007) Sae2 is an endonuclease that processes hairpin DNA cooperatively with the Mre11/Rad50/Xrs2 complex. Mol Cell 28: 638-651.
36. Vaze MB, Pellicioli A, Lee SE, Ira G, Liberi G, et al. (2002) Recovery from checkpoint-mediated arrest after repair of a double-strand break requires Srs2 helicase. Mol Cell 10: 373-385.
37. Bastin-Shanower SA, Fricke WM, Mullen JR, Brill SJ (2003) The mechanism of Mus81-Mms4 cleavage site selection distinguishes it from the homologous endonuclease Rad1-Rad10. Mol Cell Biol 23: 3487-3496.
38. Mayer ML, Pot I, Chang M, Xu H, Aneliunas V, et al. (2004) Identification of protein complexes required for efficient sister chromatid cohesion. Mol Biol Cell 15: 1736-1745.
39. Liu Y, Kao HI, Bambara RA (2004) Flap endonuclease 1: a central component of DNA metabolism. Annu Rev Biochem 73: 589-615.
40. Zheng L, Zhou M, Chai Q, Parrish J, Xue D, et al. (2005) Novel function of the flap endonuclease 1 complex in processing stalled DNA replication forks. EMBO Rep 6: 83-89.
41. Parrish JZ, Yang C, Shen B, Xue D (2003) CRN-1, a Caenorhabditis elegans FEN-1 homologue, cooperates with CPS-6/EndoG to promote apoptotic DNA degradation. Embo J 22: 3451-3460.
42. Zheng L, Dai H, Zhou M, Li M, Singh P, et al. (2007) Fen1 mutations result in autoimmunity, chronic inflammation and cancers. Nat Med 13: 812-819.
43. Guerra L, Nemec KN, Massey S, Tatulian SA, Thelestam M, et al. (2008) A novel mode of translocation for cytolethal distending toxin. Biochim Biophys Acta.
44. Alberts AS, Qin H, Carr HS, Frost JA (2005) PAK1 negatively regulates the activity of the Rho exchange factor NET1. J Biol Chem 280: 12152-12161.
45. Weterings E, Chen DJ (2007) DNA-dependent protein kinase in nonhomologous end joining: a lock with multiple keys? J Cell Biol 179: 183-186.
46. Lucero H, Gae D, Taccioli GE (2003) Novel localization of the DNA-PK complex in lipid rafts: a putative role in the signal transduction pathway of the ionizing radiation response. J Biol Chem 278: 22136-22143.
47. Feng J, Park J, Cron P, Hess D, Hemmings BA (2004) Identification of a PKB/Akt hydrophobic motif Ser-473 kinase as DNA-dependent protein kinase. J Biol Chem 279: 41189-41196.
48. Muller C, Paupert J, Monferran S, Salles B (2005) The double life of the Ku protein: facing the DNA breaks and the extracellular environment. Cell Cycle 4: 438-441.
49. Hehlgans S, Haase M, Cordes N (2007) Signalling via integrins: implications for cell survival and anticancer strategies. Biochim Biophys Acta 1775: 163-180.
50. Zhang H, Ozaki I, Mizuta T, Matsuhashi S, Yoshimura T, et al. (2002) Beta 1-integrin protects hepatoma cells from chemotherapy induced apoptosis via a mitogen-activated protein kinase dependent pathway. Cancer 95: 896-906.
51. Chiarugi P, Giannoni E (2008) Anoikis: a necessary death program for anchorage-dependent cells. Biochem Pharmacol 76: 1352-1364.
52. Zaidel-Bar R, Itzkovitz S, Ma'ayan A, Iyengar R, Geiger B (2007) Functional atlas of the integrin adhesome. Nat Cell Biol 9: 858-867.

53. Stuffers S, Brech A, Stenmark H (2009) ESCRT proteins in physiology and disease. Exp Cell Res 315: 1619-1626.
54. Falguieres T, Luyet PP, Gruenberg J (2009) Molecular assemblies and membrane domains in multivesicular endosome dynamics. Exp Cell Res 315: 1567-1573.
55. Sevrioukov EA, Moghrabi N, Kuhn M, Kramer H (2005) A mutation in dVps28 reveals a link between a subunit of the endosomal sorting complex required for transport-I complex and the actin cytoskeleton in Drosophila. Mol Biol Cell 16: 2301-2312.
56. Pan S, Wang R, Zhou X, Corvera J, Kloc M, et al. (2008) Extracellular Alix regulates integrin-mediated cell adhesions and extracellular matrix assembly. Embo J 27: 2077-2090.
57. Jahn R, Scheller RH (2006) SNAREs--engines for membrane fusion. Nat Rev Mol Cell Biol 7: 631-643.
58. Zhang Y, Shu L, Chen X (2008) Syntaxin 6, a regulator of the protein trafficking machinery and a target of the p53 family, is required for cell adhesion and survival. J Biol Chem 283: 30689-30698.
59. Crowe SE (2005) Helicobacter infection, chronic inflammation, and the development of malignancy. Curr Opin Gastroenterol 21: 32-38.
60. Lax AJ (2005) Bacterial toxins and cancer — a case to answer? Nature Reviews Microbiology 3: 343-349.

Figure legend

Figure 1. Screening of the EUROSCARF deletion library
A) CdtB induces cell cycle arrest in the G2 phase and inhibits cell growth in *S. cerevisiae*. Yeast cells (strain BY4743) transfected with the control (CTR) or the pDCH-CdtB (CdtB) plasmids were incubated for 7h in presence of either 2% glucose or 2% galactose/raffinose. Analysis of the cell cycle distribution was assessed by PI staining and flow cytometry as described in *Material and Methods* (upper panel). Serial five-fold dilutions of the yeast culture were incubated on plates containing selective medium supplemented with 2% glucose or 2% galactose/raffinose for 72h (lower panel).
B) Screening of EUROSCARF library. Replica plating of five-fold serial dilutions of the wild-type cells (wt) and deletion mutatants transformed with the pDCH-CdtB plasmid were incubated on plates containing selective medium supplemented with 2% glucose (CdtB OFF) or 2% galactose/raffinose (CdtB ON) for 72h. The left panel shows a selection of the tranformants. The right panel shows the summary of the growth pattern of all the 4492 transformants. The strains that grown up only to the third dilution step (1/125) or less are scored as CdtB hypersensitive.
C) Survival assay. Eight selected deletion mutants and the wild type cells (wt) transfected with the pDCH-CdtB or the control plasmids were incubated overnight in selection medium containing 2% raffinose (CdtB OFF). Equal number of cells were transferred to 3ml synthetic medium containing raffinose/galactose (CdtB ON), and incubated for the indicated period of times at 30°C. One thousand cells were taken at time 0h and 48h and plated on glucose selective plates. Colony forming units (CFUs) were counted after 48h incubation at 30°C. The number of CFU at 48h has been normalized against the number of CFU at time 0 in order to exclude any error due to different growth rate of the transformants. The percentage of cell survival was calculated as follow (CFU of cells carrying the pDCH-CdtB plasmid/CFU of cells carrying vector control plasmid) x 100.
** highly statistically significant; * statistically significant.
D) Functional grouping of the genes identified in the screen.

Figure 2. Actin cytskeleton network
A) The black squares indicate the 20 human orthologs of the genes found in the EUROSCARF screen. Four hubs were identified: two formed by proteins involved in DNA damage (red circle), one formed by proteins associated with MAPK pathway (green circle). A fourth group is identified with the blue circle.
B) Part of the network presented in panel A. The green boxes highlight the genes that were further analyzed in mammalian cell lines.

Figure 3. VCL and FEN1 knock down increases the rate of cell death upon intoxication
A) HeLa cells were transfected with non-silencing siRNA (siCTR), TSG101, VCL, or FEN1 specific siRNA. Expression of endogenous protein levels were analyzed by western blot 72h after transfection. Actin is used as loading control. **B)** HeLa cells were transfected with non-silencing siRNA (siCTR), TSG101, VCL, or FEN1 specific siRNA, and further left untreated or exposed to CDT (2μg/ml) for 72h. Cell death was assessed by immunoflurescence, using the conformational-dependent anti-Bax 6A7 antibody. **C)** Quantification of the Bax positive cells. One out of two experiments is shown. **D)** Data are presented as ratio of the number of Bax positive cells upon intoxication and the number of Bax positive cells in untreated control. Mean of two independent experiments.

Figure 4. Actin stress fiber formation and RhoA activation upon knock down of VCL, FEN1 and TSG101

A) Non transfected HeLa cells or cells transfected with non-silencing siRNA (siCTR), TSG101, VCL, or FEN1 specific siRNA were left untreated (-DSB) or exposed to IR (20Gy) or CDT (2μg/ml) for 48h (+DSB). The actin cytoskeleton was visualized by TRITC-phalloidin staining. Cells exhibiting more than 5 stress fibers were scored as positive.

B) Quantification of cells with stress fibers**.** The values represent the percentage of cells with stress fibers (mean ±SD of 3 independent experiments, two performed with CDT and one performed with IR).

C) HeLa cells, non transfected or cells transfected with non-silencing siRNA (siCTR), TSG101, VCL, or FEN1 specific siRNA, were left untreated (-DSB), or exposed to CDT ((2μg/ml; +DSB), and further incubated for 4h. Activation of RhoA was assessed by RhoA specific G-LISA^{TM} (mean ±SD of 3 independent experiments). Pos: internal positive control of the RhoA specific G-LISA^{TM} assay.

Figure 5. VCL and FEN1 knock down prevent phosphorylation of p38 MAPK upon induction of DNA damage.

A) Non transfected HeLa cells or cells transfected with non-silencing siRNA (siCTR), TSG101, VCL, or FEN1 specific siRNA were left untreated (-DSB), or exposed to ionizing radiation (20Gy, +DSB), and further incubated for 4h in complete medium. Samples were subjected to western blot analysis using an α-p38 phospho-specific antibody (p-p38) or an α-p38 specific antibody (p-38). **B)** Quantification of the experiment presented in panel A. Data are presented as ratio between the optical density of the p-p38 specific band in irradiated cells and the optical density of the p-p38 specific band in untreated cells (mean ±SD of 3 independent experiments).

Figure 6. Summary of the data presented in this work. RhoA activation regulates two distinct pathways in response to DNA damage: i) induction of actin stress fibers, which requires both the RhoA kinase ROCKI and II, and TSG101; ii) activation of p38 MAPK, associated with a delayed cell death, which is FEN1 and VCL dependent.

Table 1. Genes identified in the EUROSCARF screen

Group	Function	# genes	Yeast genes[a]	Human orthologs
1	Replication recombination repair	13	*DCC1*, *DDC1*, *DIA2*, *ELG1*, *MMS4*, *MUS81*, *RAD27*, *RAD50*, *RAD51*, *RAD57*, *SAE2*, *SHU1*, *SRS2*	*DSCC1*, *DIAPH3*, *MUS81*, *FEN1*, *RAD50*, *RAD51*, *XRCC3*, *UBA2*, *UBE2B*
2	Checkpoint	5	*CHK1*, *MEC3*, *MRC1*, *RAD9*, *TOF1*	*CHEK1*, *PIP3-E*, *MRC1L.1*, *RAD9A*,
3	Chromatin silencing telomeres	8	*CST6*, *ESC1*, *NAM7*, *NAT3*, *NMD2*, *NPT1*, *UPF3*, YPL205C	*CST6*, *UPF1*, *NAT5*, *UPF2*, *SLC17A1*, *UPF3A*
4	Mitotic chromosome transmission	5	*CHL1*, *CHL4*, *CTF4*, *MCM21*, *MCM22*	*DDX11*, *CENPN*, *REPS2*, *NFIC*
5	Vacuolar/ Golgi/ endocytosis	10	*DRS2*, *PEP7*, *PEP12*, *PMR1*, *SNF7*, *VPS3*, *VPS4*, *VPS8*, *VPS21*, *VPS23*, *VPS24*	*ATP8A2*, *LAP3*, *STX12*, *ATP2C1*, *CHMP4B*, *VPS4B*, *VPS8*, *RAB5A*, *TSG101*, *VPS24*
6	Mitochondrial	8	*ADK1*, *ALT1*, *FMP37*, *HFA1*, *MRPL10*, *OAR1*, *PDB1*, *SOD2*	*AK2*, *GPT*, *MRPL10*, *PDHB*, *SOD2*
7	Cytokinesis, spindle, cytoskeleton rearrangements	6	*CTF3*, *NIP100*, *PTC1*, *RVS161*, *SLT2*, *SRV2*	*PTCH2*, *BIN3*, *MAPK7*, *CAP1*
8	Translation/Ribosomal	6	*KAP123*, *RPL27A*, *RPL36A*, *RPS0B*, *RPS17A*, *ZUO1*	*IPO4*, *RPL27A*, *RPL36AL*, *LOC387867*, *RPS17*, *DNAJC2*
9	Transcription/ RNA metabolism	3	*BUR2*, *CKA2*, *NPL3*	*CST4*, *CSNK2A1*, *TAF15*,
10	Ubiquitin proteasome system	2	*DOC1*, *SHP1*	*TBX6*, *NSFL1C*
12	Others	6	*LAT1*, *LIP5*, *MKC7*, *RTS1*, *TPD3*, *TPS1*	*DLAT*, *LIAS*,, *PPP2R5C*, *PPP2R1A*, *TPSAB1/TPSB2*
13	Unknown	5	YBR099C, YDR109C, YEL045C, YMR252C, YOR376W	
			78 genes	**59 genes**

a: the red color identifies genes that present human orthologs.

Table 2: Proteins encoded by the human orthologs identified in genome-wide screen and their interacting partners

Protein	Interacting partners
APC10	APC2, RAD2
APC2	APC10
ATP6V1E1	SOS1
B56G/PPP2R5C	PR65B, ERK2
BMK1/ERK5	RAF1
CAP2	ACTG1
CHEK1	TP53BP1, CLSPN, TIMELESS, CSNK2A1P
CLSPN	CHEK1
CSNK2A1P/CSNK2A1/CSK2	CHEK1, FGFB, FGF1, APV, WAS, PAK1
NAT3	RAD2
PKLR	ARHGEF6, PAK1
PPM1A	MSN, PI3K
PR65B/PPP2R1B	B56G
FEN1	GP3A, APC10, RAD50, GP2B, NAT3, VCL
RAD50	RAD2
RSN/CLIP1	P195 (SAR1)
TIMELESS	TIPIN, CHEK1
TIPIN	TIMELESS
TP53BP1	CHEK1
TSG101	P195, ROCK1

Figure 1A

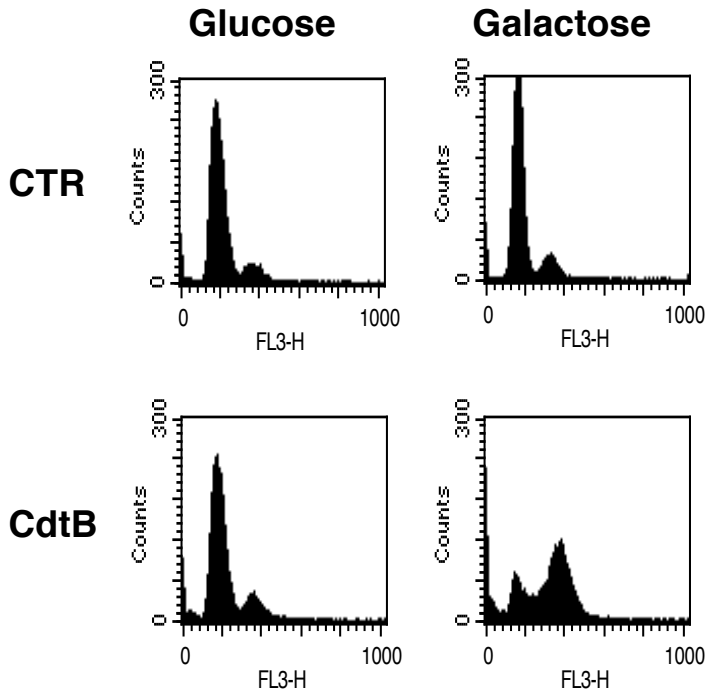
Glucose
Galactose
CTR
CdtB
Counts
300
0
1000
FL3-H

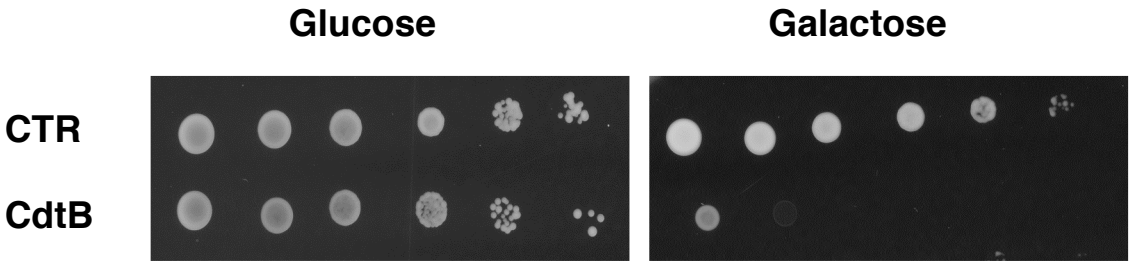
Glucose
Galactose
CTR
CdtB

Figure 1B

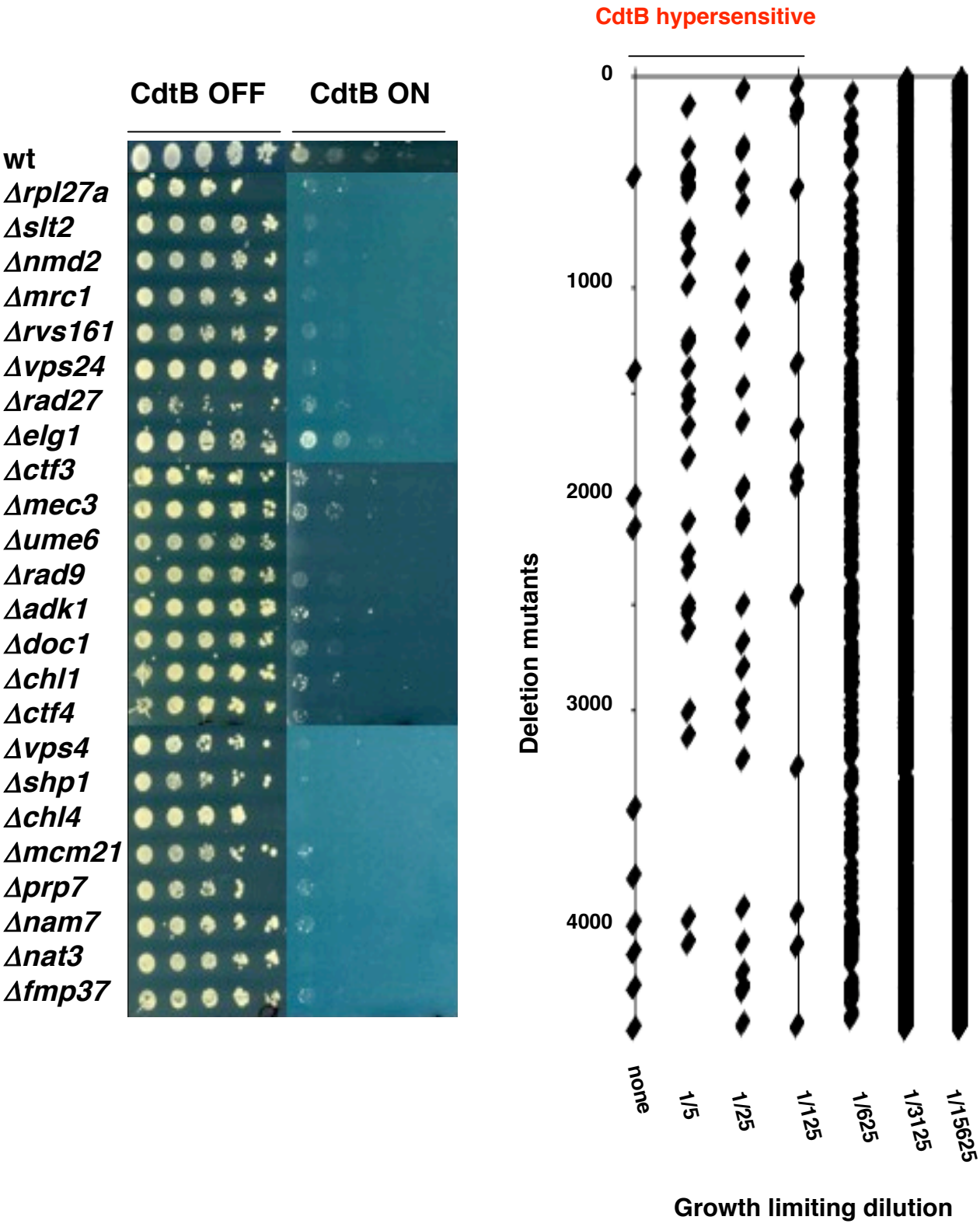
CdtB OFF
CdtB ON
wt
Δrpl27a
Δslt2
Δnmd2
Δmrc1
Δrvs161
Δvps24
Δrad27
Δelg1
Δctf3
Δmec3
Δume6
Δrad9
Δadk1
Δdoc1
Δchl1
Δctf4
Δvps4
Δshp1
Δchl4
Δmcm21
Δprp7
Δnam7
Δnat3
Δfmp37
CdtB hypersensitive
0
1000
2000
3000
4000
Deletion mutants
none
1/5
1/25
1/125
1/625
1/3125
1/15625
Growth limiting dilution

Figure 1C

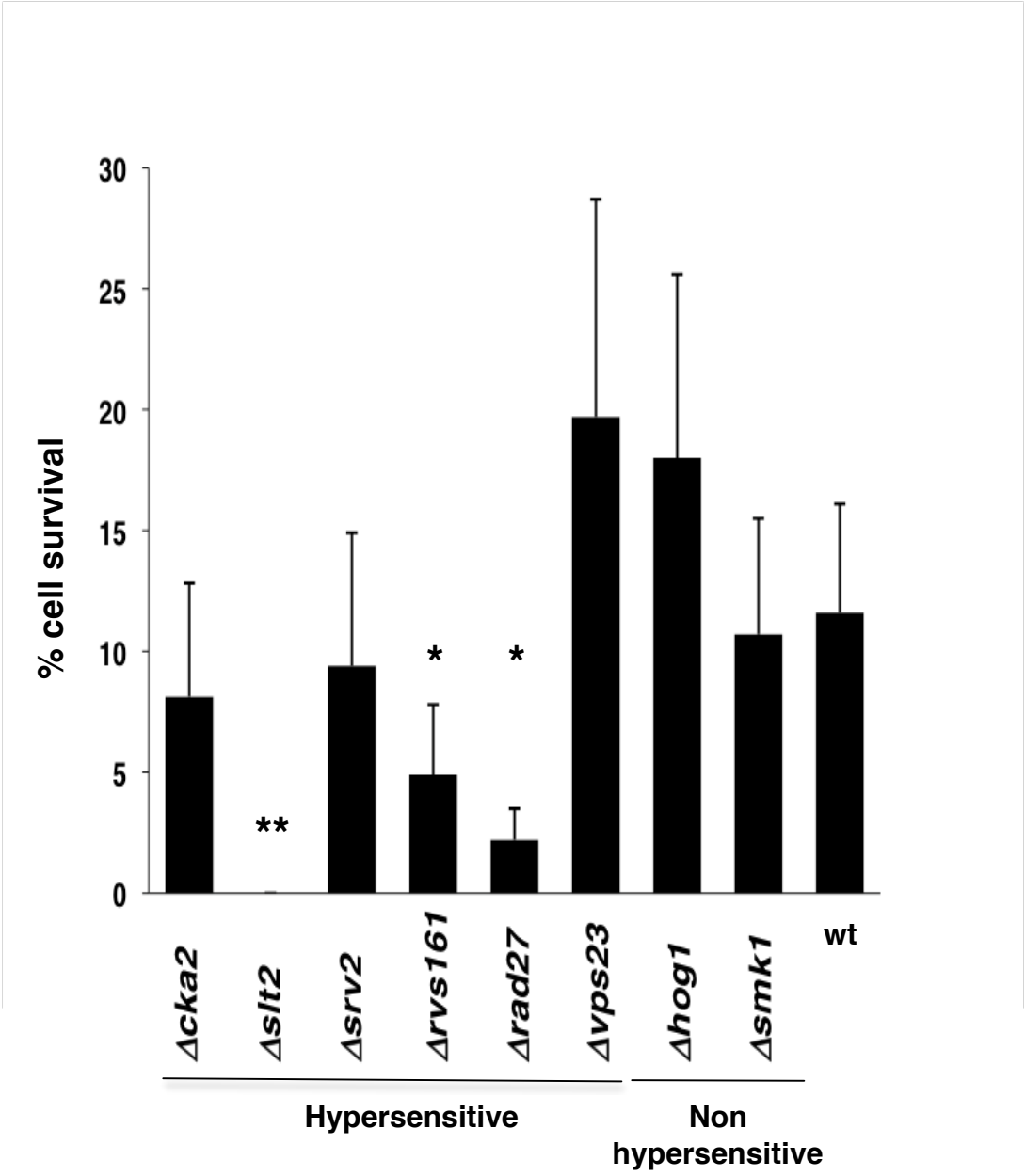
% cell survival
30
25
20
15
10
5
0
**
*
*
Δcka2
Δslt2
Δsrv2
Δrvs161
Δrad27
Δvps23
Δhog1
Δsmk1
wt
Hypersensitive
Non hypersensitive

Figure 1D

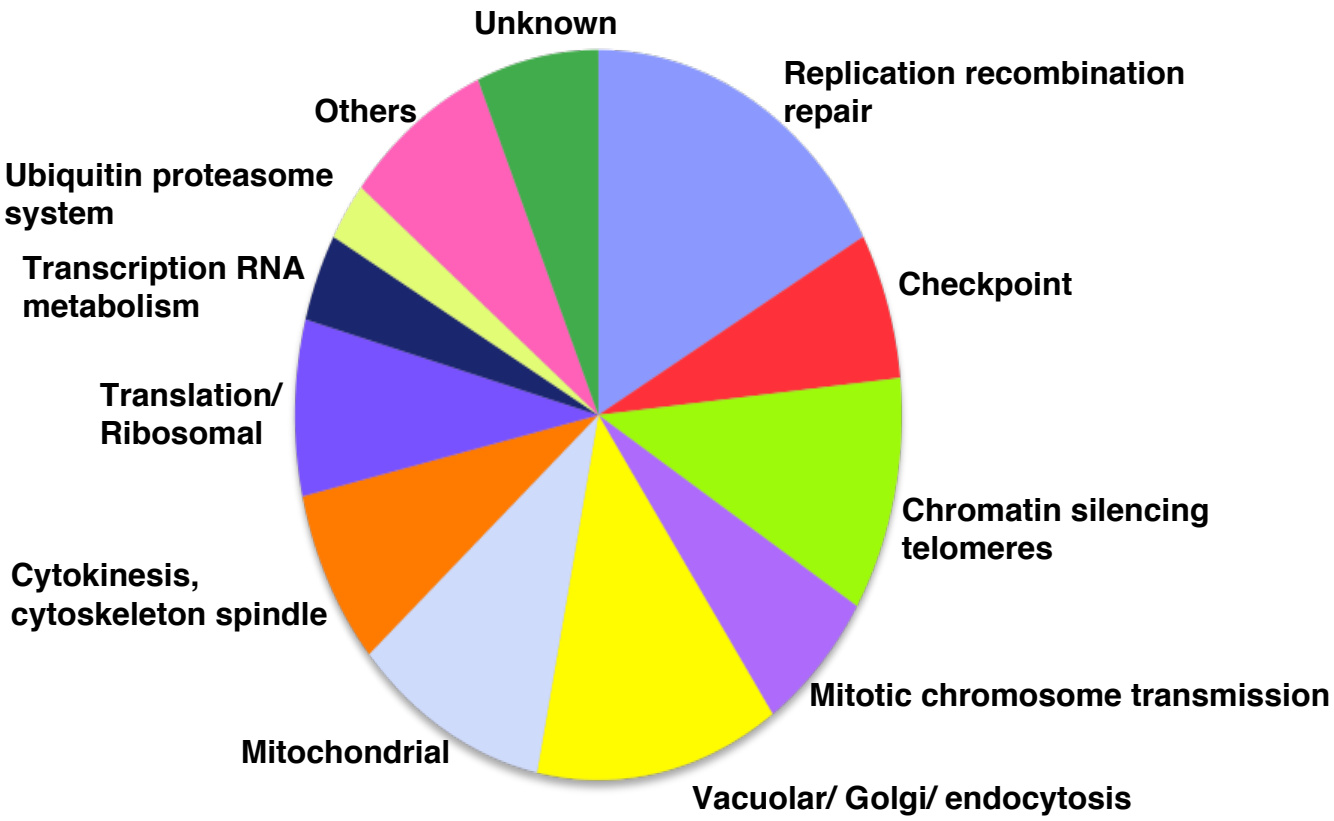
Unknown
Replication recombination repair
Others
Ubiquitin proteasome system
Checkpoint
Transcription RNA metabolism
Translation/ Ribosomal
Chromatin silencing telomeres
Cytokinesis, cytoskeleton spindle
Mitotic chromosome transmission
Mitochondrial
Vacuolar/ Golgi/ endocytosis

Figure 2A

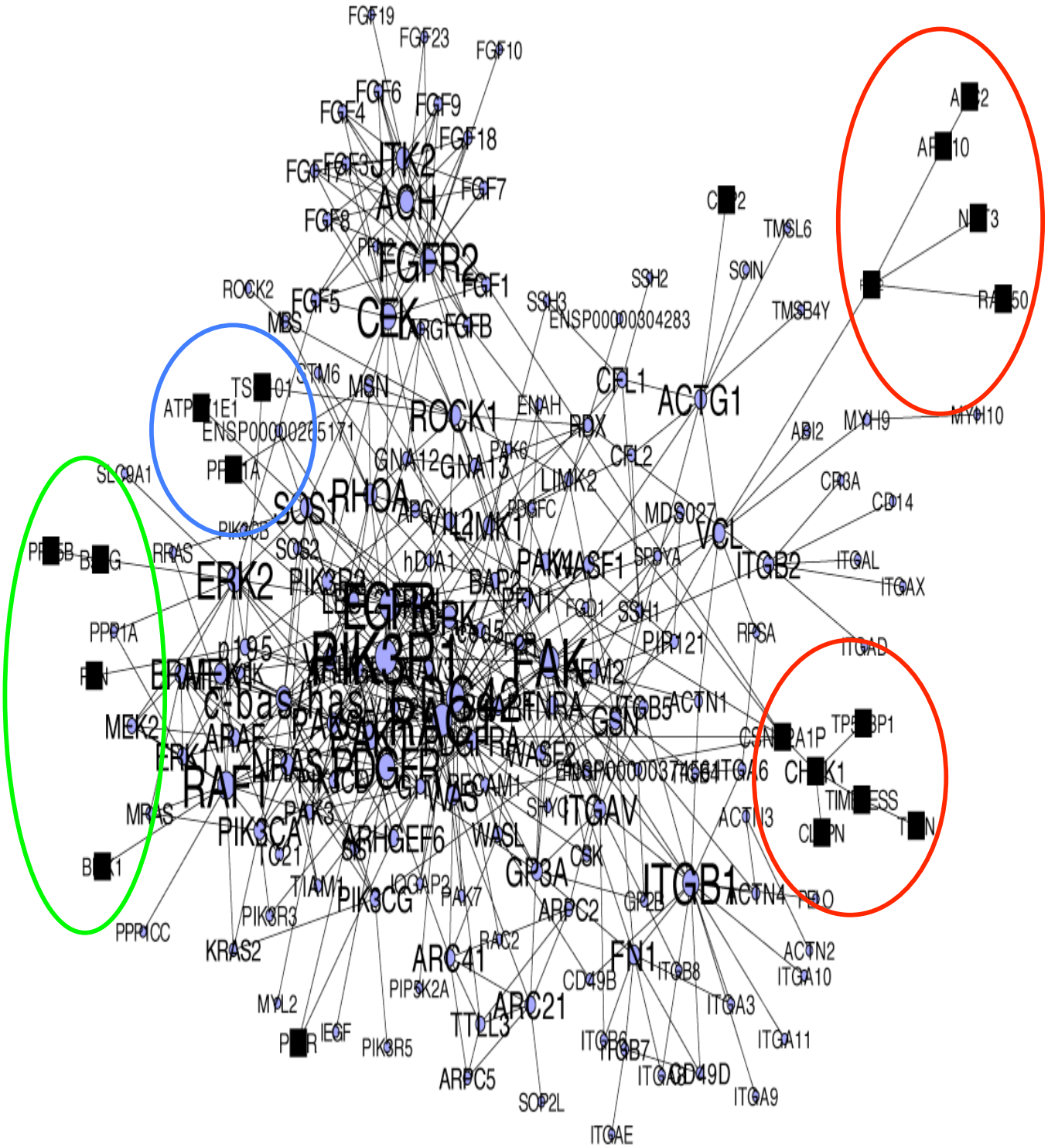

Red = DNA damage
Green = MAPK pathways
Blue = not functionally homogenous

Figure 2B

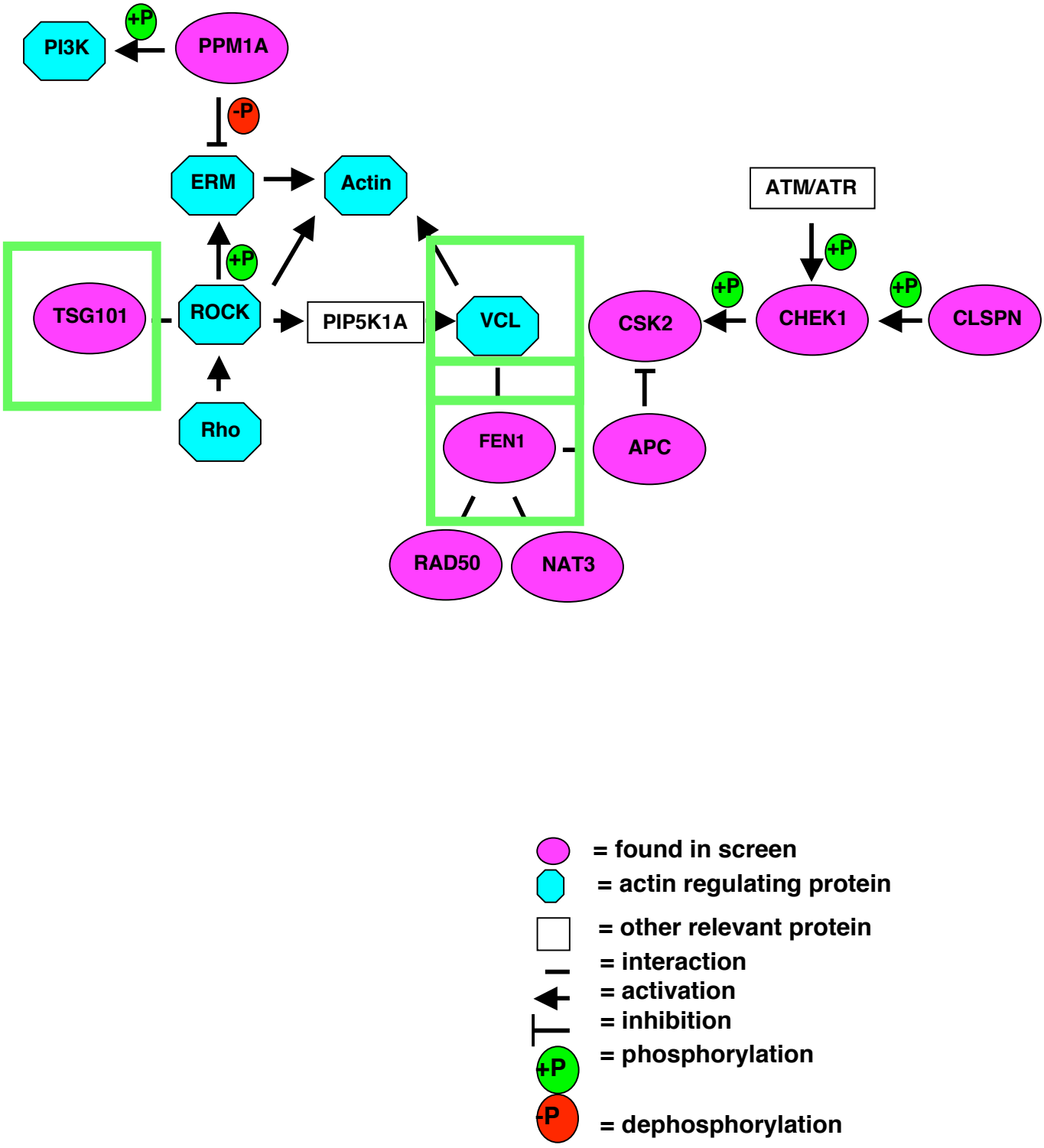
PI3K
+P
PPM1A
-P
ERM
Actin
ATM/ATR
+P
+P
TSG101
ROCK
PIP5K1A
VCL
+P
CSK2
CHEK1
+P
CLSPN
Rho
FEN1
APC
RAD50
NAT3
= found in screen
= actin regulating protein
= other relevant protein
= interaction
= activation
= inhibition
= phosphorylation
= dephosphorylation

Figure 3

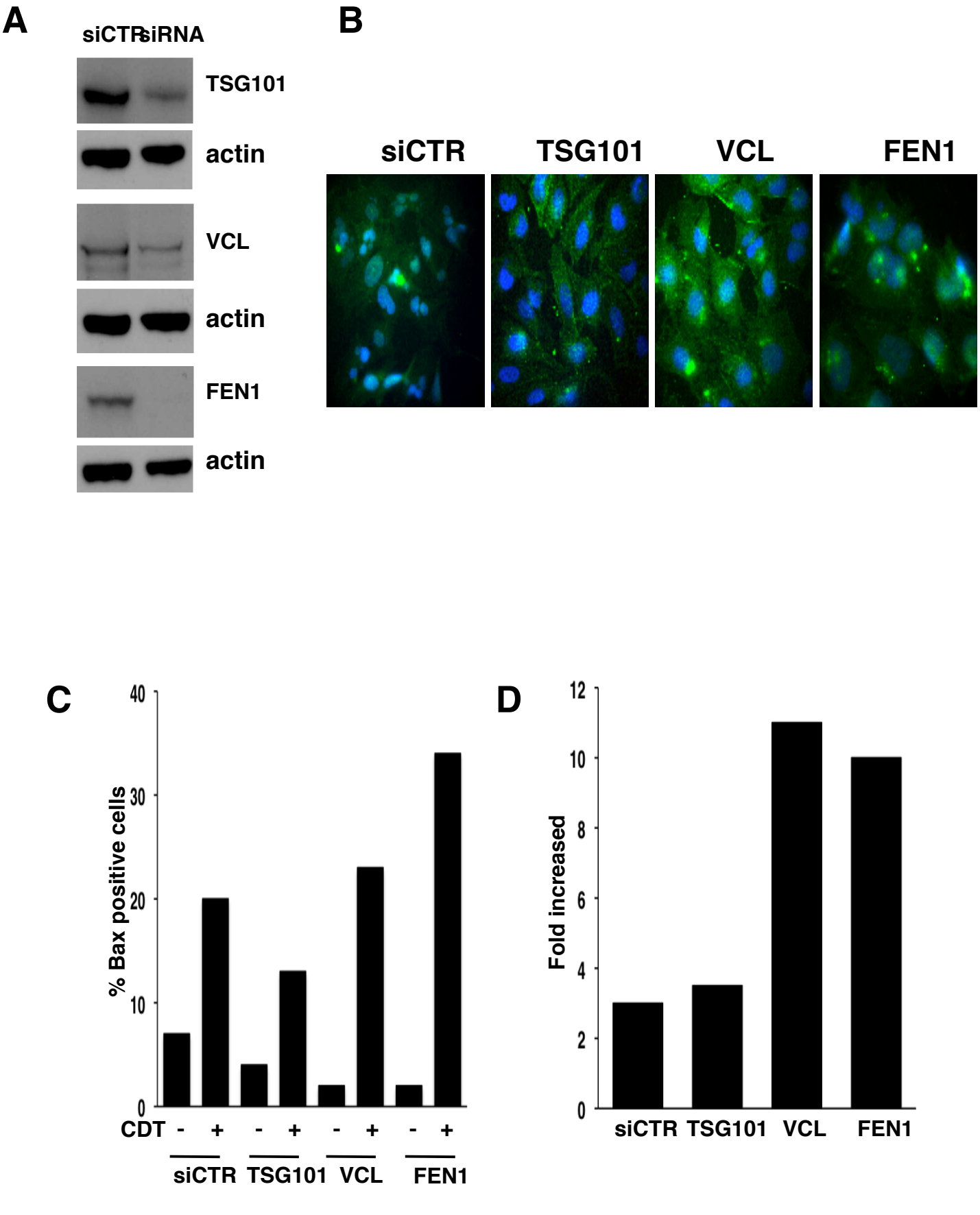
A
siCTR
siRNA
TSG101
actin
VCL
actin
FEN1
actin
B
siCTR
TSG101
VCL
FEN1
C
% Bax positive cells
40
30
20
10
0
CDT - + - + - + - +
siCTR TSG101 VCL FEN1
D
Fold increased
12
10
8
6
4
2
0
siCTR TSG101 VCL FEN1

Figure 4

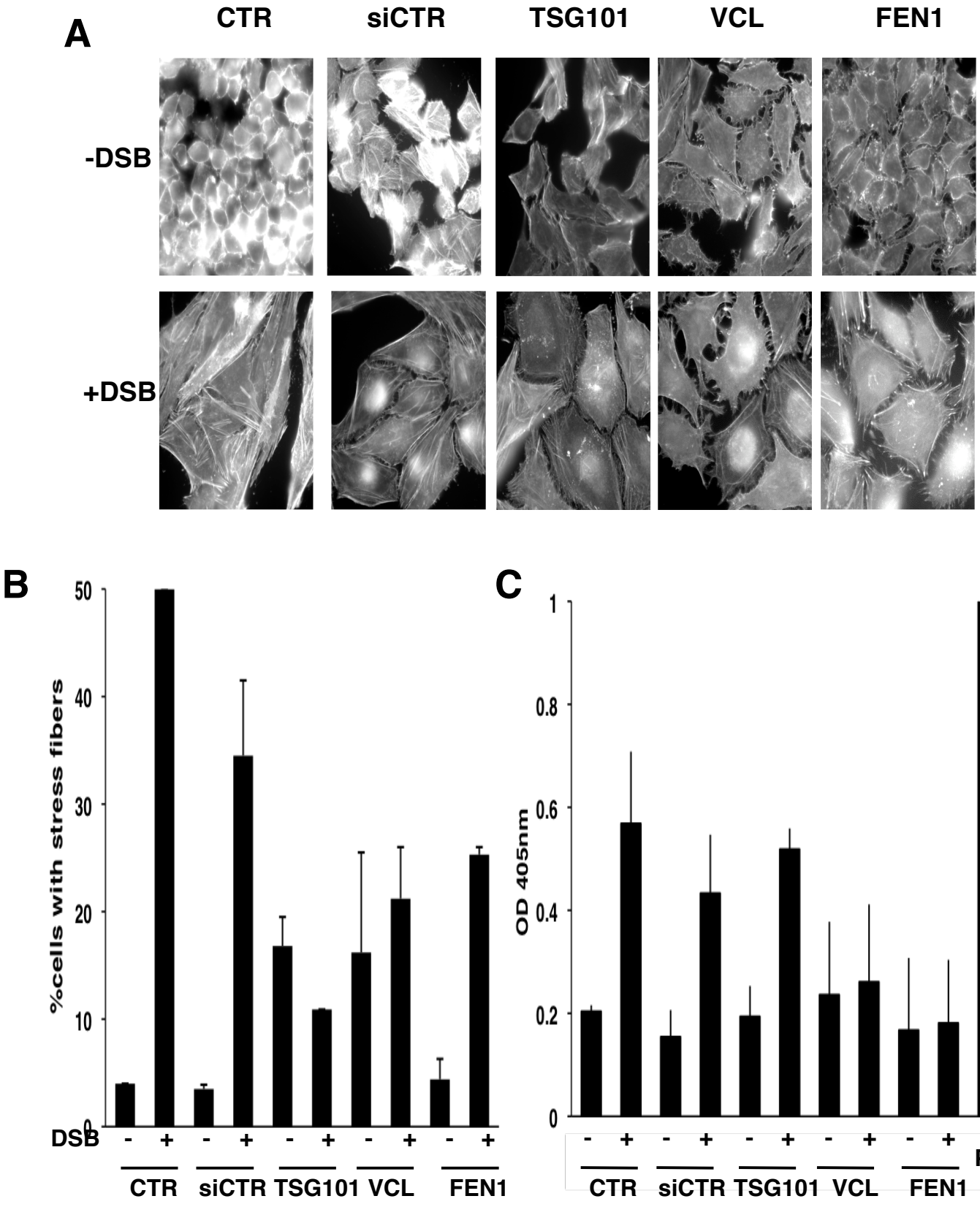
A
CTR
siCTR
TSG101
VCL
FEN1
-DSB
+DSB
B
%cells with stress fibers
50
40
30
20
10
0
DSB
- + - + - + - + - +
CTR
siCTR
TSG101
VCL
FEN1
C
OD 405nm
1
0.8
0.6
0.4
0.2
0
- + - + - + - + - +
Pos
CTR
siCTR
TSG101
VCL
FEN1

Figure 5

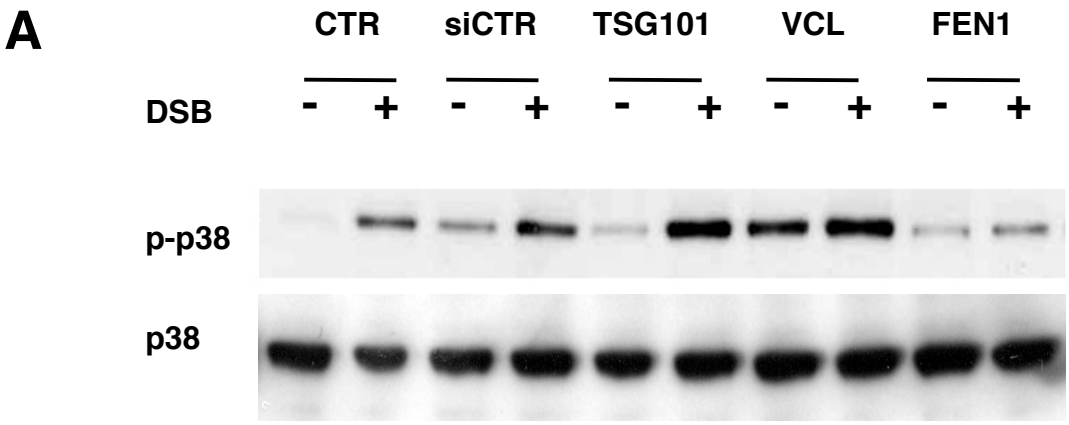
A
CTR
siCTR
TSG101
VCL
FEN1
DSB
- + - + - + - + - +
p-p38
p38

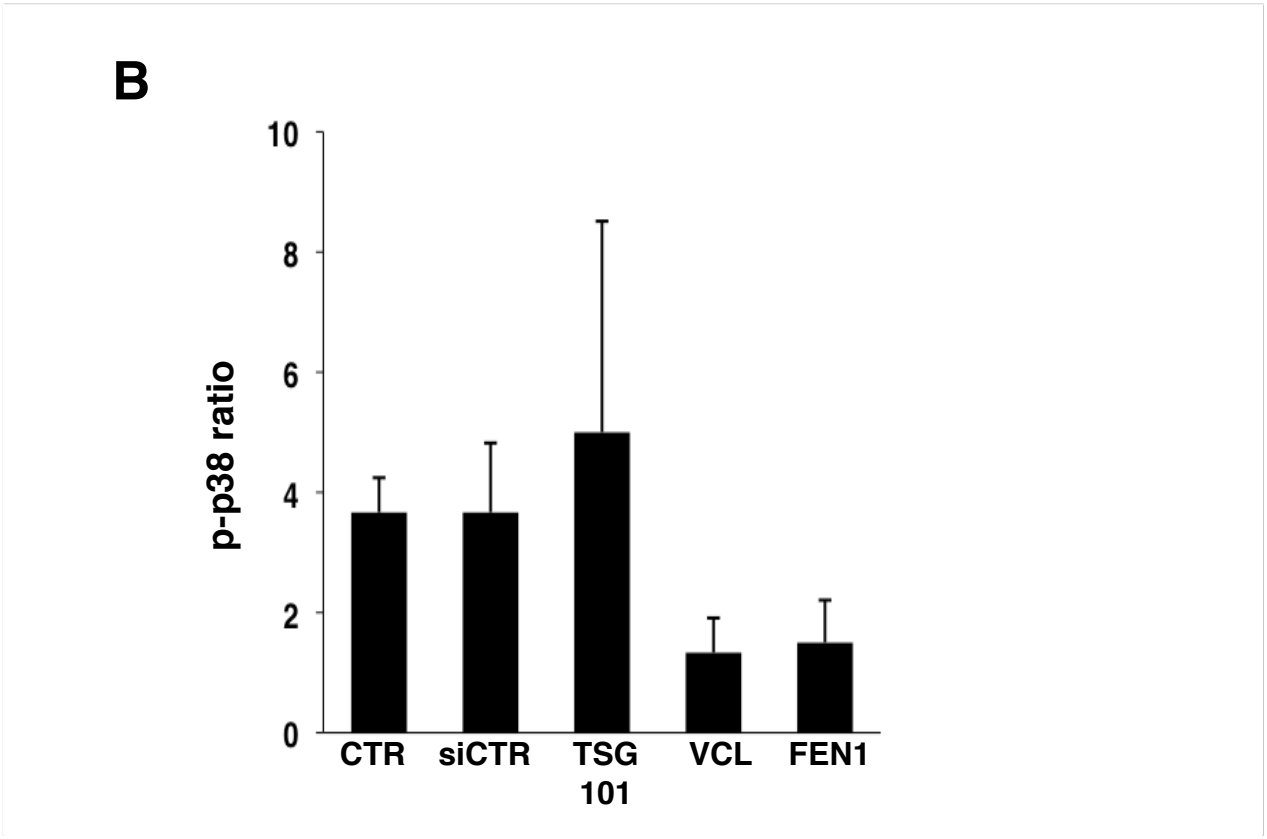
B
p-p38 ratio
10
8
6
4
2
0
CTR
siCTR
TSG 101
VCL
FEN1

Figure 6

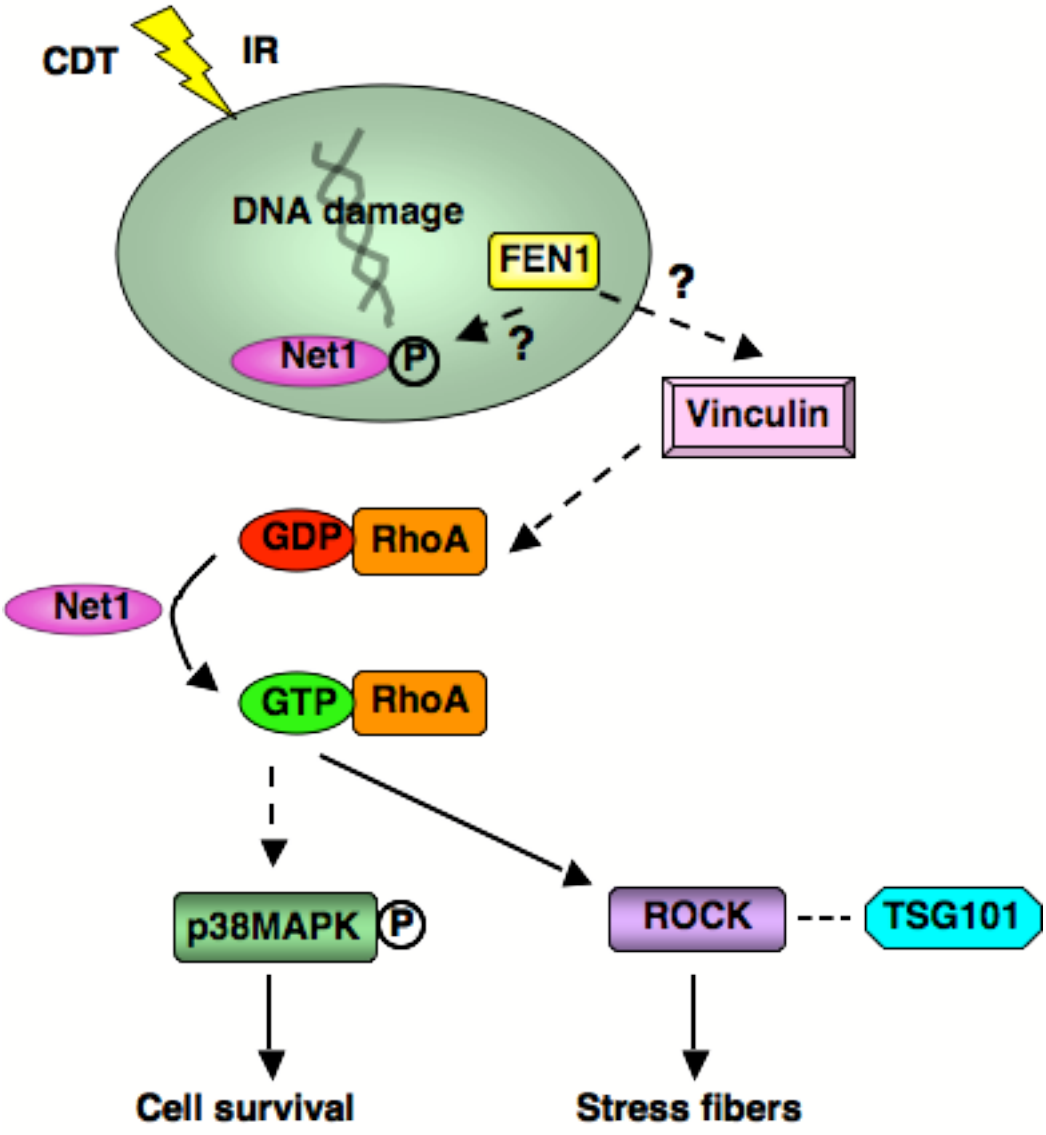
CDT
IR
DNA damage
FEN1
?
Net1
P
?
Vinculin
GDP
RhoA
Net1
GTP
RhoA
p38MAPK
P
ROCK
TSG101
Cell survival
Stress fibers

Supplementary data

PCR

PCR was performed as previously described in Single Tube Confirmation PCR Protocol (http://www-sequence.stanford.edu/group/yeast_deletion_project/single_tube_protocol.html). Briefly, one colony was suspended in 50µl of 60U/ml Zymolase 20T solution (Seikagaku Corporation) and incubated at 37°C for 1h, followed by 10min at 95°C. PCR was performed as followed: five microliter of each primer was added in the PCR tubes followed by 5µl of yeast suspension. The PCR master mix was added and the PCR was carried out accordingly using the following conditions: Step1, 3min at 95°C; Step 2, 15sec at 94°C, 15sec at 57°C, 1min at 72°C, repeated for 35 cycles; Step3, 3min at 72°C). PCR products were analyzed in 1.5% agarose gels.

Supplementary Table 1: PCR primer sequences[a]

ORF	Encoded protein	Primer name	Primer sequence (5' to 3')
YLR226W	BUR2	C_BUR2	TTTTGAATCATATTGAAACAAGGGT
		D_BUR2	TCGAAAATATTATTGATGCTTGTGA
YOR061W	CKA2	C_CKA2	TTGATCCTACGGAACGTAAACTAAG
		D_CKA2	GAACAATTCCAAAACTATTCCATTG
YLR381W	CTF3	C_CTF3	AACGCTAAATTTTTCACGATAACTG
		D_CTF3	ACTTTTTGAAATTAGGTAGGGATGC
YCL016C	DCC1	C_DCC1	ATACCGTTTATAGCTCAGTGGTACG
		D_DCC1	TTGATTTCAACATCTTCCAGTTGTA
YOR080W	DIA2	C_DIA2	TCCAATTGTTAATTTGGATGAAGAT
		D_DIA2	TGGAACAATTTCCTCTTATGATGTT
YGL240W	DOC1	C_DOC1	ATAACTACGATACGTTTTGGCAGAG
		D_DOC1	ATGAAATTTTTGAAGAACAAAGCAC
YAL026C	DRS2	C_DRS2	GTGGGCAAGAAAAAATTGTCAGAA
		D_DRS2	TAAGGTACGTACCCAGTCGAAGCAA
YGL080W	FMP37	C_FMP37	GGTGTTTTCATGAAGTATGCTCTTT
		D_FMP37	AATACAAAGGAGATGAGAGGGAAAT
YMR207C	HFA1	C_HFA1	AGAAAATGATAGAGACGATGATTCG
		D_HFA1	GAATGTCAGATTTTCTCTTTTCGG
YER110C	KAP123	C_KAP123	TTCATGAAATGCTAGAAGCCTTAGT
		D_KAP123	ATCAACTTTACAGGACGAAACTCAC
YLR288C	MEC3	C_MEC3	AATTGTGAATGAATTAGATTGGCAT
		D_MEC3	GTGCAGTTCATGTAGCCTTTAAAAT
YPL174C	NIP100	C_NIP100	AGAAATGTTCAACTTCGTGAGTACC
		D_NIP100	CATGATAGCGTGTCTAAAATGTACG
YOR209C	NPT1	C_NPT1	TTCTCGAAGATTATCTGTTATTCCG
		D_NPT1	GTGAATGAATTAAGAAAGCAAAGGA
YBR221C	PDB1	C_PDB1	ATCAAAACTGTCAAGAAGACAAACC
		D_PDB1	CGTATTCTAACCATGAAACAGGAAC
YOR036W	PEP12	C_PEP12	AACTTGTGAGGGATGTCAGTTACTC
		D_PEP12	ACTTATGAAGCCTACGTGTTATTCG
YDR323C	PEP7	C_PEP7	TTGCTAAATATGATAGCATGCAAAA
		D_PEP7	CTGCTCCTCTTTCTTCTTAGCATTA
YGL167C	PMR1	C_PMR1	GGACTGTCTCTGTTAGGTCAAATGT
		D_PMR1	TTTGTCGAAGGTATAAATGAGGAAG
YDL006W	PTC1	C_PTC1	ATTATAGAGCAAAACATTTTGGCAG
		D_PTC1	CTATTGACTTGTAAACCGTGTTGTG
YCR009C	RVS161	C_RVS161	ACAAAGTTTTCGACGTATTTCAAAG
		D_RVS161	CGTATCTTATTCCTCGCTTCTATTG
YDR129C	SAC6	C_SAC6	CCTTAGAAAACACCAACTATGCAGT
		D_SAC6	CATTTTCTGCATATTTCAAAGAACC
YGL175C	SAE2	C_SAE2	GACTACGAATTTGCGTTTGATAACT
		D_SAE2	CCTGGTAAGTTAGGTGTCATTTGTT
YBL058W	SHP1	C_SHP1	GAAGACAACACTTCACAATCACAAC

		D_SHP1	CTTCATACAACCCAATTATGACACA
YHR030C	SLT2	C_SLT2	AAAAGAGCTGGAGTTTGGATTAGAT
		D_SLT2	TAAAGGGCTTCTCAGTGAATACATC
YIR025W	SNF7	C_SNF7	GTGGAAGAGGCTCATCATTTAGATA
		D_SNF7	AACTACAAGGCAAGCAAGAGTTAGA
YNL138W	SRV2	C_SRV2	ATTCAAGTTAACCATTCCCTACCTC
		D_SRV2	AAATGGTAAATGATCGTCGTGTATT
YOR089C	VPS21	C_VPS21	AGCAGTTGGTAAATCGTCAATAGTC
		D_VPS21	CAATATTAACTAATCCATCTCCCGA
YKL041W	VPS24	C_VPS24	AGGGAGGTAAATTCATTGGTTAGAC
		D_VPS24	TATGTGGATGAAGTGAAAGAAGTGA
YDR495C	VPS3	C_VPS3	AAAATACATAGGCAAGCAGAACTTG
		D_VPS3	CCAGAAGATTTTCATAGGCAAGTAA
YPR173C	VPS4	C_VPS4	AAACAAGAAAACTAACACCATGCTC
		D_VPS4	TTTGTTACAGGAGTTAAATCAAGCC
YAL002W	VPS8	C_VPS8	ATGTACAGCGCCACCAAGATATGA
		D_VPS8	TAGGTGTCGTGAAGTACTTTCGCTT
Kanamycin cassette	Kan^R	C_Kan	TGATTTTGATGACGAGCGTAAT

a: The primer sequences were obtained from:

http://www-sequence.stanford.edu/group/yeast_deletion_project/strain_homozygous_diploid.txt)

Supplementary Table 2: Confirmation PCR for 30 out of the 80 homozygous deletion mutants[a]

ORF	Encoded protein	PCR product for the Kanamycin cassette	PCR product for the ORF coding region
YLR226W	BUR2	+	-
YOR061W	CKA2	+	-
YLR381W	CTF3	+	-
YCL016C	DCC1	+	-
YOR080W	DIA2	+	-
YGL240W	DOC1	+	-
YAL026C	DRS2	+	-
YGL080W	FMP37	+	-
YMR207C	HFA1	+	-
YER110C	KAP123	+	-
YLR288C	MEC3	+	-
YPL174C	NIP100	+	-
YOR209C	NPT1	+	-
YBR221C	PDB1	+	-
YOR036W	PEP12	+	-
YDR323C	PEP7	+	-
YGL167C	PMR1	+	-
YDL006W	PTC1	+	-
YCR009C	RVS161	+	-
YDR129C	SAC6	+	-
YGL175C	SAE2	+	-
YBL058W	SHP1	+	-
YHR030C	SLT2	+	-
YIR025W	SNF7	+	-
YNL138W	SRV2	+	-
YOR089C	VPS21	+	-
YKL041W	VPS24	+	-
YDR495C	VPS3	+	-
YPR173C	VPS4	+	-
YAL002W	VPS8	+	-

a: Strains were considered as homozygous deletion mutants when positive for the PCR product corresponding to the kanamycin cassette and negative for the PCR product relative to the ORF coding region.

Myc is required for activation of the ATM-dependent checkpoints in response to DNA damage

Lina Guerra[1#], Ami Albihn[2#], Riccardo Guidi[1], Susanna Tronnersjö[2], Bo Stenerlöw[3], Christine Josenhans[4], James G. Fox[5], David B. Schauer[6], Monica Thelestam[1], Lars-Gunnar Larsson[2], Marie Henriksson[2] and Teresa Frisan[1*]

[1]Departments of Cell and Molecular Biology and [2]Microbiology, Tumor and Cell Biology, Karolinska Institutet, Stockholm, Sweden. [3]Division of Biomedical Radiation Sciences, Rudbeck Laboratory, Uppsala University, Sweden. [4]Institute for Medical Microbiology and Hospital Epidemiology, Hannover Medical School, Germany. MIT, Divisions of [5]Comparative Medicine and [6]Biological Engineering, Cambridge, Massachusetts, U.S.A.

Running title: Myc regulates DNA damage-induced ATM response

# These authors contributed equally to the work.

*Address correspondence to: Teresa Frisan, Dept. Cell and Molecular Biology, Karolinska Institutet, Stockholm, Sweden, Box 285, S-171 77 Stockholm, Sweden. Tel: +46-8-52487162, Fax: +46-8-337412, e-mail: Teresa.Frisan@ki.se

Abstract

The MYC protein controls cellular functions such as differentiation, proliferation, and apoptosis. In response to genotoxic agents, cells expressing MYC undergo apoptosis. However, the MYC-regulated effectors acting upstream of the mitochondrial apoptotic pathway are still unknown. In this study, we demonstrate that expression of Myc is essential to activate the Ataxia telangiectasia mutated (ATM)-dependent DNA damage checkpoint responses in cells exposed to ionizing radiation (IR) or the cytolethal distending toxin (CDT). Phosphorylation of the ATM kinase and its downstream effectors, such as histone H2AX, were impaired in the *myc* null rat cell line HO15.19, compared to the *myc* positive TGR-1 and HOmyc3 cells. Nuclear foci formation of the Nijmegen Breakage Syndrome (Nbs)1 protein, essential for efficient ATM activation, was also abrogated in absence of *myc*. Interestingly, phosphorylation of the ATM- and Rad3-related (ATR) substrate Chk1 was not hampered in the HO15.19 cells in response to irradiation. Accordingly, the cellular response to UV irradiation, known to activate an ATR-dependent checkpoint, was similar in all the cell lines, independently of the *myc* status. These data demonstrate that Myc is required for activation of the ATM-dependent pathway, which recognizes DNA damage and orchestrates the checkpoint responses in order to preserve genomic integrity.

Keywords: Myc, ionizing radiation (IR), cytolethal distending toxin (CDT), DNA damage response, Ataxia Telangiectasia Mutated (ATM), checkpoint responses

Introduction

The MYC transcription factor regulates a wide variety of cellular functions such as normal cell turnover, differentiation, cellular motility, and apoptosis (reviewed in [1]). Since it controls the delicate balance between cell proliferation and cell death, MYC expression can be found deregulated in many different types of tumors [2-4]. The oncogenic capacity of MYC is not only dependent on its ability to regulate expression of genes that enhance cell proliferation (e.g up-regulation of E2F) or suppress cell cycle arrest (e.g. down-regulation of $p21^{CIP1}$ or $p15^{INK4B}$, reviewed in [5]), but it may contribute to tumorigenesis by induction of DNA damage, and consequent genomic instability [6, 7] (and reviewed in [8]).

Stress signals, such as growth factor deprivation, hypoxia, and exposure to genotoxic agents trigger MYC dependent apoptosis [9, 10]. The apoptotic response is dependent on release of cytochrome C from the mitochondria through activation or up-regulation of the pro-apoptotic members of the Bcl-2 family [9, 11-13]. Our previous studies were aimed at understanding the role of MYC in cells exposed to conventional DNA damaging cytotoxic drugs. We found that doxorubicin, camptothecin and etoposide induced a strong apoptotic response in the Rat1 cell line TGR-1, expressing physiological levels of Myc, via activation of Bid and Bax. Cell death in response to camptothecin and etoposide was further enhanced by the pro-apototic enzyme PKCδ. The apoptotic response was dependent on Myc expression, since activation of these proteins was not detected in the *myc* null cells HO15.19 [14, 15]. However, the molecular signaling pathway that regulates the MYC dependent Bax activation in response to DNA damage is not known.

In normal cells, exposure to genotoxic agents triggers activation of checkpoint responses that lead to cell cycle arrest or cell death. A key protein in orchestrating this complex response to DNA double strand breaks (DSB) is the Ataxia telangiectasia mutated (ATM) kinase [16]. ATM exists as an inactive dimer, which undergoes a conformational change upon induction of DNA DSB. The change in protein structure stimulates intermolecular autophosphorylation on Ser1981, resulting in dissociation of the dimer, and consequent activation of the kinase [17]. Full activation of ATM requires interaction with the MRN complex (Mre11/Rad50/Nbs1), which enhances

the recruitment of ATM to the site of DNA damage [18, 19]. Proteins identified as ATM substrates regulate recruitment of DNA repair complexes (e.g. H2AX), activate checkpoint responses to block cell proliferation (e.g. Chk2 kinase), or induce apoptosis (e.g. the tumor suppressor p53) [20]. Despite the well-established role of MYC in activating p53-dependent apoptosis, the exact role of MYC in regulating the DNA damage response (apoptosis versus repair) remains poorly understood [21-24].

To identify the MYC-regulated effectors acting upstream of the mitochondrial apoptotic pathway in response to genotoxic stress, we have used Rat1 cells with different Myc status: the parental TGR-1 cells expressing physiological levels of Myc, the *myc* null cells HO15.19, and the HOmyc3 cells, where expression of the murine Myc has been reconstituted [25, 26]. We demonstrated that Myc deletion impairs activation of the ATM dependent DNA damage checkpoint responses to agents causing DNA double strand breaks (ionizing radiation and cytolethal distending toxin), including impairment of nuclear foci formation of the MRN complex, lack of phosphorylation of ATM and its downstream targets, such as histone H2AX. These data contribute to identify MYC as an important regulator of one of the key pathways that control genomic stability in normal cells.

Material and methods

Cell lines

Myc null HO15.19 Rat1 fibroblasts were generated from parental TGR-1 cells by homologous recombination, deleting both *myc* alleles, and HOmyc3 cells were generated by reconstitution of the murine *myc* gene into the HO15.19 cells [25, 26]. Cells were cultivated in Dulbecco's modified eagle medium (DMEM), supplemented with 10% fetal calf serum (FCS) and 5 mM L-glutamine (complete medium) in a humid atmosphere containing 5% CO_2.

Treatments

CDT intoxication. Cells were incubated for the indicated time periods with bacterial lysate (diluted 1:2000 in complete medium) derived from the *Helicobacter hepaticus* strain ATCC51449, expressing the wild type CDT, or the control strain *H. hepaticus cdtB*, (HhcdtBm7) expressing a mutant inactive CDT [27]. Bacteria were cultured on a rotary shaker to mid-logarithmic growth phase in liquid medium (Brucella broth, supplemented with 10% horse serum) and in a microaerobic atmosphere (10% hydrogen, 10% CO_2, 80% nitrogen). Bacteria were then centrifuged from the liquid medium, and the pellet washed twice with PBS, and sonicated for 5 min in a Branson sonfier. The lysate was subsequently stored frozen at -20°C. The lysate dilution of 1: 2000 represents the minimal dose sufficient to induce cell cycle arrest in 100% of the cell population.

Ionizing radiation. Cells were irradiated (20 Gy), washed once with PBS and incubated for indicated time periods in complete medium.

UV irradiation. Cells were irradiated for 3 min with a short wave UV lamp (model UVG-11, 254 nm, 220 V, 0.12 AMPS, 50 Hz, UVP, Upland, USA), washed once with PBS and incubated in complete medium for the indicated time periods.

Cell cycle analysis

Cells were trypsinized, centrifuged and washed once with PBS. The cell pellet was resuspended and fixed overnight with 1 ml cold 70% ethanol at 4°C. The cells were subsequently centrifuged and resuspended in 0.1 ml propidium iodide (PI) solution (0.05 mg ml^{-1} PI and 0.25 mg ml^{-1} RNase in PBS) for 30 min at 37°C. Flow

cytometry analysis was performed using a FACScan cytometer (Becton Dickinson). Data from 10^4 cells were collected and analyzed using the CellQuest software (Becton Dickinson).

Immunofluorescence

Fifty thousand cells/well, plated on round 13 mm glass coverslips in 24-well plates in complete medium, were left untreated or irradiated, and incubated for indicated time periods. Cells were fixed with 4% paraformaldehyde, and permeabilized with 0.5% Triton X-100 for 30 min at RT. Slides were blocked in PBS with 3% BSA for 30 min and incubated for 1 h at RT with a α-Nbs1 mAb antibody (BD Transduction Laboratories) diluted 1:50 in PBS. Slides were washed three times for 5 min in PBS, and then incubated with fluorescein-conjugated (FITC)-conjugated anti-mouse antibody (DAKO); diluted 1:100 in PBS for 30 min at RT. Nuclei were counterstained with Hoechst 33258 (Sigma, 0.5 μg ml^{-1}) for 1 min at RT. Slides were mounted and viewed by fluorescence microscopy.

Western blot analysis

Proteins were separated in SDS-polyacrylamide gels, transferred to PVDF membranes (Millipore) and probed with the relevant antibodies. The following antibodies were used: α-H2AX (Upstate Biotechnology), α-phospho-ATM (Ser1981, Novus Biologicals), α-ATM (Genway), α-p53 (Santa Cruz Biotechnology, Inc.), α-actin (Sigma), α-phospho-Chk1 (Ser345), α-phospho-(Ser/Thr)-ATM/ATR substrate (Cell Signaling) and α-Nbs1 (BD Transduction Laboratories). Blots were developed with enhanced chemiluminescence using the appropriate horseradish peroxidase-labeled secondary antibody, according to the instructions from the manufacturer (GE Healthcare).

Detection of DNA double strand breaks by pulsed-field gel electrophoresis

Twenty-five thousand cells per well were grown in 12-well plates in complete medium containing 4000Bq/ml [methyl-^{14}C]-thymidine for 48 h. The cells were then washed 3 times with PBS and chased for 2 h in RPMI complete medium. Subsequently, cells were treated with IR (20 Gy) and collected at the indicated time points by trypsinization in a 150 μl volume. The cell suspension was mixed with 150 μl low

gelling-point agarose (InCert) at 37°C to a final agarose concentration of 0.6%, and pipetted into plastic moulds for 100-µl plugs. Moulds were incubated at 4°C for 20 min to solidify the plugs. The solid plugs were transferred into 1ml ice-cold lysis buffer (2% sarkosyl, 1mg ml^{-1} proteinase K, in 0.5M Na_3-EDTA, pH 8.0) and incubated overnight at 4°C, followed by a second lysis step in high salt solution (1.85 M NaCl, 0.15 M KCl, 5 mM $MgCl_2$, 2 mM EDTA, 4 mM Tris, 0.5% Triton X-100, pH 7.5) overnight at 4ºC [28]. Plugs were washed three times for 1 h in 0.1 M EDTA and double stranded DNA was separated on an agarose gel (0.8% SeaKem Gold, BMA) in a PFGE unit (Gene Navigator, Amersham Bioscience, Uppsala, Sweden) in TBE x 0.5 as previously described [28]. Following electrophoresis, the gels were sliced at the position of the 5.7 Mbp chromosome from *S. pombe* (BMA), and ^{14}C in the gel segments was measured by liquid scintillation. The fraction of radioactivity corresponding to DNA smaller than 5.7 Mbp was used to quantify the number of double strand breaks [29] assuming an induction of 25 DSB per diploid cell per Gy [28].

Results

Myc has been shown to enhance the apoptotic effect of DNA damaging agents, such as etoposide and camptothecin, by activation of the pro-apoptotic protein Bax, and the downstream caspases 3 and 9 [14, 15]. To identify the Myc-regulated effectors acting upstream of the mitochondrial apoptotic pathway, we used the Rat1 fibroblasts TGR-1 expressing wild type levels of Myc and the isogenic *myc* null HO15.19 cell line. As DNA damaging agent, we chose ionizing radiation since the cellular responses to such genotoxic stress are well characterized [20]. Upon irradiation, the Myc expressing TGR-1 cells were arrested in the G2 phase of the cell cycle 12 h after treatment. Arrest in G2 was followed by cell death, assessed as increase of the sub-G1 population with fragmented DNA, 24 h and 48 h after irradiation (Figure 1). On the contrary, a partial arrest in G2 was observed in the *myc* null cells HO15.19 24 h to 48 h after treatment, and signs of cell death occurred only 72 h-96 h post-irradiation (Figure 1).

We next tested whether the delay in DNA damage-induced cell death observed in the *myc* null cells was due to a faster kinetics of DNA repair. TGR-1 and HO15.19 cells were irradiated and further incubated at 37°C for the indicated time periods. The ^{14}C-labeled-DNA was subsequently separated by pulsed-field gel electrophoresis (PFGE) and visualized by ethidium bromide (Figure 2A). Double-strand breaks were then quantified by measuring the ^{14}C-activity for DNA fragments smaller than 5.7 Mbp in a liquid scintillator. As shown in Figure 2B, the disappearance of DNA fragments did not occur with faster kinetics in the HO15.19 cells compared to the control TGR-1, indicating that Myc did not interfere with the rate of DNA repair in these experimental settings.

The ATM kinase is a key protein responsible for activation of the cellular responses to DNA double strand breaks [20]. Therefore we assessed whether the delayed cell death induced by irradiation in the *myc* null cells was associated with an altered ATM response to irradiation. Phosphorylation of ATM on Ser1981 was observed in TGR-1 cells 30 min after irradiation and was sustained at least up to 8 h post-treatment. In this time frame we failed to detect any consistent ATM phosphorylation on Ser1981 in the HO15.19 cells (Figure 3A and data not shown). This result prompted us to

investigate whether Myc was essential also for the activation of ATM effector proteins in response to DNA damage. Using an antibody specific for phosphorylated ATM/ATR substrates, we detected two phospho-proteins of approximately 35 kDa and 110 kDa, respectively in the TGR-1 cells (Figure 3B). Since the levels of phosphorylation peaked at 2 h post-treatment, we chose to use shorter time course kinetics in the subsequent experiments. Phosphorylation of these two ATM/ATR substrates was absent in the HO15.19 cells, at least up to 8 h after irradiation (Figure 3C and data not shown). As the sizes of these proteins do not correspond to any of the known ATM substrates, their identity still remains unknown.

To confirm that the delayed response to genotoxic stress in the HO15.19 cells was due to the absence of *myc* and not an artifact due to clonal selection, we used the HOmyc3 cell line, where expression of the murine *myc* gene was reconstituted into the HO15.19 background [25]. The HOmyc3 cells responded in a similar way to irradiation as did TGR-1, undergoing arrest in the G2 phase of the cell cycle 12 h after treatment, followed by cell death, assessed as increase of the sub-G1 population with fragmented DNA, 24 h and 48 h after irradiation (Figure 3D). In line with this observation, irradiation of the HOmyc3 cells induced ATM phosphorylation similarly to that observed in the parental TGR-1 cells (Figure 3E).

To test whether the delayed cell death in the HO15.19 cells was dependent on the type of DNA damage, we used two additional genotoxic stresses: the bacterial cytolethal distending toxin (CDT), which induces DNA double strand breaks similarly to IR [30], and UV irradiation, which causes dipyrimidine photoproducts. CDT intoxication induced arrest in the parental TGR-1 cell line and the *myc* reconstituted HOmyc3 cells 24 h after treatment. Similarly to irradiation, arrest in G2 was followed by cell death, assessed as increase of the sub-G1 population with fragmented DNA 72 h and 96 h after intoxication (cp Figure 3D and Figure 4A upper panel). Intoxication of the HO15.19 cells induced partial G2 arrest at 24 h, followed by a complete accumulation of cells in this phase of the cell cycle by 72 h, while minimal signs of cell death were observed as late as 96 h after treatment (Figure 4A upper panel). The delayed response of the HO15.19 cells was also confirmed by cell morphology. A massive cell detachment was observed in intoxicated TGR-1 and HOmyc3 cells at 48 h post-intoxication, while this effect was not seen in the HO15.19 cell line up to 96 h (Figure

4A, lower panel). As shown in Figure 4B, UV irradiation induced cell death with similar kinetics in all the cell lines tested, independently of the *myc* status, as assessed by accumulation of cells with fragmented DNA (upper panel) or by cell morphology (lower panel).

ATM autophosphorylation on Ser1981 is dependent on Nbs1, a member of the Mre11/Rad50/Nbs1 (MRN) complex, which acts as a sensor for DNA breaks and is required for efficient activation of the ATM-dependent response [18, 19]. Therefore, we assessed the extent of Nbs1 activation in HOmyc3, TGR-1, and HO15.19 cells in response to irradiation and CDT intoxication. As expected, a prevalent perinuclear distribution of Nbs1 was detected in the HOmyc3 and TGR-1 cells untreated or exposed to the mutant inactive CDT (Figure 5A and data not shown), while exposure to IR was associated with formation of distinct nuclear foci in 80% and 90% of the cells 30 min and 2 h after irradiation, respectively, in both cell lines (Figures 5A and 5B). The number of cells presenting Nbs1 nuclear foci started to decrease 4 h after exposure to IR (Figure 5B). Similar perinuclear distribution of Nbs1 was observed in the *myc* null cells HO15.19 (Figure 5B). However, irradiation-induced foci formation occurred only in approximately 40% of cells 30 min post-treatment, and the number of cells presenting nuclear Nbs1 foci further decreased at later time periods (Figure 5B). A different kinetics of Nbs1 foci formation was observed in TGR-1 and HOmyc3 upon CDT intoxication. Up to 70% of the cells presented nuclear Nbs1 foci 2 h post-intoxication, and this percentage was not significantly decreased 4 h after treatment (Figure 5B, lower panel).
Consistent with a delayed response of the *myc* null cells HO15.19 to agents causing DNA double strand breaks, nuclear re-distribution of Nbs1 was observed in 30% to 40% of the *myc* null cells HO15.19, both at 2 h and 4 h after treatment (Figure 5B, lower panel).

To further confirm that the ATM response to DNA double strand breaks is delayed in absence of *myc*, we assessed levels of Nbs1 expression and the activation status of two other well-charaterized ATM-dependent substrates: the histone H2AX and p53 [20]. Since the cellular responses to IR and CDT are largely identical, we used IR for the next sets of experiments [30]. A two- to three-fold increased expression of Nbs1 was detected by western-blot analysis in HOmyc3 and TGR-1 cells 2 h after

treatment, compared to the untreated controls, while this effect was not observed in the *myc* null cells (Figure 6A). Similarly, HOmyc3 and TGR-1 cells presented a two- to three-fold increase of H2AX phosphorylation (γH2AX) 30 min after irradiation. In contrast, the increase in the levels of γH2AX was almost completely absent in irradiated HO15.19 cells (Figure 6B).

Irradiation induces ATM-dependent phosphorylation of the p53 protein on Ser15 [31]. This prevents its degradation via the uquibitin proteasome system, leading to p53 stabilization and consequent accumulation of the protein, which can be monitored by western-blot analysis. Kinetics experiments showed that accumulation of p53 was a late event, detected 24 h after irradiation in TGR-1 and HOmyc3 cell lines (Figure 6C). This response was further delayed in the *myc* null cells HO15.19, where stabilization of p53 was not detected until 48 h after exposure to IR (Figure 6D).

Interestingly, the Chk1 kinase, which is a known ATR substrate, was already phosphorylated 30 min after irradiation in all the three cell lines (Figure 6E), suggesting that Chk1 phosphorylation was independent of cellular Myc levels.

Collectively, these data demonstrated that MYC plays a key role in the regulation of the ATM-dependent checkpoint responses to DNA damage.

Discussion

Genomic stability is the main barrier that prevents carcinogenesis. Therefore it is not surprising that a number of checkpoint responses are activated to counteract the effects of diverse genotoxic stresses [32]. Our data demonstrated that the proto-oncogene MYC plays an important role in the regulation of the cellular responses to gentoxic stress, since *myc* null cells present impaired recruitment of the MRN complex to form nuclear foci and delayed ATM-dependent checkpoint responses to agents inducing DNA double strand breaks (IR and CDT) (**Figures 3 to 6**). In essence, this protein may play an important role for maintaining genome stability, when expressed at levels observed in non-malignant cells.

ATM may be defined as a bona fide tumor suppressor gene, since Ataxia-telangiectasia (AT) patients, carrying loss-of-function mutations of *ATM*, present chromosomal abnormality, radiation sensitivity, and increased susceptibility to cancer development. In addition, deletion of *atm* in mice results in development of thymic lymphoma [33-36]. Loss-of-function of other key regulators of the DNA damage response, such as the Nbs1 protein in patients affected by the Nijmegen breakage syndrome, causes clinical and cellular phenotypes similar to those observed in AT patients. Based on this evidence and on the data presented in this work it is conceivable that MYC may have a similar role, and therefore loss-of-function of *MYC* in association with enhanced survival signals and/or oncogene activation may lead to increased tumor development in response to chronic genotoxic stress.

Interestingly, deletion of *myc* did not prevent phosphorylation of Chk1 in response to IR (**Figure 6E**). The phospho-specific antibody used in this set of experiments was directed against the site known to be phosphorylated by the ATR kinase (Ser 345 in human cells) [37]. Therefore, we concluded that Myc regulated the activation of the ATM-, but not the ATR-dependent checkpoint pathway induced by irradiation. This is consistent with the observation that UV irradiation, a potent stimulus for ATR activation [38], elicits cell death with similar kinetics in all the three cell lines tested, independently of the *myc* status (**Figure 4B**). These data confirm that the delayed response to IR and CDT observed in the *myc* null cells HO15.19 was not an artifact due to their slower proliferative capacity [13, 26].

The selective effect on the ATM responses may depend on the fact that Nbs1, one of the proteins essential for the full kinase activation [39], is a direct target of MYC. Over-expression of MYC under a tetracycline inducible system in Epstein-Barr virus transformed B cells is associated with increased levels of Nbs1, while knock down of the endogenous levels of MYC by siRNA in 293T cells induced strong down-regulation of Nbs1 [40]. Furthermore, the Myc/Max complex has been shown to bind and enhance transcriptional activation of the *Nbs1* promoter [40]. Accordingly, we observed an up-regulation of the Nbs1 expression in TGR-1 and HOmyc3, compared with the *myc* null cells HO15.19 2h after irradiation (**Figure 6A)**. Furthermore, we observed a strong impairment in irradiation- and intoxication-induced nuclear translocation and foci formation of Nbs1 in the HO15.19 cells (**Figures 5A and 5B**), suggesting that Myc exerts an addition level of control, apart from gene regulation, in the DNA damage-induced activation of the MRN complex. The different kinetics of foci formation observed in irradiated versus intoxicated cells is consistent with the fact that CDT is a constantly active enzyme, which induces an increased number of lesions over time.

Over-expression of MYC in normal human fibroblasts enhances the basal levels of phosphorylation of H2AX and disrupts the repair of DNA DSBs in response to IR. This effect leads to enhanced chromosomal breaks and translocations [41]. In contrast, we observed a similar kinetics of DNA repair in response to irradiation in TGR-1 cells, which express physiological levels of Myc, compared to the *myc* null HO15.19 cells (**Figure 2**). Interestingly, a 3-fold higher Myc expression in the reconstituted HOmyc3 cells [25] was not sufficient to increase the basal levels of H2AX phosphorylation compared to those observed in the parental control TGR-1 (**Figure 6B**), indicating that there is a threshold after which the levels of MYC expression are associated with an abnormal response to DNA damage.

Physiological levels of Myc trigger apoptosis in TGR-1 cells exposed to DNA damaging agents, such as etoposide and camptothecin, via activation of the pro-apoptotic proteins Bax and PKCδ [14, 15]. This response is either absent or delayed in HO15.19 cells. In this work, we showed that cell death was delayed in HO15.19 cells also in response to irradiation and CDT intoxication (**Figures 1 and 4).** The late activation of cell death is in agreement with the late stabilization of the tumor

suppressor gene p53, which was not observed until 48 h post-irradiation (**Figure 6** and [42]). Maclean *et al* recently reported that MYC over-expression via a retroviral vector regulates ATM-dependent activation of p53 4 h after irradiation in primary human foreskin fibroblasts [43]. However, the involvement of MYC in the regulation of upstream activators of ATM, such as Nbs1, was not characterized.

The delayed response of the *myc* null cells HO15.19 to CDT intoxication is very interesting. Epidemiological evidences indicate that chronic infection with the CDT producing bacterium *Salmonella enterica serovar typhi* is associated with increased risk of hepatobiliar carcinoma [44], but the exact mechanism(s) by which bacterial infections can contribute to carcinogenesis is still poorly characterized. In light of the data reported in this work, MYC loss-of-function and consequent delayed cell death in chronic infections with CDT-producing bacteria may promote or enhance genomic instability, and favour tumor initiation and/or progression.

From the data presented in this work, the sequence of events regulated by Myc in response to irradiation or CDT intoxication can be summarized as follows: Myc is essential for the rapid nuclear foci formation of Nbs1. This event triggers full activation of ATM and subsequent phosphorylation of its down-stream effectors and transducer molecules (**Figure 7**). In the presence of a substantial DNA damage that cannot be repaired, activation of the checkpoint response is likely to result in mitochondria-dependent apoptosis [14, 15].

The MYC protein regulates a plethora of cellular responses with outcomes spanning from cell proliferation to cell death. Even in the context of genomic stability this dual role of MYC holds true. Indeed, over-expression of MYC can induce DNA damage both in a ROS-dependent and -independent manner, thus contributing to genome instability and chromosomal abnormalities [6, 7]. In contrast, expression of physiological levels of MYC is important for the proper activation of the DNA damage checkpoint responses. This effect suggests that MYC may exert a tumor suppressor-like function, by contributing to the repair of damaged DNA, and eventually induce the elimination of cells carrying genomic instability. Our work has contributed to the elucidation of this previously poorly characterized role of MYC.

Acknowledgements

We thank Dr J.M. Sedivy (Brown University, RI, USA) for the kind gift of the TGR-1 and HO15.19 cell lines, and Dr. M. Cole (Dartmouth Medical School, NH, USA) for kindly providing the HOmyc3 cell line. This work has been supported by the Swedish Research Council, the Swedish Cancer Society, the Åke Wiberg Foundation, and the Karolinska Institutet to TF, and by the Swedish Cancer Society and the Karolinska Institutet to MH. TF is supported by the Swedish Research Council.

References

[1] C. Grandori, S.M. Cowley, L.P. James, R.N. Eisenman, The Myc/Max/Mad network and the transcriptional control of cell behavior, Annu Rev Cell Dev Biol 16 (2000) 653-699.

[2] M. Vita, M. Henriksson, The Myc oncoprotein as a therapeutic target for human cancer, Semin Cancer Biol 16 (2006) 318-330.

[3] C.E. Nesbit, J.M. Tersak, E.V. Prochownik, MYC oncogenes and human neoplastic disease, Oncogene 18 (1999) 3004-3016.

[4] R. Ponzielli, S. Katz, D. Barsyte-Lovejoy, L.Z. Penn, Cancer therapeutics: targeting the dark side of Myc, Eur J Cancer 41 (2005) 2485-2501.

[5] S. Adhikary, M. Eilers, Transcriptional regulation and transformation by Myc proteins, Nat Rev Mol Cell Biol 6 (2005) 635-645.

[6] O. Vafa, M. Wade, S. Kern, M. Beeche, T.K. Pandita, G.M. Hampton, G.M. Wahl, c-Myc can induce DNA damage, increase reactive oxygen species, and mitigate p53 function: a mechanism for oncogene-induced genetic instability, Mol Cell 9 (2002) 1031-1044.

[7] S. Ray, K.R. Atkuri, D. Deb-Basu, A.S. Adler, H.Y. Chang, L.A. Herzenberg, D.W. Felsher, MYC can induce DNA breaks in vivo and in vitro independent of reactive oxygen species, Cancer Res 66 (2006) 6598-6605.

[8] F. Kuttler, S. Mai, c-Myc, Genomic Instability and Disease, in: V. J-N (Ed.), Genome and Disease, S. Karger AG, Basel, 2006, Vol. 1, pp. 171–190.

[9] J.A. Nilsson, J.L. Cleveland, Myc pathways provoking cell suicide and cancer, Oncogene 22 (2003) 9007-9021.

[10] S. Pelengaris, M. Khan, G. Evan, c-MYC: more than just a matter of life and death, Nat Rev Cancer 2 (2002) 764-776.

[11] P. Juin, A.O. Hueber, T. Littlewood, G. Evan, c-Myc-induced sensitization to apoptosis is mediated through cytochrome c release, Genes Dev 13 (1999) 1367-1381.

[12] P. Juin, A. Hunt, T. Littlewood, B. Griffiths, L.B. Swigart, S. Korsmeyer, G. Evan, c-Myc functionally cooperates with Bax to induce apoptosis, Mol Cell Biol 22 (2002) 6158-6169.

[13] E.L. Soucie, M.G. Annis, J. Sedivy, J. Filmus, B. Leber, D.W. Andrews, L.Z. Penn, Myc potentiates apoptosis by stimulating Bax activity at the mitochondria, Mol Cell Biol 21 (2001) 4725-4736.

[14] A. Albihn, J. Loven, J. Ohlsson, L.M. Osorio, M. Henriksson, c-Myc-dependent etoposide-induced apoptosis involves activation of Bax and caspases, and PKCdelta signaling, J Cell Biochem 98 (2006) 1597-1614.

[15] A. Albihn, H. Mo, Y. Yang, M. Henriksson, Camptothecin-induced apoptosis is enhanced by Myc and involves PKCdelta signaling, Int J Cancer 121 (2007) 1821-1829.

[16] M.F. Lavin, S. Kozlov, ATM activation and DNA damage response, Cell Cycle 6 (2007) 931-942.

[17] C.J. Bakkenist, M.B. Kastan, DNA damage activates ATM through intermolecular autophosphorylation and dimer dissociation, Nature 421 (2003) 499-506.

[18] J.H. Lee, T.T. Paull, Direct activation of the ATM protein kinase by the Mre11/Rad50/Nbs1 complex, Science 304 (2004) 93-96.

[19] J.H. Lee, T.T. Paull, ATM activation by DNA double-strand breaks through the Mre11-Rad50-Nbs1 complex, Science 308 (2005) 551-554.

[20] Y. Shiloh, ATM and related protein kinases: safeguarding genome integrity, Nat Rev Cancer 3 (2003) 155-168.

[21] K.H. Maclean, U.B. Keller, C. Rodriguez-Galindo, J.A. Nilsson, J.L. Cleveland, c-Myc augments gamma irradiation-induced apoptosis by suppressing Bcl-XL, Mol Cell Biol 23 (2003) 7256-7270.

[22] I.R. Radford, Initiation of ionizing radiation-induced apoptosis: DNA damage-mediated or does ceramide have a role?, Int J Radiat Biol 75 (1999) 521-528.

[23] J.H. Sheen, R.B. Dickson, Overexpression of c-Myc alters G(1)/S arrest following ionizing radiation, Mol Cell Biol 22 (2002) 1819-1833.

[24] J.H. Sheen, J.K. Woo, R.B. Dickson, c-Myc alters the DNA damage-induced G2/M arrest in human mammary epithelial cells, Br J Cancer 89 (2003) 1479-1485.

[25] A. Bush, M. Mateyak, K. Dugan, A. Obaya, S. Adachi, J. Sedivy, M. Cole, c-myc null cells misregulate cad and gadd45 but not other proposed c-Myc targets, Genes Dev 12 (1998) 3797-3802.

[26] M.K. Mateyak, A.J. Obaya, S. Adachi, J.M. Sedivy, Phenotypes of c-Myc-deficient rat fibroblasts isolated by targeted homologous recombination, Cell Growth Differ 8 (1997) 1039-1048.
[27] Z. Ge, Y. Feng, M.T. Whary, P.R. Nambiar, S. Xu, V. Ng, N.S. Taylor, J.G. Fox, Cytolethal distending toxin is essential for Helicobacter hepaticus colonization in outbred Swiss Webster mice, Infect Immun 73 (2005) 3559-3567.
[28] B. Stenerlow, K.H. Karlsson, B. Cooper, B. Rydberg, Measurement of Prompt DNA Double-Strand Breaks in Mammalian Cells without Including Heat-Labile Sites: Results for Cells Deficient in Nonhomologous End Joining, Radiat Res 159 (2003) 502-510.
[29] B. Stenerlöw, E. Höglund, J. Carlsson, Induction and rejoining of large DNA fragments after ion radiation, Radiation Research 151 (1999) 642-648.
[30] M. Thelestam, T. Frisan, Cytolethal distending toxins, Rev Physiol Biochem Pharmacol 152 (2004) 111-133.
[31] Y. Aylon, M. Oren, Living with p53, dying of p53, Cell 130 (2007) 597-600.
[32] J. Bartek, J. Bartkova, J. Lukas, DNA damage signalling guards against activated oncogenes and tumour progression, Oncogene 26 (2007) 7773-7779.
[33] Y. Shiloh, M.B. Kastan, ATM: genome stability, neuronal development, and cancer cross paths, Adv Cancer Res 83 (2001) 209-254.
[34] J. Boultwood, Ataxia telangiectasia gene mutations in leukaemia and lymphoma, J Clin Pathol 54 (2001) 512-516.
[35] C. Barlow, S. Hirotsune, R. Paylor, M. Liyanage, M. Eckhaus, F. Collins, Y. Shiloh, J.N. Crawley, T. Ried, D. Tagle, A. Wynshaw-Boris, Atm-deficient mice: a paradigm of ataxia telangiectasia, Cell 86 (1996) 159-171.
[36] M. Liyanage, Z. Weaver, C. Barlow, A. Coleman, D.G. Pankratz, S. Anderson, A. Wynshaw-Boris, T. Ried, Abnormal rearrangement within the alpha/delta T-cell receptor locus in lymphomas from Atm-deficient mice, Blood 96 (2000) 1940-1946.
[37] Y. Chen, Y. Sanchez, Chk1 in the DNA damage response: conserved roles from yeasts to mammals, DNA Repair (Amst) 3 (2004) 1025-1032.
[38] Y. Shiloh, ATM and ATR: networking cellular responses to DNA damage, Current Opinion in Genetics & Development 11 (2001) 71-77.
[39] J.H. Lee, T.T. Paull, Activation and regulation of ATM kinase activity in response to DNA double-strand breaks, Oncogene 26 (2007) 7741-7748.
[40] Y.C. Chiang, S.C. Teng, Y.N. Su, F.J. Hsieh, K.J. Wu, c-Myc directly regulates the transcription of the NBS1 gene involved in DNA double-strand break repair, J Biol Chem 278 (2003) 19286-19291.
[41] A. Karlsson, D. Deb-Basu, A. Cherry, S. Turner, J. Ford, D.W. Felsher, Defective double-strand DNA break repair and chromosomal translocations by MYC overexpression, Proc Natl Acad Sci U S A 100 (2003) 9974-9979.
[42] S. Adachi, A.J. Obaya, Z. Han, N. Ramos-Desimone, J.H. Wyche, J.M. Sedivy, c-Myc is necessary for DNA damage-induced apoptosis in the G(2) phase of the cell cycle, Mol Cell Biol 21 (2001) 4929-4937.
[43] K.H. Maclean, M.B. Kastan, J.L. Cleveland, Atm deficiency affects both apoptosis and proliferation to augment Myc-induced lymphomagenesis, Mol Cancer Res 5 (2007) 705-711.
[44] A.J. Lax, Bacterial toxins and cancer — a case to answer?, Nature Reviews Microbiology 3 (2005) 343-349.

Figure legend

Figure 1. Myc deletion delays cell death upon induction of DNA damage
TGR-1 and the *myc* null HO15.19 cells were left untreated or irradiated (20 Gy) and further incubated in complete medium for the indicated periods of time. Analysis of the cell cycle distribution was assessed by PI staining and flow cytometry as described in Material and Methods. One out of four experiments is shown.

Figure 2. Myc does not affect the rate of DNA repair
A) Pulsed-field gel electrophoresis (PFGE). Fifty thousand TGR-1 or HO15.19 cells were grown in a 12 well-plate in complete medium containing 4000 Bq [methyl-^{14}C]-thymidine for 72 h. The cells were then washed twice in PBS, chased for 2 h in complete medium before irradiation (20 Gy), and further processed for PFGE analysis at the indicated periods of time. One out of two independent experiments is shown. **B)** Quantification of DNA fragmentation at the indicated time periods.

Figure 3. Activation of ATM and ATM-dependent responses upon induction of DNA damage is Myc dependent
A) TGR-1 and HO15.19 cells were left untreated or exposed to IR (20 Gy), and further incubated in complete medium for the indicated periods of time. The levels of ATM phosphorylation were assessed by western-blot analysis using a α-phospho-ATM antibody. Actin was used as an internal loading control. One out of four independent experiments is shown. **B)** TGR-1 cells were left untreated or exposed to IR (20 Gy), and further incubated in complete medium for the indicated periods of time. Phosphorylation of ATM/ATR substrates was assessed by western-blot analysis. The arrows indicate two proteins of approximately 35kDa and 110kDa, respectively that were phosphorylated in response to irradiation. One out of four independent experiments is shown. **C)** TGR-1 and HO15.19 cells were left untreated or exposed to IR (20 Gy), and further incubated in complete medium for the indicated periods of time. Phosphorylation of ATM/ATR substrates was assessed as described in Figure 3B. **D)** TGR-1, and the *myc* reconstituted HOmyc3 cells were left untreated or irradiated (20 Gy), and were further incubated in complete medium for the indicated periods of time. Analysis of the cell cycle distribution was assessed as described in Material and Methods. One out of two independent experiments is shown. **E)** TGR-1, HOmyc3, and HO15.19 cells were left untreated or exposed to IR (20 Gy), and further incubated in complete medium for 2 h. The levels of ATM phosphorylation were assessed as described in Figure 3A. Actin and total ATM were used as internal loading controls.

Figure 4. Myc deletion delays cell death in response to CDT intoxication but not to UV irradiation
TGR-1, the *myc* reconstituted cells HOmyc3, and the *myc* null HO15.19 cells were exposed to bacterial lysates (1:2000) expressing the mutant (CTR) or the wild type form (CDT) of *H. hepaticus* CDT **(A),** or left untreated or exposed to UV irradiation **(B)**, and further incubated in complete medium for the indicated periods of time. Analysis of the cell cycle distribution (upper panel) was assessed by PI staining and flow cytometry as described in Material and Methods. One out of three experiments is shown. The lower panel shows phase contrast micrographs of the cells taken at the indicated time points (Magnification 40x).

Figure 5. Myc deletion impairs Nbs1 foci formation in response to DNA damage
A) TGR-1, the *myc* reconstituted HOmyc3, and the *myc* null HO15.19 cells were exposed to bacterial lysates (1:2000) expressing the mutant (CTR) or the wild type form (CDT) of *H. hepaticus* CDT, or irradiated (IR, 20 Gy) and further incubated in complete medium for the indicated periods of time. The Nbs1 protein was detected by indirect immunostaining, as described in Material and Methods. The figure shows the sub-cellular distribution of Nbs1 at 2 h post-treatment. **C)** Quantification of the number of cells expressing Nbs1 nuclear foci (one hundred cells were counted for each treatment). A cell with more than 5 nuclear foci was scored as positive. Mean ± SD of three independent experiments; * statistically significant decreased in Nbs1 foci formation.

Figure 6. Myc deletion prevents Nbs1 up-regulation and delays H2AX and p53 activation in response to DNA damage
TGR-1, the *myc* reconstituted HOmyc3, and the *myc* null HO15.19 cells were left untreated or exposed to IR (20 Gy) and further incubated in complete medium for the indicated periods of time. The levels of Nbs1 (**A**), γ-H2AX (**B**) and phospho-Chk1 (pChk1) (**E**) were assessed by western-blot analysis as described in Material and Methods.
C) TGR-1 and the *myc* reconstituted HOmyc3 cells were left untreated or exposed to IR (20 Gy) for the indicated periods of time. The levels of p53 were assessed by western-blot analysis. **D)** TGR-1, the *myc* reconstituted HOmyc3 and the HO15.19 cells were left untreated or exposed to IR (20 Gy) for the indicated periods of time. The levels of p53 were assessed by western-blot analysis. Actin was used as an internal loading control. One out of three independent experiments is shown.

Figure 7. Model for the MYC-dependent responses to irradiation or CDT intoxication. In response to IR or CDT, MYC induces up-regulation and nuclear foci formation of Nbs1. This event triggers activation (phosphorylation) of ATM, leading to phosphorylation of its down-stream effectors and transducer molecules. Phosphorylation of the ATR-dependent target kinase Chk1 is independent of MYC expression.

Figure 1

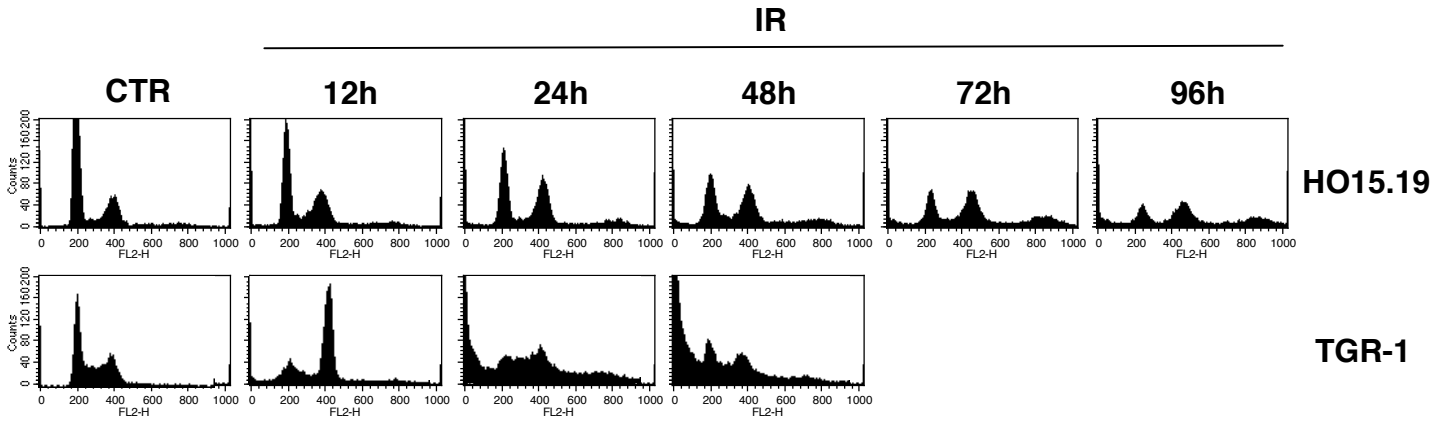

Figure 2

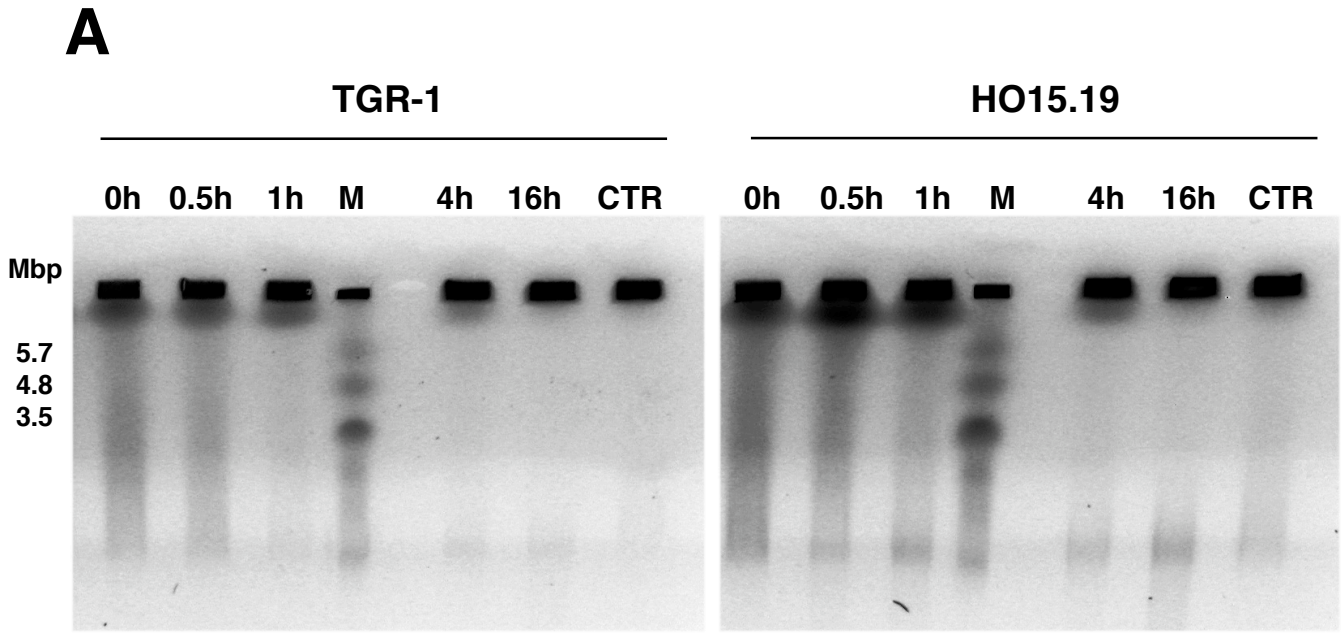
A
TGR-1
HO15.19
0h 0.5h 1h M 4h 16h CTR
0h 0.5h 1h M 4h 16h CTR
Mbp
5.7
4.8
3.5

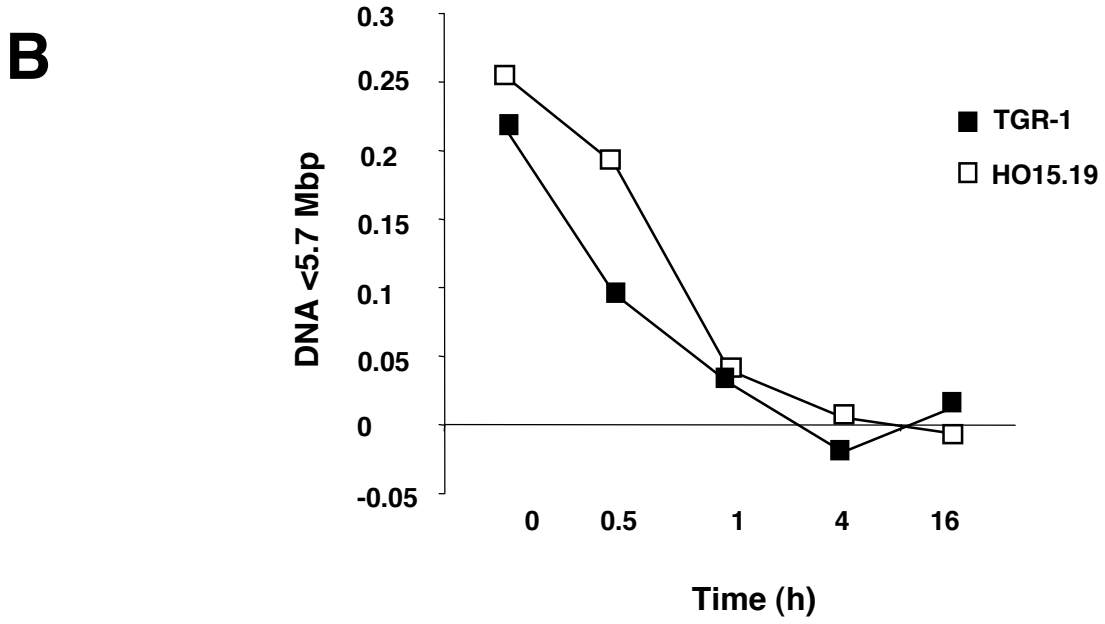
B
DNA <5.7 Mbp
0.3
0.25
0.2
0.15
0.1
0.05
0
-0.05
0
0.5
1
4
16
Time (h)
TGR-1
HO15.19

Figure 3

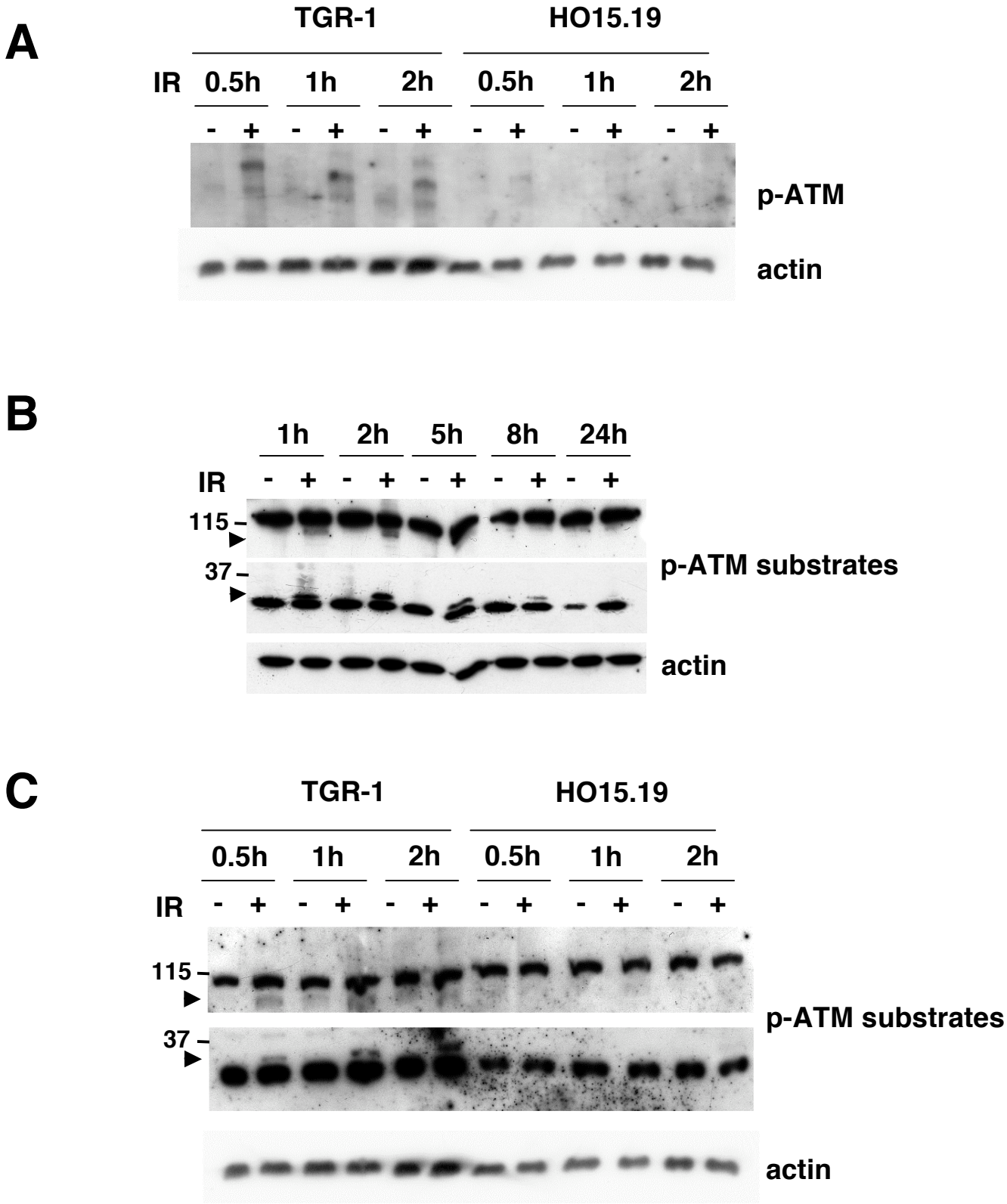
A
TGR-1
HO15.19
IR
0.5h
1h
2h
0.5h
1h
2h
- + - + - + - + - + - +
p-ATM
actin
B
1h
2h
5h
8h
24h
IR
- + - + - + - + - +
115
37
p-ATM substrates
actin
C
TGR-1
HO15.19
0.5h
1h
2h
0.5h
1h
2h
IR
- + - + - + - + - + - +
115
37
p-ATM substrates
actin

Figure 3

D

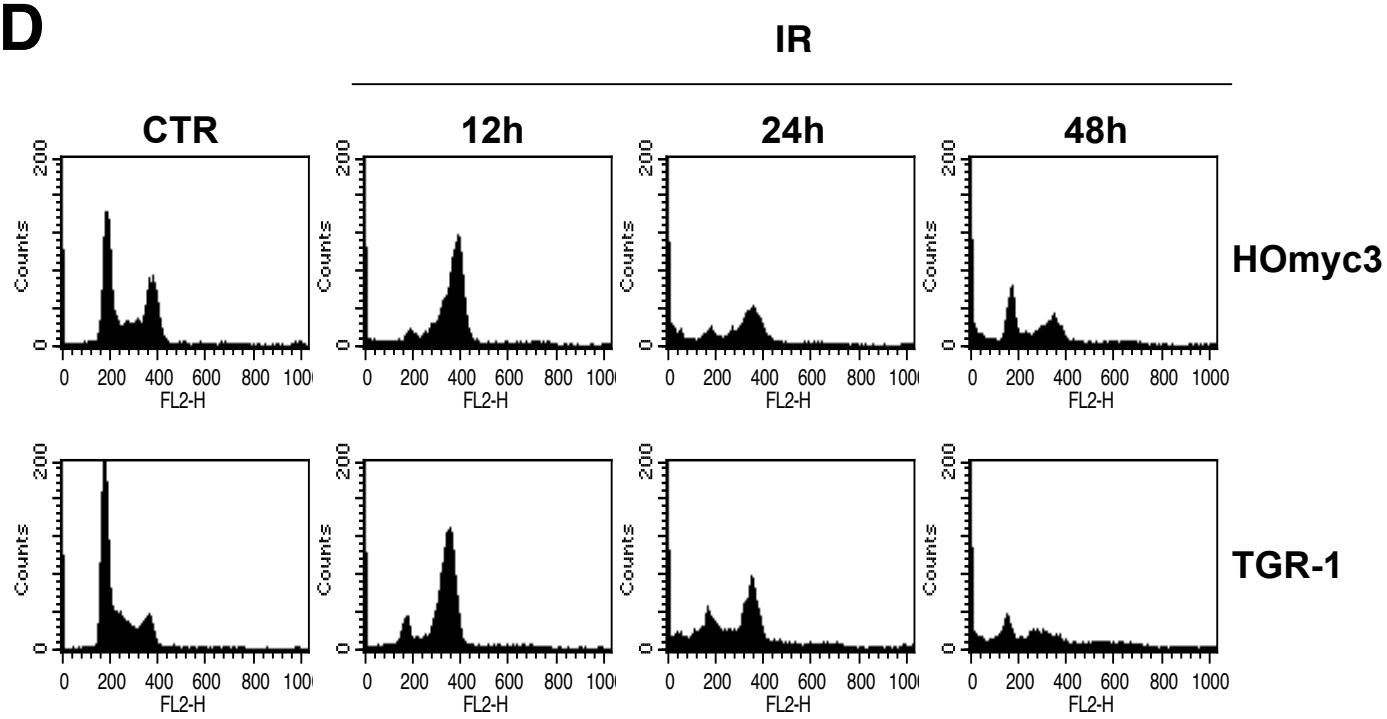
IR
CTR
12h
24h
48h
HOmyc3
TGR-1
Counts
FL2-H

E

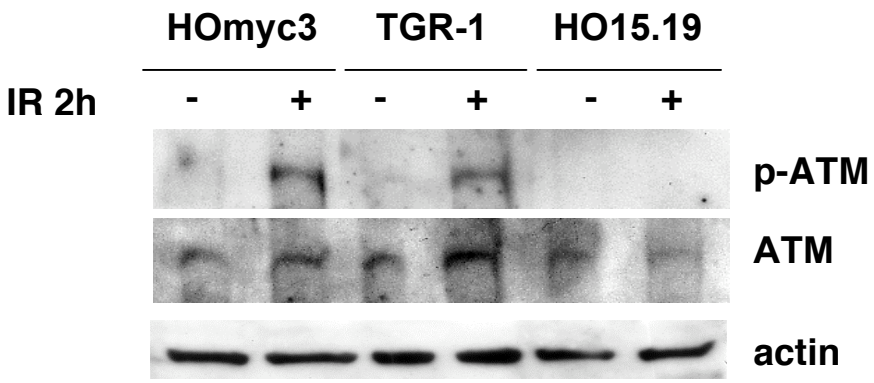
HOmyc3
TGR-1
HO15.19
IR 2h
- + - + - +
p-ATM
ATM
actin

Figure 4A

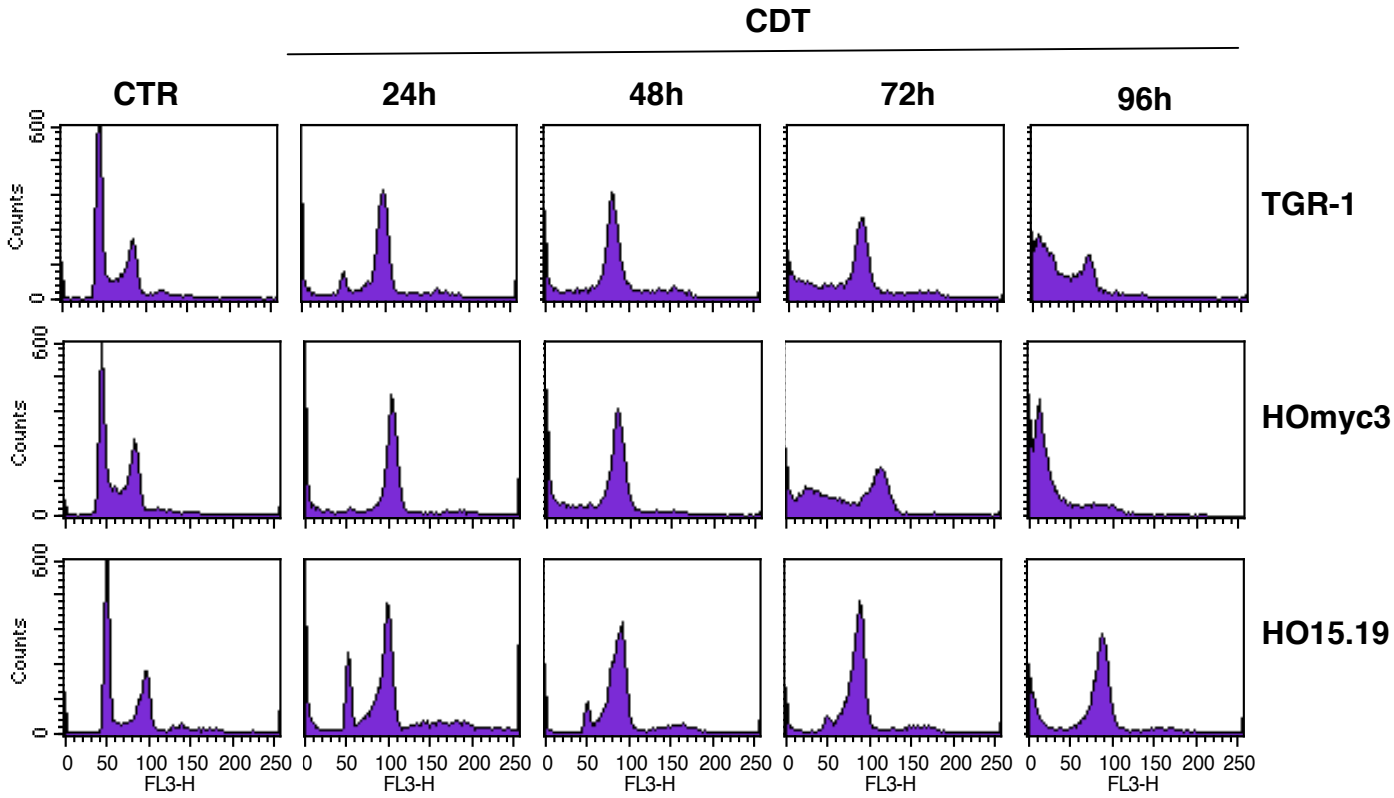
CDT
CTR
24h
48h
72h
96h
TGR-1
HOmyc3
HO15.19
Counts
600
0
0 50 100 150 200 250
FL3-H

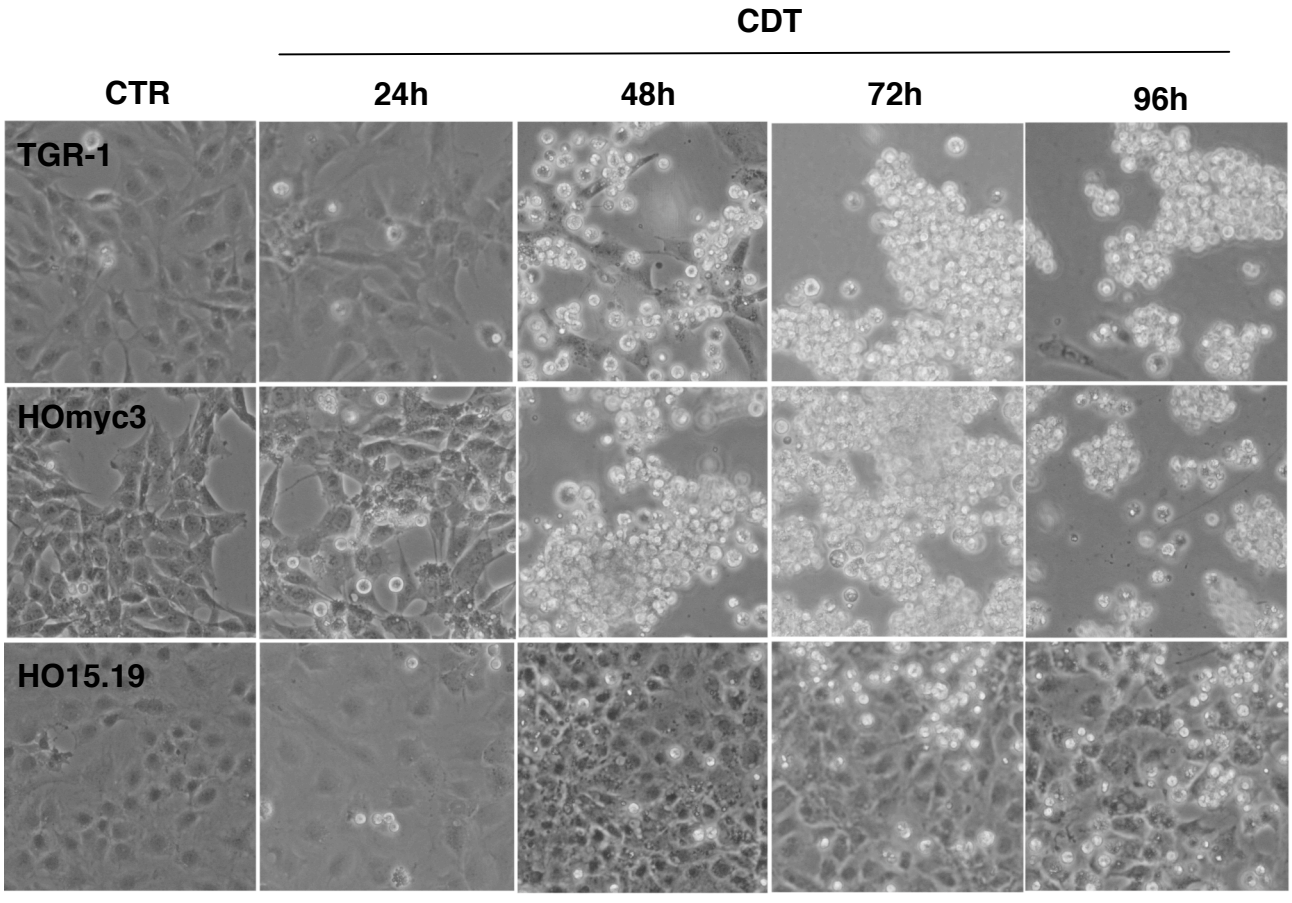
CDT
CTR
24h
48h
72h
96h
TGR-1
HOmyc3
HO15.19

Figure 4B

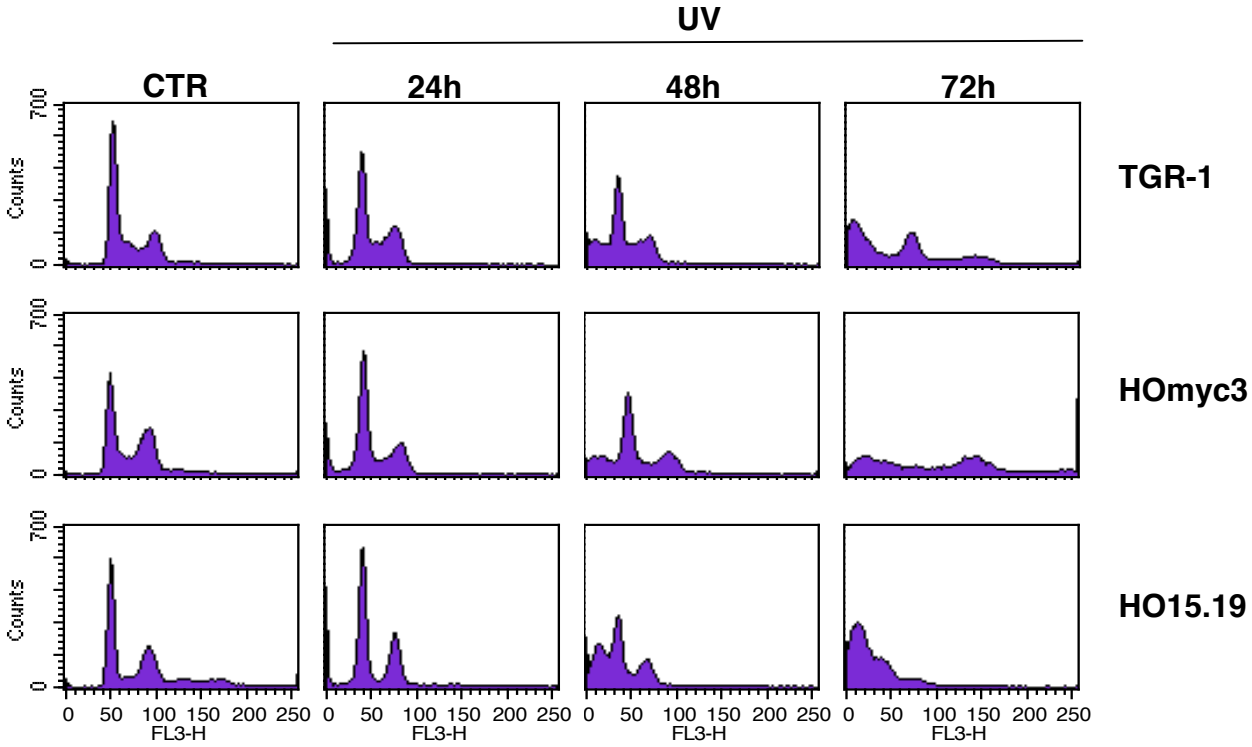
UV
CTR
24h
48h
72h
TGR-1
HOmyc3
HO15.19
Counts
700
0
0 50 100 150 200 250
FL3-H

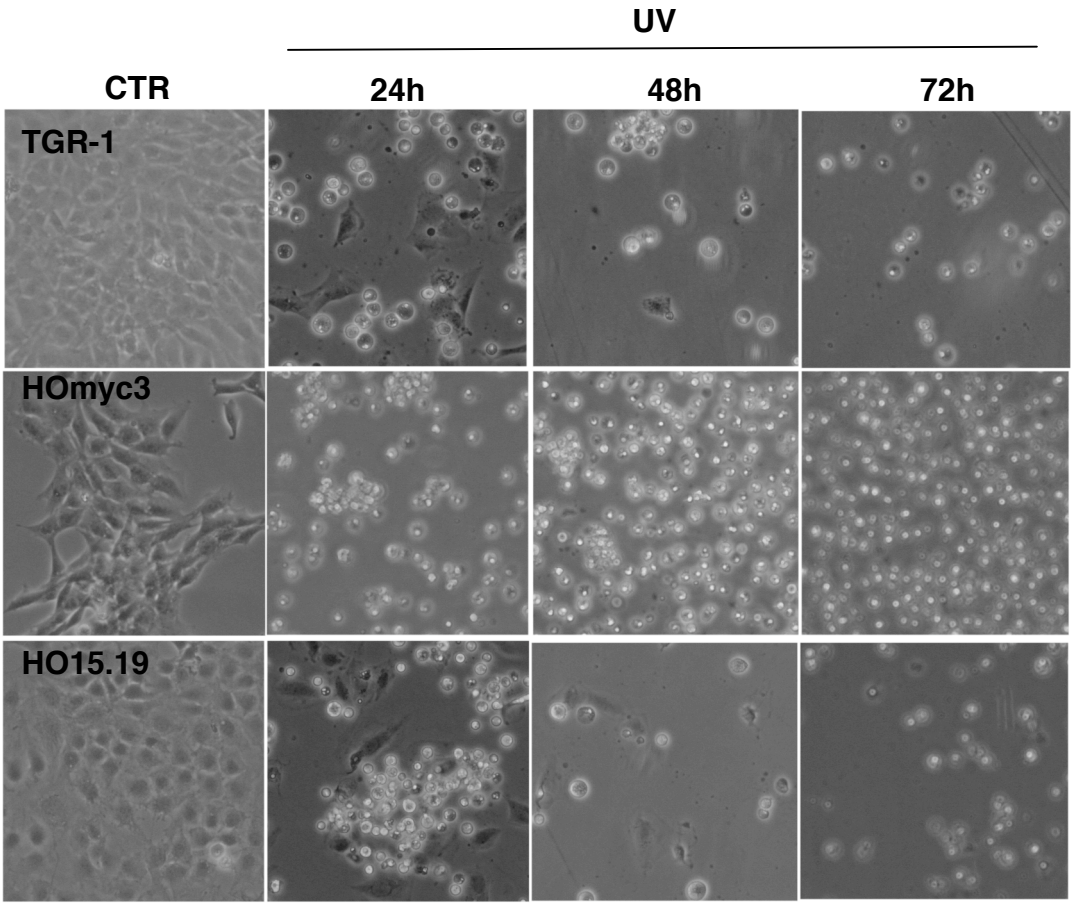
UV
CTR
24h
48h
72h
TGR-1
HOmyc3
HO15.19

Figure 5A

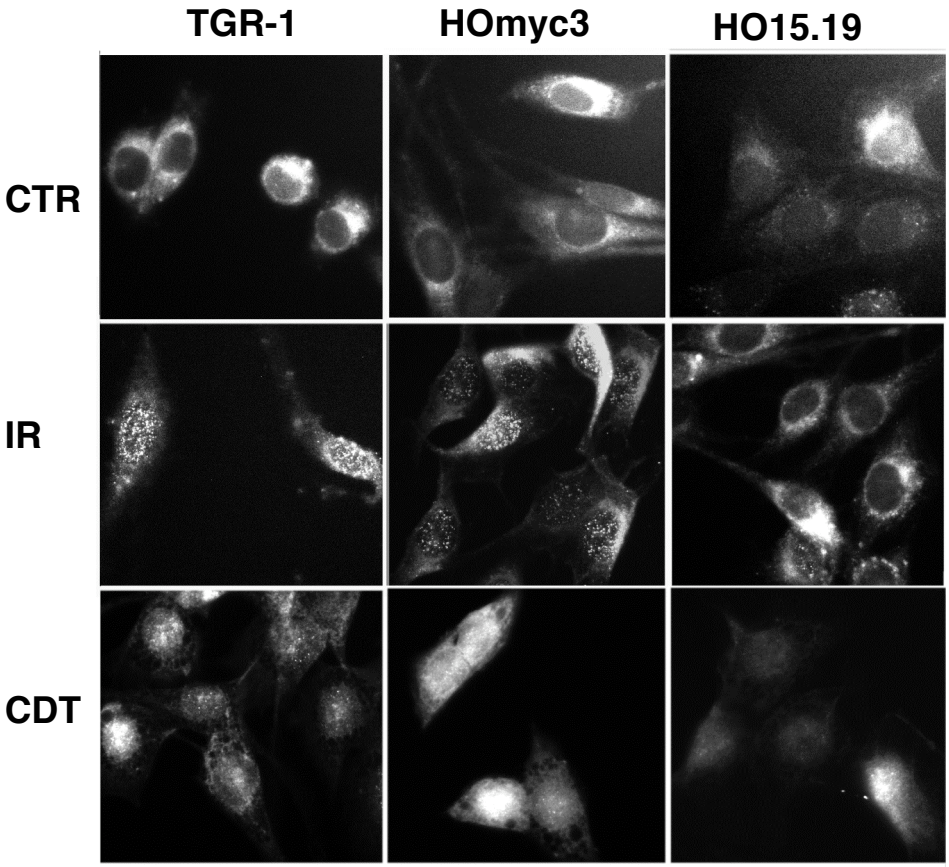

Figure 5B

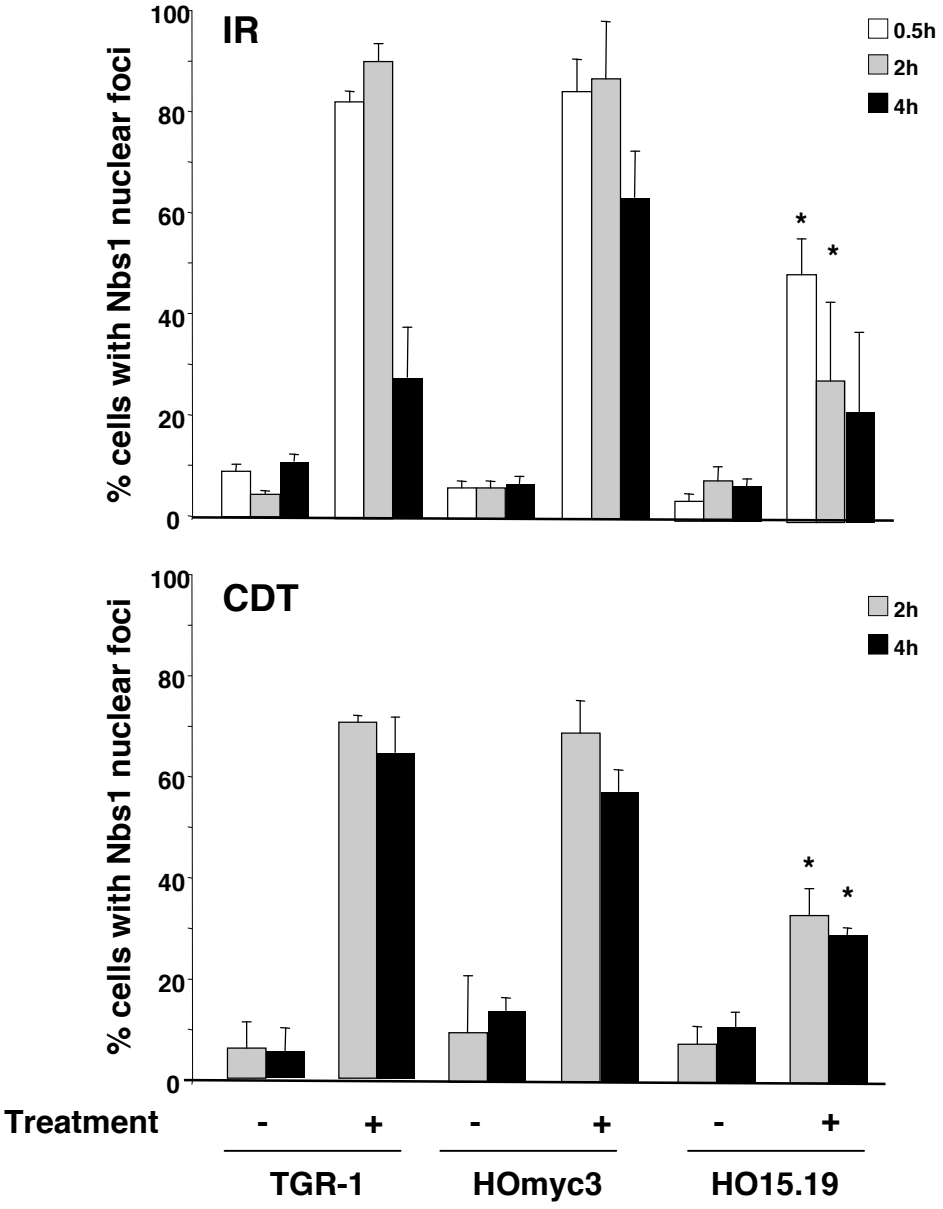
IR
0.5h
2h
4h
% cells with Nbs1 nuclear foci
100
80
60
40
20
0
*
*
CDT
2h
4h
% cells with Nbs1 nuclear foci
100
80
60
40
20
0
*
*
Treatment
-
+
-
+
-
+
TGR-1
HOmyc3
HO15.19

Figure 6

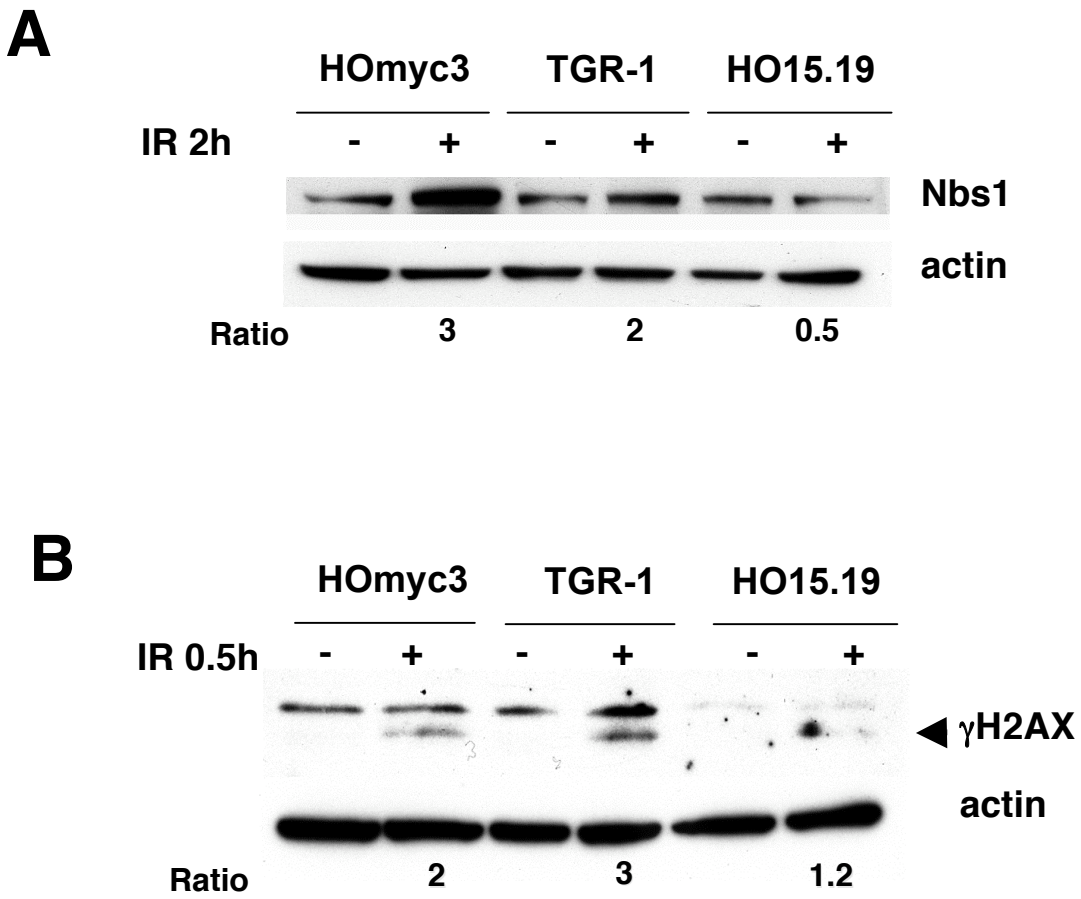
A
HOmyc3
TGR-1
HO15.19
IR 2h
- + - + - +
Nbs1
actin
Ratio
3
2
0.5
B
HOmyc3
TGR-1
HO15.19
IR 0.5h
- + - + - +
γH2AX
actin
Ratio
2
3
1.2

Figure 6

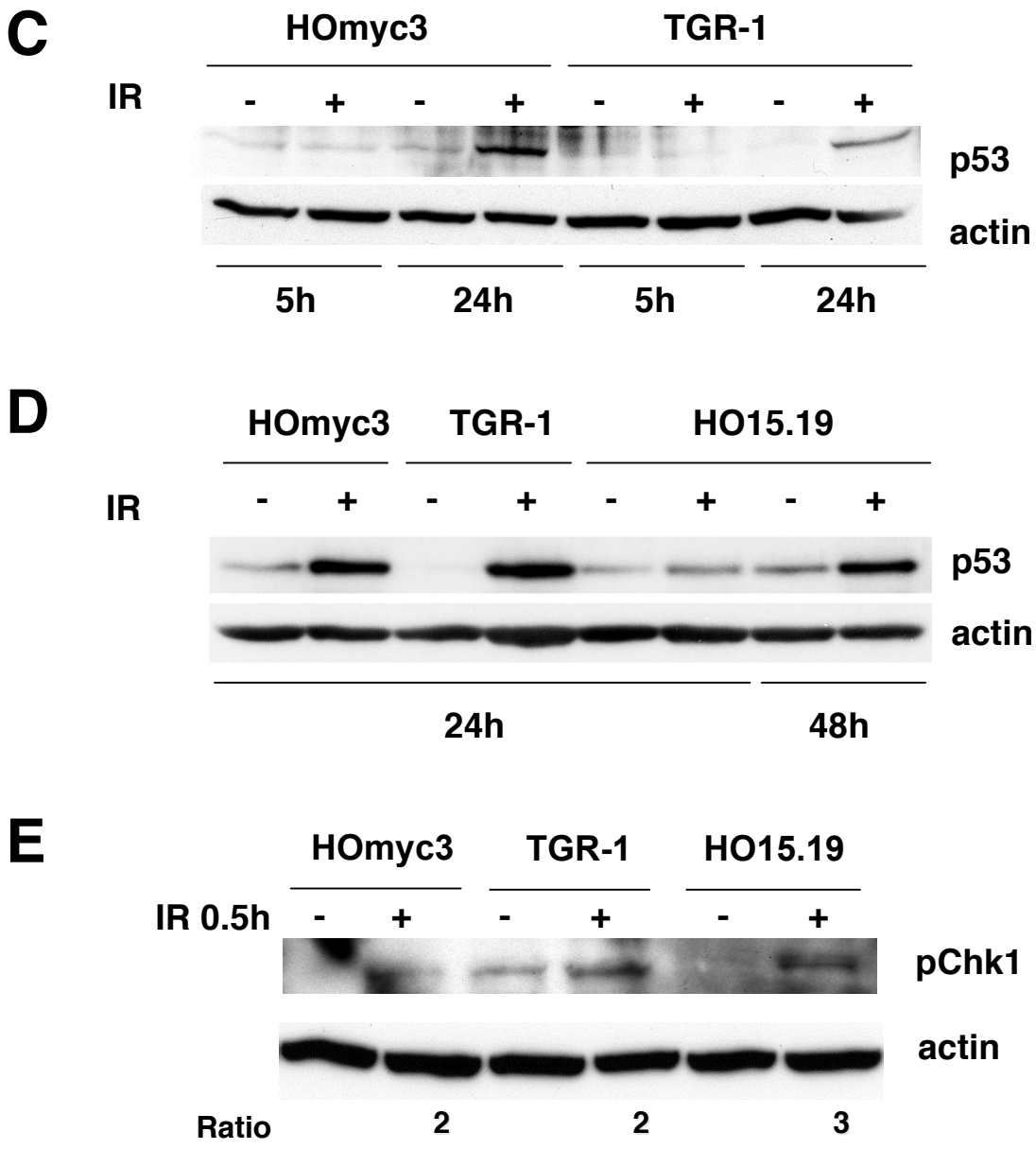
C
HOmyc3
TGR-1
IR
- + - + - + - +
p53
actin
5h
24h
5h
24h
D
HOmyc3
TGR-1
HO15.19
IR
- + - + - + - +
p53
actin
24h
48h
E
HOmyc3
TGR-1
HO15.19
IR 0.5h
- + - + - +
pChk1
actin
Ratio
2
2
3

Figure 7

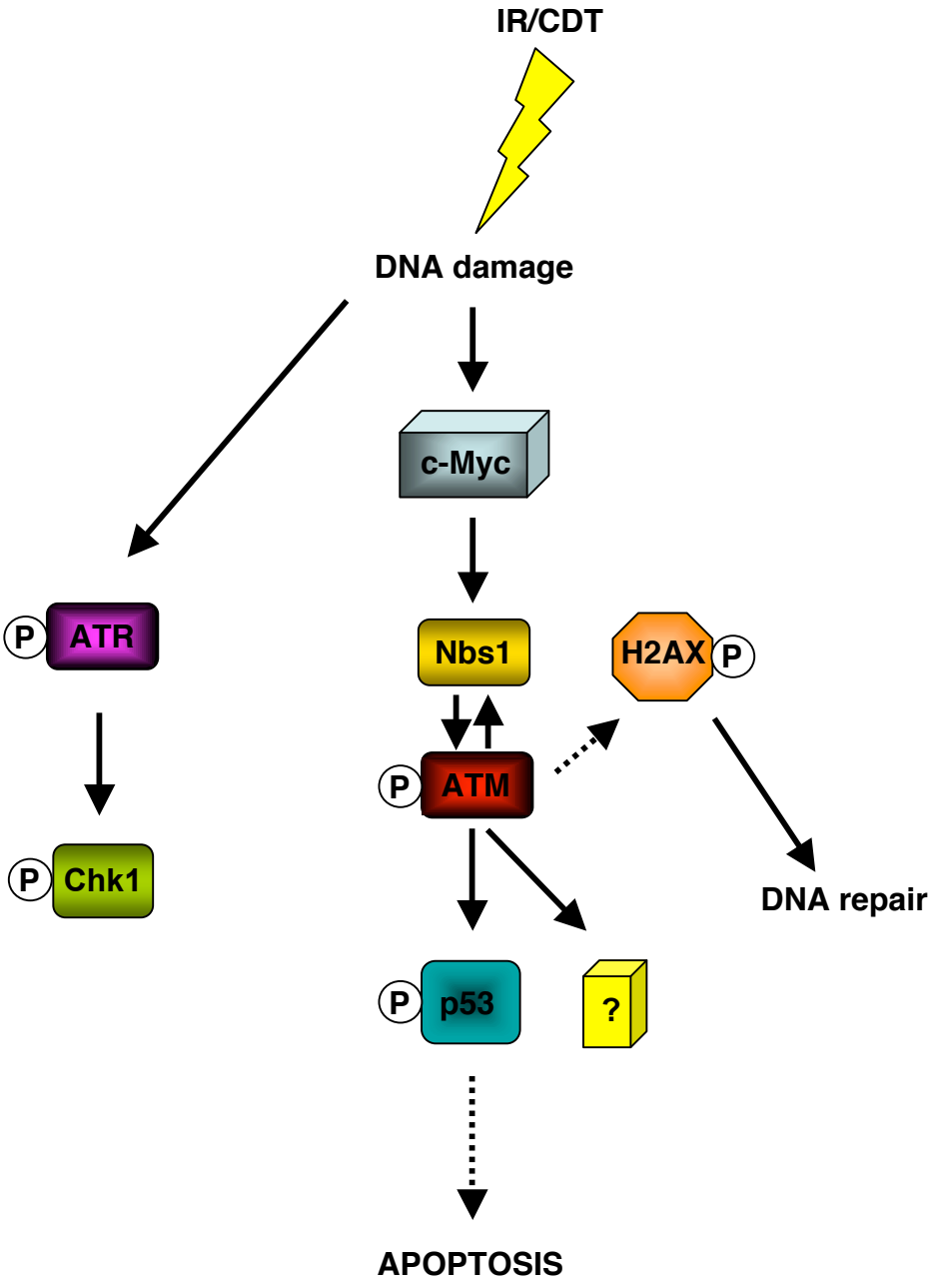
IR/CDT
DNA damage
c-Myc
P
ATR
Nbs1
H2AX
P
P
ATM
P
Chk1
DNA repair
P
p53
?
APOPTOSIS